PhD

Thesis

Lorentz-symmetry violation and new experimental signatures in particle physics as possible directions beyond the Standard Model

João Paulo da Silva Melo

Centro Brasileiro de Pesquisas Físicas

Rio de Janeiro - RJ

March, 2026

"LORENTZ-SYMMETRY VIOLATION AND NEW EXPERIMENTAL SIGNATURES IN PARTICLE PHYSICS AS POSSIBLE DIRECTIONS BEYOND THE STANDARD MODEL"

JOÃO PAULO DA SILVA MELO

Tese de Doutorado em Física apresentada no Centro Brasileiro de Pesquisas Físicas do Ministério da Ciência Tecnologia e Inovação. Fazendo parte da banca examinadora os seguintes professores:

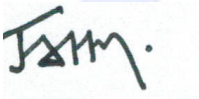

José Abdalla Helayel-Neto - Orientador/CBPF

Documento assinado digitalmente
PHILIPE OSORIO DE FABRITIIS
Data: 16/05/2026 11:10:34-0300
Verifique em https://validar.iti.gov.br

Philipe Osório de Fabritiis – CBPF

Documento assinado digitalmente
HUMBERTO BELICH JUNIOR
Data: 17/04/2026 20:48:20-0300
Verifique em https://validar.iti.gov.br

Humberto Belich Junior - UFES

Documento assinado digitalmente
MANOEL MESSIAS FERREIRA JUNIOR
Data: 27/04/2026 09:31:43-0300
Verifique em https://validar.iti.gov.br

Manoel Messias Ferreira Junior – UFMA

Documento assinado digitalmente
ANTONIO DUARTE PEREIRA JUNIOR
Data: 27/04/2026 15:06:44-0300
Verifique em https://validar.iti.gov.br

Antônio Duarte Pereira Junior - UFF

Rio de Janeiro, 24 de março de 2026.

Agradecimentos

O caminho até a conclusão desta tese de doutorado foi construído com muito esforço, aprendizado e amizade. Sou profundamente grato a todos que estiveram presentes e foram essenciais ao longo dessa jornada. A seguir, destaco alguns agradecimentos especiais.

Em primeiro lugar, agradeço aos meus pais, Genaina e João, e ao meu irmão, Jonatas, pelo amor incondicional, pelo incentivo constante e por sempre acreditarem na minha jornada para me tornar físico. Muito do que sou e do que realizei nesta tese vem das lições que recebi de vocês, especialmente o valor do trabalho duro, da persistência e da resiliência. Muito obrigado por tudo.

Agradeço, com todo o meu carinho, à minha companheira Mirian, minha física favorita. Obrigado por acreditar em mim e dar apoio nos momentos mais difíceis deste doutorado. Com você, os desafios se tornaram mais leves. Sou profundamente grato por tudo.

Agradeço ao meu orientador e – como é bom poder dizer isso – amigo, Prof. Helayël. Seus ensinamentos vão muito além do pragmatismo de manipular equações, assimilar e criar novos conceitos físicos; eles apontam para uma forma de vida em que toda forma de arte, ciência e os espaços públicos devam ser verdadeiramente compartilhados. Trabalhar com o senhor foi, é e sempre será um privilégio. Obrigado por tudo e, em especial, por acolher todos nós do interior, tantas vezes esquecidos neste Brasil.

Agradeço aos professores e amigos, o poeta Álvaro e o conselheiro Tião, pelos cursos estimulantes e por toda a Física que pude aprender com vocês; por compartilharem visões políticas, pelo acolhimento em momentos difíceis e pelas incontáveis resenhas futebolísticas, nas quais vocês insistem em não aceitar que a torcida do Flamengo é, sim, terceirizada. Mas, acima de tudo, agradeço por compartilharem ideais e valores em comum com os do Prof. Helayël.

Agradeço aos residentes do Diracstão, que me receberam da forma mais amigável e calorosa possível quando cheguei ao Rio de Janeiro: Bernard, Henrique, Herus, Jeff, Mateus Paixão (atleticano sofredor), Philipe e Weillison. Agradeço também aos novos residentes: Clara, Guilherme Scorza, Gustavo Levy, Mirian, Rodrigo Lima e Rodrigo Pinheiro. Minhas lembranças mais divertidas do CBPF sempre estarão ligadas à convivência com vocês, os residentes da República do Diracstão.

Agradeço aos camaradas Carlos Zarro, Leonardo Ospedal, Mario Junior e Pedro Malta pelas oportunidades de colaboração, nas quais aprendi muita Física nova e que foram essenciais para a realização desta tese e para a minha formação. Em especial, ao Léo Ospedal, agradeço pelos cursos, pela gentileza e pelas conversas sempre amigáveis.

Agradeço ao meu amigo e colaborador Wagno. Nossa amizade é um dos grandes presentes desta tese de doutorado. Agradeço também aos demais camaradas que orbitam Juiz de Fora: Guilherme Yoshi, Hemilly, Letícia, Nicolas, Públio e Samuel; e ao meu grande amigo

do caos e dos sistemas dinâmicos, João Batista. Todos vocês sempre apoiaram e incentivaram os passos dados ao longo dessa jornada.

Agradeço aos professores Doria, Emil e Sérgio Duarte por todas as conversas estimulantes no terceiro andar e pelo carinho que sempre tiveram por mim e todos os outros estudantes.

Agradeço também aos camaradas Artur Semião, Chauca, Felipe Sobrero, Lucas Hayashi, Mateus Poltronieri, Marcos, Taís, Dudu e Botta pelo convívio repleto de alegrias e boas resenhas no CBPF e, em especial, aos dois últimos, junto ao sempre amável Herinho, pelo acolhimento e apoio em momentos difíceis na República do Vascão.

Não posso deixar de agradecer aos professores Aquyquo Franco e Edson Wander, que, respectivamente, acendeu minha chama pela Física ainda no ensino médio e a alimentou durante a graduação. Muito obrigado, de coração.

Registro também meu agradecimento às amáveis secretárias Cláudia e Elisete, bem como às queridas colaboradoras da limpeza Dona Edina, Val e Miriam. Vocês fazem parte das memórias mais felizes da ala D do terceiro andar. Agradeço ainda às sempre solícitas secretárias do COEDU, Bete e Larissa, a todo o pessoal da segurança, em especial ao camarada Bola, e também ao pessoal da manutenção de computadores da COTEC.

Por fim, agradeço ao CNPq e à FAPERJ por cumprirem a sua função social de amparar e financiar a pesquisa científica no Brasil e no Estado do Rio de Janeiro, respectivamente, e em especial pelo apoio financeiro concedido ao longo do meu doutorado.

"The opposite of a correct statement is a false statement. But the opposite of a profound truth may well be another profound truth."

- Niels Bohr

Resumo

Esta tese é dedicada ao estudo da violação da simetria de Lorentz (*Lorentz-symmetry violation* – LSV) e a novas direções fenomenológicas em física de partículas como possíveis caminhos além do Modelo Padrão. Iniciamos com uma revisão do desenvolvimento histórico do tema da LSV, partindo do trabalho seminal de Dirac, em 1951, que lançou as bases dessa linha de pesquisa, e avançando até propostas mais recentes e contemporâneas. Em seguida, apresentamos uma visão geral da Extensão do Modelo Padrão (*Standard-Model Extension* — SME), um arcabouço geral que incorpora todos os possíveis termos de violação da simetria de Lorentz no Modelo Padrão e também discute suas implicações na presença da gravidade. Na sequência, investigamos como a LSV pode afetar o teorema de Furry e gerar correções à eletrodinâmica de Euler–Heisenberg. No contexto de uma extensão supersimétrica, estudamos como uma violação da simetria de Lorentz que quebra a hierarquia entre espaço e tempo no setor fermiônico pode ser transmitida ao setor escalar. Mostramos também que esse cenário supersimétrico induz contribuições ao momento de dipolo elétrico do elétron. A discussão sobre a LSV é concluída com uma análise das consequências fenomenológicas de uma correção à equação de Dirac que viola a simetria de Lorentz advinda da Gravitação Quântica em Laços. Em seguida, mudamos o foco para a física de partículas além do Modelo Padrão e exploramos um modelo teórico baseado em um campo de Kalb–Ramond massivo, descrito por um tensor antissimétrico de posto dois, e seu papel em contextos de interações fracas e eletromagnéticas. Nesse cenário, obtemos limites para o espaço de parâmetros utilizando física atômica, espalhamento de Bhabha e restrições provenientes da imposição do crtério da unitariedade. Por fim, delineamos perspectivas futuras motivadas pelos resultados obtidos nesta tese, bem como de outros cenários interessantes.

Palavras-chave: Física Além do Modelo Padrão, Violação da Simetria de Lorentz, Novas Partículas Leves, Fenomenologia.

Abstract

This thesis is devoted to the study of Lorentz-symmetry violation (LSV) and to new phenomenological directions in particle physics as possible paths beyond the Standard Model. We begin with a review of the historical development of the LSV subject, starting from Dirac's seminal work in 1951, which laid the foundations of this line of research, and moving toward more recent and modern proposals. We then present an overview of the Standard-Model Extension (SME), a general framework that includes all possible Lorentz-violating terms within the Standard Model and also addresses their implications in the presence of gravity. Next, we investigate how LSV can affect Furry's theorem and generate corrections to Euler–Heisenberg electrodynamics. Within a supersymmetric extension, we study how Lorentz violation that breaks the hierarchy between space and time in the fermionic sector can be transmitted to the scalar sector. We also show that this supersymmetric scenario induces contributions to the electron electric dipole moment. The discussion of LSV concludes with an analysis of the phenomenological consequences of a Lorentz-violating correction to the Dirac equation inspired by Loop Quantum Gravity. We then shift our focus to particle physics beyond the Standard Model and explore a framework based on a massive Kalb–Ramond field, described by a rank-2 antisymmetric tensor, and its role in weak and electromagnetic interactions contexts. In this setting, we derive bounds on the parameter space using atomic physics, Bhabha scattering, and unitarity constraints. Finally, we outline future directions motivated by the results obtained in this thesis, as well as other interesting scenarios.

Keywords: Beyond Standard Model Physics, Lorenz-Symmetry Violation, New Light Particles, Phenomenology.

Thesis-related publications

The content of this thesis is based on the following publications:

[1] J.P.S. Melo, J.A. Helayël-Neto, *From the Aether questioned by Dirac to the Standard Model: the diachrony of Lorentz-symmetry violation*, Rev. Bras. Ens. Fís. **45**, e20220211 (2023).

[2] J.P.S. Melo, J.A. Helayël-Neto, *Re-assessing special aspects of Dirac fermions in presence of Lorentz-symmetry violation*, Annals Phys. **470**, 169790 (2024).

[3] J.P.S. Melo, M.J. Neves, J.M.A. Paixão, J.A. Helayël-Neto, *Loop quantum gravity effects on electromagnetic properties of charged leptons*, Eur. Phys. J. C **84**, 938 (2024).

[4] J.P.S. Melo, W. Cesar e Silva, J.A. Helayël-Neto, *SUSY QED with Lorentz-Asymmetric Fermionic Matter and a Glance at the Electron's EDM*, Fortsch. Phys. **73**, 2400203 (2025).

[5] P.C. Malta, J.P.S. Melo, C.A.D. Zarro, *Experimental signatures of Kalb-Ramond-like particles*, JHEP **05**, 093 (2025).

[6] J.P.S. Melo, M. Reetz, L.P.R. Ospedal, J.A. Helayël-Neto, *From interacting fields to interparticle potentials: a pedagogical approach*, Rev. Bras. Ens. Fís. **48**, e20250466 (2026).

[7] W. Cesar e Silva, J.P.S. Melo, J.A. Helayël-Neto, *Extending the Euler-Heisenberg action to include effects of local Lorentz-symmetry violating backgrounds*, arXiv:2603.20880 [**Accepted for publication in Physical Review D**].

Contents

Chapter

1

Introduction and contextualization

The Standard Model (SM) of particle physics provides a remarkably successful framework for describing the fundamental constituents of matter and their interactions. Based on the principles of quantum field theory and local gauge invariance, it unifies the electromagnetic, weak, and strong interactions within a single, consistent theoretical structure. Over the past decades, its predictions have been confirmed with high precision in a wide range of experiments, from collider physics to precision tests at low energies. Despite this success, the SM is widely regarded as an effective theory, as it does not incorporate gravity and leaves several fundamental questions unanswered, such as the origin of neutrino masses, the nature of dark matter, and the hierarchy of energy scales. These open issues motivate the exploration of extensions of the SM that may reveal new physics beyond its established domain of validity and this perspective will guide the present thesis.

The SM of particle physics and fundamental interactions (strong and unified electroweak interactions) assumes the validity of special relativity and does not include a gravitational sector. The interactions between fields are renormalizable in four spacetime dimensions, free of anomalies, and respect unitarity. Another premise of the SM is that the matter content is exclusively fermionic in nature (since the Higgs can be viewed as an interacting boson that gives mass to particles) and neutrinos are always massless and do not oscillate. Moreover, initially, the action of the model consists of massless fields invariant under the gauge symmetry $SU(3)_{\mathrm{C}} \times SU(2)_{\mathrm{L}} \times U(1)_{\mathrm{R}}$, where $SU(3)_{\mathrm{C}}$ is the internal symmetry group associated with the fields that have the two quantum numbers related to the color charges present in quarks and gluons sector. On the other hand, $SU(2)_{\mathrm{L}}$ is associated with weak isospin acting on a doublet of left-chiral fermions, and $U(1)_{\mathrm{R}}$ is associated with weak hypercharge acting on a singlet of right-chiral fermions. However, an additional field — the Higgs field, which is also located in a doublet of $SU(2)_{\mathrm{L}}$ — is introduced. This field is responsible for a mechanism of spontaneous symmetry breaking in an energy scale of ~ 246 GeV, where $SU(3)_{\mathrm{C}} \times SU(2)_{\mathrm{L}} \times U(1)_{\mathrm{R}} \to SU(3)_{\mathrm{C}} \times U(1)_{\mathrm{EM}}$, with $U(1)_{\mathrm{EM}}$ being the internal symmetry group of Quantum Electrodynamics (QED). This group emerges as a combination of $U(1)_{\mathrm{R}}$ and a $U(1)$ factor present in $SU(2)_{\mathrm{L}}$, giving rise to the electric charge. The Higgs field is also responsible for giving mass to charged leptons and quarks via Yukawa couplings. For a review see [1, 2].

The SM is described by a set of nineteen physical parameters, which is a very large

number if we are aiming for a fundamental theory. A fundamental theory should have few postulates and a small set of parameters, yet be capable of accurately describing the current phenomenology and predicting a wide range of new results. This strongly suggests that the SM is an effective theory, originating from a more fundamental microscopic theory with fewer parameters. These nineteen parameters are as follows: the three coupling constants associated with each of the symmetry groups, g_s for $SU(3)_{\mathrm{C}}$, g for $SU(2)_{\mathrm{L}}$, and g' for $U(1)_{\mathrm{R}}$. There is also the Weinberg angle, θ_W, which describes the mixing between the gauge fields associated with the $SU(2)_L$ and $U(1)_R$ groups and determines the relations between the electroweak coupling constants and fixes the relative strengths of the weak and electromagnetic interactions. With the spontaneous symmetry breaking via the Higgs mechanism, the electric charge e becomes a function of g, g', and θ_W which are more fundamental. We also have two parameters associated with the Higgs potential: its mass, m_{H}^2, and its self-coupling constant, λ. Additionally, there are three Yukawa coupling constants, y_e, y_μ, and y_τ associated with the charged leptons, and six more associated with the quarks: y_u, y_d, y_t, y_b, y_c, and y_s. Furthermore, there are three mixing angles and one phase from the Cabibbo-Kobayashi-Maskawa(CKM)-matrix, which describes the probabilities of the quarks d, s, and b mix in weak interactions, influencing the transitions between them and thus affecting their effective masses [3]. Last but not least, we have the θ parameter that arises in the gauge sector of Quantum Chromo Dynamics (QCD) as a topological term proportional that is a total derivative at the classical level, but it becomes physically relevant due to the existence of nontrivial gauge-field configurations, known as instantons, which connect inequivalent QCD vacua with different topological winding numbers. As a consequence, the θ term induces CP violation in the strong interactions, leading to observable effects such as a nonvanishing neutron electric dipole moment [4]. As a result, we see that fifteen of these parameters (m_{H}^2, λ, the Yukawa couplings, and CKM matrix parameters) are related to the Higgs sector with m_{H}^2 being the only one that has a dimension, what indicates that the Higgs sector is the least understood in the SM.

Despite its tremendous success in predicting new particles and fitting very well with many of the existing experimental data, there are issues that challenge the SM. For example, since the beginning, the SM does not introduce a mass for neutrinos. However, neutrino oscillations, which were observed in experiments such as solar and atmospheric neutrino experiments, indicate that neutrinos have mass [5]. To describe neutrino oscillations, it is necessary to introduce a matrix analogous to the CKM-matrix for neutrino mixing. This is the so-called PMNS-matrix, proposed by Pontecorvo, Maki, Nakagawa, and Sakata, which connects the flavor states, which are the types of neutrinos that interact with leptons, and the mass states, which are the states in which neutrinos actually exist with defined masses [7]. Since neutrinos have mass, the remaining question is whether they are Dirac or Majorana fermions, which adds 7 additional parameters to the SM if the neutrino is a Dirac fermion (3 masses, 3 mixing angles, and 1 phase), or 9 additional parameters if it is a Majorana fermion (3 masses, 3 mixing angles, and 3 phases) [7]. If neutrinos are Dirac fermions, they

have distinct antiparticles and lepton number is conserved. On the other hand, if they are Majorana particles, neutrinos and antineutrinos are the same physical entity, which implies lepton-number violation and allows natural mechanisms to generate small masses, such as the seesaw mechanism, as well as rare processes like neutrinoless double beta decay. For more details, see [8].

The naturalness criterion and the hierarchy problem are also technicalities that can challenge the SM. Naturalness reflects the idea that the fundamental parameters of the theory should not require extremely precise tuning for the results to be consistent with experimental observations [9, 10]. A central example of the application of the naturalness criterion is the hierarchy problem that involves the mass of the Higgs boson. In the SM, the Higgs mass receives radiative corrections that depend on the energy scales of new physics. These corrections can be extremely large, reaching the Planck scale (10^{19} GeV, see Figure 1), but, experimentally, they absurdly exceed the physical mass of the Higgs and the natural scale of weak interactions (10^{2} GeV, see Figure 1). In the SM, an extremely fine-tuned adjustment would be necessary between the terms of the Higgs mass and its radiative corrections, which violates the naturalness criterion [9, 10]. Some proposed solutions to the hierarchy problem are based on supersymmetry, by introducing supersymmetric partners to cancel the large radiative corrections, keeping the Higgs mass natural [11]. Also in theories of extra dimensions, proposing the hierarchy as a geometric effect related to the propagation of the Higgs in additional dimensions. There are also proposals for additional symmetries that stabilize the Higgs mass, avoiding fine-tuning [12].

The naturalness criterion is also applied to other issues in the SM, such as, for example, the problem of the neutron's electric dipole moment. This is associated with the violation of charge conjugation (C) followed by a parity transformation (P) is allowed in QCD due to the presence of the aforementioned θ-parameter of the QCD vacuum, which brings a electric dipole moment form factor possibility for the neutron [9]. However, the problem arises from the fact that experiments place an upper bound on the neutron EDM that is much smaller than the theoretical expectation, which would be of order $d_n \sim 10^{-16}\,\theta\, e\cdot\text{cm}$ [13, 14]. The current experimental limit on the neutron EDM is $d_n < 1.8 \times 10^{-26}, e\cdot\text{cm}$ [15]. To reproduce this result, the parameter θ must have an upper bound of order $\theta \lesssim 10^{-10}$. This fact is unexpected because, from a theoretical perspective, there is no fundamental reason for θ to be so small, and there is no explanation within the SM for why θ should essentially be zero. One of the main proposals to solve this problem is the Peccei-Quinn mechanism, in which, through a new global symmetry called the Peccei-Quinn symmetry, the θ-parameter takes the form of a scalar field and is automatically zero in a dynamical solution [16, 17]. This new field is the so-called axion, which would be an extremely light particle responsible for cancelling the CP violation in the strong interactions.

An interesting fact about the hierarchy also relates to the vast difference between the Yukawa coupling constants of the charged leptons and quarks with the Higgs sector. For example, between the electron's coupling constant to the Higgs, y_e, and the top quark's

coupling constant to the Higgs, y_t, there is a discrepancy of 10^6 orders of magnitude [18]. The SM is unable to provide a reasonable explanation for this discrepancy. A detailed analysis of this issue, together with proposals to address it, can be found in Ref. [18]. It is also important to emphasize that, unlike the masses of charged leptons and quarks, in the SM, there is no microscopic description of the origin of the Higgs boson mass, m_{H}^2, which appears in the model's action as a term manually added to ensure everything works properly, see Refs. [19–21] for review and proposals to address this issue.

Another aspect of the Higgs sector involves the question whether the Higgs boson is truly elementary or not. There are technical considerations behind this question that are connected to the concepts of quantum triviality and the Landau pole, which are fundamental ideas imposing limits on the scalar nature of the Higgs boson self-coupling, $\lambda|\Phi|^2$, in the SM [22]. Triviality suggests that, at very high energy scales, the Higgs self-coupling may approach zero, rendering the interaction inactive, while the Landau pole occurs when the effective coupling grows indefinitely, making the theory inconsistent at high energies [22,23]. These phenomena imply that, for the SM to remain valid up to very high energy scales, such as the Planck scale, λ must lie within precise limits to avoid triviality and maintain the stability of the Higgs vacuum. However, these constraints raise questions about the Higgs boson's elementarity as a possible alternative, considering it a composite particle as proposed in theories beyond the SM, such as technicolor [23,24]. Thus, quantum triviality and the Landau pole draw attention to the need to explore physics beyond the SM, reinforcing the idea that it is likely an effective theory.

A possible evidence of violations of SM physics also begins to emerge from the results of the BaBar experiment, a collaboration at the Stanford Linear Accelerator Center (SLAC), designed to study phenomena involving B mesons and their antiparticles. In certain channels, the decay rates of the $\bar{B}$ meson are more abundant than those predicted by the SM. This raises the possibility that such decays may involve channels not accounted for in the SM, hinting at the existence of a particle spectrum beyond the SM [25,26]. An additional aspect that could challenge the SM is related to the upper limit of the electron's electric dipole moment, d_e. The most recent upper limit estimates a value of $d_e < 4.1 \times 10^{-30}$ e·cm for this observable [27,28], while the most precise SM calculation predicts $d_e = 5.8 \times 10^{-40}$ e·cm [29], resulting in a discrepancy of 10^{10} orders of magnitude compared to the experimental limit.

The gyromagnetic factor, $g_p = 2(1 + a_p)$, of particles p receives corrections due to quantum fluctuations of other fields that interact with the particle's own field, and these corrections can be accounted for by a_p, called the magnetic anomaly. In this sense, investigating the magnetism of the muon through its gyromagnetic factor is important to restrict new physics models beyond the SM, since the ratio of the square of the muon mass to the square of the electron mass is of the order of 4×10^4, indicating that the muon's magnetism is 4×10^4 times more sensitive to effects of massive new physics particles than the electron's magnetism, given that a_p of the particle is proportional to the square of the particle's mass.

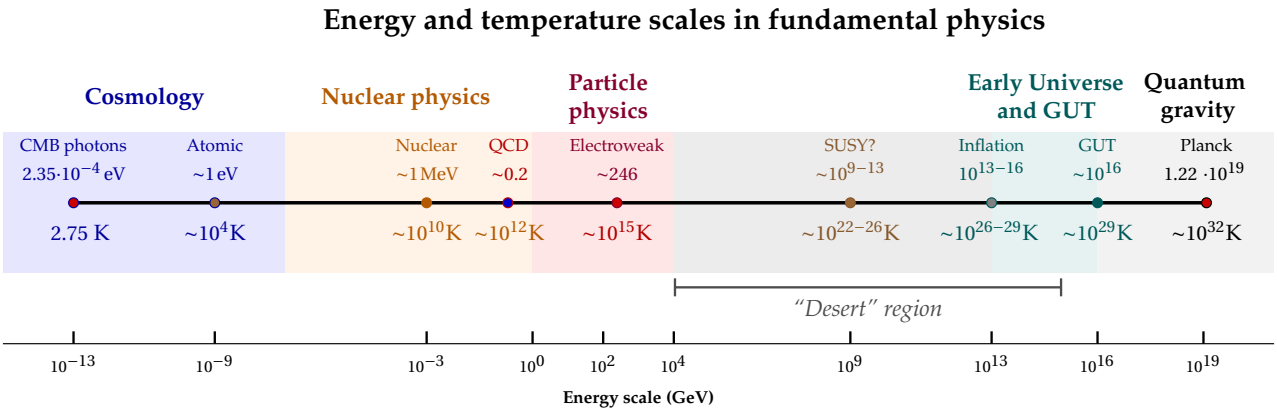

Figure 1 – The energy scales of the Universe increase from left to right. With the exception of the gray regions, where we do not yet have a clear and well-established physical theory, the other regions are associated with well-defined physical descriptions. Up to the electroweak scale, we have strong experimental evidence that supports the corresponding physical framework. At the energy scale of inflation, there are good reasons to believe that we are close to the correct physical description. However, from the scale of grand unification onward, there is still significant uncertainty about the correct path toward a consistent theory of quantum gravity. The entire region usually referred to as the "desert" may hide secrets of new physics, and perhaps even new paradigms that we are not yet able to access.

Recent measurements at the Fermi National Accelerator Laboratory (FNAL) reported the muon magnetic anomaly as $a_\mu(\text{FNAL}) = 116\,592\,040(54) \times 10^{-11}$ with a precision of 0.46 parts per million (ppm) in 2021 [30], and $a_\mu(\text{FNAL}) = 116\,592\,055(24) \times 10^{-11}$ with 0.20 ppm precision in 2023 [31]. These results improved the world average to $a_\mu(\text{exp}) = 116\,592\,061(41) \times 10^{-11}$ (0.35 ppm) and $a_\mu(\text{exp}) = 116\,592\,059(22) \times 10^{-11}$ (0.19 ppm), respectively. The improved 2023 result showed a 5.0σ deviation from the Standard Model (SM) prediction, $a_\mu(\text{theory}) = 116\,591\,810(43) \times 10^{-11}$. At that time, experiment and theory appeared to disagree at the tenth decimal place with 5.0σ significance [31]. Such a result strongly motivated the search for new physics beyond the SM. However, this tension was resolved with new results in 2025. On the experimental side, FNAL updated the world average to $a_\mu(\text{exp}) = 1\,165\,920\,715(145) \times 10^{-12}$ (0.35 ppm) [33]. On the theoretical side, using improved computational techniques and more precise experimental input, the prediction was refined to $a_\mu(\text{theory}) = 116\,592\,033(62) \times 10^{-11}$ [34]. These updated results indicate that there is no significant tension between the SM and experiment at the current level of precision [34]. A future experiment in Japan at the Japan Proton Accelerator Research Complex (J-PARC) will perform new measurements in the early 2030s. The J-PARC muon $g-2$/EDM (E34) collaboration [35] aims to measure both the muon gyromagnetic factor and its electric dipole moment (EDM), with the potential either to reveal new deviations or to further confirm the SM prediction.

An interesting fact about the Universe relates to the question of how it, which seems to be exclusively dominated by baryonic matter, emerged from an initial state where matter and antimatter were present in equal quantities [36]. According to the SM, there is no reason for the creation of a greater amount of matter in favor of antimatter, which should have resulted in mutual annihilation between them, leading to a Universe very different from the one we

know. However, the question that remains is: how did matter prevail over antimatter? This asymmetry in the production of matter over antimatter during the early moments after the Big Bang is an open problem and fundamental to contemporary physics, both in the context of cosmology and particle physics [36]. We can also reflect on the reason why the content of matter in the SM is dominated by fermions and there is no mention of scalar matter [37]. This is more of an aesthetic question, motivated by the viewpoint that the primordial universe tends to be more symmetric, with symmetries broken by phase transition mechanisms as the universe cools and time progresses. However, since the SM does not address the reason for this asymmetry between fermionic matter and scalar matter, this question remains open as an avenue for new Physics [37].

Another very important fact about the SM is that it makes no reference to the origin or the composition of dark matter and dark energy [38]. We know this is a highly significant issue, as the matter and energy density of the universe is given by $\Omega_0 = \Omega_\Lambda + \Omega_{DM} + \Omega_{SM}$, where Ω_{SM} represents the 4.9% of baryonic matter, photons, and neutrinos content of the Universe, while Ω_{DM} is associated with the 26.8% of dark matter, and Ω_Λ is associated with the cosmological constant responsible for the 68.3% of dark energy, according to Particle Data Group [39]. Additionally, gravitational interactions are not considered in the SM from the outset [1, 2].

In summary, the SM is very powerful and, despite several tensions and many theoretical/phenomenological proposals beyond its formalism, it has resisted very well to new observational and experimental tests, such as those from accelerator experiments in 14 TeV at LHC. To better understand this situation, we present the diagram shown in Figure 1, where the energy scale of the Universe increases from left to right, starting in the present era dominated by the temperature of the Cosmic Microwave Background (CMB) radiation. Although there are several open challenges at each of these energy scales, we expect that the correct physics has been identified for all scales from the electroweak scale at 10^2 GeV up to the LHC energy scale at 10^4 GeV, which is very well described by the SM, with no indications of new physics. Beyond this energy scale, there is a region corresponding to an interval with an uncertainty of about $\sim 10^{11}$ GeV regarding which physics should describe it. This region is commonly referred to as the *desert*. Some proposals, which have not yet been experimentally confirmed, such as supersymmetry and inflation, are candidates to fill part of this *desert*. Beyond it, the expectation is that physics is governed by a grand unified theory (GUT), in which the three interactions of the SM are unified into a single one, while gravity still remains separate. Only at the Planck scale is it expected that a possible unification of gravity with the other interactions may occur, as in string theory. There are also arguments that such a unification may not be necessary at this energy scale, and that this regime could instead be governed by the effects of a consistent quantum description of gravity, such as loop quantum gravity.

In this thesis, we adopt the point of view that new physics beyond the SM can be accessed by exploring new perspectives that may help to address some of the tensions

mentioned above and, in some way, fill part of the desert that still lacks a coherent physical description. We begin by highlighting one of the main topics of this thesis, which is based on the observation that the SM is strongly grounded in Lorentz symmetry, as established by Special Relativity. This naturally leads to the following question: is there any evidence for a possible violation of Lorentz symmetry? If the answer is affirmative, based on recent experimental and observational searches, this would require us to consider extensions of the SM capable of accommodating a wide range of phenomena arising from such violations. Another perspective adopted in this thesis is the search for new particle physics beyond the SM through the study of Kalb–Ramond fields. In this context, we explore the possibility that these fields may contribute to the dark matter puzzle, using high-precision experiments to constrain the parameter space of a possible particle emerging from vacuum of this field. For a recent review addressing anomalies that may indicate possible directions toward physics beyond the Standard Model, see Ref. [40].

An important point to highlight, which the reader will notice throughout the text, is that we always try to place our efforts, whenever possible, in a low-energy context related to Condensed Matter Physics. We take the view that this scenario can serve as a laboratory for high-energy physics. That is, because models can be tested at low energies, we can develop new techniques for quantum field theory in this context, improve them, and finally transfer these results to high-energy physics. This justifies our attention to these contexts, which are often left outside the scope of the high-energy physics community.

This thesis is organized as follows: Part I, comprising Chapters 2 to 6, is devoted to the study of Lorentz-symmetry violation. More specifically, In Chapter 2, we review the historical development of the subject, starting from Dirac's seminal work in 1951, which laid the foundations of this line of research, and moving toward more recent and contemporary proposals. In Chapter 3, we present a review of the Standard-Model Extension (SME), a general framework that incorporates all possible Lorentz-violating terms within the Standard Model and also discusses the implications of such violations in the context of gravity. In Chapter 4, we investigate how Lorentz-symmetry violation can affect Furry's theorem and lead to corrections in Euler–Heisenberg electrodynamics. Next, in Chapter 5, we study, within a supersymmetric extension, how Lorentz violation that breaks the hierarchy between space and time in the fermionic sector can be transmitted to the scalar sector. We also show how this supersymmetric scenario induces contributions to the electron electric dipole moment. The discussion of Lorentz symmetry violation concludes in Chapter 6, where we analyze phenomenological consequences of a Lorentz-violating correction to the Dirac equation arising from Loop Quantum Gravity. Part II is dedicated to physics beyond the Standard Model and is presented in Chapter 7. In this chapter, we explore a framework based on a massive Kalb–Ramond field, described by a rank-2 antisymmetric tensor, and its role in weak and electromagnetic interactions contexts. In this setting, we derive bounds on the parameter space using atomic physics, Bhabha scattering, and unitarity constraints. Finally, Part III contains Chapter 8, where we outline future directions motivated by the results obtained in

this thesis, including possible postdoctoral research paths. The thesis also includes a set of Appendices and a list of Bibliographical References that support the main text. Throughout this work, we adopt natural units, with $c = \hbar = \varepsilon_0 = 1$, and the Minkowski metric signature $(+,-,-,-)$. Any additional definitions or conventions will be clearly stated when needed.

Part I

The Lorentz-symmetry violation endeavor

Chapter

2

Is Lorentz-symmetry violation a reasonable possibility?

Lorentz-symmetry, a cornerstone of the SM, has endured for almost a century. Yet, even this deeply-rooted symmetry may reveal subtle deviations, needing to survive rigorous testing through high-precision measurements. In the first instance, one might think of Lorentz-symmetry violation (LSV) as a denial of the Theory of Special Relativity, whose underlying symmetry is described by the proper orthochronous Lorentz group, SO(1,3). However, it is essential to clarify that this is not the case. Just as a uniform external magnetic field established in three-dimensional space breaks down rotational symmetry, characterized by the group $SO(3)$, some anisotropy in space-time corresponds to the violation of $SO(1,3)$ symmetry. The entire investigation within the scope of LSV is motivated by the quest to understand the possible origins of spacetime anisotropies present in the quantum vacuum. These origins could potentially indicate new physics beyond the SM. In fact, in scenarios involving LSV, researchers are also attempting to comprehend the very structure of the quantum vacuum, which exhibits electromagnetic properties such as birefringence or dichroism [41, 42].

The discussion about a possible scenario with LSV was initially addressed by Dirac in his quest of an aether, where the idea of a new QED with the existence of a background vector that would establish a preferred direction was put forward to understand whether this vector could reveal the nature of the ultraviolet divergences in quantum field theory [43]. Consequences of that approach were explored in [44]. After this period, the discussion returns in the 60s with the considerations of a possible composite photon, all within a scenario of spontaneous Lorentz-symmetry (LS) breaking [45]. Shortly after, the possibility of the graviton being a Goldstone boson in the presence of a LSV background vector [46, 47] was discussed, and LSV was also contemplated in the framework of Particle Physics to analyze how it affects the velocity dependence of the muon lifetime [48]. These works were part of the pursuit of understanding possible situations in which LSV could have measurable effects. In the 70s, the context LSV comes into play with the investigation of the beta function of a non-covariant Yang-Mills theory and shows that the fixed point occurs in a regime where LS is restored [49]. In the 80s, in the context of Grand Unification, the discussion of the possibility of proton decay came to light with a possibility that it occurs with slight deviations of LS [50, 51]. The 80s also witnessed the proof of the finiteness of $\mathcal{N} = 4$ Yang-Mills theories

at all orders of perturbative expansion. However, this proof was not manifestly covariant, which initiated a discussion about the extent to which LS could be taken as a fundamental and inviolable symmetry [52–54].

The Dirac's work and the subsequent articles marks the embryonic discussions that gained consistency with the Superstrings, and culminated in the current discussions on LSV. After the so-called first String Revolution, the seminal work by V. A. Kostelecký and S. Samuel came out and the authors showed, within the context of open strings, that there are tensor fields that may acquire nontrivial vacuum expectation values, condensing in the vacuum and breaking LS [55]. This work serves as the starting point for the next phase of LSV investigation, which is more inspired by String Theory (ST) and effective models that attempt to discuss new physical scenarios beyond the SM. They also established a number of phenomenological constraints on LSV physics [56]. Subsequently, S. M. Carroll, G. B. Field, and R. Jackiw (CFJ) explored limits on LSV via a $(1+3)$D version of the Chern-Simons topological model in $(1+2)$D [57]. In the CFJ model, there is a background vector field that establishes a spacetime anisotropy altering the Maxwell's equations, and they make use of astrophysical data to estimate the scale of its components. Some important considerations from the modified dispersion relation of the model arise, such as the effect of birefringence, and two aspects ought to be investigated, namely, the potential violation of causality and the stability property of the vacuum. We refer the reader to the works [58,59], where these issues are explored in detail.

The so-called Standard-Model Extension (SME) comes into play through works by D. Colladay, V. A. Kostelecký and others [60–62]. The SME incorporates all the characteristics of the usual SM (i.e., the same local symmetries $SU(3)\times SU(2)\times U(1)$, being free from higher-order derivatives, and renormalizable) along with General Relativity but considers the possibility of violating Lorentz- and CPT-symmetry [62]. In a sense, LS remains valid, as the theory behaves normally under rotations or boosts, considering that the so-called passive Lorentz transformations of the observer are performed in the laboratory frame. In the SME context, LSV only appears when the fields are rotated or altered with respect to the expected tensor values describing the vacuum state, known as active Lorentz transformations of particles [61,62]. Among the various contemporary approaches to investigate LSV, the SME is the most widely used theoretical framework to study phenomenology from multiple perspectives. The SME incorporates the CFJ model and opens new avenues of exploration to demonstrate that there are situations where LSV effects can manifest at energy scales accessible in particle accelerators and through current or upcoming astrophysical and cosmological observations. In the next chapter, we present a brief review of the main aspects of the SME.

Soon afterwards, discussions related to LSV tests based on Modified Dispersion Relations (MDRs) for photons came to light [63–66], which can contribute, using high-energy photons accessed in astrophysical measurements, in the analysis of possible deviations compared to standard dispersion relations indicating the presence of LSV or some effects of quantum gravity. Additionally, in the context of MDRs, an important work by R. Gambini and J.

Pullin came out, which did not rely on ST or the usual quantum gravity formalism, such as first-order formalism or semiclassical approach. Instead, it was based on the Loop Quantum Gravity (LQG) framework. They obtained modified Maxwell equations and demonstrated vacuum birefringence [67]. Two other important works regarding MDRs, characterizing dispersion relations that could indicate the existence of LSV, are [68, 69].

In 1999, N. Seiberg and E. Witten introduced the Non-Commutative Field Theories, which exhibit LS breaking, and it can be seen as a low-energy limit of ST [70]. This approach to investigating LSV can be found in the literature and a very seminal work in this regard is [71]. Also S. Coleman and S. L. Glashow introduced, from first principles, the hypothesis that there could be LSV at extremely high energies, near the Planck scale $\sim 10^{19}$ GeV [72]. Later, came another approach to LSV, known as Doubly-Special Relativity (DSR), which involves a theory of double relativity, in the sense that there are two invariants: the speed of light and an energy scale, equivalent to a minimum length associated with the Planck scale [73, 74]. Then, there is a direct LSV in the algebra of the Poincaré group due to the presence of this minimum invariant length scale. This modification of the Poincaré group algebra is achieved through a mathematical procedure called Wigner-Inönü contraction. Starting from an Anti-de Sitter group, a Wigner-Inönü contraction is performed, resulting in the so-called κ-Poincaré algebra. This new algebra is a deformation of the usual Poincaré algebra, characterized by a length scale that modifies the well-known LS [75].

With all this background provided, it could be stated that LSV investigation implies that LS is an indispensable fact of nature at the scales we live but the question of to what extent can we uphold this symmetry is an open issue. We have good reasons to believe that it should break at extremely short distance scales, this is at ultra-high energies. Therefore, in low energies, we do not expect to observe a complete LSV, but rather its manifestations through very subtle effects, as they can be suppressed by some power of the Planck scale. Experimental and observational searches for these subtle effects have yielded good limits on the parameters that govern LSV. The most recent results are published annually in the so-called "*Data Tables for Lorentz and CPT Violation*" [76]. Another interesting work provides a general review of LSV phenomenology and gives indications on what data to search for to establish limits on LSV [77]. These searches generally focus on evaluating phenomenologies related to the motion of objects in an anisotropic background [78, 79], atomic clocks in space [80–82], vacuum birefringence of light [83–86], spin precession effects [87–89], atomic energy level shifts and spectroscopy [90, 91], neutrino physics [92–99], modified dispersion relations for high-energy photons and observations of gamma-ray bursts [63, 85, 100–107], among others [108–113], establishing constraints on the parameters which characterize them.

The topic of LSV is a pursuit of new physics that goes beyond the SM, with the hope of shedding light on various questions such as: indicating a path towards quantum gravity (ST, LQG, etc.); addressing the hierarchy problem in gauge theories; understanding the origin of the Higgs boson mass; explaining the asymmetry between matter and antimatter in the universe; resolving the neutron electric dipole moment problem; dark matter; investigating

neutrino oscillations and their masses; among others. In this regard, recent works marks the intersection between LSV and Condensed Matter Physics (CMP), opening a very promising line of investigation in establishing a connection between the field and Dirac and Weyl semi-metals, offering the prospect of new laboratory experiments with materials that could provide new regions of validity and new limits on the parameters associated with LSV [114–116]. This new direction in the field is highly auspicious since it will create another channel of communication between the High Energy Theory/Phenomenology and the CMP communities.

Chapter

3

The Standard Model Extension framework

Among the different approaches to study LSV, the Standard-Model Extension (SME) is a systematic framework to describe possible deviations from exact Lorentz- and CPT-symmetry. The SME was developed as an effective field theory and adds extra terms to the SM and to General Relativity to represent possible Lorentz- and CPT-violating effects. These extra terms can naturally appear in several theoretical scenarios and may produce observable effects in high-precision experiments, such as those discussed in Chapter 2. As an effective field theory, the SME focuses on low-energy effects of new physics while remaining consistent with the basic principles of quantum field theory [62].

More specifically, Lorentz symmetry violation is expected to appear as very small physcial effects of spontaneous spacetime symmetry breaking at extremely high energies, where a more fundamental theory including quantum gravity effects is expected to apply. The typical energy scale of a fundamental theory with gravity is given by the Planck mass, $M_P \sim 10^{19}$GeV, which is about seventeen orders of magnitude larger than the electroweak scale of the Standard Model, $m_W \sim 10^2$GeV (see Figure 1). This large separation of scales means that any observable effects from such a fundamental theory are expected to be very strongly suppressed. In general, they scale with some power of the ratio $m_W/M_P \simeq 10^{-17}$. As a result, observing these very small effects at accessible energies requires experiments with extremely high precision.

Special relativity implies invariance under Lorentz transformations. In this sense, to implement possible effects of LSV, there are two main possibilities. The first is to modify or deform the usual Lorentz transformations, as in the case of DSR mentioned in Chapter 2. This approach can have disadvantages, since Lorentz transformations, as usually taught, are observer transformations. Modifying them may cause the physics to depend on the choice of observer coordinates or, in order to avoid this problem, require additional assumptions to preserve the invariance of equations that originally assume Lorentz invariance. Moreover, such modifications may depend on the particle species, leading to awkward situations in which different fields require different modified observer Lorentz transformations. In contrast, the SME adopts a second point of view to implement possible effects of LSV, which aims to preserve invariance under all observer transformations, while allowing Lorentz violation to appear only in particle transformations.

Additionally, when discussing LSV in the SME context, it is important to emphasize

that the CPT theorem states that CPT symmetry (this is charge conjugation (C), parity transformation (P), and time reversal (T)) emerges under certain assumptions, combining Lorentz symmetry with quantum-mechanical principles. Therefore, if CPT symmetry is violated, at least one of the assumptions required to prove the CPT theorem must be invalid. Since both Lorentz invariance and CPT invariance involve spacetime transformations, it is natural to suspect that CPT violation implies Lorentz symmetry breaking. This relationship was rigorously proven in [117–119].

In the following sections, we present a brief review of the main aspects of the SME in curved space time, Minkowski spacetime and some of its challenges. Here we give only a few brief comments on the SME. Further details can be found in the references listed in Chapter 2.

3.1 The SME full action

To describe LSV, a general framework was developed to study tiny physical correction effects in well established theoretical and experimental scenarios, including classical and quantum aspects of mechanics, gravitation, and field theory. To understand this framework, we begin by presenting the full SME action in a Riemann-Cartan spacetime is given by (see [62] for more details)

$$S_{\text{SME}} = S_{\text{SM}} + S_{\text{LSV}} + S_{\text{GR}} + \cdots , \tag{3.1}$$

where S_{SM} represents the SM action written in a Riemann-Cartan spacetime and including its couplings to gravity. The term S_{LSV} groups all contributions that violate Lorentz- and CPT-symmetries with minimal gravitational couplings. Finally, S_{GR} refers to the gravitational sector, constructed from the vierbein and spin connection, and also extended to include possible Lorentz- and CPT-violating effects. The ellipses indicates the possibility of adding higher-order LSV terms (nonminimal) at low energies. Such terms lead to nonrenormalizable contributions in the flat-spacetime limit, higher-order gravitational coupling terms, and operators of dimension greater than four that produce couplings between curvature and torsion and the Standard Model fields [62]. There is also the possibility of nonminimal terms that break the gauge invariance of the SM [120].

The Ref. [62] establishes that the action of a theory with local Lorentz violation and gravity must be formulated in the vierbein formalism in order to accommodate spinor fields and allow for nonvanishing curvature and torsion, while at the same time preserving diffeomorphism invariance. In this formalism, the vierbein (or tetrad) $e_\mu{}^a(x)$ defines an orthonormal basis in the local tangent space at each spacetime point and acts as the fundamental gravitational field in the first-order formalism. Its determinant, denoted by $e \equiv \det(e_\mu{}^a)$, provides the invariant volume element $e\,d^4x$ and satisfies $e = \sqrt{-g}$, where g is determinant of spacetime metric $g_{\mu\nu}(x)$. The vierbein establishes a map between curved spacetime indices and local Lorentz indices, allowing the spacetime metric to be written as $g_{\mu\nu} = e_\mu{}^a e_\nu{}^b \eta_{ab}$, with $\eta_{ab} = \text{diag}(-1,+1,+1,+1)$. It is assumed that the spacetime covariant derivative satisfies the metricity condition, $\mathscr{D}_\lambda g_{\mu\nu} =$

$0 = \mathscr{D}_\lambda e_\mu{}^a$. This formulation allows the spin connection ($\omega_\mu{}^{ab}$) to be treated as an independent field and provides a natural framework for coupling gravity to spinor fields [1].

Although Lorentz-symmetry may be broken at the level of particle transformations (spacetime transformations acting on the fields), the action must remain covariant under observer Lorentz transformations (changes of reference frames) and diffeomorphism (smooth change of spacetime coordinates that does not change the physics). This requires the Lorentz-violating coefficients to be tensorial objects with local Lorentz indices, transforming covariantly under changes of reference frame, while behaving as fixed quantities (scalars) under particle transformations. These coefficients appear in the action contracted with operators constructed from the vierbein, the spin connection, and the matter fields, ensuring coordinate independence.

Additionally, in this curved spacetime formalism, the LSV coefficients are required to depend locally on the spacetime coordinates, in contast to the position adopted in flat spacetime. The consequences of adopting a spacetime-dependent LSV background were analyzed in [62]. In that work, Kostelecký points out that assuming constant LSV coefficients greatly simplifies the physical analysis, particularly with respect to the conservation of energy and momentum. He offers several motivations for this assumption: i) high-energy effects are typically associated with coefficients displaying nontrivial spacetime dependence, which suggests that constant coefficients are more suitable for low-energy effective descriptions; ii) if Lorentz violation originates at the Planck scale and an inflationary epoch took place in the early universe, it is plausible that present-day configurations exhibit approximately constant values over cosmological scales; and iii) for sufficiently slow variations, constant coefficients may be viewed as the leading term in a series expansion. In spite of that, it is important to emphasize that all such considerations rely on specific physical assumptions. From a formal perspective, in [62] is argued that any vector or tensor field with smooth integral curves can serve as a valid background configuration. Therefore, treating the LSV coefficients as constant should be regarded as a theoretical choice rather than a fundamental requirement.

Kostelecký also pointed out that assuming constant LSV terms in a Riemann–Cartan spacetime leads to integrability conditions that are globally satisfied only for specific geometries, such as parallelizable manifolds. These manifolds, characterized by vanishing curvature, are quite rare in four or more dimensions and are generally not of interest in gravitational theories [62]. Given this, it is reasonable to consider LSV backgrounds with spacetime-dependent coefficients, at least locally. However, adopting such a premise introduces significant consequences for the conservation laws of the canonical energy-momentum tensor. In particular, the canonical energy-momentum tensor associated with LSV theories is conserved only under the assumption of constant background coefficients; only in this case is translation invariance preserved [122]. Therefore, in principle, subtle deviations from energy-momentum conservation could signal a possible violation of Lorentz symmetry.

[1] For more details about the vierbein formalism, which is essential for coupling fermions to the gravitational field, see Ref. [121]. The Ref.[121] already presents this formalism in scenarios with LSV.

Adopting the notation of [62], in the fermionic sector the color index on the quarks is suppressed for simplicity and the generation index is $A = 1,2,3$ so that the charged leptons are denoted by $\ell_A = (e,\mu,\tau)$, the neutrinos by $\nu_A = (\nu_e,\nu_\mu,\nu_\tau)$, and the quarks by $u_A = (u,c,t)$ and $d_A = (d,s,b)$. The left- and right-handed chiral projections of a spinor ψ are $\psi_{\rm L} = \frac{1}{2}(1-\gamma_5)\psi$ and $\psi_{\rm R} = \frac{1}{2}(1+\gamma_5)\psi$, respectively. The right-handed leptons ($R_A = (\ell_A)_{\rm R}$) and quarks ($U_A = (u_A)_{\rm R}$ and $D_A = (d_A)_{\rm R}$) are $U(1)_{\rm Y}$ singlets. The left-handed leptons and quarks form $SU(2)_{\rm I}$ doublets such as $L_A = \big((\nu_A)_{\rm L},(\ell_A)_{\rm L}\big)^T$ and $Q_A = \big((u_A)_{\rm L},(d_A)_{\rm L}\big)^T$. In the bosonic sector, the gluons are denoted by Hermitian fields G_μ in the adjoint representations of $SU(3)_{\rm C}$, the Hermitian fields W_μ and B_μ are associated with the the adjoint representations of $SU(2)_{\rm I}$ and hypercharge $U(1)_{\rm Y}$ sectors, respectively. The field strengths are $G_{\mu\nu}$, $W_{\mu\nu}$, and $B_{\mu\nu}$, also respectively. The Higgs field ϕ is a $SU(2)_{\rm I}$ doublet which assumes the form $\phi = \frac{1}{\sqrt{2}}(0,v)^T$ in the unitary gauge, with v being the Higgs field vacuum expectation value. Given these definitions, according to [62] the Lagrangian densities that make up $S_{\rm SM}$ are $\mathscr{L}_{\rm SM} = \mathscr{L}_{\rm lepton} + \mathscr{L}_{\rm quark} + \mathscr{L}_{\rm Yukawa} + \mathscr{L}_{\rm Higgs} + \mathscr{L}_{\rm gauge}$.

Starting with the lepton sector we have

$$\mathscr{L}_{\rm lepton} = \frac{i}{2}ee^\mu{}_a\bar{L}_A\gamma^a\vec{\mathscr{D}}_\mu L_A + \frac{i}{2}ee^\mu{}_a\bar{R}_A\gamma^a\vec{\mathscr{D}}_\mu R_A. \tag{3.2}$$

The quark sector is given by

$$\mathscr{L}_{\rm quark} = \frac{i}{2}ee^\mu{}_a\bar{Q}_A\gamma^a\vec{\mathscr{D}}_\mu Q_A + \frac{i}{2}ee^\mu{}_a\bar{U}_A\gamma^a\vec{\mathscr{D}}_\mu U_A + \frac{i}{2}ee^\mu{}_a\bar{D}_A\gamma^a\vec{\mathscr{D}}_\mu D_A. \tag{3.3}$$

In the Eqs. (3.2) and (3.3) is adopted the definition $\bar{\chi}\Gamma^a\vec{\mathscr{D}}_\mu\psi \equiv \bar{\chi}\Gamma^a\mathscr{D}_\mu\psi - (\bar{\chi}\bar{\mathscr{D}}_\mu)\Gamma^a\psi$ with the covariant derivative $\mathscr{D}_\mu$ (and its complex conjugate $\bar{\mathscr{D}}_\mu$) containing both spacetime and $SU(3)_C \times SU(2)_I \times U(1)_Y$ sectors. Explicitly we have

$$\mathscr{D}_\mu\psi = \frac{i}{4}\omega_{\mu\,ab}\sigma^{ab}\psi + D_\mu\psi, \tag{3.4}$$

$$(\bar{\chi}\bar{\mathscr{D}}_\mu) = -\frac{i}{4}\omega_{\mu\,ab}\bar{\chi}\sigma^{ab} + (D^\dagger_\mu\bar{\chi}), \tag{3.5}$$

where D_μ is the usual Yang-Mills SM covariant derivative [1,2] and $\sigma^{ab} = \frac{i}{2}[\gamma^a,\gamma^b]$.

The next sector presented in [62] is that responsible for the Yukawa couplings,

$$\mathscr{L}_{\rm Yukawa} = -\Big[\big(Y_L\big)_{AB}e\bar{L}_A\phi R_B + \big(Y_U\big)_{AB}e\bar{Q}_A\phi U_B + \big(Y_D\big)_{AB}e\bar{Q}_A\phi D_B\Big] + \text{H.c}, \tag{3.6}$$

where $\big(Y_L\big)_{AB}$, $\big(Y_U\big)_{AB}$, and $\big(Y_D\big)_{AB}$ are the Yukawa-coupling matrices. Following this, the Higgs sector is presented in the form

$$\mathscr{L}_{\rm Higgs} = -e\big(\mathscr{D}_\mu\phi\big)^\dagger\mathscr{D}^\mu\phi + \mu^2e\phi^\dagger\phi - \frac{\lambda}{4!}e\big(\phi^\dagger\phi\big)^2. \tag{3.7}$$

Finally, the gauge sector is (in the absence of θ terms)

$$\mathscr{L}_{\rm gauge} = -\frac{1}{2}\,\text{Tr}\,(G_{\mu\nu}G^{\mu\nu}) - \frac{1}{2}\,\text{Tr}\,(W_{\mu\nu}W^{\mu\nu}) - \frac{1}{4}eB_{\mu\nu}B^{\mu\nu}. \tag{3.8}$$

The next sectors in the SME are those which introduces LSV from the SM fields and have mass dimension four or less (the minimal sector). These LSV corrections are constructed by combining coefficients for Lorentz violation with SM field to produce a quantity that is both local observer Lorentz invariant and general observer coordinate invariant and can be divided in two classes: one regarding to the CPT-even corrections and other regarding to the CPT-odd corrections. This is,

$$\begin{aligned}\mathscr{L}_{\text{LSV}} = \mathscr{L}^{\text{CPT}+}_{\text{lepton}} + \mathscr{L}^{\text{CPT}-}_{\text{lepton}} + \mathscr{L}^{\text{CPT}+}_{\text{quark}} + \mathscr{L}^{\text{CPT}-}_{\text{quark}} + \mathscr{L}^{\text{CPT}+}_{\text{Yukawa}} \\ + \mathscr{L}^{\text{CPT}-}_{\text{Yukawa}} + \mathscr{L}^{\text{CPT}+}_{\text{Higgs}} + \mathscr{L}^{\text{CPT}-}_{\text{Higgs}} + \mathscr{L}^{\text{CPT}+}_{\text{gauge}} + \mathscr{L}^{\text{CPT}-}_{\text{gauge}}.\end{aligned} \tag{3.9}$$

Following this perspective, the Ref. [62] presents the Lagrangian for the CPT-even lepton and quark sectors in the form

$$\begin{aligned}\mathscr{L}^{\text{CPT}+}_{\text{lepton}} + \mathscr{L}^{\text{CPT}+}_{\text{quark}} = &-\frac{i}{2}(C_L)_{\mu\nu AB} e e^{\mu}{}_a \bar{L}_A \gamma^a \vec{\mathscr{D}}^{\nu} L_B - \frac{i}{2}(C_R)_{\mu\nu AB} e e^{\mu}{}_a \bar{R}_A \gamma^a \vec{\mathscr{D}}^{\nu} R_B \\ &-\frac{i}{2}(C_Q)_{\mu\nu AB} e e^{\mu}{}_a \bar{Q}_A \gamma^a \vec{\mathscr{D}}^{\nu} Q_B - \frac{i}{2}(C_U)_{\mu\nu AB} e e^{\mu}{}_a \bar{U}_A \gamma^a \vec{\mathscr{D}}^{\nu} U_B \\ &-\frac{i}{2}(C_D)_{\mu\nu AB} e e^{\mu}{}_a \bar{D}_A \gamma^a \vec{\mathscr{D}}^{\nu} D_B.\end{aligned} \tag{3.10}$$

In (3.10) the coefficients $(C_I)_{\mu\nu AB}$ (with $I = L, R, Q, U, D$) are dimensionless and can be taken to be Hermitian in generation space. The coefficients, and those what follows, are defined considering a Minkowski-spacetime background containing weak gravitational field what enable us to write the metric as $g_{\mu\nu} = \eta_{\mu\nu} + h_{\mu\nu}$ with the metric fluctuation $h_{\mu\nu}$ being symmetric. This consideration lead us to write [62]

$$\begin{aligned} e_{\mu a} &\approx \eta_{\mu a} + \frac{1}{2} h_{\mu a} + \chi_{\mu\nu}, \\ e &\approx 1 + \frac{1}{2} h, \\ \omega_{\mu ab} &\approx -\frac{1}{2}\partial_a h_{\mu b} + \frac{1}{2}\partial_b h_{\mu a} + \partial_\mu \chi_{ab} + K_{a\mu b},\end{aligned} \tag{3.11}$$

where $\chi_{\mu\nu}$ is the antisymmetric part of the vierbein fluctuation and $K_{a\mu b}$ is the contorsion tensor. When considering this regime, and extracting from the Lagrangian only the terms that are linear in small quantities (see Ref. [62] for more details), one finds that $(C_I)_{\mu\nu AB}$ takes the form $(C_{I\text{eff}})_{\mu\nu} = c_{I\mu\nu} - \frac{1}{2} h_{\mu\nu} + \chi_{\mu\nu}$, where, for brevity, the generator indices have been omitted.

The CPT-odd sector for leptons and quarks are given by

$$\begin{aligned}\mathscr{L}^{\text{CPT}-}_{\text{lepton}} + \mathscr{L}^{\text{CPT}-}_{\text{quark}} = &-(a_L)_{\mu AB} e e^{\mu}{}_a \bar{L}_A \gamma^a L_B - (a_R)_{\mu AB} e e^{\mu}{}_a \bar{R}_A \gamma^a R_B \\ &-(a_Q)_{\mu AB} e e^{\mu}{}_a \bar{Q}_A \gamma^a Q_B - (a_U)_{\mu AB} e e^{\mu}{}_a \bar{U}_A \gamma^a U_B \\ &-(a_D)_{\mu AB} e e^{\mu}{}_a \bar{D}_A \gamma^a D_B,\end{aligned} \tag{3.12}$$

where the $(a_I)_{\mu AB}$ coefficients have mass dimension one and were obtained adopting the aforementioned weak-field form of the vierbein and spin connection.

There is a possibility for a CPT-even Yukawa sector given by

$$\mathscr{L}^{\text{CPT}+}_{\text{Yukawa}} = -\frac{1}{2}\Big[\left(H_L\right)_{\mu\nu AB} e e^{\mu}{}_a e^{\mu}{}_b \bar{L}_A \phi \sigma^{ab} R_B + \left(H_U\right)_{\mu\nu AB} e e^{\mu}{}_a e^{\mu}{}_b \bar{Q}_A \phi \sigma^{ab} U_B + \left(H_D\right)_{\mu\nu AB} e e^{\mu}{}_a e^{\mu}{}_b \bar{Q}_A \phi \sigma^{ab} D_B\Big] + \text{H.c.} \tag{3.13}$$

The $\left(H_I\right)_{\mu\nu AB}$ coefficients are antisymmetric in spacetime indices, dimensionless, and are not Hermitian in the generation space.

There is also a CPT-even sector for the Higgs field which can be expressed as

$$\mathscr{L}^{\text{CPT}+}_{\text{Higgs}} = \frac{1}{2}\left(k_{\phi\phi}\right)^{\mu\nu} e \left(\mathscr{D}_\mu \phi\right)^\dagger \mathscr{D}_\nu \phi + \text{H.c.} - \frac{1}{2}\left(k_{\phi W}\right)^{\mu\nu} e \phi^\dagger W_{\mu\nu} \phi - \frac{1}{2}\left(k_{\phi B}\right)^{\mu\nu} e \phi^\dagger \phi B_{\mu\nu}, \tag{3.14}$$

where all LSV coefficients are dimensionless. Both $\left(k_{\phi W}\right)$ and $\left(k_{\phi B}\right)$ are real and $\left(k_{\phi\phi}\right)$ has a symmetric real part and antisymmetric imaginary part. The Higgs field also presents a possibility for a CPT-odd sector

$$\mathscr{L}^{\text{CPT}-}_{\text{Higgs}} = i\left(k_\phi\right)^\mu e \phi^\dagger D_\mu \phi + \text{H.c.} \tag{3.15}$$

Here, the $\left(k_\phi\right)^\mu$ has dimension of mass coefficient and is complex.

In the gauge sector the CPT-even contributions are

$$\mathscr{L}^{\text{CPT}+}_{\text{gauge}} = -\frac{1}{2}\left(k_G\right)_{\kappa\lambda\mu\nu} e \,\text{Tr}\left(G^{\kappa\lambda} G^{\mu\nu}\right) - \frac{1}{2}\left(k_W\right)_{\kappa\lambda\mu\nu} e \,\text{Tr}\left(W^{\kappa\lambda} W^{\mu\nu}\right) - \frac{1}{4}\left(k_G\right)_{\kappa\lambda\mu\nu} e B^{\kappa\lambda} B^{\mu\nu}, \tag{3.16}$$

with all LSV coefficients being real, antisymmetric on the first two indices and on the last two, and symmetric under interchange of the first and last pairs of indices. Additionally, there is the possibility of a CPT-odd contributions for the gauge sector. They are invariant under infinitesimal gauge transformations and have a Chern-Simons form given by

$$\mathscr{L}^{\text{CPT}-}_{\text{gauge}} = \left(k_3\right)_\kappa \varepsilon^{\kappa\lambda\mu\nu} e \,\text{Tr}\left(G_\lambda G_{\mu\nu} - \tfrac{2}{3} i g_s G_\lambda G_\mu G_\nu\right) + \left(k_2\right)_\kappa \varepsilon^{\kappa\lambda\mu\nu} e \,\text{Tr}\left(W_\lambda W_{\mu\nu} - \tfrac{2}{3} i g W_\lambda W_\mu G_\nu\right) + \left(k_1\right)_\kappa \varepsilon^{\kappa\lambda\mu\nu} e B_\lambda G_{\mu\nu} + \left(k_0\right)_\kappa e B^\kappa. \tag{3.17}$$

In (3.17) all LSV coefficients are real, $\left(k_0\right)_\kappa$ has dimension of mass cubed and $\left(k_{1,2,3}\right)_\kappa$ have mass dimension.

It is also important to mention that, although they depend on the spacetime coordinates, not all LSV coefficients lead to measurable physical effects. This happens because, in some situations, it is possible to perform a field redefinition that completely removes the dependence on a given LSV parameter. For example, in the Higgs sector one can perform a field redefinition by a phase factor of the form $\phi(x) = e^{-ig(x)}\rho(x)$, choosing $g(x) = (k_\phi)_\mu x^\mu$ to absorb the effects of the coefficient $(k_\phi)_\mu$. The Ref. [62] also argues that certain field redefinitions can be performed to relate coefficients from one sector to those of other sectors.

These Lagrangians presented so far define the action $S_{\text{SM}} + S_{\text{LSV}}$ in a phase prior to the spontaneous symmetry breaking caused by the Higgs mechanism. For further discussions of the Higgs mechanism in the context of the minimal SME in curved spacetime, see Ref. [43], and for discussions in Minkowski spacetime, see Ref. [60, 61].

It now remains to consider the gravitational sector of the SME, which is defined in Ref. [62] in such a way that

$$S_{\mathrm{GR}} = \frac{1}{2\kappa}\int d^4x\mathscr{L}_{\mathrm{GR}}, \tag{3.18}$$

where $\kappa = 8\pi G_N$ and

$$\mathscr{L}_{\mathrm{GR}} = \mathscr{L}^{\mathrm{LI}}_{e,\omega} + \mathscr{L}^{\mathrm{LSV}}_{e,\omega} + \cdots, \tag{3.19}$$

with $\mathscr{L}^{\mathrm{LI}}_{e,\omega}$ and $\mathscr{L}^{\mathrm{LSV}}_{e,\omega}$ being the Lorentz invariant and the LSV pieces, respectively, and both are constructed in term of the vierbein and the spin connection. The ellipsis indicates a possible dependence on other dynamical gravitational fields, which may be fundamental or composite and may contain both Lorentz-invariant and Lorentz-violating contributions. The $\mathscr{L}^{\mathrm{LI}}_{e,\omega}$ part can be written as an expansion of powers of the curvature, torsion and covariant derivatives. In the leading order we have

$$\mathscr{L}^{\mathrm{LI}}_{e,\omega} = eR - 2e\Lambda + \cdots, \tag{3.20}$$

which is the Einstein-Hilbert Lagrangian, $\mathscr{L}_{\mathrm{EH}} = eR$, plus a cosmological constant term.

As before, $\mathscr{L}^{\mathrm{LSV}}_{e,\omega}$ is constructed by combining Lorentz-violating coefficients with gravitational field operators (vierbein, spin connection, and their derivatives) to obtain a quantity invariant under local observer Lorentz and general coordinate transformations. The Ref. [62] expresses theses operator in terms od curvature, torsion and covariant derivatives. Then, in leading order of expansion, we have

$$\mathscr{L}^{\mathrm{LSV}}_{e,\omega} = e\big(k_T\big)^{\lambda\mu\nu}T_{\lambda\mu\nu} + e\big(k_R\big)^{\kappa\lambda\mu\nu}R_{\kappa\lambda\mu\nu} + e\big(k_{TT}\big)^{\alpha\beta\gamma\lambda\mu\nu}T_{\alpha\beta\gamma}T_{\lambda\mu\nu} + e\big(k_{DT}\big)^{\kappa\lambda\mu\nu}\mathscr{D}_\kappa T_{\lambda\mu\nu} + \cdots. \tag{3.21}$$

Here, all LSV coefficients are real and inherit the symmetries of the operators with which they are contracted. All coefficients presented in Eq. (3.21) are dimensionless, with the exception of $(k_T)^{\lambda\mu\nu}$, which has mass dimension. For a more detailed discussion of this sector, see Ref. [62].

Another important aspect in gravitational theories of the Einstein–Cartan type in the SME context is the distinction between spontaneous and explicit LSV. In Ref. [121], it is clearly argued that when the violation is spontaneous, the Lorentz-violating coefficients correspond to vacuum values of dynamical fields. This preserves consistency between the Bianchi identities, the Noether identities, and the equations of motion, and avoids conflicts with the covariant conservation of the energy–momentum tensor. In contrast, in explicit breaking, the Lorentz coefficients are nondynamical background fields. This can lead to so-called *no-go* results, originally discussed in Ref. [62], which are characterized by inconsistencies between geometric identities and gravitational dynamics, especially in Riemannian or Riemann–Cartan geometries. The work [121] emphasizes that although some explicit breaking scenarios may avoid these problems through specific mechanisms, the most natural and generally consistent approach to Lorentz violation in gravity remains

spontaneous breaking. This is the assumption adopted in most phenomenological analyses of the gravitational sector of the SME. In Section 3.4, we comment on how Finsler geometry may help to slove some of the problems related to explicit Lorentz breaking.

3.1.1 The full SME action in Minkowski spacetime

Most work in the SME context are focused on the QED sector in flat spacetime, which we will discuss in Section 3.2. However, there are also developments beyond this sector, including studies in the non-Abelian sector [111,123] and in the gravitational sector [124–126], which aim to obtain experimental bounds on Lorentz-violating effects.

Here we restrict ourselves to the interesting aspects of the SME in curved spacetime. However, the complete SME action in flat spacetime, as well as a detailed discussion of technical difficulties, possible phenomenological applications, and comparisons with experiments, can be found in the seminal works that established the SME [60,61]. The action is very similar to the one presented here, with the addition of terms involving $\gamma^\mu\gamma_5$ and $\sigma^{\mu\nu}$ in the lepton sector.

This first contact with the SME is quite technical and not very transparent, but it is still worthwhile because it provides a general view of how the formalism is constructed and how it connects with the usual Standard Model. In the next section, we present a clearer discussion of the SME and its phenomenology by introducing its minimal and nonminal QED sectors in flat spacetime. We then also present how the main experimental and observational limits on these symmetry-breaking coefficients are obtained.

3.2 The QED sectors of the mSME and nmSME in Minkowski spacetime

The renormalizable and gauge invariant QED sector of the mSME is constructed in terms of constant background LSV tensors (the simplest choice, with no physical obstruction to more elaborate choices; see Sec. 3.1) and consists in the following action in flat spacetime [62]:

$$S_{\text{QED-mSME}} = \int d^4x \Big[\bar{\psi}\left(i\Gamma^\mu D_\mu - M\right)\psi - \frac{1}{4}F^{\mu\nu}F_{\mu\nu} - \frac{1}{4}(k_F)^{\mu\nu\lambda\rho}F_{\mu\nu}F_{\lambda\rho} - \frac{1}{2}\varepsilon_{\mu\nu\kappa\lambda}(k_{AF})^\mu A^\nu F^{\kappa\lambda} \Big], \tag{3.22}$$

where the dimensionless constant background tensor $(k_F)^{\mu\nu\lambda\rho}$ is a CPT-even term that carries similar symmetry properties of Riemann curvature tensor in gravitation context. The constant background vector $(k_{AF})^\mu$ is a CPT-odd term with dimensions of inverse of length, and it is responsible for the usual CFJ term. In the matter sector, $D_\mu = \partial_\mu + ieA_\mu$ is the usual covariant derivative and we also have

$$\Gamma^\mu = \gamma^\mu + c^{\mu\nu}\gamma_\nu + d^{\mu\nu}\gamma_\nu\gamma_5 + e^\mu + if^\mu\gamma_5 + \frac{1}{4}g^{\lambda\nu\mu}\Sigma_{\lambda\nu}, \tag{3.23}$$

$$M = m + im_5\gamma_5 + a_\mu\gamma^\mu + b_\mu\gamma^\mu\gamma_5 + \frac{1}{4}H_{\mu\nu}\Sigma^{\mu\nu}, \tag{3.24}$$

with γ^μ and $\gamma_5 = i\gamma^0\gamma^1\gamma^2\gamma^3$ being the usual Dirac matrices obeying the Clifford algebra $\{\gamma^\mu, \gamma^\nu\} = 2\eta^{\mu\nu}$, and defining the proper and orthochronous $SO(1,3)$ generators in the spinor representation as $\Sigma^{\mu\nu} = \sigma^{\mu\nu}/2 = i[\gamma^\mu, \gamma^\nu]/4$. The terms in Eqs. (3.23) and (3.24) can be generally expressed as $\Gamma^\mu = \gamma^\mu + \delta\Gamma^\mu_{\text{LSV}}$ and $M = m + \delta M_{\text{LSV}}$, where $\delta\Gamma^\mu_{\text{LSV}}$ and δM_{LSV} represent small and constant Lorentz- and CPT-violating corrections. The former is dimensionless, while the latter has mass dimension.

Requiring the Lagrangian to be Hermitian implies that all the LSV coefficients must be real. The coefficients a_μ, b_μ, e_μ, and $g_{\mu\nu\lambda}$ are all CPT-odd, whereas f_μ is CPT-even. This is because f_μ can be absorbed into the $c_{\mu\nu}$ coefficients via an appropriate spinor redefinition and only appears in physical observables through bilinear combinations $f_\mu f_\nu$ [127]. It is also worth emphasizing that, in certain cases, a field redefinition can be performed to eliminate some of the background terms appearing in Eqs. (3.23) and (3.24). In other words, these terms can be absorbed into a reparametrization of the spinor field ψ. A typical example is the a_μ term, which can be removed by the transformation $\psi(x) = e^{-ia\cdot x}\chi(x)$. Similarly, the b_μ term could also be eliminated through a suitable redefinition, but only in the absence of the fermion mass term, m. Another term that can be easily removed is m_5, through a chiral rotation of the form $\psi = e^{i\alpha\gamma_5}\psi'$, with a global parameter given by $\alpha = -\frac{1}{2}\tan^{-1}\left(\frac{m_5}{m}\right)$, and a corresponding redefinition of the mass term: $m \to m' = m\cos(2\alpha) - m_5\sin(2\alpha)$ [127]. A rigorous analysis of field redefinitions that can eliminate redundant background choices can be found in [128].

Regarding the Lorentz and CPT invariance of the action (3.22), it is important to recall that these symmetries are defined with respect to the free field theory, $\mathscr{L}_0 = \bar{\psi}(i\gamma^\mu\partial_\mu - m)\psi$. From this perspective, the distinction between observer and particle transformations becomes essential. In a certain sense, Lorentz symmetry remains preserved: the theory behaves normally under rotations and boosts as long as one considers passive Lorentz transformations – those associated with changes of coordinates in the laboratory frame. Within the framework of the SME, LSV only emerges when fields are actively transformed—that is, when particle transformations alter their orientation relative to fixed background tensor fields that characterize the vacuum. In this context, LSV terms such as $(k_F)^{\mu\nu\lambda\rho}$, $(k_{AF})^\mu$, $\delta\Gamma^\mu_{\text{LSV}}$, and δM_{LSV} transform as tensors, vectors, or scalars under observer transformations, but remain invariant (i.e., behave as scalars) under particle transformations. This distinction allows these terms to be consistently treated as constant background fields [60]. Furthermore, it is worth noting that m_5 does not introduce an apparent violation of Lorentz symmetry, as the combined presence of m and m_5 still yields a Lorentz-invariant mass term at the level of the dispersion relation [122].

Most phenomenological developments of the SME are found in the QED sector within the framework of the mSME in flat spacetime. This sector is a good laboratory to explore basic ideas and later search for generalizations. Some notable works in this sector include [41] in the photonic sector, [129] in the fermionic sector, and [130] exploring relations between these sectors.

The QED sector of the nmSME is quite similar to that of the mSME. This similarity is expressed as [131, 132]

$$S_{\text{QED-nmSME}} = \int d^4x \Big[\bar{\psi} \left(i\hat{\Gamma}^\mu D_\mu - \hat{M} \right) \psi - \frac{1}{4} F^{\mu\nu} F_{\mu\nu} - \frac{1}{4} (\hat{k}_F)^{\mu\nu\lambda\rho} F_{\mu\nu} F_{\lambda\rho} - \frac{1}{2} \varepsilon_{\mu\nu\kappa\lambda} (\hat{k}_{AF})^\mu A^\nu F^{\kappa\lambda} \Big], \tag{3.25}$$

where $\hat{\Gamma}^\mu$, $\hat{M}$, $(\hat{k}_{AF})^\mu$, and $(\hat{k}_F)^{\mu\nu\lambda\rho}$ now represent non-minimal version of the minimal LSV coefficients in the action (3.22). In the photon sector, the non-minimal coefficients involve terms of higher derivatives and are given by the series [131, 133]

$$(\hat{k}_{AF})_\mu = \sum_{D\,\text{odd}} (k_{\text{AF}}^{(D)})_\mu{}^{\alpha_1 \cdots \alpha_{D-3}} \partial_{\alpha_1} \cdots \partial_{\alpha_{D-2}}, \tag{3.26}$$

$$(\hat{k}_F)_{\mu\nu\lambda\rho} = \sum_{D\,\text{even}} (k_F^{(D)})_{\mu\nu\lambda\rho}{}^{\alpha_1 \cdots \alpha_{D-4}} \partial_{\alpha_1} \cdots \partial_{\alpha_{D-4}}, \tag{3.27}$$

where each coefficient is labeled by the mass dimension $D \geq 3$ of the corresponding field operator (that is, the respective term in the action containing the photon field and its derivatives), and the Lorentz indices α_i are associated with spacetime derivatives. In the CFJ sector (CPT-odd), the first non-minimal contribution appears at $D = 5$ and takes the form $(k_{\text{AF}}^{(5)})_\mu{}^{\nu\kappa} \partial_\nu \partial_\kappa$. In contrast, in the CPT-even sector, the first non-minimal contribution arises at $D = 6$ and has the form $(k_F^{(6)})_{\mu\nu\lambda\rho}{}^{\kappa\sigma} \partial_\kappa \partial_\sigma$. A very interesting work that explore theoretical and phenomenological aspects of these possibilities in the nonminimal photonic sector is [133].

In the fermion sector, the action of nmSME can also be expressed as [132]

$$S_{\text{QED-nmSME}} \supset S_\psi = \frac{1}{2} \int d^4x \bar{\psi} (i\gamma^\mu \partial_\mu - m_\psi + \hat{Q}) \psi + \text{H.c.}, \tag{3.28}$$

where $\hat{Q}$ is a Hermitian matrix operator involving both Lorentz-invariant and LSV contractions with derivative operators $i\partial_\mu$. In Ref. [132], a point of view is adopted in which higher-order Lorentz-violating terms in $\hat{Q}$ are considered negligible, since they are strongly suppressed by the Planck mass. Moreover, $\hat{Q}$ is taken to be invariant under spacetime translations, thereby preserving energy-momentum conservation. This theoretical choice implies that $\hat{Q}$ is a constant spacetime operator, and the focus is placed on pure Lorentz violation, which minimizes complications in both theoretical and experimental analyses. A subsequent decomposition of $\hat{Q}$ is then performed, allowing for the enumeration and characterization of the coefficients for Lorentz violation appearing in Eq. (3.28), such as

$$\hat{Q} = \sum_I \hat{Q}^I \gamma_I = \hat{\mathscr{S}} + i\hat{\mathscr{P}}\gamma_5 + \hat{\mathscr{V}}_\mu \gamma^\mu + \hat{\mathscr{A}}_\mu \gamma^\mu \gamma_5 + \frac{1}{2} \hat{\mathscr{T}}_{\mu\nu} \sigma^{\mu\nu}, \tag{3.29}$$

where the sixteen $\hat{Q}^I$ operators $\{\hat{\mathscr{S}}, \hat{\mathscr{P}}, \hat{\mathscr{V}}_\mu, \hat{\mathscr{T}}_{\mu\nu}\}$ have mass dimension one and are scalar functions of $i\partial_\mu$. Therefore, the $\hat{Q}^I$ operators, in the momentum space where $i\partial_\mu = p_\mu$, can be expanded as

$$\hat{Q}^I = \sum_{D=3}^{\infty} Q^{I(D)\alpha_1 \cdots \alpha_{D-3}} p_{\alpha_1} \cdots p_{\alpha_{D-3}}, \tag{3.30}$$

where the coefficients $Q^{I(D)\alpha_1\cdots\alpha_{D-3}}$ are real and spacetime independent.

In the momentum space, there is a map between the $\hat{Q}$ and the $\hat{\Gamma}^\mu p_\mu - \hat{M}$ notation of the mSME, which comes from the equality [132]

$$\gamma^\mu p_\mu - m_\psi + \hat{Q} = \hat{\Gamma}^\mu p_\mu - \hat{M}, \tag{3.31}$$

where

$$\hat{\Gamma}^\mu = \gamma^\mu + \hat{c}^{\mu\nu}\gamma_\nu + \hat{d}^{\mu\nu}\gamma_\nu\gamma_5 + \hat{e}^\mu + i\hat{f}^\mu\gamma_5 + \frac{1}{4}\hat{g}^{\lambda\nu\mu}\Sigma_{\lambda\nu}, \tag{3.32}$$

$$\hat{M} = m_\psi + \hat{m} + i\hat{m}_5\gamma_5 + \hat{a}_\mu\gamma^\mu + \hat{b}_\mu\gamma^\mu\gamma_5 + \frac{1}{4}\hat{H}_{\mu\nu}\Sigma^{\mu\nu}. \tag{3.33}$$

Here, the terms $\hat{c}^{\mu\nu}$ and $\hat{d}^{\mu\nu}$ are CPT-even and dimensionless, while $\hat{e}^\mu$, $\hat{f}^\mu$, and $\hat{g}^{\lambda\nu\mu}$ are CPT-odd and also dimensionless. Additionally, $\hat{m}$, $\hat{m}_5$, and $\hat{H}_{\mu\nu}$ are CPT-even with mass dimension one, whereas $\hat{a}^\mu$ and $\hat{b}^\mu$ are CPT-odd with the same mass dimension. The operators $\hat{m}$ and $\hat{m}_5$ consist solely of higher-derivative terms of nonrenormalizable dimension, while all the other operators appearing in Eq. (3.33) have counterparts in the mSME. In Eq. (3.31), the operator $\hat{\Gamma}^\mu$ appears contracted with the momentum p_μ, which motivates the introduction of contracted operators given by

$$\hat{c}^\mu \equiv \hat{c}^{\mu\nu}p_\nu, \quad \hat{d}^\mu \equiv \hat{d}^{\mu\nu}p_\nu, \quad \hat{e} \equiv \hat{e}^\mu p_\mu, \quad \hat{f} \equiv \hat{f}^\mu p_\mu, \quad \text{and} \quad \hat{g}^{\lambda\nu} \equiv \hat{g}^{\lambda\nu\mu}p_\mu. \tag{3.34}$$

In terms of these operators, one can write

$$\hat{\mathscr{S}} = \hat{e} - \hat{m}, \quad \hat{\mathscr{P}} = \hat{f} - \hat{m}_5, \quad \hat{\mathscr{V}}^\mu = \hat{c}^\mu - \hat{a}^\mu, \quad \hat{\mathscr{A}}^\mu = \hat{d}^\mu - \hat{b}^\mu, \quad \text{and} \quad \hat{\mathscr{T}}^{\mu\nu} = \hat{g}^{\mu\nu} - \hat{H}^{\mu\nu}. \tag{3.35}$$

These expressions provide the explicit link between the decompositions (3.29) and (3.31).

Explicitly, these ten LSV operators in (3.32) and (3.33) can be written in the form of a series such that of Eq. (3.30). As an example, we can consider the $\hat{b}^\mu$ operator which can be written in the form

$$\hat{b}^\mu = \sum_{D\,\text{odd}} b^{(D)\mu\alpha_1\cdots\alpha_{D-3}}p_{\alpha_1}\cdots p_{\alpha_{D-3}}, \tag{3.36}$$

where the number of independent $b^{(D)\mu\alpha_1\cdots\alpha_{D-3}}p_{\alpha_1}$ coefficients for a given D is equals to $\frac{2}{3}D(D-1)(D-2)(D-3)$.

Overall, Ref. [132] offers the most detailed treatment of the nonminimal fermion sector, incorporating operators of arbitrary mass dimension. In this study, the authors also derive compact expressions for the exact dispersion relation and spinor projection operators, and construct effective Hamiltonians for fermions. A key achievement is the organization of LSV coefficients through a decomposition in spin-weighted spherical harmonics, which establishes a clear framework for potential experimental investigations. The general theory is then applied to specific scenarios, including isotropic models, the nonrelativistic and ultrarelativistic limits, as well as the mSME. Within these limits, the authors obtain explicit formulas for dispersion relations, fermion group velocities, and spin-precession frequencies.

Operator	Type	D	CPT	Coefficients	Number
$\hat{m}$	Scalar	odd ≥ 5	even	$m^{(D)\alpha_1\cdots\alpha_{D-3}}$	$\frac{1}{6}D(D-1)(D-2)$
$\hat{m}_5$	Pseudoscalar	odd ≥ 5	even	$m_5^{(D)\alpha_1\cdots\alpha_{D-3}}$	$\frac{1}{6}D(D-1)(D-2)$
$\hat{a}^\mu$	Vector	odd ≥ 3	odd	$a^{(D)\mu\alpha_1\cdots\alpha_{D-3}}$	$\frac{2}{3}D(D-1)(D-2)(D-3)$
$\hat{b}^\mu$	Pseudovector	odd ≥ 3	odd	$b^{(D)\mu\alpha_1\cdots\alpha_{D-3}}$	$\frac{2}{3}D(D-1)(D-2)(D-3)$
$\hat{c}^\mu$	Vector	even ≥ 4	even	$c^{(D)\mu\alpha_1\cdots\alpha_{D-3}}$	$\frac{2}{3}D(D-1)(D-2)(D-3)$
$\hat{d}^\mu$	Pseudovector	even ≥ 4	even	$d^{(D)\mu\alpha_1\cdots\alpha_{D-3}}$	$\frac{2}{3}D(D-1)(D-2)(D-3)$
$\hat{e}$	Scalar	even ≥ 4	odd	$e^{(D)\alpha_1\cdots\alpha_{D-3}}$	$\frac{1}{6}D(D-1)(D-2)$
$\hat{f}$	Pseudoscalar	even ≥ 4	odd	$f^{(D)\alpha_1\cdots\alpha_{D-3}}$	$\frac{1}{6}D(D-1)(D-2)$
$\hat{g}^{\mu\nu}$	Tensor	even ≥ 4	odd	$g^{(D)\mu\nu\alpha_1\cdots\alpha_{D-3}}$	$D(D-1)(D-2)$
$\hat{H}^{\mu\nu}$	Tensor	odd ≥ 3	even	$H^{(D)\mu\nu\alpha_1\cdots\alpha_{D-3}}$	$D(D-1)(D-2)$

Table 1 – The ten non-minimal operators and coefficients for a Dirac fermion and their properties. Table reproduced from Ref. [132].

The formalism is further linked to other approaches, and astrophysical data are used to set constraints on isotropic ultrarelativistic coefficients associated with LSV.

In Chapter 6, we present a work that can be understood from the point of view of the nonminimal fermionic sector of QED within the SME in flat spacetime. In the next section, we will discuss how these LSV coefficients from both the mSME and the nmSME can be compared with actual experiments and where the best limits on them can be found.

3.3 The data tables for Lorentz and CPT violation

The last important point of this brief review of the SME is the compilation of definitions and bounds on its Lorentz- and CPT-violating coefficients, provided by the so-called Data Tables for Lorentz and CPT Violation, which are updated annually by V. A. Kostelecký and N. Russell [76]. In [76], tables and lists with the measured and derived values of the coefficients are presented for the matter, photon, neutrino, and gravity sectors, along with the definitions and relevant properties of these coefficients. It is adopted natural units, where $\hbar = c = \varepsilon_0 = k_B = 1$, and all values are reported in the standard Sun-centered inertial (SCI) reference frame [78,79], which provides a convenient and widely used framework for experimental comparisons.

A reference frame on Earth's surface is inadequate, since it is non-inertial and, consequently, an external background cannot appear fixed in such a frame since it would be observed as rotating. For this reason the SCI reference frame is a convenient choice considering that it can be regarded as approximately inertial on the time scale of typical experiments, given that its motion around the galaxy has a period of ~ 200 million years. Moreover, it is experimentally accessible, and its axes can be conveniently aligned with those of the Earth as

shown in Figure 2.

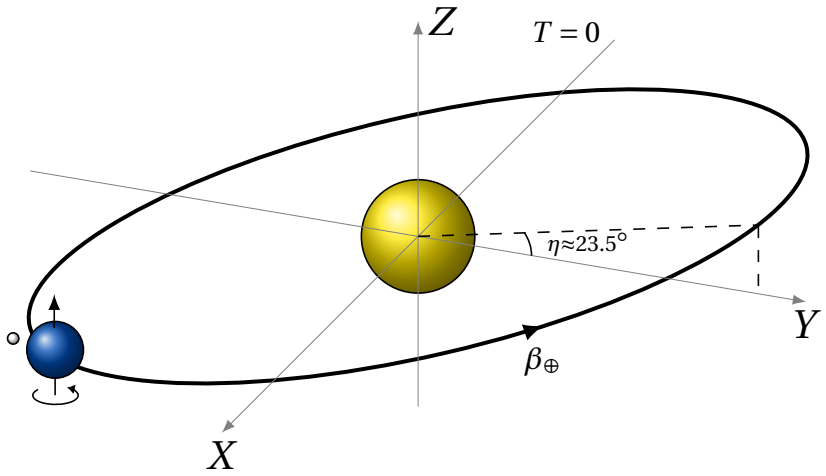

Figure 2 – Schematic drawing of the standard Sun-centered inertial (SCI) reference frame, reproduced from Refs. [76,78,79]. The Z axis is parallel to the Earth's rotation axis, X points from the Sun to the vernal equinox, and Y completes a right-handed system. $\beta_\oplus = 10^{-4}$ is the Earth's orbital velocity and $\eta = 23.5^\circ$ is the inclination of Earth's axis relative to the orbital plane. $T = 0$ is the origin time.

Thus, for an Earth-based observer the background appears to rotate, implying that experimental signals affected by LSV will generally exhibit time-dependent modulations, particularly at sidereal frequencies. Moreover, even isotropic backgrounds in the SCI become anisotropic in the Earth's frame due to its rotational and translational motions, which generate boosts. Hence, violations of rotational invariance constitute a key signature of Lorentz violation in Earth experiments.

According to Refs. [76, 78, 79], the axes of the SCI are defined as follows: the Z axis is parallel to the Earth's rotation axis, X points from the Sun to the vernal equinox, and Y completes a right-handed system (see Figure 2). The origin of time $T = 0$ is set at the 2000 vernal equinox[2]. For the standard Earth-bound frame at a point in the northern hemisphere, the z axis is vertical to the surface (pointing to the local zenith), the x axis points south, and the y axis points east. The local time $T_\oplus$ is defined as the time measured in the SCI from one of the instants when y aligns with Y. To relate the LSV coefficients from the laboratory frame (LAB), where they usually depend on time, to the SCI, where they remain constant, we introduce a generic background V^μ. The components of this vector in both frames are linked through

$$V^\mu_{\text{LAB}} = \Lambda^\mu{}_\nu V^\nu_{\text{SCI}}, \tag{3.37}$$

where $\Lambda^\mu{}_\nu$ is an observer Lorentz transformation between an Earth's frame and the SCI. The V^μ components in the LAB and SCI frames are, respectively, defined as $V^\mu_{\text{LAB}} \equiv \left(V^0_{\text{LAB}}, V^i_{\text{LAB}}\right)$

[2] The vernal equinox is the moment when the Sun crosses the celestial equator moving northward. It marks the beginning of spring in the northern hemisphere and serves as a reference point in celestial coordinate systems, corresponding to zero right ascension (the celestial analogue of longitude).

and $V^{\mu}_{\rm SCI} \equiv \left(V^{T}_{\rm SCI}, V^{I}_{\rm SCI}\right)$ with $i = (x, y, z)$ and $I = (X, Y, Z)$. The Lorentz transformation $\Lambda^{\mu}{}_{\nu}$ is given by the components (see Appendix A of Ref. [111])

$$\Lambda^{0}{}_{T} = 1, \;\; \Lambda^{0}{}_{I} = -\boldsymbol{\beta}^{I}, \;\; \Lambda^{i}{}_{T} = -(R\cdot\boldsymbol{\beta})^{i}, \;\; \text{and} \;\; \Lambda^{i}{}_{I} = -R^{iI}, \tag{3.38}$$

where $\boldsymbol{\beta} = \boldsymbol{v}/c$ in natural units and $\boldsymbol{v}$ being the LAB velocity relative to the SCI and R^{iJ} is a spatial rotation. In the present situation, the $\gamma = \sqrt{1-\boldsymbol{\beta}^2}$ is approximately equals to one, since the speed of Earth relative to the Sun is small when compared to c. If one is able to calculate the $\boldsymbol{\beta}^{I}$ and R^{iJ} components in terms of the Earth's orbital velocity ($\beta_{\oplus} = 10^{-4}$), Earth's rotational velocity ($\beta_{L} = r_{\oplus}\omega_{\oplus} < 10^{-6}$), Earth's angular orbital velocity ($\Omega_{\oplus} = 2\pi/\text{year} \approx 2\times10^{-7}s^{-1}$), Earth's angular rotational velocity ($\omega_{\oplus} = 2\pi/\text{day} \approx 7\times10^{-5}s^{-1}$), the inclination of Earth's axis relative to the orbital plane denoted by η, and the experiment's co-latitude denoted by χ (the angle between the Earth's rotation axis and the laboratory z-axis), then it will be possible to complete the link proposed by Eq. (3.37). These components are explicitly presented in Ref. [111] and have the form

$$\boldsymbol{\beta}^{X} = \beta_{\oplus}\sin\left(\Omega_{\oplus}T\right) - \beta_{T}\sin\left(\omega_{\oplus}T_{\oplus}\right), \tag{3.39}$$

$$\boldsymbol{\beta}^{Y} = -\beta_{\oplus}\cos\left(\eta\right)\cos\left(\Omega_{\oplus}T\right) - \beta_{L}\cos\left(\omega_{\oplus}T_{\oplus}\right), \tag{3.40}$$

$$\beta^{Z} = -\beta_{\oplus}\sin\left(\eta\right)\cos\left(\Omega_{\oplus}T\right), \tag{3.41}$$

and

$$R^{iJ} = \begin{pmatrix} \cos\left(\chi\right)\cos\left(\omega_{\oplus}T_{\oplus}\right) & \cos\left(\chi\right)\sin\left(\omega_{\oplus}T_{\oplus}\right) & -\sin\left(\chi\right) \\ -\sin\left(\chi\right) & \cos\left(\chi\right) & 0 \\ \sin\left(\chi\right)\cos\left(\omega_{\oplus}T_{\oplus}\right) & \sin\left(\chi\right)\sin\left(\omega_{\oplus}T_{\oplus}\right) & \cos\left(\chi\right) \end{pmatrix}. \tag{3.42}$$

Therefore, $\Lambda^{0}{}_{I}$ and $\Lambda^{i}{}_{I}$ components are completely obtained. The last one, $\Lambda^{i}{}_{T} = -(R\cdot\boldsymbol{\beta})^{i}$, takes the form

$$\Lambda^{x}{}_{T} = -\left(R^{xX}\boldsymbol{\beta}^{X} + R^{xY}\boldsymbol{\beta}^{Y} + R^{xZ}\boldsymbol{\beta}^{Z}\right), \tag{3.43}$$

$$\Lambda^{y}{}_{T} = -\left(R^{yX}\boldsymbol{\beta}^{X} + R^{yY}\boldsymbol{\beta}^{Y}\right), \tag{3.44}$$

$$\Lambda^{z}{}_{T} = -\left(R^{zX}\boldsymbol{\beta}^{X} + R^{zY}\boldsymbol{\beta}^{Y} + R^{zZ}\boldsymbol{\beta}^{Z}\right). \tag{3.45}$$

As the Earth's velocity relative to the Sun is small ($\boldsymbol{\beta}$ small), the components $\Lambda^{0}{}_{I}$ and $\Lambda^{i}{}_{T}$ can be neglected, since they produce small effects of order $\boldsymbol{\beta}$. Taking this into account, Eq. (3.37) leads us to write

$$V^{0}_{\rm LAB} = V^{T}_{\rm SCI} + O(\boldsymbol{\beta}), \tag{3.46}$$

$$V^{i}_{\rm LAB} = R^{iI}V^{I}_{\rm SCI} + O(\boldsymbol{\beta}). \tag{3.47}$$

This type of transformation is used for all limits on the LSV parameters in the matter, photon, neutrino, and gravity sectors presented in the annually updated Data Tables for Lorentz and CPT Violation by V. A. Kostelecký and N. Russell [76]. In the next section, we conclude our brief review with comments on new perspectives for the SME and on central open problems.

3.4 Comments on the concordance problem, the relation with Condensed Matter Physics, and Finsler geometry

Up to this point, the SME has been viewed as an effective field theory designed to describe effects of CPT- and Lorentz-symmetry violation in gravitational scenarios and in the SM at low energies, and several phenomenological possibilities to test the formalism have been presented. However, the SME suffers from a pathology known as the concordance problem. This pathology is related to the physical interpretation of regimes in which the Lorentz-violating coefficients cannot be treated perturbatively in the chosen reference frame, or when a system that is initially perturbative is observed from a highly boosted reference frame and becomes nonperturbative. In these cases, the effective description may exhibit apparently pathological features, such as the occurrence of negative-energy states, which brings doubts about the physical consistency of the theory. For more details, see Refs. [90,134]. In general, this problem is avoided in the SME by requiring that the LSV coefficients are small and that only so-called concordant reference frames are considered, that is, frames in which the perturbative expansion remains valid. Although this approach works from a phenomenological point of view, it avoids the problem instead of solving it physically, leaving open the question of the consistency of the SME in nonperturbative regimes [134].

As pointed out in the Chapter 2 (and will be will be pointed in the Chapter 5) , a recent effort to explore parallels between the SME and condensed matter systems (in particular Weyl and Dirac semimetals) has begun. In these systems, Dirac-like equations with effective violations of emergent Lorentz invariance appear, without any restriction on the magnitude of these violations, even in the low-energy regime. This suggests that the concordance problem is not necessarily a fundamental obstacle, but rather a question of physical interpretation of the ground state of the theory, as argued in Refs. [115,116,134,135]. In this context, Refs. [115,116,134,135] present a proposal for a physical solution to the concordance problem, explicitly discussed for the case of a Dirac fermion in Minkowski spacetime in the presence of a nonzero coefficient b_μ. In this model, the concordance problem appears through the presence of particles and antiparticles with negative energies when the components of b_μ become large compared to the fermion mass, either directly in the chosen reference frame or after a large boost transformation. The solution proposed in [115,116,134,135] is based on thermodynamic arguments inspired by the physics of Weyl semimetals. In these materials, the ground state is defined by a Fermi surface associated with a thermal reservoir, and all energy states below this surface are occupied. In an analogous way, in the model with b_μ, the idea of a physical bath is introduced to define the vacuum state of the theory. The condition of thermodynamic equilibrium requires the Fermi level to be zero, so that all negative-energy states are filled in the physical vacuum. Considering this point of view, the presence of negative-energy particles and antiparticles in the ground state does not imply instability, since there are no available states for transitions that would allow the extraction of energy from the vacuum. As a result, the vacuum remains stable, even in presence of large LSV.

Finally, Ref. [134] emphasizes that the existence of this physical bath fixes a preferred reference frame associated with the ground state, removing ambiguities related to large observer boosts. Although different observers may describe the system in different ways, the physics remains invariant, since the bath frame (suggested to be the cosmological frame defined by the cosmic microwave background [134]) determines the real physical state of the system. In this way, the concordance problem is effectively resolved, at least for the class of models analyzed, without the need to artificially restrict the Lorentz-violating coefficients or the admissible reference frames.

Another important current concern in the context of the SME is the line of research that proposes Finsler geometry as a natural extension of Riemannian geometry in effective theories with Lorentz and diffeomorphism violation, as discussed in Section 3.1. In Section 3.1, the effects of Lorentz violation were introduced through coefficients that contract with field operators. When these coefficients have an external origin and, therefore, the symmetry breaking is explicit, this leads to problems in particle dynamics and in the geometric structure of spacetime if one keeps the assumption of a purely Riemannian geometry. The Refs. [134, 136] clarifies this situation by arguing that the metric in Riemannian geometry depends only on the position in spacetime, while the dynamics of particles subject to Lorentz-violating coefficients also depends on the direction of motion in the tangent space of the base manifold. The argument further explains that this incompatibility does not indicate an inconsistency of the SME, but rather a limitation of Riemannian geometry to describe effective classical particle trajectories in the presence of explicit Lorentz violation. In this sense, Finsler geometry then emerges as the appropriate mathematical framework, since it generalizes the notion of a metric by allowing simultaneous dependence on position and direction in the tangent space.

More specifically, Finsler geometry is a natural generalization of Riemannian geometry, in which the notion of length is not determined only by a quadratic metric, but by a more general function defined on the tangent bundle. Instead of a metric of the form $g_{\mu\nu}(x)$, the fundamental structure is given by a Finsler function $F(x, y)$, which is positive and homogeneous of degree one in the tangent vector y^μ, from which the line element and the geodesics of the space are defined. This explicit dependence on both position and direction makes Finsler geometry intrinsically anisotropic, allowing the description of spaces whose geometric properties vary with direction. A review work on this subject, with implications for physics, can be found in Ref. [137–139].

More specifically, Refs. [134, 139] point to the case of Dirac fermions propagating in a fixed curved spacetime with SME coefficients. In this case, it is known that the analytic continuation of the classical trajectory of a relativistic wave packet generally corresponds to a geodesic of a Finsler geometry, and not of a Riemannian geometry. This correspondence establishes a direct link between the Lagrangian structure of the SME and Finsler geometry, providing a clear geometric interpretation of Lorentz-violation effects. In Ref. [134], and the references therein, more technical aspects of the physical consequences of this point of view are discussed. In summary, the main message is that the study of Finsler geometry in the SME

context is not only a convenient mathematical tool, but a natural physical consequence of the presence of explicit Lorentz violation. The adoption of this geometry resolves conceptual tensions between particle dynamics and the structure of spacetime, offering a coherent and unified geometric description of fermion propagation in gravitational backgrounds with Lorentz-violating coefficients. This perspective reinforces the idea that the SME not only parametrizes experimental deviations from Lorentz symmetry, but also points to a deep generalization of the classical notion of spacetime.

In this Chapter, we aim to provide an overview of the SME, a very powerful formalism that, independently of the origin of Lorentz-symmetry breaking at high energies in the primordial universe, guides us toward understanding the phenomenological implications and the structure of spacetime resulting from this absence of invariance in low energies. In the following Chapters, we will focus on investigating LSV in several contexts, always seeking to place our efforts within (or to clarify how they differ from) the scope of the SME.

Chapter

4

Integrating out fermions to get LSV effective photonic actions

Within the SME effective field theory (EFT) framework, it is natural to consider extensions of electrodynamics beyond the linear Maxwell regime, as discussed in Section 3.2. In this context, nonlinear electromagnetic theories have been studied in the presence of LSV. These theories can appear as effective descriptions resulting from spontaneous Lorentz-symmetry breaking in Abelian and gauge-invariant models [140]. They may also arise as low-energy limits of scenarios inspired by quantum gravity, such as the semiclassical regime of Loop Quantum Gravity [65, 67–69]. Similar nonlinear structures are found in brane-world models, where Dirac–Born–Infeld–type actions can emerge dynamically due to spontaneous Lorentz-symmetry breaking, even though these models mainly focus on the gravitational and brane sectors [141]. Alternatively, Lorent-symmetry can be explicitly broken in nonlinear electrodynamics. A representative example is Very Special Relativity, in which a Born–Infeld action can be consistently embedded in a gauge-invariant theory with a reduced symmetry group. This leads to modified electromagnetic interactions, such as a $\frac{1}{r^3}$ correction to the Coulomb potential [142]. More recently, phenomenological studies have explored nonlinear electromagnetic theories coupled to axion fields and Lorentz-violating operators in the presence of a CFJ-type anisotropic background [143].

Focusing on Euler-Heisenberg (EH) electrodynamics, the analysis of potential modifications caused by LSV expands somewhat, but remains underexplored in terms of phenomenological implications. The EH electrodynamics can be understood as a low-energy effective action, applicable in physical scenarios where the phenomena of interest occur at energy scales much smaller than the masses of the fundamental fermionic degrees of freedom in QED. Although these heavy fermions appear only as virtual states at such low energies, they induce observable effects that are captured by an effective action describing the photon degrees of freedom. This low-energy effective action is obtained by integrating out the heavy fermionic modes from the full quantum theory [144–146].

The physics behind this procedure is that light- light interaction is absent at the classical level, where the linearity of Maxwell's equation guarantees a superposition principle for the electromagnetic field. On the other hand, in QED a four photon interaction is possible by next order perturbation through the involvement of a charged fermion loop as shown in

Figure 3. This is a difficult loop to compute directly, but one can get the answer integrating out fermions in QED in limit of low-frequency ($\omega \ll m$) obtaining a fourth order term in e, which has the form for the effective action [145]

$$\Gamma_{\rm EH} = \frac{\alpha^2}{90m^2}\left[F^4 + \frac{7}{4}\left(F_{\mu\nu}\tilde{F}^{\mu\nu}\right)^2\right], \tag{4.1}$$

where $\alpha = \frac{e^2}{4\pi}$ is the fine-structure constant. This effective approach is equivalent to computing light-by-light scattering through a tree-level Feynman diagram and represents the physical content of the aforementioned procedure, as illustrated in in Figure 3. In this regard it is also important to emphasize that light-by-light scattering has been experimentally observed at the LHC in ultraperipheral heavy-ion collisions. The ATLAS Collaboration first reported evidence for light-by-light scattering in Pb–Pb collisions at $\sqrt{s_{NN}} = 5.02$ TeV [147], and later achieved a clear observation with high statistical significance [148]. Independent measurements by the CMS Collaboration confirmed these results, showing good agreement with SM predictions [149].

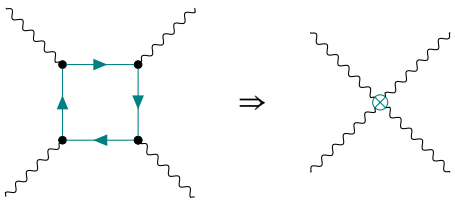

Figure 3 – On the left, we show the Feynman diagram for photon–photon scattering in QED, constructed from the interaction vertex $-eA_\mu\bar{\psi}\gamma^\mu\psi$. On the right, we present an effective approach that allows this quantum effect, arising from fermionic loop contributions, to be captured implicitly by integrating out the heavy modes of QED.

In a low-energy scenario, nonlinear responses play an important role in condensed matter systems and contribute to experimental effects related to magnetization under extreme fields, both in Weyl [150] and Dirac semi-metals [151]. Recently, it was shown that these observations originate from an Euler–Heisenberg–type effect and, as a consequence, lead to the prediction of a whole new class of magnetoelectric effects in materials [152]. As argued in Chapters 2 and 3 (and as we will reinforce in Chapter 5), excitations related to LSV were also found in these types of materials. Therefore, studying how emergent Lorentz-symmetry breaking and nonlinear effects combine can be of great interest in these scenarios.

Given this perspective, LSV-type corrections can be obtained for EH electrodynamics by taking into account the effects of the modified fermionic sector of QED within the SME framework. These modifications involve mass-type corrections given by $M = m + \delta M_{\rm LSV}$ and kinetic corrections of the form $\Gamma^\mu = \gamma^\mu + \delta\Gamma^\mu_{\rm LSV}$, where $\delta M_{\rm LSV}$ and $\delta\Gamma^\mu_{\rm LSV}$ represent all contributions that break Lorentz- and CPT-symmetries in the mass and kinetic sectors of the fermions, respectively, as we saw in Section 3.2 and Ref. [62].

Several recent works investigate how LSV can modify the EH effective action. In [153], radiative corrections induced by a Lorentz-violating background tensor $c_{\mu\nu}$, introduced

through the structure $\delta\Gamma^{\mu}_{\text{LSV}}$, are computed. The resulting effective theory reveals phenomena such as photon splitting and modifications to Maxwell's equations. In [154], the one-loop effective action for the photon field is computed in the presence of a nonminal CPT-breaking interaction term given by $d^{\mu}F_{\mu\nu}\bar{\psi}\gamma^{\nu}\psi$, where d^{μ} is a constant background vector, using the proper-time method with zeta-function regularization. Although higher-derivative operators are generated, is shown that the leading-order corrections do not affect electromagnetic wave propagation in vacuum, suggesting that other photon-related phenomena must be considered to probe this type of Lorentz violation. In another interesting work [155], the authors perform one-loop calculations within the framework of the SME, deriving a generalized EH action that incorporates corrections from both constant axial and tensor Lorentz-violating backgrounds. An additional study [156] applies the proper-time method to scalar QED with both CPT-even and CPT-odd Lorentz-violating terms, yielding an exact modified action and exploring its implications for light propagation and scattering processes. Finally, a recent work [157] explores the effective action at first order in $H_{\mu\nu}$ and obtains a closed expression up to third order in $F_{\mu\nu}$. The authors show that their results violate Furry's theorem. However, they do not explicitly calculate terms of fourth order in the electromagnetic field strength.

In the present Chapter, we shall address this issue by analyzing the additional contributions that arise in the EH effective framework when Lorentz-violating backgrounds are allowed to depend on spacetime. Focusing on the fermionic sector of the SME, we compute, via the proper-time method, the complete set of corrections to photon–photon scattering induced by spacetime-dependent couplings of the form $a_{\mu}\gamma^{\mu}$, $im_5\gamma_5$, and $b_{\mu}\gamma^{\mu}\gamma_5$. Our analysis aims to clarify how such generalized backgrounds modify the structure of the effective action and to assess the physical consequences of these corrections. Additionally, we revisit the calculation of the photonic effective action by considering $b_{\mu}\gamma^{\mu}\gamma_5$ and $H_{\mu\nu}\sigma^{\mu\nu}$ as constant LSV backgrounds. In this analysis, we show violations of Furry's theorem and discuss ambiguities in the calculation of the effective action. These ambiguities arise from the dependence on the specific procedure used to construct the functional determinant of the Dirac operator modified by LSV effects. Finally, we intend to present modified Maxwell's equations for this last scenario and discuss possible physical applications.

In order to obtain this photonic EFT, we write down the functional generator of the starting point model as

$$Z[A^{\mu}] = \mathcal{N}\int \mathscr{D}\bar{\psi}\mathscr{D}\psi e^{iS[A^{\mu},\bar{\psi},\psi]}. \tag{4.2}$$

The next step is integrate the massive modes $\bar{\psi}$ and ψ which results in

$$\det\hat{\theta} = e^{\text{Tr}\ln\hat{\theta}}, \tag{4.3}$$

where the $\hat{\theta}$ is the differential operator present in the fermionic kinetic term $(\bar{\psi}\hat{\theta}\psi)$. The effective photonic action is given by

$$\Gamma[A^{\mu}] = i\ln Z[A^{\mu}] = i\ln\det\hat{\theta} = i\,\text{Tr}\ln\hat{\theta}. \tag{4.4}$$

In order to compute the effective action (4.4), we can perform explicit calculations using the Feynman diagram loop expansion [158], the zeta-function regularization approach [146], and the aforementioned Schwinger proper-time method [145]. This last one is the approach adopted in this Chapter.

4.1 One-loop effective action with spacetime-dependent LSV coefficients

In this Section, based on the Fock-Shcwinger [145] proper time method, we employ a procedure similar to that adopted in Refs. [154, 155] to evaluate the functional determinant of the modified Dirac operator in presence of spacetime coordinates dependent LSV background. As argued in Section 3.1 and Ref. [62], choosing a constant LSV background is a physical but not mandatory assumption, and it cannot be applied to scenarios where gravitational interactions are present. Such scenarios are well known to host extreme astrophysical events, in which nonlinear effects in photon propagation are expected [159]. These extreme environments are also of strong interest in the search for measurable effects of LSV [160]. Therefore, our decision to consider an LSV background that can vary from point to point in spacetime is well justified.

Since our interest is to integrate out only the fermionic matter fields, while keeping the gauge field as a classical constant background, the starting point is the fermionic functional trace associated with the action (3.22) with $\delta\Gamma^{\mu}_{\rm LSV}$, $H_{\mu\nu}$, k_F, and $k_{AF}=0$ equals to zero. Therefore, we consider

$$i\ln\det\left(i\not{D}-\mathscr{M}\right)=i\,\mathrm{Tr}\ln\left(i\not{D}-\mathscr{M}\right)=\frac{i}{2}\,\mathrm{Tr}\left[\ln\left(i\not{D}-\mathscr{M}\right)+\ln\left(-i\not{D}-\mathscr{M}^{\star}\right)\right]=\frac{i}{2}\,\mathrm{Tr}\ln\mathscr{O}, \tag{4.5}$$

where Tr denotes the functional trace including integration over spacetime coordinates and trace over spinor indices. In the second equality of Eq. (4.5), the second term is obtained from the first one by multiplying on the left by the matrix γ_5 and using the cyclic properties of the trace to obtain the result. For convenience, we introduce the compact notation

$$\mathscr{M}\equiv m+im_5\gamma_5+a_\mu\gamma^\mu+b_\mu\gamma^\mu\gamma_5,\qquad \mathscr{M}^{\star}\equiv m+im_5\gamma_5-a_\mu\gamma^\mu-b_\mu\gamma^\mu\gamma_5, \tag{4.6}$$

and adopt the Feynman slash notation $\not{D}\equiv\gamma^\mu D_\mu$. The squared operator $\mathscr{O}$ can be written in the form

$$\mathscr{O}=\left(i\not{D}-\mathscr{M}\right)\left(-i\not{D}-\mathscr{M}^{\star}\right)=\mathscr{K}\left[1+\mathscr{K}^{-1}\mathscr{X}\right], \tag{4.7}$$

with $\mathscr{K}\equiv D^2+m^2-e\Sigma^{\mu\nu}F_{\mu\nu}$ representing the minimal second-order differential operator, and the Lorentz-violating part given by

$$\begin{aligned}\mathscr{X}\equiv&-a^2+b^2-m_5^2+i\left(\partial\cdot a+2\,a\cdot D\right)+i\gamma_5\left(\partial\cdot b+2m_5m\right)+2im_5\not{b}-\gamma_5\left(\not{\partial}m_5\right.\\&\left.+2m_5\not{D}+2im_5\not{a}\right)+4\Sigma^{\mu\nu}\left(2ia_{[\mu}b_{\nu]}\gamma_5-2\gamma_5b_{[\mu}D_{\nu]}-\partial_{[\nu}a_{\mu]}-\gamma_5\,\partial_{[\nu}b_{\mu]}\right).\end{aligned} \tag{4.8}$$

Since the Lorentz-violating parameters are expected to be small (see Chapters 2 and 3 for discussions), the decomposition (4.7) proves particularly useful, as it allows for a systematic

expansion of the effective action in which $\mathscr{X}$ can be treated as a small perturbation around the minimal operator $\mathscr{K}^{-1}\mathscr{X}$,

$$\Gamma = -\frac{i}{2}\,\mathrm{Tr}\ln\mathscr{O} = -\frac{i}{2}\,\mathrm{Tr}\ln\mathscr{K} - \frac{i}{2}\,\mathrm{Tr}\left(\mathscr{K}^{-1}\mathscr{X}\right) + \frac{i}{4}\,\mathrm{Tr}\left(\mathscr{K}^{-1}\mathscr{X}\,\mathscr{K}^{-1}\mathscr{X}\right) + \cdots, \tag{4.9}$$

where the where the ellipsis indicate higher-order terms in $\mathscr{X}$. In the present Section, we restrict our analysis to contributions up to second order in the LSV background parameters. In this regard, it is important to note that the third term in Eq. (4.9) contains cubic and quartic powers of the Lorentz-violating structures and, hence, these contributions will be neglected in what follows. The term $\frac{i}{2}\,\mathrm{Tr}\ln\mathscr{K}$ is responsible for generating the usual Euler-Heisenberg contribution to electrodynamics, as discussed in [145, 146] and given by Eq. (4.1). In other words, Eq. 4.9 allows us to write an action of the form

$$\Gamma = \Gamma_0 + \Gamma_{\mathrm{LSV}}, \tag{4.10}$$

where $\Gamma_0 \equiv \Gamma_{\mathrm{EH}}$ denotes the Lorentz-invariant part of the effective action corresponding to the standard QED contribution and Γ_{LSV} encodes the contributions induced by the LSV background.

For the analysis that follows, we perform an analytic continuation from Minkowski to Euclidean spacetime (see Appendix A for details and conventions). We then apply a Wick rotation of the time coordinate in the squared operator $\mathscr{O}$ and the effective action takes the form

$$\bar{\Gamma} = -i\Gamma. \tag{4.11}$$

After this step, we keep only terms up to first and second order in the LSV parameters and express the inverse of the minimal operator using the Fock-Schwinger proper-time representation [145, 161]

$$\frac{1}{\bar{\mathscr{K}}} = \int_0^\infty ds\, e^{-s\bar{\mathscr{K}}}. \tag{4.12}$$

In what follows, we omit the bars to denote Euclidean quantities for notational simplicity. Nevertheless, the covariant derivative and all quantities in Euclidean space are assumed to follow the conventions established in Appendix A omitting the bars. By following this procedure, we obtain, at first order in the LSV parameters, the contribution to the effective action given by

$$\begin{aligned}\Gamma_{\mathrm{LSV}}\big|^{(1)} = -\frac{i}{2\mu^2}\,\mathrm{Tr}\int_0^\infty ds\Big\{ e^{\frac{s}{\mu^2}(D^2-m^2-e\Sigma^{\lambda\sigma}F_{\lambda\sigma})}\Big[\partial\cdot a + 2\,a\cdot D + \gamma_5\big(\partial\cdot b + 2m_5 m\big) \\ + 2i\Sigma^{\mu\nu}\big(\partial_\nu a_\mu + \gamma_5\partial_\nu b_\mu + 2\gamma_5 b_\mu D_\nu\big)\Big]\Big\},\end{aligned} \tag{4.13}$$

while the second-order LSV contribution terms are

$$\begin{aligned}\Gamma_{\rm LSV}\big|^{(2)} = &-\frac{1}{2\mu^2}\,\mathrm{Tr}\int_0^\infty ds\Big\{e^{\frac{s}{\mu^2}(D^2-m^2-e\Sigma^{\lambda\sigma}F_{\lambda\sigma})}\Big[a^2-b^2+m_5^2-4i\Sigma^{\mu\nu}\gamma_5 a_\mu b_\nu\Big]\Big\}\\ &-\frac{1}{4\mu^4}\,\mathrm{Tr}\int_0^\infty ds\int_0^\infty d\tau\Big\{e^{\frac{s}{\mu^2}(D^2-m^2-e\Sigma^{\lambda\sigma}F_{\lambda\sigma})}\Big[\partial\cdot a+2\,a\cdot D+\gamma_5\big(\partial\cdot b\\ &+2m_5 m\big)+2i\Sigma^{\mu\nu}\big(\partial_\nu a_\mu+\gamma_5\partial_\nu b_\mu+2\gamma_5 b_\mu D_\nu\big)+i\gamma_5\big(\partial\!\!\!/\, m_5+2m_5 D\!\!\!/\big)\Big]e^{\frac{\tau}{\mu^2}D^2}\\ &\times e^{-\frac{\tau}{\mu^2}(m^2+e\Sigma^{\gamma\rho}F_{\gamma\rho})}\Big[\partial\cdot a+2\,a\cdot D+\gamma_5\big(\partial\cdot b+2m_5 m\big)+2i\Sigma^{\alpha\beta}\big(\partial_\beta a_\alpha\\ &+\gamma_5\partial_\beta b_\alpha+2\gamma_5 b_\alpha D_\beta\big)+i\gamma_5\big(\partial\!\!\!/\, m_5+2m_5 D\!\!\!/\big)\Big]\Big\}. \end{aligned}\tag{4.14}$$

In both Eqs. (4.13) and (4.14) μ denotes a mass scale introduced to render the proper-time parameter dimensionless and also plays the role of a regulating parameter from the point of view of spectral zeta-function regularization [146]. It is also worth noting that in Eqs. (4.13) and (4.14) we have already discarded terms containing an odd number of γ-matrices, since their traces vanish identically.

In what follows, we evaluate these contributions separately, since the expressions are lengthy and technically involved, particularly in the second-order case. Many of the steps presented below were obtained with the aid of computer-based calculations. For this reason, only the general idea and the main flow of the calculations will be outlined. The terms involving two proper-time integrals require extensive Clifford algebra manipulations, in particular due to the presence of products of several Lorentz generators in combination with γ_5. For this reason, the computation of these structures was carried out separately, order by order in the field strength, and independently cross-checked using the xAct package in Mathematica software.

4.1.1 First-order LSV corrections

Considering the functional trace, defined as $\mathrm{Tr} = \mathrm{tr}\int d^4x\,\delta^4(x-x')\big|_{x=x'}$, and making use of the trace cyclic property to change $e^{-\frac{\tau}{\mu^2}D^2}$ position, the expression (4.13) reads

$$\begin{aligned}\Gamma_{\rm LSV}\big|^{(1)} = &-\frac{i}{2\mu^2}\int d^4x\int_0^\infty ds\Big\{e^{-\frac{sm^2}{\mu^2}}\,\mathrm{tr}\,e^{-\frac{s}{\mu^2}(e\Sigma^{\lambda\sigma}F_{\lambda\sigma})}\Big[\partial\cdot a+2\,a\cdot D+\gamma_5\big(\partial\cdot b+2m_5 m\big)\\ &+2i\Sigma^{\mu\nu}\big(\partial_\nu a_\mu+\gamma_5\partial_\nu b_\mu+2\gamma_5 b_\mu D_\nu\big)\Big]e^{\frac{s}{\mu^2}D^2}\delta^4(x-x')\big|_{x=x'}\Big\}. \end{aligned}\tag{4.15}$$

At this stage, the heat-kernel function is introduced through the result [146]

$$K(s) = e^{\frac{s}{\mu^2}D^2}\delta^4(x-x')\big|_{x=x'} = \frac{\mu^4}{16\pi^2 s^2}\det{}^{1/2}\left[\frac{iesF}{\mu^2\sinh\left(\frac{ies}{\mu^2}F\right)}\right].\tag{4.16}$$

It is worth noting that the terms containing a single gauge–covariant derivative acting on the kernel vanish, since [146]

$$D^\mu e^{\frac{s}{\mu^2}D^2}\delta^4(x-x')\big|_{x=x'} = 0.\tag{4.17}$$

Taking these considerations into account, we can write Eq. (4.15) in the form

$$\Gamma_{\rm LSV}\big|^{(1)} = \frac{i\mu^4}{32\pi^2}\int d^4x\int_0^\infty ds\left\{\frac{1}{s^2}\,e^{-\frac{sm^2}{\mu^2}}\,\mathrm{tr}\,e^{-\frac{s}{\mu^2}(e\Sigma^{\lambda\sigma}F_{\lambda\sigma})}\Big[\partial\cdot a-\gamma_5\big(\partial\cdot b-2m_5 m\big)\right.$$
$$\left.+2i\Sigma^{\mu\nu}\big(\partial_\nu a_\mu-\gamma_5\partial_\nu b_\mu\big)\Big]\det{}^{1/2}\left[\frac{iesF}{\mu^2\sinh\left(\frac{ies}{\mu^2}F\right)}\right]\right\}. \tag{4.18}$$

In the weak background electromagnetic field approximation, where $[D_\mu, F_{\nu\kappa}] = \partial_\mu F_{\nu\kappa} = 0$ and which is useful to a avoid higher-order derivative terms, we proceed with the expansion

$$\det{}^{1/2}\left[\frac{iesF}{\mu^2\sinh\left(\frac{ies}{\mu^2}F\right)}\right] = 1+\frac{e^2s^2}{12\mu^4}\,\mathrm{Tr}\,(F^2)+\frac{e^4s^4}{72\mu^8}\left[\frac{1}{4}F^4+\frac{1}{5}\,\mathrm{Tr}\,(F^4)\right]+O\big(F^6\big). \tag{4.19}$$

In this way, the traces of the exponentials are explicitly given by

$$\begin{aligned}\mathrm{tr}\left[e^{-\frac{s}{\mu^2}(e\Sigma^{\lambda\sigma}F_{\lambda\sigma})}\right] &= \mathrm{tr}\left[\delta^\mu_\mu-\frac{es}{\mu^2}\Sigma^{\lambda\sigma}F_{\lambda\sigma}+\frac{e^2s^2}{2\mu^4}\left(\Sigma^{\lambda\sigma}F_{\lambda\sigma}\right)^2-\frac{e^3s^3}{6\mu^6}\left(\Sigma^{\lambda\sigma}F_{\lambda\sigma}\right)^3\right.\\ &\quad\left.+\frac{e^4s^4}{24\mu^8}\left(\Sigma^{\lambda\sigma}F_{\lambda\sigma}\right)^4+\cdots\right]\\ &= 4+\frac{e^2s^2}{\mu^4}F^2+\frac{e^4s^4}{2\mu^8}\left(\frac{1}{4}F^4-\frac{1}{3}F^{\mu\nu}F_{\nu\alpha}F^{\alpha\beta}F_{\beta\mu}\right)+O\big(F^6\big),\end{aligned} \tag{4.20}$$

$$\mathrm{tr}\left[e^{-\frac{s}{\mu^2}(e\Sigma^{\lambda\sigma}F_{\lambda\sigma})}\gamma_5\right] = -\frac{e^2s^2}{\mu^4}(\tilde{F}^{\mu\nu}F_{\mu\nu})-\frac{e^4s^4}{12\mu^8}F^2(\tilde{F}^{\mu\nu}F_{\mu\nu})+O\big(F^6\big), \tag{4.21}$$

$$\mathrm{tr}\left[e^{-\frac{s}{\mu^2}(e\Sigma^{\lambda\sigma}F_{\lambda\sigma})}\Sigma^{\mu\nu}\right] = -\frac{2es}{\mu^2}F^{\mu\nu}-\frac{e^3s^3}{\mu^6}\left[\frac{1}{2}F^2F^{\mu\nu}+\frac{2}{3}F^{\mu\lambda}F_{\lambda\sigma}F^{\sigma\nu}\right]+O\big(F^5\big), \tag{4.22}$$

and

$$\begin{aligned}\mathrm{tr}\left[e^{-\frac{s}{\mu^2}(e\Sigma^{\lambda\sigma}F_{\lambda\sigma})}\Sigma^{\mu\nu}\gamma_5\right] &= \frac{2es}{\mu^2}\tilde{F}^{\mu\nu}+\frac{e^3s^3}{12\mu^6}\Big[F^2\tilde{F}^{\mu\nu}+\tilde{F}_{\lambda\sigma}F^{\lambda\sigma}F^{\mu\nu}+2\tilde{F}_{\lambda\sigma}F^{\mu\lambda}F^{\sigma\nu}-F^{\mu\lambda}F_{\lambda\sigma}\tilde{F}^{\sigma\nu}\\ &\quad-\tilde{F}^{\mu\lambda}F_{\lambda\sigma}F^{\sigma\nu}\Big]+O\big(F^5\big),\end{aligned} \tag{4.23}$$

with $\tilde{F}_{\mu\nu} = \frac{i}{2}\varepsilon_{\mu\nu\alpha\beta}F^{\alpha\beta}$ denoting the dual field strength tensor in the Euclidian spacetime.

By inserting the expressions derived above into Eq. (4.18), evaluating the proper-time integrals (see Appendix A for a list of these integrals), and neglecting contributions that, in the weak background electromagnetic field approximation, reduce to total derivative terms after integration by parts, we obtain the only surviving first-order LSV contribution to the effective action returning to the Minkowski spacetime given by

$$\Gamma_{\rm LSV}\big|^{(1)} = -\frac{e^2}{16\pi^2 m}\int d^4x\, m_5\tilde{F}^{\mu\nu}F_{\mu\nu}\,. \tag{4.24}$$

The axial mass parameter $m_5(x)$ gives rise to a nontrivial contribution to the effective action at first order in LSV in Eq. (4.24) with the same local structure as an axion–photon

coupling [166]. In contrast, for constant m_5, this contribution reduces to a surface term, up to integration by parts, and hence does not lead to physical modifications of the electromagnetic dynamics. Nevertheless, even in the spacetime-dependent case, $m_5(x)$ should be regarded as an external pseudoscalar background rather than a propagating axion field, since no kinetic or potential terms for m_5 are generated at this order.

An interesting point that can be raised concerns the relevance of terms similar to the action (4.24) in condensed matter systems. Nonpropagating excitations, although in some cases dependent on space-time coordinates, which correspond to an axion-like parameter, have already been reported in several low-energy scenarios; for a detailed discussion, see the review [162]. Some of these excitations are particularly noteworthy because they arise in materials with emergent Lorentz-symmetry, as discussed in Refs. [163–165]. In this context, approaches such as the one adopted in this work may be useful for the description of these systems.

Since the action (4.24) is the only term contributing at first-order in LSV, we show in what follows that additional axion-like terms induced by Lorentz breaking emerge at second-order in LSV corrections.

4.1.2 Second-order LSV corrections

We now turn to the evaluation of the second-order contributions to Lorentz violation encoded in $\Gamma_{\rm LSV}\big|^{(2)}$. The first line of (4.14) contains only a proper-time integral and can thus be computed in a straightforward way by applying the same procedures used in the derivation of the first-order LSV corrections. In particular, one makes use of the cyclic property of the trace and the expansions given in Eqs. (4.19) - (4.21), what allows us to write Eq. (4.14) in the form

$$\begin{aligned}\Gamma_{\rm LSV}\big|^{(2)} = &-\frac{1}{2\mu^2}\int d^4x\int_0^\infty ds\Big\{e^{-\frac{sm^2}{\mu^2}}\,\mathrm{tr}\,e^{-\frac{s}{\mu^2}(e\Sigma^{\lambda\sigma}F_{\lambda\sigma})}\Big[a^2-b^2+m_5^2-4i\Sigma^{\mu\nu}\gamma_5 a_\mu b_\nu\Big]K(s)\Big\}\\
&-\frac{1}{4\mu^4}\int d^4x\int_0^\infty ds\int_0^\infty d\tau\Big\{e^{-\frac{(s+\tau)m^2}{\mu^2}}\,\mathrm{tr}\,e^{-\frac{s}{\mu^2}(e\Sigma^{\lambda\sigma}F_{\lambda\sigma})}\Big[\partial\cdot a+2\,a\cdot D+\gamma_5\big(\partial\cdot b\\
&+2m_5 m\big)+2i\Sigma^{\mu\nu}\big(\partial_\nu a_\mu+\gamma_5\partial_\nu b_\mu+2\gamma_5 b_\mu D_\nu\big)+i\gamma_5\big(\not\partial\, m_5+2m_5\not D\big)\Big]e^{-\frac{\tau}{\mu^2}(e\Sigma^{\gamma\rho}F_{\gamma\rho})}\\
&\times e^{\frac{\tau}{\mu^2}D^2}\Big[\partial\cdot a+2\,a\cdot D+\gamma_5\big(\partial\cdot b+2m_5 m\big)+2i\Sigma^{\alpha\beta}\big(\partial_\beta a_\alpha+\gamma_5\partial_\beta b_\alpha+2\gamma_5 b_\alpha D_\beta\big)\\
&+i\gamma_5\big(\not\partial\, m_5+2m_5\not D\big)\Big]e^{-\frac{\tau}{\mu^2}D^2}e^{\frac{(s+\tau)}{\mu^2}D^2}\delta^4(x-x')\Big\}.\end{aligned}\tag{4.25}$$

On the other hand, the part of Eq. (4.25) containing two proper-time integrals involves more complicated operator structures. Their treatment requires the use of nontrivial commutation relations between derivative operators and spacetime dependent LSV parameters. To evaluate such commutators, we employ the identities derived from the Baker-Campbell-Hausdorff series to write

$$
\begin{aligned}
e^{\frac{\tau}{\mu^2}D^2}\left(\partial_\mu b^\mu + 2b^\mu D_\mu\right)e^{-\frac{\tau}{\mu^2}D^2} &= \partial_\mu b^\mu + 2b^\mu D_\mu + \frac{\tau}{\mu^2}[D^2, \partial_\mu b^\mu + 2b^\mu D_\mu] \\
&\quad + \frac{\tau^2}{2\mu^4}[D^2,[D^2,\partial_\mu b^\mu + 2b^\mu D_\mu]] + \ldots \\
&= \left(e^{-\frac{2ie\tau}{\mu^2}F}\right)_\mu{}^\nu \left(\partial_\nu b^\mu + 2b^\mu D_\nu\right) + (\partial_\nu b^\mu)\Pi_\mu{}^\nu, \qquad (4.26)
\end{aligned}
$$

with

$$
\begin{aligned}
\left(e^{-\frac{2ie\tau}{\mu^2}F}\right)_\mu{}^\nu (\partial_\nu b^\mu + 2b^\mu D_\nu) = \Big[\delta_\mu^\nu + \frac{2i\tau e}{\mu^2}F_\mu{}^\nu - \frac{2\tau^2 e^2}{\mu^4}F_{\mu\lambda}F^{\lambda\nu} - \frac{4i\tau^3 e^3}{3\mu^6}F_{\mu\lambda}F^{\lambda\gamma}F_\gamma{}^\nu \\
+ \frac{2\tau^4 e^4}{3\mu^8}F_{\mu\lambda}F^{\lambda\gamma}F_{\gamma\zeta}F^{\zeta\nu} + O\left(F^5\right)\Big](\partial_\nu b^\mu + 2b^\mu D_\nu) \qquad (4.27)
\end{aligned}
$$

and

$$
\begin{aligned}
\Pi_\mu{}^\nu = \frac{2\tau}{\mu^2}\Big\{ & 2D_\mu D^\nu + ieF_\mu{}^\nu + \frac{ie\tau}{\mu^2}\left[4F_{\mu\lambda}D^\lambda D^\nu + 2F^{\nu\lambda}D_\lambda D_\mu + 3ieF_{\mu\lambda}F^{\lambda\nu}\right] \\
& - \frac{2e^2\tau^2}{3\mu^4}\left[6F_{\mu\lambda}F^{\lambda\gamma}D_\gamma D^\nu + 2F^{\nu\lambda}F_{\lambda\gamma}D^\gamma D_\mu + 6F_{\mu\lambda}F^{\nu\gamma}D_\gamma D^\lambda - 5ieF_{\mu\lambda}F^{\lambda\gamma}F_\gamma{}^\nu\right] \\
& - \frac{ie^3\tau^3}{3\mu^6}\Big[8F_{\mu\lambda}F^{\lambda\gamma}F_{\gamma\zeta}D^\zeta D^\nu + 2F^{\nu\lambda}F_{\lambda\gamma}F^{\gamma\zeta}D_\zeta D_\mu - 5ieF_{\mu\lambda}F^{\lambda\gamma}F_{\gamma\zeta}F^{\zeta\nu} \\
& + 4\left(3F_\mu{}^\lambda F_\gamma{}^\nu + 2F_{\mu\gamma}F^{\nu\lambda}\right)F_{\lambda\zeta}D^\zeta D^\gamma\Big] + \frac{4e^4\tau^4}{15\mu^8}\Big[5F_{\mu\lambda}F^{\lambda\gamma}F_{\gamma\zeta}F^{\zeta\xi}D_\xi D^\nu \\
& + F^{\nu\lambda}F_{\lambda\gamma}F^{\gamma\zeta}F_{\zeta\xi}D^\xi D_\mu + 5\left(2F_\mu{}^\lambda F_\gamma{}^\nu F_\lambda{}^\zeta + F_{\mu\gamma}F^{\nu\lambda}F_\lambda{}^\zeta + 2F_\mu{}^\zeta F^{\nu\lambda}F_{\lambda\gamma}\right)F_{\zeta\xi}D^\xi D^\gamma\Big] + O\left(F^5\right)\Big\}. \qquad (4.28)
\end{aligned}
$$

Another useful relation is

$$
\begin{aligned}
e^{\frac{\tau}{\mu^2}D^2}b^\mu e^{-\frac{\tau}{\mu^2}D^2} &= b^\mu + \frac{2\tau}{\mu^2}(\partial_\gamma b^\mu)\Big[\delta_\rho^\gamma + \frac{ie\tau}{\mu^2}F^\gamma{}_\rho - \frac{2e^2\tau^2}{3\mu^4}F^{\gamma\sigma}F_{\sigma\rho} - \frac{ie^3\tau^3}{3\mu^6}F^{\gamma\sigma}F_{\sigma\zeta}F^\zeta{}_\rho \\
&\quad + \frac{2e^4\tau^4}{15\mu^8}F^{\gamma\sigma}F_{\sigma\zeta}F^{\zeta\xi}F_{\xi\rho} + O\left(F^5\right)\Big]D^\rho \\
&= b^\mu + (\partial_\gamma b^\mu)\bar{\Pi}^\gamma{}_\rho D^\rho. \qquad (4.29)
\end{aligned}
$$

It is worth emphasizing that these relations are valid for a background with constant field strength, i.e., $[D_\mu, D_\nu] = -ieF_{\mu\nu}$ = constant which we have been assuming. Using these results, we can proceed to compute the relevant contributions to the effective action, which are given by

$$
\begin{aligned}
\Gamma_{\rm LSV}\big|^{(2)} = &-\frac{\mu^2}{32\pi^2}\int d^4x\int_0^\infty ds\,\frac{1}{s^2}\,e^{-\frac{sm^2}{\mu^2}}\Big\{\Big[4+\frac{e^2s^2}{\mu^4}F^2+\frac{e^4s^4}{2\mu^8}\Big(\frac{1}{4}F^4-\frac{1}{3}F^{\mu\nu}F_{\nu\alpha}F^{\alpha\beta}F_{\beta\mu}\Big)\Big]\\
&\times\big(a^2+b^2-m_5^2\big)-i\frac{8es}{\mu^2}\tilde{F}^{\mu\nu}a_\mu b_\nu-i\frac{e^3s^3}{3\mu^6}\Big[F^2\tilde{F}^{\mu\nu}+\tilde{F}_{\lambda\sigma}F^{\lambda\sigma}F^{\mu\nu}+2\tilde{F}_{\lambda\sigma}F^{\mu\lambda}F^{\sigma\nu}\\
&-F^{\mu\lambda}F_{\lambda\sigma}\tilde{F}^{\sigma\nu}-\tilde{F}^{\mu\lambda}F_{\lambda\sigma}F^{\sigma\nu}\Big]a_\mu b_\nu\Big\}-\frac{1}{4\mu^4}\int d^4x\int_0^\infty ds\int_0^\infty d\tau\,\Big\{e^{-\frac{(s+\tau)m^2}{\mu^2}}\\
&\times\,\mathrm{tr}\,e^{-\frac{s}{\mu^2}(e\Sigma^{\lambda\sigma}F_{\lambda\sigma})}\Big[2i\Sigma^{\mu\nu}\big(\partial_\nu a_\mu-\gamma_5\partial_\nu b_\mu\big)-\gamma_5\big(\partial\cdot b+2\,b\cdot D-2m_5m\big)+\partial\cdot a\\
&+2\,a\cdot D-\gamma_5\big(\not{\partial}\,m_5+2m_5\not{D}-2m\not{b}\big)\Big]\,e^{-\frac{\tau}{\mu^2}(e\Sigma^{\gamma\rho}F_{\gamma\rho})}\Big[2i\Sigma^{\mu\nu}\big(\partial_\nu a_\mu-\gamma_5\partial_\nu b_\mu\big)\\
&+\big(e^{\frac{2ie\tau}{\mu^2}F}\big)_\mu{}^\nu\big(\partial_\nu a^\mu+2a^\mu D_\nu-\gamma_5\partial_\nu b^\mu-2\gamma_5 b^\mu D_\nu-\gamma_5\gamma^\mu\partial_\nu m_5-2\gamma_5\gamma^\mu m_5D_\nu\big)\\
&+\big(\partial_\nu a^\mu-\gamma_5\partial_\nu b^\mu-\gamma_5\gamma^\mu\partial_\nu m_5\big)\Pi_\mu{}^\nu+2\gamma_5 m\big(m_5+\not{b}\big)+2\gamma_5 m\big(\partial_\gamma m_5+\partial_\gamma\not{b}\big)\bar{\Pi}^\gamma{}_\rho D^\rho\Big]\\
&\times\,e^{\frac{(s+\tau)}{\mu^2}D^2}\delta^4(x-x')\Big\},
\end{aligned}
\tag{4.30}
$$

where the result of the action of two gauge-covariant derivatives on the kernel can be expressed as [146]

$$
\begin{aligned}
D^\mu D^\nu e^{\frac{(s+\tau)}{\mu^2}D^2}\delta^4(x-x')\big|_{x=x'} &= \left[\frac{-ieF}{e^{2ie(s+\tau)F/\mu^2}-1}\right]^{\nu\mu}K(s+\tau)\\
&=\Big[-\frac{\mu^2}{2(s+\tau)}\delta^{\mu\nu}-\frac{ie}{2}F^{\mu\nu}+\frac{e^2(s+\tau)}{6\mu^2}F^{\mu\kappa}F_\kappa{}^\nu\\
&\quad+\frac{e^4(s+\tau)^3}{90\mu^6}F^{\mu\kappa}F_{\kappa\theta}F^{\theta\eta}F_\eta{}^\nu\Big]K(s+\tau).
\end{aligned}
\tag{4.31}
$$

The terms involving two proper-time integrals require extensive Clifford algebra manipulations, in particular due to the presence of products of several Lorentz generators in combination with γ_5. For this reason, the computation of these structures was carried out separately, order by order in the field strength, and independently cross-checked using the xAct package in Mathematica [167]. After evaluating the corresponding traces, performing the integrations over the proper times s and τ, and returning to Minkowski spacetime, one arrives at

$$
\Gamma_{LSV}|^{(2)} = \sum_{n=1}^{4}\Gamma_{F^n},
\tag{4.32}
$$

where n labels the power of the field strength appearing in each term of the effective action. For $n=1$, we then obtain corrections linear in F and second-order in the LSV background, given by

$$
\Gamma_{F^1} = \frac{e}{16\pi^2 m}\int d^4x\left\{\left[\frac{1}{\epsilon}-\gamma_E+\ln\left(\frac{\mu^2}{m^2}\right)\right]2a_\mu b_\nu\tilde{F}^{\mu\nu}+2m_5(\partial_\mu a_\nu)\tilde{F}^{\mu\nu}\right\},
\tag{4.33}
$$

where γ_E is the Euler-Mascheroni constant. The term $a_\mu b_\nu F^{\mu\nu}$ in the action (4.33) originates from a purely divergent contribution. This corresponds to shifting the vacuum, since this

infinity contribution appears in the tadpole of the photon field. In contrast, the term proportional to $m_5(\partial_\mu a_\nu)\tilde{F}^{\mu\nu}$ is finite and suggests that LSV background can effectively act as a source term in Maxwell equations.

For $n=2$, the contribution takes the following form

$$\Gamma_{F^2} = \frac{e^2}{16\pi^2 m^2}\int d^4x\left[\frac{1}{3}\left(m_5^2+b^2\right)F^2+\frac{1}{6}(a\cdot b)F_{\mu\nu}\tilde{F}^{\mu\nu}\right]. \tag{4.34}$$

In this quadratic sector of the effective action, the second-order corrections in LSV contribute to the Maxwell equations in a nontrivial way. It is important to note that, as in the case of the contribution to the photon kinetic sector given by Eq. (4.24), the new terms appearing in Eq. (4.34) also contain axion-like contributions. However, it should be emphasized that these are not dynamical axions, but rather axion-type parameters that may be related to possible phenomenological applications.

Now, for $n=3$, we obtain that

$$\Gamma_{F^3} = \frac{e^3}{16\pi^2 m^4}\int d^4x\left\{\frac{37}{96}a^\mu b^\nu F_{\mu\nu}\left(F\cdot\tilde{F}\right)-\frac{7}{5}\frac{m_5}{m}\left(\partial^\mu a^\nu\right)F_{\mu\nu}\left[F^2-\frac{1}{2}(F\cdot\tilde{F})\right]\right\}. \tag{4.35}$$

Finally, but not least, we obtain the contribution for $n=4$, given by

$$\begin{aligned}\Gamma_{F^4} = -\frac{e^4}{16\pi^2 m^6}\int d^4x\Bigg\{&\frac{m_5^2}{4}\left[\frac{1}{9}F^4+\frac{7}{45}\left(F\cdot\tilde{F}\right)\right]+\frac{523}{5472}\left(a\cdot b\right)F^2\left(F\cdot\tilde{F}\right)\\&+\frac{b^2}{45}\left[F^4+2\left(F\cdot\tilde{F}\right)^2\right]+\frac{2}{45}b^\mu b_\nu F_{\mu\kappa}F^{\kappa\nu}F^2-\frac{817}{720}a^\mu b_\nu F_{\mu\kappa}F^{\kappa\nu}\left(F\cdot\tilde{F}\right)\\&-\frac{m_5}{m}\left[\frac{31}{60}\left(\partial^\mu a_\nu\right)F_{\mu\kappa}F^{\kappa\nu}\left(F\cdot\tilde{F}\right)+\frac{2}{25}\left(\partial\cdot b\right)\left(F\cdot\tilde{F}\right)^2-12\left(\partial^\mu b_\nu\right)F_{\mu\kappa}F^{\kappa\nu}F^2\right]\Bigg\}.\end{aligned} \tag{4.36}$$

To write these expressions elegantly for the effective action corrections, we use the identities $F_{\mu\kappa}\tilde{F}^{\kappa\nu}=-\frac{1}{4}\delta^\nu_\mu, F\cdot\tilde{F}$ and $F_{\mu\nu}F^{\mu\nu}=F\cdot F$.

The results (4.33) and (4.35) point to a violation of Furry's theorem. This theorem states that any Feynman diagram containing a closed fermion loop with an odd number of external photon lines gives a vanishing contribution to physical amplitudes [168]. This occurs because the QED interaction is invariant under charge conjugation, while the photon field changes sign under this transformation. As a consequence, diagrams related by reversing the direction of the fermion loop cancel each other exactly when the number of photon vertices is odd. Furry's theorem plays an important role in simplifying perturbative calculations in QED and explains, e.g., why processes such as single-photon or three-photon amplitudes generated by a fermion loop do not contribute to the effective action.

The seminal work [169] studies the validity of Furry's theorem in the presence of first-order corrections in LSV and shows that only CPT-even fermionic sectors are expected to violate this theorem. In our case, where the LSV background depends on spacetime, the terms that violate Furry's theorem arise from the mixing of two distinct LSV sectors and appear only at second-order, with an overall CPT-even dependence. This indicates that the results

on the violation of Furry's theorem obtained in Ref. [169] can be extended to second-order contributions in LSV.

Finally, we obtain the second-order LSV contribution to photon–photon scattering, given by Eq. (4.36). Actually, this set of quartic terms in the field strengths of the photon can be discussed in the context of the anomalous vertices in the electroweak theory. Moreover, the Z^0 field also couples, through weak coupling constant, to electron-positron field so that as similar neutral four-vertices can also appear associated Z^0 field [170, 171]. This means that they may be used to constrain the corresponding parameters through photon–photon scattering data from the ATLAS and CMS experiments [147–149]. Also, we should point out that quartic terms cast in Eq. (4.36) yield tree-level contributions to the photon-photon scattering.

At this point, it is worth commenting on the absence of CFJ-type terms, of the form $\sim A_\mu \tilde{F}^{\mu\nu}$. In Ref. [130], it was shown that the calculation of the vacuum polarization with first-order insertions of the term $b_\mu \gamma^\mu \gamma_5$ and constant b_μ, leads to a CFJ-type correction to the effective action at second-order in the photon field, with $(k_{AF})^\mu = \frac{3}{16\pi^2} b^\mu$. However, it was emphasized that this result depends on the regularization scheme employed. In our calculation, the electromagnetic background is frozen, $F_{\mu\nu} =$ constant, hence avoiding contributions involving higher-derivative and CFJ-type terms. Once we freeze the field strength, it is equivalent to adopting the Fock–Schwinger gauge, $A_\mu = -\frac{1}{2} F_{\mu\nu} x^\nu$, and consequently it becomes clear that the effective action is written entirely in terms of $F_{\mu\nu}$. There is no way the gauge potential explicitly appears.

A additional remark concerns the fact that, if we restrict ourselves to the regime in which the coefficients are constant, in addition to discarding terms involving derivatives acting on the LSV background, we must also neglect the contributions depending on a_μ and m_5 at all orders in the field strength of the corrected effective action. This follows from the fact that one can perform a field redefinition from the outset to eliminate these terms, indicating that they cannot generate physical effects, as discussed in Sect. 6.1.

In this regard, by setting the parameters a_μ and m_5 to zero and assuming b_μ to be constant in Eq. (4.34), one obtains

$$\Gamma_{F^2} = \frac{e^2}{48\pi^2 m^2} \int d^4x \, b^2 F^2. \tag{4.37}$$

In contrast to the result presented in work [155], when considering in Eq. (4.37) the particular case in which b_μ is light-like, we find that the quadratic photon sector does not receive contributions from second-order in LSV. This discrepancy stems from the use of different parametrizations in the construction of the quadratic operator given in Eq. (4.5). In the present work, we make use of the properties of the γ_5 matrix together with the cyclicity of the trace, whereas Ref. [155] adopts a parametrization that effectively changes the sign of the mass term m and of $b_\mu \gamma^\mu \gamma_5$. As a consequence, a relative sign difference in the mass term m inside of $\mathscr{M}^*$, Eq. (4.6), appears when comparing the two approaches.

This ambiguity in the parametrization of the quadratic Dirac operator is related to the so-called multiplicative anomaly (see, e.g., [172–174] for the details). In the next section, we revisit the calculation of the effective action with contributions from two constant Lorentz-violating parameters, b_μ and $H_{\mu\nu}$, and analyze this issue in a fully general scenario, with arbitrary parametrization. In the present work, we choose to use the parametrization implemented through the γ_5 matrix, since it is the only one consistent with all results available in the literature obtained via explicit Feynman-diagram loop calculations in presence of LSV, such as those reported in [169, 179].

In the next subsection, we analyze how the quadratic sector, composed of the results (4.24) and (4.34), modifies Maxwell's equations and the conservation of the energy–momentum tensor. We also derive the local dispersion relation associated with this corrections.

4.1.3 Modified Maxwell equations

The kinetic sector that contributes to vacuum Maxwell equations is given by

$$\Gamma_{\text{kinetic}} = \Gamma_{\text{Maxwell}} + \Gamma_{\text{LSV}}\big|^{(1)} + \Gamma_{F^2} = -\frac{1}{4}\int d^4x \Big[\big(1+c_1\big)F^2 + (c_2+c_3)\tilde{F}^{\mu\nu}F_{\mu\nu}\Big], \tag{4.38}$$

where we have used the definition of the fine-structure constant $\alpha = \frac{e^2}{4\pi}$ and the following compact notations:

$$c_1 = -\frac{\alpha}{3\pi m^2}\big(m_5^2 + b^2\big), \tag{4.39}$$

$$c_2 = -\frac{\alpha}{6\pi m^2}(a\cdot b), \tag{4.40}$$

$$c_3 = \frac{\alpha}{\pi m} m_5\,. \tag{4.41}$$

From the variational principle applied to the photon field, we obtain the covariant Maxwell equations in the form

$$\big(1+c_1\big)\partial_\mu F^{\mu\nu} + \big(\partial_\mu c_1\big)F^{\mu\nu} + \big[\partial_\mu\big(c_2+c_3\big)\big]\tilde{F}^{\mu\nu} = 0, \tag{4.42}$$

where the Bianchi identity $\partial_\mu \tilde{F}^{\mu\nu} = 0$ holds. Since LSV is expected to be small, Eq. (4.42) can be rewritten as $\partial_\mu F^{\mu\nu} = \big(1+c_1\big)^{-1}(...)$, allowing for a perturbative expansion of the right-hand side in powers of c_1. Keeping terms up to second-order in the LSV parameters, Eq. (4.42) reduces to

$$\partial_\mu F^{\mu\nu} = \big(\partial_\mu c_1\big)F^{\mu\nu} + \big[\partial_\mu\big(c_2+c_3\big)\big]\tilde{F}^{\mu\nu}. \tag{4.43}$$

The energy–momentum tensor conservation can be explicitly verified by contracting the right-hand side of Eq. (4.43) with $F_{\nu\rho}$ and subsequently constructing a continuity equation of the form $\partial_\mu(\dots)$. This procedure leads to

$$\partial_\mu\Big[\big(1+c_1\big)T^\mu{}_\kappa\Big] = \big(1+c_1\big)J^\mu F_{\mu\kappa} + \frac{1}{4}(\partial_\kappa c_1)F_{\alpha\beta}F^{\alpha\beta} + \frac{1}{4}\big[\partial_\kappa\big(c_2+c_3\big)\big]F_{\alpha\beta}\tilde{F}^{\alpha\beta}, \tag{4.44}$$

where $T^{\mu}{}_{\kappa} = F^{\mu\nu}F_{\nu\kappa} + \frac{1}{4}\delta^{\mu}_{\kappa}F_{\alpha\beta}F^{\alpha\beta}$ is the standard energy–momentum tensor of Maxwell electrodynamics. In Eq. (4.44), the source term J^{ν} may arise either from the coupling of the photon field to matter or from a purely LSV-induced source term originating from the effective action (4.33), when it is divergence-free. We observe that allowing the LSV background to depend on the spacetime coordinates leads to a violation of the conservation of the energy–momentum tensor, which is restored in the limit of a constant background.

This non-conservation of the energy-momentum tensor requires a careful assessment of the domain of validity of the effective description. It is well known that whenever a Lorentz-violating background exhibits spacetime dependence, the associated energy-momentum tensor is generally not conserved [62] and, in certain cases, a symmetric energy-momentum tensor cannot even be consistently defined [122, 176]. The immediate physical interpretation of this non-conservation is that the electromagnetic field can exchange energy with the Lorentz-violating background, thereby either losing or gaining energy. However, this non-conservation arises from the fact that we are considering only a subsystem in which the coefficients $a_{\mu}(x)$, $b_{\mu}(x)$, and $m_5(x)$ are regarded as nondynamical effective external backgrounds. In this framework, Lorentz symmetry is broken explicitly, and the apparent non-conservation of the electromagnetic energy-momentum tensor can be interpreted as an exchange of energy and momentum with the background sector. See Refs. [55, 60, 62] for further discussion. In Ref. [62], it is shown that energy-momentum conservation is restored once the full dynamical system is considered. In particular, when the Lorentz-violating background arises from spontaneous Lorentz-symmetry breaking, the effective Lorentz-violating coefficients correspond to vacuum expectation values of underlying dynamical fields rather than prescribed external sources. As a consequence, the background itself carries dynamical degrees of freedom, and any apparent non-conservation of energy and momentum in the observable sector can be understood as an exchange with the fields responsible for the spontaneous breaking. In this framework, the total energy-momentum tensor is conserved.

In Refs. [62, 121, 175], a series of no-go results were established and discussed, demonstrating the incompatibility between explicit local Lorentz-symmetry breaking and the geometric framework underlying gravitational theories formulated on Riemann and Riemann–Cartan manifolds. In such geometries, diffeomorphism invariance together with the Bianchi identities impose constraints on the gravitational field equations that require the appropriate covariant conservation of the energy-momentum tensor. This consistency condition can be naturally satisfied when Lorentz symmetry is broken spontaneously, since the Lorentz-violating coefficients then arise as vacuum expectation values of underlying dynamical fields and obey their own equations of motion. Consequently, in flat spacetime, spacetime-dependent nondynamical backgrounds may be consistently employed as an effective description, provided that the sector described by the theory is not regarded as a closed system. In this case, the apparent non-conservation of the energy-momentum tensor can be interpreted as an exchange of energy and momentum with the external background. The true content of the no-go results is therefore a restriction on the gravitational extension of such constructions, rather than on

their use as effective field theories in Minkowski spacetime.

In the following, we demonstrate that the spacetime-dependent coefficients $a_\mu(x)$, $b_\mu(x)$, and $m_5(x)$ produce nontrivial corrections to the photon local dispersion relation. These modifications cause the vacuum to behave as an optically active medium, supporting non-propagating modes typically associated with dichroism, inducing the possbility of absorption and attenuation effects in electromagnetic wave propagation. To investigate these phenomena, we start from the $\nu = 0$ component of Eq. (4.43), which allow us to write the Gauss law for the electric field as

$$\boldsymbol{\nabla}\cdot\boldsymbol{E} = \big(\boldsymbol{\nabla} c_1\big)\cdot\boldsymbol{E} + \big[\boldsymbol{\nabla}\big(c_2+c_3\big)\big]\cdot\boldsymbol{B}\,. \tag{4.45}$$

Similarly, the Ampère–Maxwell equation in vacuum becomes

$$\boldsymbol{\nabla}\times\boldsymbol{B} - \partial_t\boldsymbol{E} = \big(\boldsymbol{\nabla} c_1\big)\times\boldsymbol{B} - \big(\partial_t c_1\big)\boldsymbol{E} - \big[\boldsymbol{\nabla}\big(c_2+c_3\big)\big]\times\boldsymbol{E} - \big[\partial_t\big(c_2+c_3\big)\big]\boldsymbol{B}\,. \tag{4.46}$$

As a consequence of the Bianchi identity, Gauss's law for magnetism and Faraday–Lenz law remain unchanged:

$$\boldsymbol{\nabla}\cdot\boldsymbol{B} = 0, \tag{4.47}$$

$$\boldsymbol{\nabla}\times\boldsymbol{E} + \partial_t\boldsymbol{B} = 0\,. \tag{4.48}$$

By taking the curl of Faraday–Lenz law and using the Ampère–Maxwell equation, the wave equation for the electric field takes the form

$$\begin{aligned}&\Big\{\Big[\partial_t^2 - \boldsymbol{\nabla}^2 - \big(\boldsymbol{\nabla} c_1\big)\cdot\boldsymbol{\nabla} - \big(\partial_t c_1\big)\partial_t\Big]\delta_{ij} + \nabla_i\nabla_j + \big(\nabla_j c_1\big)\nabla_i \\ &+ \varepsilon_{ijl}\Big[\nabla_l\big(c_2+c_3\big)\partial_t - \partial_t\big(c_2+c_3\big)\nabla_l\Big]\Big\}E_j = 0.\end{aligned} \tag{4.49}$$

There is a central complication in the modified wave equation (4.49) related to the fact that the plane-wave ansatz (or the usual Fourier transform) is no longer the appropriate procedure to obtain the dispersion relation of the model, due to the presence of a background that depends explicitly on spacetime coordinates. To proceed, we adopt a method commonly used in the plasma physics literature for non-homogeneous media, namely the eikonal approximation for electromagnetic waves [177], which allows one to define a local dispersion relation.

The eikonal approximation consists in the introduction of a small parameter ϵ^n multiplying each derivative term in the wave equation, where n denotes the order of the derivative operator. This allows us to systematically track the different orders in a perturbative expansion that can be carried out afterward. At the end of the calculation, the limit $\epsilon \to 1$ is taken. Under these considerations, the eikonal approximation for the electric field is written as

$$E_i(t,\boldsymbol{x}) = A_i(t,\boldsymbol{x})\exp\Big[\frac{i}{\epsilon}S(t,\boldsymbol{x})\Big], \tag{4.50}$$

where the amplitude $A_i(t,\boldsymbol{x})$ and the phase $S(t,\boldsymbol{x})$ are both assumed to be real (see, e.g., Ref. [177] for more details). Thus, at zeroth order in ϵ, the wave equation is given by

$$M_{ij}(t,\boldsymbol{x})E_j = 0, \tag{4.51}$$

with

$$\begin{aligned} M_{ij}(t,\boldsymbol{x}) = &\Big[\omega^2 - \boldsymbol{k}^2 - i(\partial_t c_1)\omega + i(\boldsymbol{\nabla} c_1)\cdot\boldsymbol{k}\Big]\delta_{ij} + k_i k_j - i(\nabla_j c_1)k_i \\ &+ i\varepsilon_{ijl}\Big[\nabla_l\big(c_2+c_3\big)\omega + \partial_t\big(c_2+c_3\big)k_l\Big]. \end{aligned} \tag{4.52}$$

and taking into account the definitions

$$\nabla_i S(t,\boldsymbol{x}) \equiv k_i(t,\boldsymbol{x}) \quad \text{and} \quad \partial_t S(t,\boldsymbol{x}) \equiv -\omega(t,\boldsymbol{x}) \tag{4.53}$$

as the local wave vector and the local frequency, respectively.

Therefore, for a nontrivial electric field, the local dispersion equation (or eikonal equation) is obtained by $\mathscr{D}\big(t,\omega=-\partial_t S,\boldsymbol{x},\boldsymbol{k}=\boldsymbol{\nabla}S\big) \equiv \det M_{ij}(t,\boldsymbol{x}) = 0$. Performing this determinant calculation and considering contributions up to second-order in LSV, one finds

$$\begin{aligned} \mathscr{D}\big(\omega,\boldsymbol{k},t,\boldsymbol{x}\big) = &\,4\omega^6 - 12i(\partial_t c_1)\omega^5 - \Big[9\boldsymbol{k}^2 - 9i\boldsymbol{k}\cdot\big(\boldsymbol{\nabla}c_1\big) + 2\big(\boldsymbol{\nabla}c_3\big)^2\Big]\omega^4 + 2\Big[9i\boldsymbol{k}^2\big(\partial_t c_1\big) \\ &- 2\big(\partial_t c_3\big)\boldsymbol{k}\cdot\big(\boldsymbol{\nabla}c_3\big)\Big]\omega^3 + \Big\{2\boldsymbol{k}^2\Big[3\boldsymbol{k}^2 - \big(\partial_t c_3\big)^2 + \big(\boldsymbol{\nabla}c_3\big)^2 - 12i\big(\boldsymbol{\nabla}c_1\big)\cdot\boldsymbol{k}\Big] \\ &- \big[\big(\boldsymbol{\nabla}c_3\big)\cdot\boldsymbol{k}\big]^2\Big\}\omega^2 - 2\boldsymbol{k}^2\Big[3i\boldsymbol{k}^2\big(\partial_t c_1\big) - \big(\partial_t c_3\big)\big(\boldsymbol{\nabla}c_3\big)\cdot\boldsymbol{k}\Big]\omega - \boldsymbol{k}^4\Big[\boldsymbol{k}^2 \\ &- \big(\partial_t c_3\big)^2 - 3i\big(\boldsymbol{\nabla}c_1\big)\cdot\boldsymbol{k}\Big]. \end{aligned} \tag{4.54}$$

The modified dispersion relation (4.54) shows that the spacetime-dependent LSV contributions lead to a complex local frequency. The real part governs wave propagation, while the imaginary part, proportional to spacetime derivatives of c_1, may induce local amplification or attenuation of the wave amplitude. Indeed, by considering non-constant parameters means that the energy-momentum of the wave is not conserved, by virtue of the exchange with the background. The wave may, therefore, acquire or loose energy. When restricting the LSV sector to light-like structures, the dispersion relation becomes real, and only the parameter m_5 yields nontrivial contributions.

To close this Section, we wish to call the reader's attention to the fact that a spacetime-dependent frequency, as a consequence of non-constant/non-homogeneous LSV parameters, may lead to a red or a blue shift under specific conditions on the way the local parameters depend on time and space coordinates. We believe this a relevant issue to be inspected. The reason being that the LSV parameters are expected to originate from some more fundamental physics, valid at (high) energies close to the scale where the vacuum fluctuations are very strong. It is then reasonable to expect that the LSV entities should emerge as local parameters. Considering constant parameters is a very particular situation and, even though it is a particular case, a broad class of interesting effects beyond Standard-Model Physics may emerge.

4.2 One-loop effective action with constant LSV coefficients

In this Section, we examine the effective photonic action arising from the fermionic determinant in a sector with LSV due to constant coefficients. More specifically, we analyze the action (3.22) in presence of corrections exclusively in the fermion mass sector, given by b_μ and $H_{\mu\nu}$, with all other violating terms set to zero. The other mass sector terms are neglected because they can be eliminated by field redefinitions and therefore do not generate detectable physical effects. All procedures here are very similar to those of the previous Section. We start from the defining term of the effective action in the present case of interest, which is given by

$$i\,\mathrm{Tr}\ln\left(i\not{D}-\mathcal{M}\right)=\frac{i}{2}\,\mathrm{Tr}\left[\ln\left(i\not{D}-\mathcal{M}\right)+\ln\left(i\delta\not{D}-\mathcal{M}^{\star}\right)\right], \tag{4.55}$$

For convenience, we introduce the compact notation

$$\mathcal{M}^{\star}\equiv\zeta m+\beta b_\mu\gamma^\mu\gamma_5+\sigma H_{\mu\nu}\Sigma^{\mu\nu}. \tag{4.56}$$

Here it is important to clarify the role of the coefficients δ, ζ, β, and σ. These coefficients can take the values $+1$, -1, or 0 and encode different ways of completing the squaring procedure (here meaning the construction of the Klein–Gordon operator in the expression of the fermionic determinant). Table 2 summarizes some possibilities found in the literature. What we will see is that the final expression for the effective action depends on how we choose to fix these parameters.

	δ	ζ	β	σ
γ_5 conjugation	$-$	$+$	$-$	$+$
Charge conjugation	$-$	$+$	$+$	$-$
Ref. [155] conjugation	$+$	$-$	$-$	$-$
Ref. [178] conjugation	$+$	$-$	0	0

Table 2 – Different ways of performing the squaring procedure to construct the Klein–Gordon operator in the expression of the fermionic determinant for the effective action.

Once again, to compute the one-loop effective action for the photon field, we integrate out the fermions in the presence of constant background fields by treating the functional determinant of the Dirac operator via the proper-time method and we employ a perturbative expansion in powers of the Lorentz-violating terms. Following standard procedures, we rewrite the squared Dirac operator as

$$\mathcal{O}=\mathcal{K}\left[1+\mathcal{K}^{-1}\mathcal{Y}\right], \tag{4.57}$$

where the kinetic operator is given by $\mathcal{K}\equiv\delta(D^2-e\Sigma^{\mu\nu}F_{\mu\nu})+\zeta m^2+(\delta+\zeta)m\not{D}$, and the Lorentz-violating contributions are collected in the perturbation $\mathcal{Y}$, which includes terms up to second

order in the LSV background,

$$\mathscr{Y} \equiv \beta\big(\not{b}\not{b} + m\not{b}\gamma_5 + \gamma^\mu \not{b}\gamma_5 D_\mu + \Sigma^{\mu\nu} H_{\mu\nu}\not{b}\gamma_5\big) + \sigma\big(m\Sigma^{\mu\nu}H_{\mu\nu} - \not{b}\Sigma^{\mu\nu}H_{\mu\nu}\gamma_5 + \gamma^\alpha \Sigma^{\mu\nu}H_{\mu\nu}D_\alpha + \Sigma^{\alpha\beta}\Sigma^{\mu\nu}H_{\alpha\beta}H_{\mu\nu}\big) + \zeta m\big(\not{b}\gamma_5 + \Sigma^{\mu\nu}H_{\mu\nu}\big) + \delta\big(\Sigma^{\mu\nu}H_{\mu\nu}\not{D} - \not{b}\gamma^\mu\gamma_5 D_\mu\big). \tag{4.58}$$

In addition, it is important to note that, in all parametrizations in the Table 2, cross terms in the minimal operator $\mathscr{K}$ are avoided because one always has $\zeta = -\delta$ (In order to avoid the crossed term $m\not{D}$, which is not present in standard calculations found in the literature [145, 146, 154–157]), and we will assume this condition from now on.

In the form of Eq. (4.58), the operator $\mathscr{Y}$ contains all possible structures constructed from the backgrounds b_μ and $H_{\mu\nu}$, as well as their interplay with the covariant derivative. Note that only constant backgrounds are considered. The expansion of the effective action is then performed in powers of $\mathscr{K}^{-1}\mathscr{Y}$ in $\ln\big[1+\mathscr{K}^{-1}\mathscr{Y}\big]$, as done in Eq. (4.9). After evaluating this expression, making the Wick rotation (see Appendix A), and using the Schwinger parametrization presented in Eq. (4.12), we can write the first- and second-order LSV contributions, respectively, in the form

$$\Gamma_{\rm LSV}\big|^{(1)} = \frac{1}{2\mu^2}\int_0^\infty ds\, Tr\Big\{e^{\frac{\delta}{\mu^2}(D^2-m^2-e\Sigma^{\mu\nu}F_{\mu\nu})}\Big[\beta\big(m\not{b}\gamma_5 + \gamma^\alpha\not{b}\gamma_5 D_\alpha\big) + \sigma\big(m\Sigma^{\kappa\lambda}H_{\kappa\lambda} + \gamma^\alpha\Sigma^{\kappa\lambda}H_{\kappa\lambda}D_\alpha\big) + \zeta m\big(\not{b}\gamma_5 + \Sigma^{\kappa\lambda}H_{\kappa\lambda}\big) + \delta\big(\Sigma^{\kappa\lambda}H_{\kappa\lambda}\not{D} - \not{b}\gamma^\alpha\gamma_5 D_\alpha\big)\Big]\Big\} \tag{4.59}$$

and

$$\begin{aligned}\Gamma_{\rm LSV}\big|^{(2)} = \frac{1}{2\mu^2}\int_0^\infty ds\, Tr\Big\{e^{\frac{\delta}{\mu^2}(D^2-m^2-e\Sigma^{\mu\nu}F_{\mu\nu})}\Big[\beta\big(\not{b}\not{b} + \Sigma^{\kappa\lambda}H_{\kappa\lambda}\not{b}\gamma_5\big) - \sigma\big(\not{b}\Sigma^{\kappa\lambda}H_{\kappa\lambda}\gamma_5 - \Sigma^{\alpha\beta}\Sigma^{\kappa\lambda}H_{\alpha\beta}H_{\kappa\lambda}\big)\Big] + \frac{1}{4\mu^4}\int_0^\infty ds\int_0^\infty d\tau\, Tr\Big\{e^{\frac{\delta}{\mu^2}(D^2-m^2-e\Sigma^{\mu\nu}F_{\mu\nu})} \\ \times\Big[\beta\big(m\not{b}\gamma_5 + \gamma^\alpha\not{b}\gamma_5 D_\alpha\big) + \sigma\big(m\Sigma^{\kappa\lambda}H_{\kappa\lambda} + \gamma^\alpha\Sigma^{\kappa\lambda}H_{\kappa\lambda}D_\alpha\big) + \zeta m\big(\not{b}\gamma_5 + \Sigma^{\kappa\lambda}H_{\kappa\lambda}\big) \\ + \delta\big(\Sigma^{\kappa\lambda}H_{\kappa\lambda}\not{D} - \not{b}\gamma^\alpha\gamma_5 D_\alpha\big)\Big]e^{\frac{\delta}{\mu^2}(D^2-m^2-e\Sigma^{\rho\sigma}F_{\rho\sigma})}\Big[\beta\big(m\not{b}\gamma_5 + \gamma^\zeta\not{b}\gamma_5 D_\zeta\big) + \sigma\big(m\Sigma^{\omega\xi}H_{\omega\xi} \\ + \gamma^\zeta\Sigma^{\omega\xi}H_{\omega\xi}D_\zeta\big) + \zeta m\big(\not{b}\gamma_5 + \Sigma^{\omega\xi}H_{\omega\xi}\big) + \delta\big(\Sigma^{\mu\nu}H_{\mu\nu}\not{D} - \not{b}\gamma^\zeta\gamma_5 D_\zeta\big)\Big]\Big\},\end{aligned} \tag{4.60}$$

in which, in Eqs. (4.59) and (4.60), only terms with an even number of gamma matrices will survive.

Following procedures analogous to those used in the previous section to construct the terms leading to the heat-kernel expression and the action of covariant derivatives on it (here the procedure is simplified by the fact that the LSV coefficients are constant), and finally performing the proper-time integrals and simplifying the results, we can write the only surviving first-order LSV contribution in the form

$$\Gamma_{\rm LSV}\big|^{(1)} = -\frac{\mu^2 e^3}{16\pi^2 m^3}\int d^4x\,\frac{1}{6}(1-\sigma\delta)\Big[2H_{\mu\nu}F^{\nu\alpha}F_{\alpha\beta}F^{\beta\mu} - H_{\mu\nu}F^{\mu\nu}F^2\Big]. \tag{4.61}$$

The result (4.61) points to a violation of Furry's theorem and it is completely consistent with the analysis of Furry's theorem presented in Ref. [169], in which the authors conclude

that the theorem is violated at first order in LSV, and that the Lorentz-violating parameter has CPT-even nature. However, one should note that if we adopt the charge conjugation perspective in Table 2, for which $\sigma = -1$ and $\delta = -1$, one would obtain agreement with Furry's theorem and would go against the conclusions of Ref. [169]. This may indicate that charge conjugation should be discarded, at least in the context of the ambiguity in the parametrization, since the arguments of Ref. [169] were entirely built from the analysis of Feynman diagrams, and no ambiguous behavior of the type discussed here was encountered. Since the other parametrizations are more exotic and are introduced in their respective contexts mainly for practical convenience, we believe that the conjugation by γ_5 is the most appropriate choice, thus justifying our selection in the previous Section.

As before, it is also convenient to express the second-order Lorentz-symmetry-violating contributions to the effective action in the form

$$\Gamma_{LSV}|^{(2)} = \sum_{n=1}^{4} \Gamma_{F^n}. \tag{4.62}$$

However, in the present case, for odd orders in the field strength F, we obtain

$$\Gamma_{F^1} = \Gamma_{F^3} = 0, \tag{4.63}$$

a result that indicates full agreement with Furry's theorem. The corrections to the photon kinetic sector take the form

$$\begin{aligned}\Gamma_{F^2} = \frac{ie^2}{16\pi^2 m^2}\int d^4x\Big[&\frac{1}{3}(1+\beta+\beta\delta)b^2F^2 + \frac{2}{3}(1-\beta\delta)b_\mu b^\nu F^{\mu\kappa}F_{\kappa\nu}\\ &+\frac{1}{6}(3+\sigma+7\delta\sigma)H^2F^2 - \frac{1}{3}(1-3\sigma-3\delta\sigma)H_{\mu\kappa}H_{\lambda\nu}F^{\mu\nu}F^{\kappa\lambda}\\ &-\frac{1}{2}(1+\sigma+\delta\sigma)H_{\mu\nu}H_{\kappa\lambda}F^{\mu\nu}F^{\kappa\lambda} - 2H_{\mu\nu}H^{\nu\kappa}F_{\kappa\lambda}F^{\lambda\mu}\Big].\end{aligned} \tag{4.64}$$

The contributions to photon–photon scattering appear in the form

$$\begin{aligned}\Gamma_{F^4} = \frac{ie^4}{16\pi^2 m^6}\int d^4x\Big[&-\frac{1}{90}(2-5\beta-5\beta\delta)b^2F^4 - \frac{7}{45}\beta(1+\delta)b^2\,\mathrm{Tr}\left(F^4\right)\\ &-\frac{2}{45}b_\mu b^\nu F_{\mu\kappa}F^{\kappa\nu}F^2 - \frac{1}{45}(1+\beta\delta)b_\mu b^\nu F^{\mu\kappa}F_{\kappa\lambda}F^{\lambda\tau}F_{\tau\nu} + \frac{1}{36}(5+\sigma+13\sigma\delta)H^2F^4\\ &-\frac{1}{90}(11+7\sigma+67\sigma\delta)H^2\,\mathrm{Tr}\left(F^4\right) + \frac{44}{45}H_{\mu\nu}H_{\mu\kappa}F^{\nu\lambda}F^{\mu\rho}F_{\rho\nu}F^{\kappa\tau}F_{\tau\lambda}\\ &-\frac{1}{9}(1+3\sigma+\sigma\delta)H_{\mu\kappa}H_{\nu\lambda}F^{\mu\nu}F^{\kappa\lambda}F^2 - \frac{4}{45}(2+15\sigma+15\sigma\delta)H_{\mu\kappa}H_{\nu\lambda}F^{\mu\rho}F_{\rho\tau}F^{\tau\nu}F^{\kappa\lambda}\\ &+\frac{1}{6}(1+\sigma+7\sigma\delta)H_{\mu\nu}H_{\kappa\lambda}F^{\mu\nu}F^{\kappa\lambda}F^2 - \frac{2}{7}(1+\sigma+7\sigma\delta)H_{\mu\nu}H_{\kappa\lambda}F^{\mu\rho}F_{\rho\tau}F^{\tau\nu}F^{\kappa\lambda}\\ &-\frac{2}{9}(5+2\sigma\delta)H_{\mu\kappa}H^{\kappa\nu}F^{\mu\lambda}F_{\lambda\nu} - \frac{8}{5}(1+40\sigma\delta)H_{\mu\kappa}H^{\kappa\nu}F^{\mu\lambda}F_{\lambda\rho}F^{\rho\tau}F_{\tau\nu}\Big].\end{aligned} \tag{4.65}$$

In some way, these fourth-order terms of the field strength may inspire an analysis of photon–photon scattering data to constrain these parameters. In the next Subsection, we examine how the modifications of the photon kinetic sector affect the Maxwell equations, which may naturally lead to interesting phenomenological implications.

An interesting fact that is worth emphasizing concerns the CPT-even case $(k_F)^{\mu\nu\kappa\lambda}$, which has the same symmetry properties as the Riemann tensor and is commonly known in the literature as the *aether term*. Ref. [179] shows that a second-order photonic action containing an aether-like term can be generated at one loop in a finite way by considering the starting action

$$S = \int d^d x \bar{\psi}\Big[i\partial\!\!\!/ - m - eA\!\!\!/ - b\!\!\!/\gamma_5 - g\varepsilon^{\mu\nu\kappa\lambda} b_\mu F_{\nu\kappa}\gamma_\lambda\Big]\psi, \tag{4.66}$$

which leads to an aether-term Lagrangian density of the form

$$\mathscr{L}_{\text{aether}} = c\big(b_\mu F^{\mu\nu}\big)^2, \tag{4.67}$$

where c is a constant that depends on the spacetime dimension. Eq. (4.67) is equivalent to the CPT-even photonic term of the minimal SME,

$$\mathscr{L}_{K_F} = -\frac{1}{4}(k_F)_{\mu\nu\kappa\lambda} F^{\mu\nu}F^{\kappa\lambda}. \tag{4.68}$$

Due to the symmetry properties of $(k_F)^{\mu\nu\kappa\lambda}$, this tensor can be written in terms of c and b^μ as

$$(k_F)^{\mu\nu\kappa\lambda} = -c\Big(b^\mu b^\kappa \eta^{\nu\lambda} - b^\mu b^\lambda \eta^{\nu\kappa} + b^\nu b^\lambda \eta^{\mu\kappa} - b^\nu b^\kappa \eta^{\mu\lambda}\Big). \tag{4.69}$$

By defining $u^\mu \equiv \sqrt{|c|}\, b^\mu$, we can write

$$\mathscr{L}_{K_F} = -\frac{1}{4}(k_F)_{\mu\nu\kappa\lambda} F^{\mu\nu}F^{\kappa\lambda} = \frac{1}{2} u^\mu u_\nu F_{\mu\kappa}F^{\nu\kappa}. \tag{4.70}$$

In this sense, we have successfully generated aether-like terms in the second-order action in $F_{\mu\nu}$, given in Eq. (4.64), due to the presence of the term $\frac{2}{3}(1-\beta\delta)\, b_\mu b^\nu F^{\mu\kappa}F_{\kappa\nu}$. This term survives for all parametrizations listed in Table 2, except for the γ_5 parametrization.

4.2.1 The modified Maxwell equations

Fixing the parametrization by γ_5 in Eq. (4.64), performing the inverse Wick rotation, adding the result to the usual action that leads to the standard Maxwell equations, we obtain the action

$$\begin{aligned} S = -\frac{1}{4}\int d^4x \Big\{ &\left[1 - \kappa\left(\frac{1}{3}b^2 + \frac{1}{2}H^2\right)\right]F^2 - \frac{\kappa}{2}\Big(H_{\mu\nu}F^{\mu\nu}\Big)^2 \\ &- \frac{\kappa}{3}H_{\mu\kappa}H_{\lambda\nu}F^{\mu\nu}F^{\kappa\lambda} - 2\kappa H_{\mu\nu}H^{\nu\kappa}F_{\kappa\lambda}F^{\lambda\mu}\Big\}, \end{aligned} \tag{4.71}$$

where

$$\kappa = \frac{\alpha}{\pi m^2}. \tag{4.72}$$

Applying the variational principle to the photon field, we obtain that the covariant field equations are

$$\left[1 - \kappa\left(\frac{1}{3}b^2 + \frac{1}{2}H^2\right)\right]\partial_\mu F^{\mu\nu} - \frac{\kappa}{2}H^{\mu\nu}H_{\kappa\lambda}\partial_\mu F^{\kappa\lambda} - \frac{\kappa}{3}H^{\mu\kappa}H^{\lambda\nu}\partial_\mu F_{\kappa\lambda} - 2\kappa H_{\kappa\lambda}H^{\lambda\mu}\partial_\mu F^{\nu\kappa} = 0. \tag{4.73}$$

Since the Bianchi identity, $\partial_\mu \tilde{F}^{\mu\nu} = 0$, remains valid, there are no alterations to Faraday-Lenz law and Gauss's law for the magnetic field.

We know that $F^{i0} = -F_{i0} = \boldsymbol{E}_i$ and $F^{ij} = F_{ij} = -F^i{}_j = -\varepsilon_{ijk}\boldsymbol{B}_k$. The terms H_{0i} and H_{ij} will be identified, respectively, with two vectors $\boldsymbol{h}_i$ and $\tilde{\boldsymbol{h}}_i$ in such a way that

$$H_{0i} = \boldsymbol{h}_i, \tag{4.74}$$

$$H_{ij} = \varepsilon_{ijk}\tilde{\boldsymbol{h}}_k. \tag{4.75}$$

Given these considerations and taking the $\nu = 0$ component in Eq. (4.73), we obtain that Gauss's law for the electric field is given by

$$\begin{aligned}&\left[1 - \frac{\kappa}{3}\left(b_0^2 - \boldsymbol{b}^2 - 3\boldsymbol{h}^2 + 3\tilde{\boldsymbol{h}}^2\right)\right]\boldsymbol{\nabla}\cdot\boldsymbol{E} + \frac{\kappa}{3}\Big[2(\boldsymbol{h}\cdot\tilde{\boldsymbol{h}})\boldsymbol{\nabla}\cdot\boldsymbol{B} + 6\boldsymbol{h}\cdot\boldsymbol{\nabla}(\boldsymbol{h}\cdot\boldsymbol{E})\\ &- 3\tilde{\boldsymbol{h}}\cdot\boldsymbol{\nabla}(\tilde{\boldsymbol{h}}\cdot\boldsymbol{E}) + \boldsymbol{h}\cdot\boldsymbol{\nabla}(\tilde{\boldsymbol{h}}\cdot\boldsymbol{B}) - 5\tilde{\boldsymbol{h}}\cdot\boldsymbol{\nabla}(\boldsymbol{h}\cdot\boldsymbol{B})\Big] = 0.\end{aligned} \tag{4.76}$$

Now taking the i-component in (4.73) we get the Ampère-Maxwell equation in the form

$$\begin{aligned}&-\left[1 - \frac{\kappa}{3}(b_0^2 - \boldsymbol{b}^2 - 3\boldsymbol{h}^2 + 3\tilde{\boldsymbol{h}}^2)\right]\partial_t\boldsymbol{E} + \left[1 + \frac{\kappa}{3}(b_0^2 - \boldsymbol{b}^2 + \boldsymbol{h}^2 - 5\tilde{\boldsymbol{h}}^2)\right]\boldsymbol{\nabla}\times\boldsymbol{B}\\ &+ \frac{\kappa}{3}\Big[5(\boldsymbol{h}\cdot\partial_t\boldsymbol{B})\tilde{\boldsymbol{h}} - 6(\boldsymbol{h}\cdot\partial_t\boldsymbol{E})\boldsymbol{h} + 3(\tilde{\boldsymbol{h}}\cdot\partial_t\boldsymbol{E})\tilde{\boldsymbol{h}} - (\tilde{\boldsymbol{h}}\cdot\partial_t\boldsymbol{B})\boldsymbol{h} - 2(\boldsymbol{h}\cdot\tilde{\boldsymbol{h}})\partial_t\boldsymbol{B}\\ &+ 2(\boldsymbol{h}\times\tilde{\boldsymbol{h}})\cdot\boldsymbol{\nabla}\boldsymbol{E} + 3\tilde{\boldsymbol{h}}\cdot(\boldsymbol{\nabla}\times\boldsymbol{E})\boldsymbol{h} + 3(\tilde{\boldsymbol{h}}\times\boldsymbol{\nabla})(\boldsymbol{h}\cdot\boldsymbol{E}) + 3\boldsymbol{h}\cdot\boldsymbol{\nabla}(\tilde{\boldsymbol{h}}\times\boldsymbol{E}) - 2(\boldsymbol{h}\times\tilde{\boldsymbol{h}})\boldsymbol{\nabla}\cdot\boldsymbol{E}\\ &+ 3\boldsymbol{h}\cdot\boldsymbol{\nabla}(\boldsymbol{h}\times\boldsymbol{B}) + 3\tilde{\boldsymbol{h}}\cdot\boldsymbol{\nabla}(\tilde{\boldsymbol{h}}\times\boldsymbol{B}) + 3\boldsymbol{h}\cdot(\boldsymbol{\nabla}\times\boldsymbol{B})\boldsymbol{h} + 3\tilde{\boldsymbol{h}}\cdot(\boldsymbol{\nabla}\times\boldsymbol{B})\tilde{\boldsymbol{h}} - 2(\tilde{\boldsymbol{h}}\times\boldsymbol{\nabla})(\tilde{\boldsymbol{h}}\cdot\boldsymbol{B})\Big] = 0.\end{aligned} \tag{4.77}$$

Therefore, we can define the electric displacement as

$$\boldsymbol{D}_i = \varepsilon_{ij}\boldsymbol{E}_j + \alpha_{ij}\boldsymbol{B}_j \tag{4.78}$$

with the electrical permittivity tensor given by

$$\varepsilon_{ij} = \left[1 - \frac{\kappa}{3}\left(b_0^2 + \boldsymbol{b}^2 - 3\boldsymbol{h}^2 + 3\tilde{\boldsymbol{h}}^2\right)\right]\delta_{ij} + \frac{\kappa}{3}\left(6\boldsymbol{h}_i\boldsymbol{h}_j - 3\tilde{\boldsymbol{h}}_i\tilde{\boldsymbol{h}}_j\right), \tag{4.79}$$

and

$$\alpha_{ij} = \frac{\kappa}{3}\Big[3(\boldsymbol{h}\cdot\tilde{\boldsymbol{h}})\delta_{ij} + \boldsymbol{h}_i\tilde{\boldsymbol{h}}_j - 3\tilde{\boldsymbol{h}}_i\boldsymbol{h}_j\Big]. \tag{4.80}$$

Finally the Gauss law for the electric field can be written in the form

$$\boldsymbol{\nabla}\cdot\boldsymbol{D} = 0. \tag{4.81}$$

The Ampère-Maxwell law can also be written as

$$\boldsymbol{\nabla}\times\mathbf{H} = \partial_t\boldsymbol{D}, \tag{4.82}$$

where

$$\boldsymbol{H}_i = \mu_{ij}^{-1}\boldsymbol{B}_j + \beta_{ij}\boldsymbol{E}_j \tag{4.83}$$

with

$$\mu_{ij}^{-1} = \left[1 + \frac{\kappa}{3}\left(b_0^2 - \boldsymbol{b}^2 + \boldsymbol{h}^2 - 5\tilde{\boldsymbol{h}}^2\right)\right]\delta_{ij} + \frac{\kappa}{3}\left(3\boldsymbol{h}_i\boldsymbol{h}_j + 5\tilde{\boldsymbol{h}}_i\tilde{\boldsymbol{h}}_j\right) \tag{4.84}$$

and

$$\beta_{ij} = \frac{\alpha}{3\pi m^2}\left[3(\boldsymbol{h}\cdot\tilde{\boldsymbol{h}})\delta_{ij} + 2\boldsymbol{h}_i\tilde{\boldsymbol{h}}_j + 2\tilde{\boldsymbol{h}}_i\boldsymbol{h}_j\right]. \tag{4.85}$$

The construction of the matrices ε_{ij} and α_{ij} is straightforward. However, in the derivation of the matrices μ_{ij}^{-1} and β_{ij}, some terms require the use of the vector identity $\boldsymbol{v}\cdot(\boldsymbol{\nabla}\times\boldsymbol{K}) = -\boldsymbol{\nabla}\cdot(\boldsymbol{v}\times\boldsymbol{K})$, together with

$$\begin{aligned}\boldsymbol{u}\cdot\boldsymbol{\nabla}(\boldsymbol{v}\times\boldsymbol{K}) - \boldsymbol{\nabla}\cdot(\boldsymbol{v}\times\boldsymbol{K})\,\boldsymbol{u} &= \varepsilon_{ijk}\boldsymbol{\nabla}_j\left[\varepsilon_{klm}(\boldsymbol{v}\times\boldsymbol{K})_l\, u_m\right] \\ &= \varepsilon_{ijk}\boldsymbol{\nabla}_j\left[\varepsilon_{klm}\varepsilon_{lno}\, v_n K_o u_m\right].\end{aligned} \tag{4.86}$$

Here, $\boldsymbol{v}$ and $\boldsymbol{u}$ are constant LSV background vectors, while $\boldsymbol{K}$ is a spacetime-dependent vector, corresponding to the fields $\boldsymbol{E}$ or $\boldsymbol{B}$.

The constitutive relations that emerge in this scenario, Eqs. (4.78) and (4.83), indicate properties of a homogeneous but bianisotropic material. However, here these characteristics should be understood as referring to a vacuum that behaves like a material medium.

4.3 Final remarks

This Chapter is very technical and still lacks direct phenomenological applications. Such applications may arise from different directions, for example by drawing a parallel with axion-like parameters that appear in condensed matter systems, or by studying the optical phenomena that can emerge from the modified Maxwell equations.

In the context of modified Maxwell equations, we expect that allowing spacetime dependence for the LSV background will lead to very rich constitutive relations, typical of a non-homogeneous, bianisotropic, and dispersive medium. In principle, this could provide a new way to impose bounds on Lorentz-violating parameters using data from high-energy laser experiments that measure optical properties of the vacuum. In this direction, one can calculate dispersion relations, perform a detailed polarization and birefringence analysis, compute the rotatory power, and investigate the possible existence of dichroism. One may also study classical causality criteria through group and phase velocities and analyze unitarity by examining the imaginary part of the pole of the modified photon propagator. All these analyses can also be carried out in the context of the effective action with constant coefficients.

Additionally, the attainment of an effective photonic action of the Euler-Heisenberg type including the space-time-dependent parameters may be of interest if we identify the four-vector, $a_\mu(x)$, and the pseudo-vector, $b_\mu(x)$, respectively with the gradients of the saxion (the CP-even axion field - the supersymmetric scalar partner of the axion [180, 181]) and the

axion field itself, in the context of Eq. (4.34). This does not mean that these identifications reproduce interactions dictated by supersymmetry. We are merely borrowing the saxion field from the supermultiplet that accommodates the axion in a supersymmetric scenario. This could be a way to introduce dark matter candidates in interaction with the photon in a sort of extended Euler-Heisenberg action. By upgrading these variable LSV parameters to the status of dynamical fields, one should also introduce their respective kinetic and mass terms. If we take this path, an effective axionic Euler-Heisenberg emerges which may be further exploited. Differently from simply adding the (purely photonic) Euler-Heisenberg action to the Axionic Electrodynamics, such a construction would incorporate the saxion and axion fields into the classes of terms with powers of the photon field-strength and its dual.

Nevertheless, it is clear that the issue of ambiguity in the quadrature procedure deserves a more careful analysis. In this sense, we also intend to continue investigating the possibility of a multiplicative anomaly in the fermionic determinant in the presence of Lorentz-symmetry-breaking terms. In the next Chapter, we will change our focus and seek to understand a particular Lorentz-symmetry breaking in a supersymmetric model.

Chapter

5

An Abelian model for fermions in presence of LSV and SUSY

In this Chapter, we present our ideas on a supersymmetric scenario with Lorentz symmetry breaking. The results of this effort were published in Ref. [219].

Considering that Lorentz symmetry violation is expected to occur at the Planck scale ($M_P \sim 10^{19}\,\mathrm{GeV}$), as argued in Chapter 2, at the same time, in this high-energy regime, Supersymmetry (SUSY) is expected to keep unbroken [182]. In this way, it becomes pretty natural to wonder about the relationship between the LSV and SUSY breaking. Berger and Kostelecký were pioneers in proposing a method for incorporating Lorentz-breaking terms into a SUSY scenario; this can be accomplished by introducing the background anisotropies of LSV into the SUSY algebra [182, 183]. Subsequently, a number of approaches to inspect supersymmetric extensions of QED with LSV have emerged. These investigations have led to important phenomena such as vacuum birefringence [184], as well as the manifestation of SUSY breaking that arises from the mass splitting of superpartners [185]. Alternatively to the original proposal presented by Berger and Kostelecký, the framework we adopt here to study LSV in a supersymmetric scenario consists in treating the Lorentz-breaking parameters as components of special (background) superfields, while SUSY algebra is kept unchanged. In this case, the central idea consists in seeking a supersymmetric formulation for the background tensor structures that constitute the spacetime anisotropies responsible for the LSV. This allows us to present a microscopic origin for the LSV parameters in terms of components of non-dynamical superfields, as it shall be subsequently described.

On the other hand, the possibility of LSV in other scenarios gives rise to interesting developments, e.g., in Condensed Matter Physics (CMP), where both SUSY and Lorentz invariance may appear as emergent symmetries. The first indication of SUSY in CMP has come out from the study of a two-dimensional Ising model [186], where an emergent SUSY becomes apparent near the critical point. In this context, the fundamental degrees of freedom may not exhibit SUSY, but an effective description via a supersymmetric action can be obtained from them. From this perspective, more recent works have contemplated scenarios of emergent SUSY in a $(2+1)$-dimensional system composed of a monolayer of carbon atoms arranged in a honeycomb lattice [187–189]. Moreover, such scenarios can also arise dynamically as pointed out, e.g., in refs. [190–193]. It should also be mentioned that there

are systems in low-energy CMP where the emergent Lorentz-symmetry plays an important role; it is the case of the so-called Dirac and Weyl materials [194–200], topological insulators [201–207] and graphene [208, 209]. At the same time, in these scenarios, the violation of this emergent symmetry has been extensively explored in refs. [210–214]. In this regard, as mentioned in Chapter 2, the interesting work [114] present a comprehensive exploration of quasi-particle excitations in the band structures of Dirac and Weyl materials and, according to the authors, the emergent Lorentz-symmetry features in these materials shed light on Lorentz violation within the SME.

Considering this perspective, the efforts of the present Chapter are motivated by the theoretical study published by Isobe and Nagaosa of quantum critical phenomena in the phase transition between trivial and topological insulators in $(3+1)$ dimensions, which is described by a Dirac fermion coupled to the electromagnetic field [215]. In their model, LSV is realized by a constant parameter present only in the fermionic piece of the action. Our proposal consists in building up an $\mathcal{N}=1$-supersymmetric $U(1)$ gauge model as an extended version of the Isobe-Nagaosa's paper with the LSV parameter no longer constant, but now taken to be space-time dependent. The main purpose is to understand how the LSV, initially manifested only in the fermionic sector, affects the sector of (charged) scalar partners in the gauge-invariant theory. For this, we shall adopt an alternative approach to implement LSV in connection with SUSY, as discussed in refs. [216, 217], in which LSV parameters are located in background superfields and they are therefore accompanied by background fermionic partners that condensate to give origin to bosonic LSV parameters.

In an interesting paper [218], Katz and Shadmi contemplate the situation in which SUSY is broken together with Poincaré invariance, once a certain field acquires a Poincaré-violating (x_μ-dependent) vacuum expectation value. This field yields a spontaneous (and, therefore, a soft) SUSY-breaking. A similar framework will be presented in details in the Sect. 5.2.3 of the present Chapter. And we shall see, in the scenario we study, that a fermion, partner of the background scalar that violates Poincaré symmetry, can form (bilinear) condensates that, in turn, break Lorentz symmetry.

The outline of this Chapter is as follows: In Sect. 5.1, we briefly review the extended Isobe-Nagaosa model, wherein the LSV parameter exhibits spacetime dependence, and present a formulation of the superspace consistent with such a model. In Sect. 5.2, we work to get a supersymmetric $U(1)$ gauge model, based on the extended Isobe-Nagaosa model, and investigate the modifications induced by Lorentz-breaking background components. Next, in Section 5.3, we study the modified field equations and dispersion relations for both the fermionic/scalar matter sectors, and for the Maxwell sector as well. These results shall be used, in what follows, to obtain the rest energy and group velocity for some particular cases. In Sect. 5.4, we derive the effective electric dipole interaction and, based on current experimental results for the electron electric dipole moment (EDM), we present an estimate for one of the background Majorana fermion condensates. Finally, in Sect. 5.5, we draw our Conclusive Considerations and Perspectives. Two Appendices supplement the main text. In

the Appendix B.1, one can find an alternative approach to generate the $v_\mu\bar{\Psi}\gamma^\mu\Psi$-term from a vector superfield. Next, in Appendix B.2, we collect useful results concerning the calculation of our dispersion relations worked out in Section 5.3. It is also worth mentioning that the efforts presented in this chapter were duly published in [219].

5.1 The extended Isobe-Nagaosa model

We start off from the following extended version of the model proposed by Isobe-Nagaosa (see ref. [122] for more details),

$$\mathscr{L} = i\bar{\Psi}\Big[\gamma^0\partial_0 - \mathrm{Re}(\xi)\gamma^i\partial_i\Big]\Psi - \frac{1}{2}\Big\{\partial_i \mathrm{Im}\big[\xi(x)\big]\Big\}\bar{\Psi}\gamma^i\Psi - m\bar{\Psi}\Psi, \tag{5.1}$$

where Ψ is a Dirac fermion and ξ is a factor that breaks Lorentz-symmetry. In the extended model (5.1), we introduce a space-time dependence on the background parameter ξ, since, in a general situation, such a parameter may not be constant and/or homogeneous, and it would be pertinent to exploit consequences of the non-constancy and non-homogeneity. In order to guarantee the reality of the action associated with (5.1), it follows that the real part of ξ, $\mathrm{Re}(\xi)$, must be a real constant parameter, while its imaginary part, $\mathrm{Im}\big[\xi(x)\big] \equiv I(x)$, carries all the eventual space-time dependence of the ξ factor. The original Isobe-Nagaosa model [215] is rescued considering $I(x)$ constant. Before moving on, it is important to stress that, as it is explicit in the Isobe-Nagaosa's topological insulator QED model, the extended version we investigate in what follows (5.1) also exhibits local U(1) invariance.

In what follows, it is convenient to introduce the covariant notation in the form

$$\tilde{\partial}_\mu = (\partial_0, \mathrm{Re}(\xi)\partial_i), \tag{5.2}$$

$$v_\mu = (0, -\partial_i I(x)). \tag{5.3}$$

Then, the Lagrangian (5.1) can be written as

$$\mathscr{L} = \frac{i}{2}\bar{\Psi}\gamma^\mu(\tilde{\partial}_\mu\Psi) - \frac{i}{2}(\tilde{\partial}_\mu\bar{\Psi})\gamma^\mu\Psi + \frac{1}{2}v_\mu\bar{\Psi}\gamma^\mu\Psi - m\bar{\Psi}\Psi. \tag{5.4}$$

We can map the Lorentz violation present in Eq. (5.4) into the mSME framework discussed in the Section 3.2 of the Chapter 3 by identifying $v_\mu \to a_\mu(x)$, where $a_\mu(x)$ is a spacelike vector and cannot be removed by a field redefinition due to its dependence on spacetime coordinates. The Lorentz violation coming from $\mathrm{Re}(\xi)$, which we conveniently observe here in the derivative operator, can be mapped into a term of the $c^{\mu\nu}$ type. In this case, we have $c^{00} = 1$, $c^{0i} = c^{i0} = c^{[ij]} = 0$, where $c^{[ij]}$ denotes the antisymmetric part of c^{ij}, and $c^{(ij)} = \mathrm{Re}(\xi)\,\delta^{ij}$, where $c^{(ij)}$ denotes the symmetric part of c^{ij}.

As a step further, considering a Dirac spinor in the Weyl representation, one can arrange the Ψ-components according to their chirality,

$$\Psi = \begin{pmatrix} \psi_\alpha \\ \bar{\chi}^{\dot{\alpha}} \end{pmatrix}, \tag{5.5}$$

where the Van der Waerden notation has been adopted. Defining $\sigma^\mu = (I_2, \sigma^i)$ and $\bar{\sigma}^\mu = (I_2, -\sigma^i)$, the γ-matrices in Weyl representation are written as

$$\gamma^\mu = \begin{pmatrix} 0 & \sigma^\mu \\ \bar{\sigma}^\mu & 0 \end{pmatrix} \quad \text{and} \quad \gamma_5 = i\gamma^0\gamma^1\gamma^2\gamma^3 = \begin{pmatrix} -I_2 & 0 \\ 0 & I_2 \end{pmatrix}. \tag{5.6}$$

Thus, the Lagrangian (5.1) acquires the form

$$\begin{aligned} \mathscr{L} = \frac{i}{2}\left[\bar{\psi}\bar{\sigma}^\mu(\tilde{\partial}_\mu\psi) - (\tilde{\partial}_\mu\bar{\psi})\bar{\sigma}^\mu\psi + \bar{\chi}\bar{\sigma}^\mu(\tilde{\partial}_\mu\chi) - (\tilde{\partial}_\mu\bar{\chi})\bar{\sigma}^\mu\chi\right] \\ + \frac{1}{2}v_\mu(\bar{\psi}\bar{\sigma}^\mu\psi - \bar{\chi}\bar{\sigma}^\mu\chi) - m(\bar{\psi}\bar{\chi} + \chi\psi), \end{aligned} \tag{5.7}$$

with two chiral sectors, left and right, described by the ψ- and χ-spinors, respectively.

5.1.1 The SUSY-extended model in superspace

In order to incorporate SUSY in the framework of the extended fermionic Lagrangian (5.7), and to carry out its coupling with the photon and photino, we adopt an approach that keeps SUSY algebra intact. We call into question that, instead of modifying SUSY algebra to include the LSV parameters, the latter are rather accommodated as components of a background superfield. To implement this point of view, one should remember the definition of four-divergence operator, $\tilde{\partial}_\mu$, presented in (5.2) and define the position four-vector as

$$\tilde{x}_\mu = \left(x_0, -\frac{1}{\mathrm{Re}(\xi)}x_i\right), \tag{5.8}$$

in such a way that $\tilde{\partial}_\mu\tilde{x}^\nu = \delta^\nu_\mu$. Then, we define the superspace coordinates, adopting the Salam-Strathdee formulation [220] (see, e.g., in ref. [221] for the textbook level introduction), as $\{\tilde{x}^\mu; \theta_\alpha, \bar{\theta}_{\dot{\alpha}}\}$ with μ being a space-time index and $\alpha = (1,2)$, as well as $\dot{\alpha} = (1,2)$, being indices of Grassmannian nature. That said, one can obtain the form of the SUSY generators,

$$Q_\alpha = -i\partial_\alpha - (\sigma^\mu)_{\alpha\dot{\beta}}\bar{\theta}^{\dot{\beta}}\tilde{\partial}_\mu, \quad \bar{Q}_{\dot{\alpha}} = i\bar{\partial}_{\dot{\alpha}} + \theta^\beta(\sigma^\mu)_{\beta\dot{\alpha}}\tilde{\partial}_\mu, \tag{5.9}$$

and establish the anti-commutation relations

$$\{D_\alpha, Q_\beta\} = \left\{\bar{D}_{\dot{\alpha}}, \bar{Q}_{\dot{\beta}}\right\} = \left\{D_\alpha, \bar{Q}_{\dot{\beta}}\right\} = \{\bar{D}_{\dot{\alpha}}, Q_\beta\} = 0, \tag{5.10}$$

with the SUSY covariant derivative operators given by

$$D_\alpha = \partial_\alpha + i(\sigma^\mu)_{\alpha\dot{\beta}}\bar{\theta}^{\dot{\beta}}\tilde{\partial}_\mu, \tag{5.11}$$

$$\bar{D}_{\dot{\alpha}} = \bar{\partial}_{\dot{\alpha}} + i\theta^\beta(\sigma^\mu)_{\beta\dot{\alpha}}\tilde{\partial}_\mu. \tag{5.12}$$

From (5.9), it is clear that the SUSY algebra is left untouched, as already mentioned. See Ref. [222] to understand how these definitions connect with the SUSY algebra; it then becomes immediate to see that the algebra remains intact.

5.2 $\mathcal{N}=1$-supersymmetric $U(1)$ gauge-field sector

In what follows, we shall apply the ideas presented in the previous Section to build up a supersymmetric version of QED. First, let us investigate the modifications the formulation of superspace, based on the fermionic matter sector, in the gauge field sector.

5.2.1 The Maxwell sector

Consider a real vector superfield, $A(\tilde{x},\theta,\bar{\theta})$, in the Wess-Zumino gauge (see, e.g., the textbook in refs. [221,222] for more details),

$$A_{\rm WZ} = i\theta^2\bar{\theta}\bar{\lambda} - i\bar{\theta}^2\theta\lambda + (\theta\sigma^\mu\bar{\theta})\tilde{a}_\mu + \frac{1}{2}\theta^2\bar{\theta}^2 K, \tag{5.13}$$

where λ is the Weyl component of a Majorana spinor, $\tilde{a}_\mu$ is the four-vector and K is an auxiliary field. To be consistent with the definitions of superspace and superfields we are considering, $\tilde{a}_\mu$ must have the form

$$\tilde{a}_\mu = \left(A_0, -\frac{1}{\mathrm{Re}(\xi)}A_i\right). \tag{5.14}$$

Here, it is clear that the Lorentz violation in the Maxwell sector is signaled exclusively by the presence of $\mathrm{Re}(\xi)$. Hence, we can expect that this sector is not affected by the space-time dependence of the background.

In this case, the generalization of the Abelian gauge condition for the modified electromagnetic four-potential is given by (see ref. [222])

$$\tilde{a}_\mu \rightarrow \tilde{a}'_\mu = \tilde{a}_\mu - \tilde{\partial}_\mu[2\mathrm{Im}(z)], \tag{5.15}$$

with $\mathrm{Im}(z)$ standing for the imaginary part of the complex scalar component of some chiral superfield. The kinetic term for $\tilde{a}_\mu$ can be generated by the contractions

$$W^\alpha W_\alpha\Big|_{\sim\theta^2} = -\frac{1}{2}\mathscr{F}^{\mu\nu}\mathscr{F}_{\mu\nu} + \frac{i}{2}{}^*\mathscr{F}^{\mu\nu}\mathscr{F}_{\mu\nu} - 2i\lambda\sigma^\mu\tilde{\partial}_\mu\bar{\lambda} + K^2, \tag{5.16}$$

$$\bar{W}_{\dot{\alpha}}\bar{W}^{\dot{\alpha}}\Big|_{\sim\bar{\theta}^2} = -\frac{1}{2}\mathscr{F}^{\mu\nu}\mathscr{F}_{\mu\nu} - \frac{i}{2}{}^*\mathscr{F}^{\mu\nu}\mathscr{F}_{\mu\nu} + 2i(\tilde{\partial}_\mu\lambda)\sigma^\mu\bar{\lambda} + (K^*)^2, \tag{5.17}$$

where $\mathscr{F}_{\mu\nu}$ is the electromagnetic field strength and λ is identified as the photino spinor field. In the expressions (5.16) and (5.17), we define the spinorial superfield, $W_\alpha = -\frac{1}{4}\bar{D}\bar{D}D_\alpha A_{\rm WS}$, with $\bar{W}_{\dot{\alpha}}$ representing its complex conjugate, and use the compact notations

$$\mathscr{F}_{\mu\nu} = \left(\tilde{\partial}_\mu\tilde{a}_\nu - \tilde{\partial}_\nu\tilde{a}_\mu\right), \quad {}^*\mathscr{F}^{\mu\nu} = \frac{1}{2}\varepsilon^{\mu\nu\kappa\rho}\mathscr{F}_{\kappa\rho}. \tag{5.18}$$

With all described above, the supersymmetric gauge field action reads as follows:

$$S_{\rm M} = \frac{1}{4}\int d^4x\left(\int d^2\theta\, W^2 + \int d^2\bar{\theta}\,\bar{W}^2\right) \tag{5.19}$$

or, in terms of the component fields,

$$S_{\rm M}=\frac{1}{2}\int d^4x\Big\{-\frac{1}{2}\mathscr{F}_{\mu\nu}^2+i\Big[(\tilde{\partial}_\mu\bar{\lambda})\bar{\sigma}^\mu\lambda-\bar{\lambda}\bar{\sigma}^\mu\tilde{\partial}_\mu\lambda\Big]+|K|^2\Big\}. \tag{5.20}$$

In Eq. (5.19) we use the compact notations W^2 and $\bar{W}^2$ for the definitions (5.16) and (5.17), respectively. It is important to notice that, in our case, the modified Maxwell sector is obtained from the matter sector as a consequence of SUSY. In Section 6.3, we shall explicitly see the modifications in Maxwell's equations due to the prescription (5.14).

5.2.2 The matter sector

Our next task is to supersymmetrize the matter sector based on the Lagrangian (5.7). This procedure will lead to the kinetic and mass terms for the scalar supersymmetric partners of ψ and χ.

To have a supersymmetric version of the left sector in (5.7), we define a chiral superfield,

$$\begin{aligned}\Phi_{\rm L}&=e^{i(\theta\sigma^\mu\bar{\theta})\tilde{\partial}_\mu}\left(\varphi+\sqrt{2}\theta\psi+\theta^2 f\right)\\&=\varphi+\sqrt{2}\theta\psi+\theta^2 f+i(\theta\sigma^\mu\bar{\theta})\tilde{\partial}_\mu\varphi-\frac{i}{\sqrt{2}}\theta^2(\tilde{\partial}_\mu\psi)\sigma^\mu\bar{\theta}-\frac{1}{4}\theta^2\bar{\theta}^2\tilde{\Box}\varphi,\end{aligned} \tag{5.21}$$

and its anti-chiral associated superfield,

$$\bar{\Phi}_{\rm L}=\varphi^*+\sqrt{2}\bar{\theta}\bar{\psi}+\bar{\theta}^2 f^*-i(\theta\sigma^\mu\bar{\theta})\tilde{\partial}_\mu\varphi^*+\frac{i}{\sqrt{2}}\bar{\theta}^2\theta\sigma^\mu\tilde{\partial}_\mu\bar{\psi}-\frac{1}{4}\theta^2\bar{\theta}^2\tilde{\Box}\varphi^*, \tag{5.22}$$

where φ is a charged scalar field, ψ is the Weyl component of a Dirac spinor and f is an auxiliary field. Similarly, for the right sector, we have

$$\bar{\Phi}_{\rm R}=s+\sqrt{2}\bar{\theta}\bar{\chi}+\bar{\theta}^2 g-i(\theta\sigma^\mu\bar{\theta})\tilde{\partial}_\mu s+\frac{i}{\sqrt{2}}\bar{\theta}^2\theta\sigma^\mu\tilde{\partial}_\mu\bar{\chi}-\frac{1}{4}\theta^2\bar{\theta}^2\tilde{\Box}s, \tag{5.23}$$

$$\Phi_{\rm R}=s^*+\sqrt{2}\theta\chi+\theta^2 g^*+i(\theta\sigma^\mu\bar{\theta})\tilde{\partial}_\mu s^*-\frac{i}{\sqrt{2}}\theta^2(\tilde{\partial}_\mu\chi)\sigma^\mu\bar{\theta}-\frac{1}{4}\theta^2\bar{\theta}^2\tilde{\Box}s^*. \tag{5.24}$$

Here, s, χ and g are the right component fields analogous to φ, ψ and f in the left sector, respectively. It is important to notice that the introduction of two chiral superfields with independent fermionic components, ψ and χ, is necessary in order to compose the (charged) Dirac fermion Ψ. The mass terms arise from the combinations

$$\Phi_{\rm R}\Phi_{\rm L}\Big|_{\sim\theta^2}=s^*f+g^*\varphi-\chi\psi\ \text{ and }\ \bar{\Phi}_{\rm L}\bar{\Phi}_{\rm R}\Big|_{\sim\bar{\theta}^2}=f^*s+\varphi^*g-\bar{\psi}\bar{\chi}. \tag{5.25}$$

To implement the Abelian gauge symmetry in the matter sector, we consider the transformation of chiral superfields under the global $U(1)$ gauge transformation by the relations (see ref. [222])

$$\Phi'_{\rm L}=e^{ie\Lambda}\Phi_{\rm L},\quad \bar{\Phi}'_{\rm L}=e^{-ie\bar{\Lambda}}\bar{\Phi}_{\rm L}, \tag{5.26}$$

$$\bar{\Phi}'_{\rm R}=e^{ie\bar{\Lambda}}\bar{\Phi}_{\rm R},\quad \Phi'_{\rm R}=e^{-ie\Lambda}\Phi_{\rm R}, \tag{5.27}$$

where e is the $U(1)$ charge of the superfields $\Phi_{L,R}$ and Λ a chiral superfield. The mass term in the supersymmetric action is automatically gauge invariant under this transformations. After some algebra, one can verify that the kinetics terms in (5.7) (now coupled with the photon and photino fields) are generated by combinations like

$$\left(\Phi_L e^{eA_{WZ}}\bar{\Phi}_L + \Phi_R e^{-eA_{WZ}}\bar{\Phi}_R\right)\big|_{\sim\theta^2\bar{\theta}^2}. \tag{5.28}$$

This term is gauge invariant if

$$e^{eA'_{WZ}} = e^{-ie\Lambda}e^{-eA_{WZ}}e^{ie\Lambda}, \quad e^{-eA'_{WZ}} = e^{ie\Lambda}e^{-eA_{WZ}}e^{-ie\Lambda}. \tag{5.29}$$

In the Abelian case, these expressions are consistent with $A' = A + \Lambda + \bar{\Lambda}$, from which the results in Eqs. (5.13) and (5.14) can be derived [222].

5.2.3 The $v_\mu(x)\bar{\Psi}\gamma^\mu\Psi$-term as a background chiral superfield

The less immediate structure to supersymmetrize is the term

$$\frac{1}{2}v_\mu\left(\bar{\psi}\bar{\sigma}^\mu\psi - \bar{\chi}\bar{\sigma}^\mu\chi\right). \tag{5.30}$$

The central point of our approach is to consider LSV in a supersymmetric scenario. The background supermultiplet which accommodates the Lorentz-symmetry violating parameters realizes the (explicit) breaking of Lorentz symmetry and, contemporarily, induces spontaneous SUSY breaking [223–225].

We have actually three alternatives to accomplish this program: 1) to introduce an extra chiral-superfield and then identify v_μ as four-gradient of a (background) scalar; 2) to define a vector superfield and consider v_μ as a genuine four-vector; 3) to introduce the LSV four-vector v_μ by means of an explicit breaking of SUSY, so that not only Lorentz symmetry but also SUSY be also explicitly broken. In this case, the background four-vector would not have background fermionic partners. The latter give rise to bilinears that may be identified with background vector or tensors. Since we are interested in considering this situation, we are going to discard path (3).

From a conceptual point of view, we can consider that the anisotropy arises from some kind of more fundamental field that may condensate to form the LSV background. As we argue, it is important to look for a microscopic origin for the anisotropy and, in this case, the first approach becomes more natural, since the background field does not appear by itself; contrary, it is derived from some more fundamental object; in our case, a scalar, as we shall soon see. Let us remember that, in general, it is the scalars that trigger transitions between different phases of the primordial Universe. Hence, they may have played an important role in the formation of anisotropic structures during the evolution of the Universe. These are motivations that support our choice of the background as a chiral superfield and not a four-vector supermultiplet.

In what follows, we shall adopt the first scenario. For completeness, though we are not going to adopt the alternative (2), we cast in Appendix B.1 the results obtained from the alternative approach, i.e., the case of a vector superfield.

Let us introduce an additional chiral superfield Ω, which is gauge invariant from the perspective of the transformation in (5.26) and (5.27). The θ-expansion of Ω reads

$$\Omega = \omega + \sqrt{2}\theta\zeta + \theta^2 h + i(\theta\sigma^\mu\bar{\theta})\tilde{\partial}_\mu\omega - \frac{i}{\sqrt{2}}\theta^2(\tilde{\partial}_\mu\zeta)\sigma^\mu\bar{\theta} - \frac{1}{4}\theta^2\bar{\theta}^2\tilde{\Box}\omega, \tag{5.31}$$

where ω is a scalar field, ζ is the Weyl component of a Majorana spinor and h is an auxiliary field. One should also notice that, differently from the physical propagating superfields, the background superfield Ω has trivial canonical dimension. The products of superfields which can reproduce (5.30) are

$$\begin{aligned}
(\Omega+\bar{\Omega})\Phi_{\rm L}e^{eA_{\rm WZ}}\bar{\Phi}_{\rm L}\Big|_{\sim\theta^2\bar{\theta}^2} =& -\frac{i}{2}\tilde{\partial}_\mu(\omega-\omega^*)\bar{\psi}\bar{\sigma}^\mu\psi + (\omega+\omega^*)\Big\{\frac{i}{2}\Big[(\tilde{\partial}_\mu\bar{\psi})\bar{\sigma}^\mu\psi - \bar{\psi}\bar{\sigma}^\mu\tilde{\partial}_\mu\psi\Big] \\
&- \frac{1}{2}\Big[(\tilde{\Box}\varphi^*)\varphi + \varphi^*\tilde{\Box}\varphi\Big] + f^*f\Big\} + f^*(h\varphi - \zeta\psi) + f(h^*\varphi^* - \bar{\zeta}\bar{\psi}) \\
&+ \frac{1}{2}\tilde{\partial}_\mu(\omega-\omega^*)\Big[(\tilde{\partial}^\mu\varphi^*)\varphi - \varphi^*\tilde{\partial}^\mu\varphi\Big] + \frac{i}{2}\Big[\varphi(\tilde{\partial}_\mu\bar{\psi})\bar{\sigma}^\mu\zeta - \varphi\bar{\psi}\bar{\sigma}^\mu\tilde{\partial}_\mu\zeta \\
&- \bar{\psi}\bar{\sigma}^\mu\zeta\tilde{\partial}_\mu\varphi\Big] - \frac{i}{2}\Big[\varphi^*\bar{\zeta}\bar{\sigma}^\mu\tilde{\partial}_\mu\psi - \varphi^*(\tilde{\partial}_\mu\bar{\zeta})\bar{\sigma}^\mu\psi - \bar{\zeta}\bar{\sigma}^\mu\psi\tilde{\partial}_\mu\varphi^*\Big] \\
&- \frac{e(\omega+\omega^*)}{2}\Big\{i\sqrt{2}(\bar{\lambda}\bar{\psi}\varphi - \lambda\psi\varphi^*) - i(\varphi^*\tilde{\partial}^\mu\varphi - \varphi\tilde{\partial}^\mu\varphi^*)\tilde{a}_\mu \\
&+ (\bar{\psi}\bar{\sigma}^\mu\psi)\tilde{a}_\mu - \Big(K + \frac{e}{2}\tilde{a}^2\Big)\varphi^*\varphi\Big\} + \frac{e}{2}\Big\{i\tilde{\partial}^\mu(\omega-\omega^*)\varphi^*\varphi\,\tilde{a}_\mu \\
&- \big[(\bar{\psi}\bar{\sigma}^\mu\zeta)\varphi + (\bar{\zeta}\bar{\sigma}^\mu\psi)\varphi^*\big]\tilde{a}_\mu - i\sqrt{2}(\bar{\lambda}\bar{\zeta} - \lambda\zeta)\varphi^*\varphi\Big\},
\end{aligned} \tag{5.32}$$

and an analog structure working to reproduce the right sector.

Choosing the scalar component ω of the background supermultiplet Ω as it is done in ref. [216],

$$(\omega+\omega^*) = 0 \quad \text{and} \quad (\omega-\omega^*) = 2i\varpi, \tag{5.33}$$

with $\varpi = v_\nu\tilde{x}^\nu$, we must impose that $\tilde{\partial}_\mu v_\nu = 0$, i.e., that the imaginary part of parameter ξ in Eq. (5.3) has an only linear dependence on the coordinates.

At this point, we again call into question the paper by Katz and Shadmi [218], where an x_μ-dependent scalar field violates Poincaré symmetry and, as a consequence, softly breaks SUSY. This is exactly what is happening above, where the imaginary part of the ω-background field is taken linearly dependent on $\tilde{x}_\mu$. Actually, this field plays the role of the spurion considered in ref. [218]. In due time, we should mention the paper by Nibbelink and Pospelov [226], where the authors classify LSV operators compatible with exact SUSY, restricting their analysis to vector and tensor backgrounds, and show that LSV operators in the context of the MSSM must have at least dimension five; they are therefore Planck mass-suppressed. This is not what we are doing here, since we are not based on exact SUSY;

contrary, we associate a soft (spontaneous) SUSY breaking with Poincaré symmetry violation. We then justify that we have LSV operators with dimensions less than five because we are not bound to considering exact SUSY. As already anticipated in the Introduction, the ζ-fermion given above, partner of the spurion in the Ω-superfield, will be responsible for condensates that realize LSV contributions to the matter action.

From these considerations, we can write our supersymmetric model as follows below:

$$S=\int d^4x\Big\{\int d^2\theta d^2\bar{\theta}\Big[\bar{\Phi}_{\rm L}e^{eA_{\rm WZ}}\Phi_{\rm L}+\bar{\Phi}_{\rm R}e^{-eA_{\rm WZ}}\Phi_{\rm R}+\frac{1}{2}(\Omega+\bar{\Omega})\Big(\bar{\Phi}_{\rm L}e^{eA_{\rm WZ}}\Phi_{\rm L} - \bar{\Phi}_{\rm R}e^{-eA_{\rm WZ}}\Phi_{\rm R}\Big)\Big]+\frac{1}{4}\Big(\int d^2\theta\, W^2+c.c.\Big)+m\Big(\int d^2\theta\,\Phi_{\rm R}\Phi_{\rm L}+c.c.\Big)\Big\}. \tag{5.34}$$

Using the field equations for the auxiliary fields, (5.34) can be formulated in terms of the physical fields:

$$\begin{aligned}
S_1=\int d^4x\Big\{&-\frac{1}{4}\mathscr{F}_{\mu\nu}^2+\frac{i}{2}\Big[(\tilde{\partial}_\mu\bar{\lambda})\bar{\sigma}^\mu\lambda-\bar{\lambda}\bar{\sigma}^\mu\tilde{\partial}_\mu\lambda\Big]-\frac{i}{2}\Big[\bar{\psi}\bar{\sigma}^\mu\tilde{\partial}_\mu\psi-(\tilde{\partial}_\mu\bar{\psi})\bar{\sigma}^\mu\psi+\bar{\chi}\bar{\sigma}^\mu\tilde{\partial}_\mu\chi\\
&-(\tilde{\partial}_\mu\bar{\chi})\bar{\sigma}^\mu\chi\Big]+\frac{1}{2}v_\mu(\bar{\psi}\bar{\sigma}^\mu\psi-\bar{\chi}\bar{\sigma}^\mu\chi)-m(\bar{\psi}\bar{\chi}+\chi\psi)+\Big[(\tilde{\partial}^\mu\varphi^*)\tilde{\partial}_\mu\varphi+(\tilde{\partial}^\mu s^*)\tilde{\partial}_\mu s\Big]\\
&+\frac{i}{2}v_\mu\Big[(\tilde{\partial}^\mu\varphi^*)\varphi-\varphi^*\tilde{\partial}^\mu\varphi+(\tilde{\partial}^\mu s^*)s-s^*\tilde{\partial}^\mu s\Big]-\Big(m^2+\frac{1}{4}h^*h\Big)(\varphi^*\varphi+s^*s)\\
&+\frac{i}{2}\Big[\varphi(\tilde{\partial}_\mu\bar{\psi})\bar{\sigma}^\mu\zeta-\varphi^*\bar{\zeta}\bar{\sigma}^\mu\tilde{\partial}_\mu\psi+s\bar{\zeta}\bar{\sigma}^\mu\tilde{\partial}_\mu\chi-s^*(\tilde{\partial}_\mu\bar{\chi})\bar{\sigma}^\mu\zeta\Big]-\frac{1}{2}\Big[\varphi\Big(m\zeta\chi-\frac{1}{2}h\bar{\zeta}\bar{\psi}\Big)\\
&+\varphi^*\Big(m\bar{\zeta}\bar{\chi}-\frac{1}{2}h^*\zeta\psi\Big)-s\Big(m\bar{\zeta}\bar{\psi}+\frac{1}{2}h^*\zeta\chi\Big)-s^*\Big(m\zeta\psi+\frac{1}{2}h\bar{\zeta}\bar{\chi}\Big)\Big]\\
&-\frac{1}{4}\Big(\bar{\zeta}\bar{\psi}\zeta\psi+\bar{\zeta}\bar{\chi}\zeta\chi\Big)-\frac{e}{2}\Big[i\sqrt{2}(\varphi\bar{\lambda}\bar{\psi}-\varphi^*\lambda\psi+s\lambda\chi-s^*\bar{\lambda}\bar{\chi})+(\bar{\psi}\bar{\sigma}^\mu\psi-\bar{\chi}\bar{\sigma}^\mu\chi)\tilde{a}_\mu\\
&+i(\varphi\tilde{\partial}^\mu\varphi^*-\varphi^*\tilde{\partial}^\mu\varphi+s\tilde{\partial}^\mu s^*-s^*\tilde{\partial}^\mu s)\tilde{a}_\mu\Big]-\frac{e}{4}\Big[(\bar{\psi}\bar{\sigma}^\mu\zeta)\varphi+(\bar{\zeta}\bar{\sigma}^\mu\psi)\varphi^*+(\bar{\chi}\bar{\sigma}^\mu\zeta)s^*\\
&+(\bar{\zeta}\bar{\sigma}^\mu\chi)s\Big]\tilde{a}_\mu-\frac{e}{2}(\varphi^*\varphi+s^*s)\Big[v^\mu\tilde{a}_\mu+\frac{i}{\sqrt{2}}(\bar{\lambda}\bar{\zeta}-\zeta\lambda)-\frac{e}{2}\tilde{a}^2\Big]-\frac{e^2}{8}(\varphi^*\varphi-s^*s)^2\Big\}.
\end{aligned} \tag{5.35}$$

Despite the lengthy expression in S_1, it is immediate to identify the fermionic model (5.1) in the first two lines. In order to speed up the analysis of the contributions arising from the presence of the background, we group the terms according to sectors. It proves much more useful to rewrite the result (5.35) in terms of 4-component spinors.

In the gauge sector, we have the following standard structure

$$S_{\rm gauge}=-\frac{1}{4}\int d^4x\Big\{\mathscr{F}_{\mu\nu}^2-i\Big[(\tilde{\partial}_\mu\bar{\Lambda})\gamma^\mu\Lambda-\bar{\Lambda}\gamma^\mu\tilde{\partial}_\mu\Lambda\Big]\Big\}, \tag{5.36}$$

where the gaugino (photino) is a Majorana fermion written as

$$\Lambda=\begin{pmatrix}\lambda_\alpha\\ \bar{\lambda}^{\dot{\alpha}}\end{pmatrix}. \tag{5.37}$$

It should be recalled that that the background component-fields are not present in the photon/photino sector, in contrast to other scenarios with LSV, such as, e.g., the supersymmetric extensions of the Carroll-Field-Jackiw model of refs. [216,227]. The reason for this is that, in our case, the gauge sector is affected only by the real part of the background parameter ξ. In fact, the modifications in the gauge sector, induced by the background, only manifest as "dilations" in Maxwell's equations, as we shall see in the next Section.

Using (5.5) and defining the covariant derivative $\tilde{D}_\mu \equiv \tilde{\partial}_\mu - \frac{ie}{2}\tilde{a}_\mu$, we can organize the fermionic sector, including the gauge coupling field, in the form

$$S_{\text{fermion}} = \int d^4x \Big\{ \frac{i}{2}\Big[(\tilde{D}^*_\mu\bar{\Psi})\gamma^\mu\Psi - \bar{\Psi}\gamma^\mu\tilde{D}_\mu\Psi\Big] + \frac{1}{2}v_\mu(\bar{\Psi}\gamma^\mu\Psi) - m\bar{\Psi}\Psi - \frac{1}{16}(\bar{Z}\gamma_\mu\gamma_5 Z)(\bar{\Psi}\gamma^\mu\gamma_5\Psi)\Big\}, \tag{5.38}$$

with the Majorana spinor Z (the background fermion), given by

$$Z = \begin{pmatrix} \zeta_\alpha \\ \bar{\zeta}^{\dot{\alpha}} \end{pmatrix}. \tag{5.39}$$

The term with dependence on the background fermionic condensate $\bar{Z}\gamma_\mu\gamma_5 Z$ that appears in the fermionic sector is an additional contribution to the mass of the Dirac spinor Ψ. In Eq. (5.31), in defining the Ω-superfield, the component fields ω, ζ and h are space-time dependent. However, since Ω is non-dynamical (it is a background superfield), we are allowed to fix its components. Indeed, in Eq. (5.33), by taking $\text{Re}(\omega) = 0$ and $\text{Im}(\omega) = v^\mu\tilde{x}_\mu$, ζ and h are taken to be constant component fields, and this choice is compatible with the SUSY transformations of the component fields. Therefore, the Z-bilinear is constant, so that it is legitimate to state that it is a contribution to the mass-like $\bar{\Psi}\gamma^\mu\gamma_5\Psi$-term. It is interesting to notice that this correction can be identified as the coefficient b_μ in one of the CPT-odd terms introduced in the SME [60,61] in order to implement the violation of the Lorentz symmetry.

The (gauge-invariant) sector of matter scalar partners reads as given below:

$$S_{\text{scalar}} = \int d^4x \Big\{ (\tilde{D}^\mu\varphi^*)\tilde{D}_\mu\varphi + (\tilde{D}^\mu s^*)\tilde{D}_\mu s - iv_\mu(\varphi^*\tilde{D}^\mu\varphi + s^*\tilde{D}^\mu s) - \Big(m^2 + \frac{1}{4}h^*h\Big)(\varphi^*\varphi + s^*s)\Big\}. \tag{5.40}$$

As in the fermionic sector, there is a correction to the scalar masses, φ and s; in this case, proportional to h^*h. This non-degeneracy in the mass spectrum indicates a SUSY breaking due to the presence of the background. Furthermore, there is also a contribution of the background vector, v_μ, to the dynamic part of the scalar sector. On the other hand, in the fermionic case, v_μ only affects the mass term, as we can see in the first line of (5.38).

Finally, we have the gaugino and matter self-interaction contributions to the Lagrangian:

$$\begin{aligned} S_{\text{mixing+int}} = -\int d^4x \Bigg\{ & \frac{ie}{\sqrt{2}}\Big[\bar{\Psi}(\varphi\mathscr{P}_{\text{R}} + s\mathscr{P}_{\text{L}})\Lambda - \bar{\Lambda}(\varphi^*\mathscr{P}_{\text{L}} + s^*\mathscr{P}_{\text{R}})\Psi\Big] \\ & + \frac{i}{2}\Big[\bar{Z}\gamma^\mu(\varphi^*\mathscr{P}_{\text{L}} - s^*\mathscr{P}_{\text{R}})\tilde{D}_\mu\Psi - (\tilde{D}^*_\mu\bar{\Psi})\gamma^\mu(\varphi\mathscr{P}_{\text{L}} - s\mathscr{P}_{\text{R}})Z\Big] \\ & + \frac{1}{2}\bar{\Psi}\Big[\Big(m\varphi - \frac{1}{2}h^*s\Big)\mathscr{P}_{\text{L}} - \Big(ms + \frac{1}{2}h\varphi\Big)\mathscr{P}_{\text{R}}\Big]Z \\ & + \frac{1}{2}\bar{Z}\Big[\Big(m\varphi^* - \frac{1}{2}hs^*\Big)\mathscr{P}_{\text{R}} - \Big(ms^* + \frac{1}{2}h^*\varphi^*\Big)\mathscr{P}_{\text{L}}\Big]\Psi \\ & + \frac{e}{2}\Big[\frac{i}{2\sqrt{2}}(\bar{\Lambda}\gamma_5 Z + \bar{Z}\gamma_5\Lambda)\Big](\varphi^*\varphi + s^*s) + \frac{e^2}{8}(\varphi^*\varphi - s^*s)^2\Bigg\}, \end{aligned} \tag{5.41}$$

with the parity operators,

$$\mathscr{P}_{\text{R}} = \frac{I_4 + \gamma_5}{2} = \begin{pmatrix} 0 & 0 \\ 0 & I_2 \end{pmatrix} \quad \text{and} \quad \mathscr{P}_{\text{L}} = \frac{I_4 - \gamma_5}{2} = \begin{pmatrix} I_2 & 0 \\ 0 & 0 \end{pmatrix}. \tag{5.42}$$

It is worth mentioning that the new couplings induced by the background fermion, Z, except for those involving the degrees of freedom of the gauge sector (a_μ and Λ), must be taken into account when calculating the dispersion relations for the matter fields, because such couplings do not characterize interaction terms (since the background is not dynamic).

5.3 Field equations and dispersion relations

With the supersymmetric action (5.35) in hand, we proceed, in this Section, to a detailed analysis of the field equations in both the matter and gauge sectors. Subsequently, in each case, we shall derive the modified dispersion relations within this framework, aiming to understand the implications of LSV in connection with SUSY.

5.3.1 The modified Maxwell's equations

The modified Maxwell's equations in the vacuum come from the $\mathscr{F}^2_{\mu\nu}$ part of the action (5.36),

$$\tilde{\partial}_\mu\mathscr{F}^{\mu\nu} = 0. \tag{5.43}$$

Let us recall that $\mathscr{F}_{\mu\nu} = \big(\tilde{\partial}_\mu\tilde{a}_\nu - \tilde{\partial}_\nu\tilde{a}_\mu\big)$. From (5.43) we obtain the modified version of the Gauss's law for the electric field and the Ampère-Maxwell equation, in the simplified form,

$$\text{Re}(\xi)\nabla\cdot\boldsymbol{\mathcal{E}} = 0, \tag{5.44}$$

$$\text{Re}(\xi)\nabla\times\boldsymbol{\mathcal{B}} = \partial_t\boldsymbol{\mathcal{E}}, \tag{5.45}$$

where, in an analogy with the usual electrodynamics, we define an effective electric field given by $\boldsymbol{\mathcal{E}} = -\text{Re}(\xi)\nabla\phi - \partial_t\mathbf{A}/\text{Re}(\xi)$, while the magnetic field remains unchanged in this scenario, i.e., $\boldsymbol{\mathcal{B}} = \nabla\times\mathbf{A}$.

On the other hand, from the Bianchi identity,

$$\tilde{\partial}_\mu {}^*\mathscr{F}_{\mu\nu} = 0, \quad {}^*\mathscr{F}_{\mu\nu} = \frac{1}{2}\varepsilon^{\mu\nu\alpha\beta}\mathscr{F}_{\alpha\beta} \tag{5.46}$$

there follow the modified Faraday-Lenz (for $\nu = i$) and the Gauss's law for the magnetic field (for $\nu = 0$):

$$\mathrm{Re}(\xi)\nabla \times \boldsymbol{\mathcal{E}} = -\partial_t \boldsymbol{\mathcal{B}}, \tag{5.47}$$

$$\mathrm{Re}(\xi)\nabla \cdot \boldsymbol{\mathcal{B}} = 0. \tag{5.48}$$

Following the standard procedure for obtaining the wave equation, let us apply a time derivative on (5.47), and use the Eqs. (5.44) and (5.45). For non-trivial field configurations, the photonic scattering relation arises from the requirement that

$$\omega = \pm \mathrm{Re}(\xi)|\mathbf{k}|. \tag{5.49}$$

For the photino, the field equation is $\gamma^\mu \tilde{\partial}_\mu \Lambda = 0$, the dispersion relation has the same form as (5.49).

One of the main consequences of SUSY is the mass degeneracy between a particle and its corresponding superpartner. Since the photon and photino share the same modified dispersion relation, it is immediate to verify that they are both massless. This is simply a confirmation that in the gauge sector there is no SUSY breaking.

5.3.2 The modified Dirac and Klein-Gordon equations

As we have seen in Section 5.2.3, due to the fact that the SUSY background is not dynamic, the mixing terms involving the spinors, Ψ and Z, also contribute to the extended Dirac action, in addition to the (pure) fermionic sector,

$$\begin{aligned} S_{\mathrm{Dirac}} = \int d^4x \Big\{ & \frac{i}{2}\Big[(\tilde{\partial}_\mu \bar{\Psi})\gamma^\mu \Psi - \bar{\Psi}\gamma^\mu \tilde{\partial}_\mu \Psi\Big] + \frac{1}{2}v_\mu(\bar{\Psi}\gamma^\mu\Psi) - m\bar{\Psi}\Psi - \frac{1}{16}(\bar{\Psi}\gamma^\mu\gamma_5\Psi)(\bar{Z}\gamma_\mu\gamma_5 Z) \\ & - \frac{i}{2}\Big[\bar{Z}\gamma^\mu(\varphi^*\mathscr{P}_{\mathrm{L}} - s^*\mathscr{P}_{\mathrm{R}})\tilde{\partial}_\mu\Psi - (\tilde{\partial}_\mu\bar{\Psi})\gamma^\mu(\varphi\mathscr{P}_{\mathrm{L}} - s\mathscr{P}_{\mathrm{R}})Z\Big] - \frac{1}{2}\bar{\Psi}\Big[\Big(m\varphi - \frac{1}{2}h^* s\Big)\mathscr{P}_{\mathrm{L}} \\ & - \Big(ms + \frac{1}{2}h\varphi\Big)\mathscr{P}_{\mathrm{R}}\Big]Z - \frac{1}{2}\bar{Z}\Big[\Big(m\varphi^* - \frac{1}{2}hs^*\Big)\mathscr{P}_{\mathrm{R}} - \Big(ms^* + \frac{1}{2}h^*\varphi^*\Big)\mathscr{P}_{\mathrm{L}}\Big]\Psi\Big\}. \end{aligned} \tag{5.50}$$

The modified Dirac equation in momentum space is given by

$$\begin{aligned} \big[(\tilde{p} - \zeta)_\mu\gamma^\mu + m + R_\mu\gamma^\mu\gamma_5\big]\Psi_0 = -\frac{1}{2}\Big\{ & \Big[(\tilde{p}_\mu\gamma^\mu + m)\varphi_0 - \frac{1}{2}h^* s_0\Big]\mathscr{P}_{\mathrm{L}} \\ & - \Big[(\tilde{p}_\mu\gamma^\mu + m)s_0 + \frac{1}{2}h\varphi_0\Big]\mathscr{P}_{\mathrm{R}}\Big\}Z, \end{aligned} \tag{5.51}$$

where $\zeta_\mu = \frac{1}{2}v_\mu$ and $R_\mu = \frac{1}{16}(\bar{Z}\gamma_\mu\gamma_5 Z)$. Let us remember that the imaginary part of ξ is a linear function of the coordinates which yields a constant v_μ.

Similarly, the action for the matter scalars reads as below:

$$
\begin{aligned}
S_{\rm KG} = \int d^4x \Big\{ & (\tilde{\partial}^\mu \varphi^*)\tilde{\partial}_\mu \varphi + (\tilde{\partial}^\mu s^*)\tilde{\partial}_\mu s + \frac{i}{2} v_\mu \Big[(\tilde{\partial}^\mu \varphi^*)\varphi - \varphi^* \tilde{\partial}^\mu \varphi + (\tilde{\partial}^\mu s^*) s - s^* \tilde{\partial}^\mu s \Big] \\
& - \left(m^2 + \frac{1}{4}|h|^2 \right)(\varphi^* \varphi + s^* s) - \frac{i}{2} \Big[\bar{Z}\gamma^\mu (\varphi^* \mathscr{P}_{\rm L} - s^* \mathscr{P}_{\rm R}) \tilde{\partial}_\mu \Psi - (\tilde{\partial}_\mu \bar{\Psi})\gamma^\mu (\varphi \mathscr{P}_{\rm L} - s \mathscr{P}_{\rm R}) Z \Big] \\
& - \frac{1}{2}\bar{\Psi} \Big[\left(m\varphi - \frac{1}{2} h^* s \right) \mathscr{P}_{\rm L} - \left(ms + \frac{1}{2} h\varphi \right) \mathscr{P}_{\rm R} \Big] Z - \frac{1}{2} \bar{Z} \Big[\left(m\varphi^* - \frac{1}{2} h s^* \right) \mathscr{P}_{\rm R} \\
& - \left(ms^* + \frac{1}{2} h^* \varphi^* \right) \mathscr{P}_{\rm L} \Big] \Psi \Big\},
\end{aligned} \tag{5.52}
$$

which gives the following modified Klein-Gordon equations:

$$
\Theta \varphi_0 = -\frac{1}{2} \bar{Z} \left[\left(\tilde{p}_\mu \gamma^\mu - \frac{1}{2} h^* \right) \mathscr{P}_{\rm L} + m \mathscr{P}_{\rm R} \right] \Psi_0, \tag{5.53}
$$

$$
\Theta s_0 = \frac{1}{2} \bar{Z} \left[\left(\tilde{p}_\mu \gamma^\mu + \frac{1}{2} h \right) \mathscr{P}_{\rm R} + m \mathscr{P}_{\rm L} \right] \Psi_0, \tag{5.54}
$$

where we introduce the useful notation $\Theta \equiv -\left[\tilde{p}^2 - 2(\tilde{p}\cdot\zeta) - m^2 - \frac{1}{4}|h|^2 \right]$.

As expected from our analysis of the mixing part (5.41), the modified field equations of the matter sector are coupled by means of the background fermion, Z. In the next Section, we shall present a way to rewrite these equations and their associated dispersion relations.

5.3.3 The matter sector and the associated dispersion relations

To obtain the fermionic dispersion relation, let us first substitute the expressions for φ_0 and s_0, i.e., (5.53) and (5.54), into the modified Dirac equation (5.51). The Fierz rearrangement,

$$
\left(\bar{Z} M \Psi_0 \right) N Z = -\frac{1}{4} \left[\left(\bar{Z} Z \right) N M + \left(\bar{Z}\gamma_5 Z \right) N \gamma_5 M + \left(\bar{Z}\gamma_\alpha \gamma_5 Z \right) N \gamma^\alpha \gamma_5 M \right] \Psi_0, \tag{5.55}
$$

where M and N are arbitrary 4×4 matrices, allows us to rewrite the pieces involving the mixing of Ψ_0 and Z in terms of background fermionic condensates, which we will denote just as $\theta = \bar{Z}Z$, $\tau = \bar{Z}\gamma_5 Z$ and $C_\alpha = \bar{Z}\gamma_\alpha \gamma_5 Z$. After some simplifications using the relations, $\gamma^\mu \gamma^\alpha \gamma^\nu = \eta^{\mu\alpha}\gamma^\nu + \eta^{\alpha\nu}\gamma^\mu - \eta^{\nu\mu}\gamma^\alpha - i\epsilon^{\mu\alpha\nu\beta}\gamma_\beta \gamma_5$ and $\Sigma^{\mu\alpha} = \frac{i}{4}[\gamma^\mu, \gamma^\alpha]$, the field equation for Ψ_0 can be written in compact form as

$$
\left[(\tilde{p} - \zeta)_\mu \gamma^\mu + m - \mathscr{R}_\mu \gamma^\mu \gamma_5 - W_{\mu\alpha} \Sigma^{\mu\alpha} \gamma_5 \right] \Psi_0 = 0, \tag{5.56}
$$

where we define the nonlocal structures

$$
\begin{aligned}
\mathscr{R}_\mu &= \frac{1}{16\Theta} \left[2\tilde{p}_\mu \tilde{p}_\nu C^\nu - 2\left(\tilde{p}\cdot\zeta + m^2 + \frac{1}{4}|h|^2 \right) C_\mu + \tilde{p}_\mu (h^* - h)\tau - \frac{1}{2}\tilde{p}_\mu (h^* + h)\theta \right], \\
W_{\mu\alpha} &= \frac{im}{4\Theta} \tilde{p}_\mu C_\alpha .
\end{aligned} \tag{5.57}
$$

The derivation of dispersion relations for the matter sector is a more involved task. In the fermionic case, in particular, the presence of the last term, $\Sigma^{\mu\alpha}$, in Eq. (5.56) makes the

structure of the Dirac equation operator more complicated to manipulate. Following the approach presented in ref. [60], we adopt the standard squaring procedure and apply the Dirac operator with an opposite mass sign to the (5.56):

$$\mathcal{O}_{2\text{-der}}\Psi_0 = 0, \tag{5.58}$$

where the operator is given by

$$\begin{aligned}\mathcal{O}_{2\text{-der}} = (\tilde{p}-\zeta)^2 - m^2 - \mathscr{R}^2 + \frac{1}{4}W_{\nu\beta}W_{\mu\alpha}\big[\left(\eta^{\nu\mu}\eta^{\beta\alpha} - \eta^{\nu\alpha}\eta^{\beta\mu}\right) + 2i(\eta^{\nu\alpha}\Sigma^{\beta\mu} + \eta^{\beta\mu}\Sigma^{\nu\alpha})\big] \\ - i(\tilde{p}-\zeta-\mathscr{R})_\nu W_{\mu\alpha}(\eta^{\nu\mu}\gamma^\alpha - \eta^{\nu\alpha}\gamma^\mu).\end{aligned} \tag{5.59}$$

To eliminate the off-diagonal terms in spinor space, we repeat the squaring procedure to Eq. (5.58). Now, let us consider the operator $\mathcal{O}_{2\text{-der}}$ with opposite sign for the off-diagonal piece, i.e., $+i(\tilde{p}-\zeta-\mathscr{R})_\kappa W_{\lambda\rho}(\eta^{\kappa\lambda}\gamma^\rho - \eta^{\kappa\rho}\gamma^\lambda)$. This procedure gives a fourth-order equation satisfied by each component of the Dirac spinor Ψ_0, such that (for non-trivial field configurations)

$$\tilde{p}^4 - 2\tilde{p}^2\left[4(\tilde{p}\cdot\zeta) + m^2 - \zeta^2 + \frac{1}{4}|h|^2\right] + 8(\tilde{p}\cdot\zeta)\left[3(\tilde{p}\cdot\zeta) + m^2\right] + m^2\left(m^2 - 2\zeta^2 + \frac{1}{2}|h|^2\right) = 0, \tag{5.60}$$

where we neglect higher-order terms in the Lorentz-breaking parameters, since it is reasonable to consider them to be small (see, e.g., in refs. [60, 228] for theoretical discussions). The result (5.60) is the most general expression up to second order in Lorentz breaking for the fermionic dispersion relation of model (5.35). It is clear its non-dependence on the background fermionic condensates θ, τ and C_α. Therefore, we can see that, up to second order in LSV, the explicit dependence on the background is manifested only through the auxiliary complex scalar h and vector $\zeta_\mu = \frac{1}{2}v_\mu$ fields. An interesting consequence of this is that the results obtained from (5.60) are automatically parity invariant.

In the case of scalar fields, φ_0 and s_0, the right-hand side of their respective equations, (5.53) and (5.54), involves a mixing of Dirac and background fermions. To express these equations in terms of the background fermionic condensates, θ, τ and C_α, we first employ the squaring procedure to Eq. (5.51). This allows us to compose an expression for Ψ_0, which can then be substituted into the modified Klein-Gordon equations. After some algebra, we get

$$\Theta\varphi_0 = \frac{1}{4\Xi}\left[X^{(1)}(\varphi_0, s_0)\theta + \mathscr{M}^{(1)}(\varphi_0, s_0)\tau + Y^{(1)}_\alpha(\varphi_0, s_0)C^\alpha\right], \tag{5.61}$$

$$\Theta s_0 = -\frac{1}{4\Xi}\left[X^{(2)}(\varphi_0, s_0)\theta + \mathscr{M}^{(2)}(\varphi_0, s_0)\tau + Y^{(2)}_\alpha(\varphi_0, s_0)C^\alpha\right], \tag{5.62}$$

where $\Xi = \left[(\tilde{p}-\zeta)^2 - m^2 - R^2\right]^2 + 4(\tilde{p}-\zeta)^2R^2 - 4\left[(\tilde{p}-\zeta)\cdot R\right]^2$, and the explicit form of X's, $\mathscr{M}$'s and Y_α's can be found in Appendix B.2. Finally, from (5.61) and (5.62), is possible to obtain the full dispersion relation for the scalars, up to second order in LSV,

$$\begin{aligned}0 = \tilde{p}^4 - 4\tilde{p}^2\left[3(\tilde{p}\cdot\zeta) + \frac{1}{2}m^2 - \zeta^2 + \frac{1}{8}|h|^2\right] + 60(\tilde{p}\cdot\zeta)^2 \\ + 4m^2\left[3(\tilde{p}\cdot\zeta) + \frac{1}{32}(\tilde{p}\cdot C) + \frac{1}{4}m^2 - \zeta^2 + \frac{1}{8}|h|^2\right].\end{aligned} \tag{5.63}$$

In contrast to the fermionic case, Eq. (5.60), the modified dispersion relation for the scalar sector has a non-trivial dependence on the background fermionic condensate C_α, in addition to terms proportional to h and v_μ components.

Now, we are in a position to exploit the effects of this LSV background on the mass spectrum of the fermionic and scalar matter sectors. Let us take the rest frame, where the linear momentum is zero, $\boldsymbol{p}=0$, and the rest energy is nothing but the rest mass. From (5.60), we verify that the fermionic rest energy results in

$$E_{0,\text{fermion}} = \pm\sqrt{m^2+\frac{1}{2}\left(\boldsymbol{v}^2+|h|^2\right)}. \tag{5.64}$$

In this scenario, the fermion in question does not allow the existence of tachyonic mass modes. Therefore, considering that LSV terms are very small compared to the mass scale of the particles, we can take the limit $m^2\to\infty$, which corresponds to the regime $m^2\gg\boldsymbol{v}^2$ and $m^2\gg|h|^2$, in the positive solution of the spectra (5.64) in order to obtain a LSV shift in the fermion mass. The result is

$$E_{0,\text{fermion}}\Big|_{m^2\to\infty} \approx m\left(1+\frac{\boldsymbol{v}^2+|h|^2}{4m^2}\right). \tag{5.65}$$

On the other hand, for the scalar sector, Equ. (5.63), let us consider two particular cases, for simplicity: *i*) in the previous Section, we have got that the induced SUSY breaking occurs even when the background auxiliary component is zero. So, assuming $h=0$, we arrive at the following non-parity invariant results

$$E^{(1)}_{0,\text{scalar}}\Big|_{h=0} = \frac{\sqrt{B}}{2}\pm\frac{1}{2}\sqrt{-B+2(2m^2+\boldsymbol{v}^2)-\frac{m^2C_0}{4\sqrt{B}}}, \tag{5.66}$$

$$E^{(2)}_{0,\text{scalar}}\Big|_{h=0} = -\frac{\sqrt{B}}{2}\pm\frac{1}{2}\sqrt{-B+2(2m^2+\boldsymbol{v}^2)+\frac{m^2C_0}{4\sqrt{B}}}. \tag{5.67}$$

In the solutions (5.66) and (5.67) we defined the notations

$$A = G+\sqrt{G^2-4\left(16m^4+16m^2\boldsymbol{v}^2+\boldsymbol{v}^4\right)^3}, \tag{5.68}$$

$$G = m^4\left[\frac{27}{64}C_0^2+64(2\,m^2+3\boldsymbol{v}^2)\right]+2\boldsymbol{v}^4(30\,m^2-\boldsymbol{v}^2), \tag{5.69}$$

$$B = \frac{1}{3}\left\{\left(\frac{A}{2}\right)^{-\frac{1}{3}}\left[\left(\frac{A}{2}\right)^{\frac{2}{3}}+16m^4+16m^2\boldsymbol{v}^2+\boldsymbol{v}^4\right]+2(2m^2+\boldsymbol{v}^2)\right\}, \tag{5.70}$$

and $C_0=\bar{Z}\gamma_0\gamma_5 Z$ is the zeroth component of the background fermionic condensate, responsible for the parity breaking in both (5.66) and (5.67) rest mass modes.

ii) In other situation, we assume that the background is invariant under parity transformations. In this case, the effects of the background fermionic condensate disappear, i.e., $C_\alpha=0$,

$$E_{0,\text{scalar}}\Big|_{C_\alpha=0} = \pm\sqrt{m^2+\boldsymbol{v}^2+\frac{1}{2}|h|^2}. \tag{5.71}$$

In this situation, the scalar mass spectrum is quite similar to the fermionic case and does not allow for the presence of tachyonic mass modes. As before, assuming that $m^2 \gg v^2$ and $m^2 \gg |h|^2$, (5.71) reduces to

$$E_{0,\text{scalar}}\Big|_{C_\alpha=0} \approx m\left(1+\frac{2v^2+|h|^2}{4m^2}\right). \tag{5.72}$$

Unlike from the photon-photino sector, the fermion-scalar sector exhibits a SUSY breaking due the difference between the scalar and fermion rest masses in both cases, parity invariant and parity breaking LSV backgrounds.

Furthermore, another interesting result which can be expressed from the modified dispersion relations is the group velocity,

$$v_g = \nabla_{\text{Re}(\xi)p} E, \tag{5.73}$$

where $\nabla_{\text{Re}(\xi)p}$ is a gradient of linear momentum $\text{Re}(\xi)p$ and E is the energy that comes from the zeroth component of $\tilde{p}_\mu$. According to the conditions $i)$ and $ii)$, we arrive at the following group velocity for the scalars

$$\begin{aligned} v^i_{g,\text{scalar}}\Big|_{h=0} = &\frac{\tilde{p}^i\left[\tilde{\boldsymbol{p}}^2+m^2-E^2-3(\tilde{\boldsymbol{p}}\cdot\boldsymbol{v})+\boldsymbol{v}^2/2\right]}{E\left[\tilde{\boldsymbol{p}}^2+m^2-E^2-3(\tilde{\boldsymbol{p}}\cdot\boldsymbol{v})+\boldsymbol{v}^2/2\right]-m^2C_0/32} \\ &-\frac{3v^i\left[\tilde{\boldsymbol{p}}^2+m^2-E^2-5(\tilde{\boldsymbol{p}}\cdot\boldsymbol{v})\right]+m^2C^i/16}{2E\left[\tilde{\boldsymbol{p}}^2+m^2-E^2-3(\tilde{\boldsymbol{p}}\cdot\boldsymbol{v})+\boldsymbol{v}^2/2\right]-m^2C_0/16}, \end{aligned} \tag{5.74}$$

in the case of $h=0$, and

$$v^i_{g,\text{scalar}}\Big|_{C_\alpha=0} = \frac{\tilde{p}^i}{E}-\frac{3v^i\left[\tilde{\boldsymbol{p}}^2+m^2-E^2-5(\tilde{\boldsymbol{p}}\cdot\boldsymbol{v})\right]}{2E\left[\tilde{\boldsymbol{p}}^2+m^2-E^2-3(\tilde{\boldsymbol{p}}\cdot\boldsymbol{v})+(2\boldsymbol{v}^2+|h|^2)/4\right]}, \tag{5.75}$$

for a parity invariant background.

And finally, the group velocity for the fermionic case is given by

$$v^i_{g,\text{fermion}} = \frac{\tilde{p}^i}{E}-\frac{v^i\left[\tilde{\boldsymbol{p}}^2+m^2-E^2-3(\tilde{\boldsymbol{p}}\cdot\boldsymbol{v})\right]}{E\left[\tilde{\boldsymbol{p}}^2+m^2-E^2-2(\tilde{\boldsymbol{p}}\cdot\boldsymbol{v})+(\boldsymbol{v}^2+|h|^2)/4\right]}, \tag{5.76}$$

where $\tilde{p}_i = \text{Re}(\xi)\,p_i$, with $i=1,2,3$. Both cases reduce to the usual situation, $v^i_g = p^i/E$, if we turn off the LSV background. Let us notice that, even in the presence of LSV terms, the expressions for the group velocities (5.74), (5.75), and (5.76) admit the condition $|v^i_g|<1$, indicating in this case that the causal structure of the theory is maintained (see, e.g., in refs. [**?**,58–60] for discussions on causality in other scenarios with Lorentz violation).

5.4 A glance at the electron's EDM

We are, at this point, ready to start off the task of inspecting the structure of the fermionic current, as the modifications that arise due to the background may induce a contribution

to the charged particle EDM interaction (see, e.g., in refs. [229, 230] for the textbook level introduction). First, due to non-local structure, it proves useful to rewrite the modified Eq. (5.56) as

$$\Big\{(1-s)\big[(\tilde{p}-\zeta)_\mu\gamma^\mu+m\big]-r_\mu\gamma^\mu\gamma_5-w_{\mu\alpha}\Sigma^{\mu\alpha}\Big\}\Psi_0=0, \tag{5.77}$$

where we introduce the following definitions

$$\begin{aligned}
r_\mu &= \frac{1}{16m^2}\left[2\tilde{p}_\mu\tilde{p}_\nu C^\nu-2\left(\tilde{p}\cdot\zeta+m^2+\frac{1}{4}|h|^2\right)C_\mu+\tilde{p}_\mu(h^*-h)\tau-\frac{1}{2}\tilde{p}_\mu(h^*+h)\theta\right],\\
w_{\mu\alpha} &= \frac{i}{4m}\tilde{p}_\mu C_\alpha,\\
s &= \frac{1}{m^2}\big[\tilde{p}^2-2(\tilde{p}\cdot\zeta)\big].
\end{aligned} \tag{5.78}$$

By multiplying the modified Eq. (5.77), with momentum $\tilde{p}$, to the left by $\bar{\Psi}_0(\tilde{p}')$, taking the Dirac conjugate of (5.77), with momentum $\tilde{p}'$, and multiplying it by $\Psi_0(\tilde{p})$ to the right, and finally summing the results we get the Gordon decomposition

$$\begin{aligned}
\bar{\Psi}_0(\tilde{p}')\gamma^\nu\Psi_0(\tilde{p}) = &-\frac{1}{2m}\bar{\Psi}_0(\tilde{p}')\Big\{\Big[(\tilde{p}+\tilde{p}'-2\zeta)^\nu-s(\tilde{p}-\zeta)^\nu-s'(\tilde{p}'-\zeta)^\nu\Big]\\
&+\frac{i}{2}\Big[\big(w'+w\big)_\mu{}^\nu-\big(w'+w\big)^\nu{}_\mu+2im(s+s')\delta^\nu_\mu\Big]\gamma^\mu\\
&-2i\Big[(\tilde{p}'-\tilde{p})_\mu+s(p-\zeta)_\mu-s'(p'-\zeta)_\mu\Big]\Sigma^{\mu\nu}+(r'-r)^\nu\gamma_5\\
&+\frac{1}{2}\big(w'-w\big)_{\mu\alpha}\epsilon^{\mu\alpha\nu\tau}\gamma_\tau\gamma_5\Psi_0(\tilde{p})-2i(r'+r)_\mu(\tilde{p}')\Sigma^{\mu\nu}\gamma_5\Big\}\Psi_0(\tilde{p}).
\end{aligned} \tag{5.79}$$

Here, the primes denote the structures carrying the momentum $\tilde{p}'$. This result, besides providing information on the vector and axial charge densities in terms proportional to the identity and γ_5, also brings to light the possible interactions that the electromagnetic current may induce in this scenario, i.e., interactions such as electric and magnetic dipole moments associated with the terms $\Sigma^{\mu\nu}$ and $\Sigma^{\mu\nu}\gamma_5$, respectively, as well as other terms that require further attention.

From the last term of (5.79), one can identify the piece from which the EDM emerges,

$$\frac{i}{8m^3}C^\tau(p'_\mu p'_\tau+p_\mu p_\tau)\bar{\Psi}_0(\tilde{p}')\Sigma^{\mu\nu}\gamma_5\Psi_0(\tilde{p}). \tag{5.80}$$

When minimally coupled to the gauge field $\tilde{a}_\nu$, the term in Eq. (5.80) corresponds to the following structure for the effective electric dipole interaction

$$\mathscr{L}_{\rm EDM}=-i\frac{\mu_{\rm B}}{8m^2}C^\tau\tilde{\partial}_\tau\big(\bar{\Psi}\Sigma^{\mu\nu}\gamma_5\Psi\big)\mathscr{F}_{\mu\nu}, \tag{5.81}$$

where $\mu_{\rm B}=e/(2m)$ is the Bohr magneton and $\mathscr{F}_{\mu\nu}$ is defined in Eq. (5.18). Following ref. [231], one can verify that, in our case, the EDM is given by

$$d=-\frac{F_3(\tilde{q}^2=0)}{2m}=\frac{\mu_{\rm B}}{4m^2}C^\tau\tilde{q}_\tau, \tag{5.82}$$

with $\tilde{q} = \tilde{p}' - \tilde{p}$ being the transfer momentum of the interaction. $F_3(\tilde{q}^2)$ is the third electromagnetic form factor associated with the EDM.

In the case of the electron EDM, denoted by d_e, the most recent experimental results, obtained by using electrons confined inside molecular ions subject to a huge intramolecular electric field, provide an upper bound of $d_e < 4.1 \times 10^{-30}$ e·cm [27,28] (see also ref. [29] for the Standard Model prediction concerning the long-distance hadronic contributions). We can use these results to estimate a bound for the modulus of the fermionic background condensate C^τ.

Let us remember that $\tilde{q}^2 = \tilde{q}^\mu \tilde{q}_\mu = 0$ for the EDM form factor configuration. Consequently, assuming a typical energy scale of the order of 1 MeV and considering the special case where C^τ is timelike, i.e., $\boldsymbol{C} = 0$, we arrive at

$$\left|C^0\right| < 2.2 \times 10^{-13}\,\text{eV}. \tag{5.83}$$

For a purely spacelike C^τ, a reference frame can be chosen in which $C^0 = 0$. In this case, it is possible to establish a bound on the magnitude of $\boldsymbol{C}$ component,

$$\left|\boldsymbol{C}\right| < \frac{1}{\text{Re}(\xi)\cdot\cos(\alpha)}\, 2.2 \times 10^{-13}\,\text{eV}, \tag{5.84}$$

where α is the angle between the spatial part of the four-momentum transfer, $\tilde{\boldsymbol{q}}$, and $\boldsymbol{C}$. We justify that the choice of splitting the two cases of C^τ time- or space-like is a common procedure in the study of LSV models. The reason is that either choice (time- or space-like) may induce different effects as far as physical observables are concerned.

Once the bound in (5.84) depends on both $\text{Re}(\xi)$ and α, we can collect all upper bounds that within a range $\alpha = [0, \pi/2)$ by plotting a graph of $\left|\boldsymbol{C}\right|$ as a function of α for a specific value of $\text{Re}(\xi)$. As an example, Figure 4 represents the plot of the upper bounds on $\left|\boldsymbol{C}\right|$ for $\text{Re}(\xi) = 0.5$, 1.0, and 1.5.

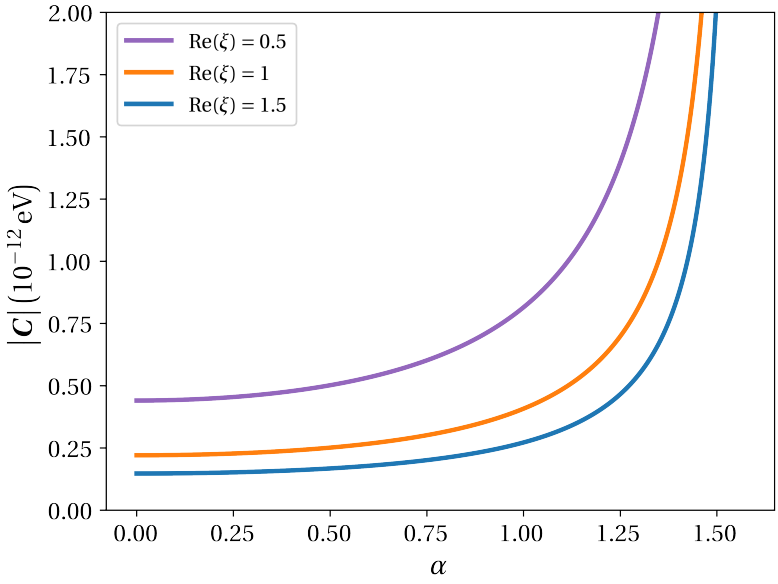

Figure 4 – Plot of the upper bounds on the spatial components of C^τ as a function of α for $\text{Re}(\xi) =$ 0.5, 1.0, and 1.5, in purple, orange, and blue, respectively.

5.5 Final considerations

In this Chapter, which was formally published in [219], we have studied the implications of a Lorentz-violating background supermultiplet of an $\mathcal{N} = 1$-supersymmetric $U(1)$ gauge model that extends the topological insulator Isobe-Nagaosa's QED model [215]. In our endeavor, we consider that the LSV parameters may have their microscopic origin traced back to a background SUSY multiplet, a chiral superfield. Instead of taking the LSV parameters for granted and extending the SUSY algebra, we keep the ordinary SUSY structure and assume the existence of the background mentioned above. Condensates of the fermionic component of the background superfield appear that are in the backstage of the scalar, pseudoscalar, and pseudovector objects that correspond to LSV parameters.

The modifications in the gauge sector that arise as a consequence of LSV in the fermionic matter consist of nothing but a dilation factor in Maxwell's equations. Indeed, the photon-photino partners are influenced only by the real component of the Lorentz-violating parameter and, therefore, we do not observe any physically relevant modifications in this sector, at least initially. On the other hand, the scalar matter is modified in both its dynamic and mass terms. Furthermore, the fermionic sector also receives an additional contribution that is proportional to the background fermionic condensate, $\bar{Z}\gamma_\mu\gamma_5 Z$. In this case, we believe that such a contribution arises due to the soft SUSY breaking induced by LSV. In this sense, it is interesting to recall that our model successfully reproduces the CPT-odd terms of the SME, with one of these terms appearing naturally as a direct consequence of SUSY breaking.

Considering the dispersion relations, we verify that, in the case of fermions, the terms proportional to the background fermionic condensates appear only as higher-order contributions in the Lorentz violation parameters. Therefore, by assuming that the latter are small compared to the mass m, such condensates do not provide relevant contributions to the rest energy nor to the fermionic group velocity. On the other hand, the scalar dispersion relation receives contribution from the background condensate $\bar{Z}\gamma_\mu\gamma_5 Z$ already in the second order.

Finally, our results from Section 6.4 indicate a possible connection between the EDM and the SUSY breaking induced by LSV. In this scenario, it is shown that SUSY matter scalars play a supportive role in the process of generating the EDM of the charged fermion.

The introduction of additional Lorentz-violating terms in the gauge sector, which induces significant modifications in the photon-photino sector, is a path to be followed as a step forward. The motivation to do that is to keep track of the interference between the effects of the different LSV terms present in the matter and the gauge sectors.

Furthermore, based on the theoretical framework developed here, we aim to explore potential applications to those condensed matter systems that exhibit (low-energy) SUSY and Lorentz symmetry as emergent phenomena in the dynamics of quasiparticle excitations. On the other hand, the modified photonic and electronic dispersion relations including both SUSY and LSV effects may be studied in connection with photon-photon, Breit-Wheeler and

Compton scatterings which may be used to impose upper limits on the parameters with the help of astrophysical data, such as measurements of (non-)attenuation of gamma-rays from active galactic nuclei (AGNs), gamma-ray bursts (GRBs) and extra galactic background light (EBL). Also, we keep in mind that QED high-precision tests can also provide estimates and constraints on the parameters of the model.

In the next Chapter, we change the perspective and study how effects coming from a microscopic structure of spacetime in the Loop Quantum Gravity framework can generate modifications in fermion dynamics through the appearance of a Lorentz-violating operator in the Dirac equation. We also discuss some phenomenological implications of this scenario.

Chapter

6

Loop Quantum Gravity effects on charged leptons

Here our journey through Lorentz-symmetry violation comes to an end, and Our efforts in this Chapter consist in reassessing a modified Dirac equation that incorporates a $\gamma^0\gamma_5$-LSV term induced as a Loop Quantum Gravity (LQG) effect. The results of this Chapter were published in Ref. [341]. Before going into the last step of our Lorentz-symmetry violation analysis, some background is necessary.

The theoretical framework of LQG is one of the most promising ways to inspect the challenges of quantum gravity, which seeks to understand the fundamental nature of the spacetime and gravity at the quantum level [232, 233]. In LQG, the spacetime is considered to be discrete rather than continuous, which is a departure from the smooth, continuous spacetime described by general relativity. The theory represents the spacetime as a network or quantum foam of interconnected loops. These loops are thought to be the building blocks of space and time at the smallest scales. The key idea in LQG is that quantities, such as area and volume, are quantized, meaning they come in discrete, indivisible units. The theory uses mathematical structures called spin networks and spin foams to describe the quantum properties of the spacetime [234–246]. LQG is still a research area in progress and it has not yet been experimentally confirmed once its principals predictions and phenomenological aspects become relevant at the order of the Planck scale ($\ell_P \sim 10^{19}$ GeV) [67–69,247]. However, indirect ways to probe the soft effects of quantum gravity at larger scales or through cosmological observations, e.g, some experiments and observations related to cosmology [248, 249], high-energy astrophysics [64,250–253], or precision measurements [254,255] might provide insights into LQG phenomenology.

The investigation on Lorentz-symmetry violation (LSV) is another significant approach to uncover evidence in the pursuit of quantum gravity, once it is also expected to happen at the Planck scale [63–65, 67, 72], where strong space-time fluctuations are expected to occur. In this context, discussions related to tests based on Modified Dispersion Relations (MDRs), using high-energy photons available from astrophysical measurements, can contribute to analyzes of possible deviations compared to standard dispersion relations, indicating the presence of LSV or some effects of quantum gravity, such as LQG [63–65]. Additionally, in this context, an important connection between the LQG and LSV frameworks is presented in [67], where

the modified Maxwell equations point vacuum birefringence. Two other important works regarding the MDRs, characterizing dispersion relations that could indicate the existence of the LSV, can be found in Refs. [68, 69].

In the context of MDRs, as argued in [256] at the leading order of LSV, the modified speed of a massless particle with energy E can be expressed as $v(E) \approx (1 - \xi E)$, where ξ refers to the LSV scale approximately of the order of a fraction of the Planck scale. Consequently, the velocity difference between two massless particles with different energies becomes apparent whenever their energies are sufficiently high, and the discrepancies in travel time accumulate over a considerable propagation distance. As a result, cosmic photons and neutrinos, particularly those originating from gamma-ray bursts (GRBs), and active galactic nuclei (AGNs) exhibiting simultaneous high energy, provide a unique window for exploring LSV during their journeys through the Universe [64]. Regarding the LSV exploration linked to GRBs, a comprehensive summary is provided in [256] stating that: for photons, without helicity dependence, we have $v(E) = (1 - E/E^{\gamma}_{\mathrm{LSV}})$, with $E^{\gamma}_{\mathrm{LSV}} \approx 3.6 \times 10^{17}$ GeV, indicating that photons are subluminal and high energy photons propagate slower than low energy ones [96, 100–107, 257, 258]; for neutrinos and anti-neutrinos, their speeds are $v(E) \approx (1 \mp E/E^{\nu}_{\mathrm{LSV}})$, with $E^{\nu}_{\mathrm{LSV}} \approx 6.5 \times 10^{17}$ GeV, indicating that neutrinos and anti-neutrinos, or Majorana neutrinos with opposite helicities, could be subluminal and superluminal with the sign of the velocity variations depending on the helicities [92, 93, 97–99, 107, 258].

In [256] the authors find out that LQG is as a good theoretical candidate for explaining the phenomenological suggestion of the speed variations of cosmic photons and neutrinos picture consistently, and suggest that others observable signals could also testify the predictions of LQG in the future. In order to show that, they introduce LQG description that consists in assuming specifics conditions and properties for the so-called weave states, which are semiclassical states with a characteristic length $\mathscr{L}$ that describes the discreteness of the spacetime represented by this state. When the de Broglie wavelength (λ) of a particle satisfies the condition $\ell_{\mathrm{P}} \ll \lambda$, in which $\ell_{\mathrm{P}} = 1.61 \times 10^{-35}$ m is the Planck length, and the characteristic length $\mathscr{L}$ satisfies the condition $\ell_{\mathrm{P}} \ll \mathscr{L} \leq \lambda$, one can compute the weave state expectation of the corresponding Hamiltonian of the particle and obtain an effective Hamiltonian from which we can read off the modified dispersion relation and the speed of such particle [69, 247]. Their results can be directly related to observable phenomena and conversely the phenomenological analyses may be used to examine the description of LQG based on wave states, leading towards better understanding of the LQG framework and further progress of LQG theories.

The Chapter is structured as follows: In Section 6.1, we present the modified Dirac equation discussed in [256]. We provide the action, and the modified fermion propagator associated with this equation. The dispersion relation is reevaluated, and additionally, we introduce the correspondent group velocity. In Section 6.2, we derive the positive and negative energy solutions for this modified Dirac equation. The Section 6.3 focuses on obtaining the conserved current associated with the $U(1)$ gauge symmetry of the model. Through

minimal coupling with the electromagnetic (EM) field, we demonstrate that this current aligns with the EM current within the framework of modified Maxwell's equations. In Section 6.4, we obtain the Gordon decomposition of the conserved current exploring its implications. Section 6.5 is devoted to obtaining spin- and velocity-dependent corrections to the Coulomb potential due to the modified current structure of the model. The Section 6.6 involves deriving the non-relativistic limit of the modified Dirac equation with minimal coupling. In Section 6.7, we delve into the question of renormalizability, concluding that the model is super-renormalizable. Finally, Section 6.8 encompasses our concluding considerations.

6.1 The modified Dirac equation from LQG

The modified Dirac equation emerging from the LQG effects in the context of [256] is

$$\left(i\gamma^{\mu}\partial_{\mu}-\frac{\hat{C}}{2\mathscr{L}}\gamma^{0}\gamma_{5}-m\right)\psi=0\,, \tag{6.1}$$

where $\mathscr{L}$ is a characteristic length constraint by the condition $\ell_{\rm P}\ll\mathscr{L}\leqslant\lambda$, in which $\ell_{\rm P}=1.61\times10^{-35}$ m is the Planck length, and λ is the de Broglie wavelength of a particle. The $\hat{C}$-operator is defined by

$$\hat{C}=\frac{\kappa_7}{2}\left(\frac{\ell_p}{\mathscr{L}}\right)^{\Upsilon_f}\ell_p^2\,\boldsymbol{\nabla}^2=\xi\,\boldsymbol{\nabla}^2\,, \tag{6.2}$$

in which Υ_f is a phenomenological parameter from LQG, κ_7 is a magnitude parameter, and ξ is the combination of these parameters that has length dimension. Thus, it is convenient to define the quantity $\vartheta\equiv\xi/(2\mathscr{L})$, with length dimension, and consequently, all the known results of the fermion theory are recovered in the limit $\vartheta\to0$. The γ^{μ}-matrices are the usual 4×4 Dirac's matrices that satisfy the relations $\gamma^{\mu}\gamma^{\nu}=\eta^{\mu\nu}-2i\Sigma^{\mu\nu}$, and $\{\gamma^{\mu},\gamma_5\}=0$. The correspondent action from Eq. (6.1) is

$$S(\bar{\psi},\psi)=\int d^4x\bar{\psi}\left(i\gamma^{\mu}\partial_{\mu}-\vartheta\gamma^{0}\gamma_{5}\boldsymbol{\nabla}^2-m\right)\psi, \tag{6.3}$$

that, upon an integration by parts, we obtain

$$S(\bar{\psi},\psi)=\int d^4x\left[\bar{\psi}\left(i\gamma^{\mu}\partial_{\mu}-m\right)\psi+\vartheta(\boldsymbol{\nabla}\bar{\psi})\cdot\gamma^{0}\gamma_{5}(\boldsymbol{\nabla}\psi)\right], \tag{6.4}$$

and the adjoint field that satisfies the equation

$$i\partial_{\mu}\bar{\psi}\gamma^{\mu}+\vartheta(\boldsymbol{\nabla}^2\bar{\psi})\gamma^{0}\gamma_{5}+m\bar{\psi}=0\,. \tag{6.5}$$

Taking a plane wave solution $\psi(x)=u(p)e^{-ip\cdot x}$, the modified Dirac equation in momentum space reads

$$\left(\gamma^{\mu}p_{\mu}+\vartheta\boldsymbol{p}^2\gamma^{0}\gamma_{5}-m\right)u(p)=0, \tag{6.6}$$

where $u(p)$ is an amplitude in the momentum space.

We can map the operator $\vartheta \boldsymbol{p}^2 \gamma^0 \gamma_5$ into the nonminimal SME framework discussed in Section 3.2. For this purpose, we return to Eq. (3.36) for $D = 5$, which allows us to write $\hat{b}_\mu = b^{(5)}_{\mu\nu\kappa}\, p^\nu p^\kappa$, where $b^{(5)}_{\mu\nu\kappa}$ has 80 independent components (see Table 1). The operator $\vartheta \boldsymbol{p}^2 \gamma^0 \gamma_5$ is contained in the term $b^{(5)}_{\mu\nu\kappa}\, p^\nu p^\kappa$ by requiring that the only nonzero components are $b^{(5)}_{0ij}\, p^i p^j$, with $b^{(5)}_{0ij}$ given by $\vartheta \delta_{ij}$. Therefore, the connection with the SME formalism is made clear.

The term $\vartheta \boldsymbol{p}^2$ appearing alongside the $\gamma^0\gamma_5$-matrix in Eq. (6.6) brings a CPT-violating contribution, as argued in [169]. The CPT theorem states that CPT symmetry arises under assumptions through the combination of Lorentz-symmetry and quantum-mechanical assumptions. Then, if CPT symmetry is broken, one or more of the assumptions necessary to prove the CPT theorem should not be valid. Once both Lorentz and CPT invariance involve spacetime transformations, it is natural to suspect that CPT violation implies Lorentz-symmetry breakdown. This statement was rigorously proven in [117–119]. However, Lorentz-symmetry breaking does not necessarily imply CPT violation.

To obtain the fermion propagator, it is convenient to define the matrix $D = p_\mu \gamma^\mu + d_\mu \gamma^\mu \gamma_5 - m$ that acts on the $u(p)$ amplitude in Eq. (6.6), where $d^\mu = (\vartheta \boldsymbol{p}^2, \boldsymbol{0})$ is a time-like vector whose the component depends on the $\boldsymbol{p}^2$. Thereby, the fermion propagator is the inverse of the D-matrix given by

$$\begin{aligned} D^{-1} = \Big[& \left(p^2 - m^2 - d^2\right)\left(m + p_\mu \gamma^\mu + d_\mu \gamma^\mu \gamma_5\right) \\ & - 2(p\cdot d)\left(d_\mu \gamma^\mu - p_\mu \gamma^\mu \gamma_5\right) - 2m\left(p^\alpha d^\beta - p^\beta d^\alpha\right)\varepsilon_{\alpha\beta\mu\nu}\Sigma^{\mu\nu}\Big]\Delta^{-1}, \end{aligned} \tag{6.7}$$

where the denominator Δ is given by

$$\Delta = (p^2 - m^2)^2 - 4(p\cdot d)^2 + 2d^2(p^2 + m^2) + d^4\,. \tag{6.8}$$

The dispersion relation of the particle is the propagator's pole at $\Delta = 0$. Restricting these results to the case of the time-like 4-vector $d^\mu = (\vartheta \boldsymbol{p}^2, \boldsymbol{0})$, the fermion dispersion relation is reduced to

$$4p^2\vartheta^2\boldsymbol{p}^4 + \left(p^2 - m^2 - \vartheta^2\boldsymbol{p}^4 + 2E\vartheta\boldsymbol{p}^2\right)\left(p^2 - m^2 - \vartheta^2\boldsymbol{p}^4 - 2E\vartheta\boldsymbol{p}^2\right) = 0. \tag{6.9}$$

The corresponding energy solutions of Eq. (6.9) are the positive, $+E_\pm(\boldsymbol{p})$, and negative, $-E_\pm(\boldsymbol{p})$, energy eigenstates, where

$$E_\pm(\boldsymbol{p}) = \sqrt{\boldsymbol{p}^2 + m^2 + \vartheta^2\boldsymbol{p}^4 \pm \vartheta(\boldsymbol{p}^2)^{3/2}}, \tag{6.10}$$

that confirm the results obtained in [256]. In the rest frame of the fermion, we have no mass splitting

$$E_0 = m. \tag{6.11}$$

This indicates that the $(\pm)$ signals in Eq. (6.10) correspond to two energy eigenstates of the same fermion.

The i-th component of the group velocity is

$$\boldsymbol{v}_i = \frac{\partial E}{\partial \boldsymbol{p}_i} = \left[\frac{6\,(E^2 - m^2 - \boldsymbol{p}^2)}{E^2 - m^2 - \boldsymbol{p}^2 - \vartheta^2\,\boldsymbol{p}^4} + \vartheta^2\,\boldsymbol{p}^2 - 5 \right] \frac{\boldsymbol{p}_i}{E}, \tag{6.12}$$

which reduces to the usual case, $\boldsymbol{p}_i/E$, whether we turn off the LSV terms. Substituting the positive energy solutions, one obtain

$$\boldsymbol{v}_\pm = \left[\frac{1 + \vartheta^2\,\boldsymbol{p}^2 \pm 6\,\vartheta\,|\boldsymbol{p}|}{\sqrt{\boldsymbol{p}^2 + m^2 + \vartheta^2\,\boldsymbol{p}^4 \pm \vartheta(\boldsymbol{p}^2)^{3/2}}} \right] \boldsymbol{p}\,. \tag{6.13}$$

The result with a $(+)$ sign on the right-hand side of Eq. (6.13) is superluminal, $|v_+| > 1$, consistent with the phenomenology discussed in [256]. At this point, it is important to emphasize that we are dealing with a possible break of Lorentz symmetry, and for this reason, the familiar causal structure of special relativity may not be such a rigid rule that must hold.

For the purposes of Section 6.4, it is interesting to present the form of the dispersion relation in the high momentum limit at leading order two,

$$E_\pm(\,\mathbf{p}) = |\boldsymbol{p}| + \frac{m^2}{|\boldsymbol{p}|} \pm \vartheta |\boldsymbol{p}|^2\,, \tag{6.14}$$

followed by the group velocity modulus associated with this regime,

$$|\boldsymbol{v}^\pm| = 1 - \frac{m^2}{2|\boldsymbol{p}|^2} \pm 2\vartheta|\boldsymbol{p}|, \tag{6.15}$$

which has the same interpretation regarding the causal aspects of Eq. (6.13).

6.2 The positive energy solutions for the modified Dirac equation

From the energy eigenstates, we can obtain the positive energy solutions for the modified Dirac equation in the laboratory reference frame. We consider the following plane wave solution for a free fermion ψ:

$$\psi(x, \pm s) = u(p, \pm s)\, e^{-ip\cdot x} = \begin{pmatrix} u_a(p, \pm s) \\ u_b(p, \pm s) \end{pmatrix} e^{-ip\cdot x}\,, \tag{6.16}$$

in which the positive energy is described by the four-momentum fermion $p^\mu = \left(E_\pm, \boldsymbol{p}\right)$, in a laboratory reference frame, and with spin projection $(\pm s)$. Using this definition, the equation field is

$$\left(E_\pm \gamma^0 - p_i \gamma^i - m + \vartheta \boldsymbol{p}^2 \gamma^0 \gamma_5\right) u(p, \pm s) = 0\,. \tag{6.17}$$

In matrix form, this equation leads to the coupled system

$$(E_\pm - m)\, u_a(p, \pm s) + \left(\vartheta \boldsymbol{p}^2 - \boldsymbol{\sigma}\cdot\boldsymbol{p}\right) u_b(p, \pm s) = 0, \tag{6.18}$$

$$(E_\pm + m)\, u_b(p, \pm s) + \left(\vartheta \boldsymbol{p}^2 - \boldsymbol{\sigma}\cdot\boldsymbol{p}\right) u_a(p, \pm s) = 0, \tag{6.19}$$

Thus, we obtain the relation

$$u_b(p,\pm s) = \frac{\boldsymbol{\sigma}\cdot\boldsymbol{p} - \vartheta \boldsymbol{p}^2}{E_\pm + m} u_a(p,\pm s). \tag{6.20}$$

Therefore, the general solution for a positive energy eigenstate in momentum space is written as

$$u(p,\pm s) = \begin{pmatrix} 1 \\ \dfrac{\boldsymbol{\sigma}\cdot\boldsymbol{p} - \vartheta \boldsymbol{p}^2}{E_\pm + m} \end{pmatrix} u_a(p,\pm s)\,. \tag{6.21}$$

As in the case of the usual Dirac equation, we construct the spin up solution from the amplitude

$$u_a(p,+s) = N_+ \begin{pmatrix} 1 \\ 0 \end{pmatrix}, \tag{6.22}$$

that substituting in Eq. (6.20), the u_b-amplitude for $(+s)$ is

$$u_b(p,+s) = \frac{N_+}{E_\pm + m} \begin{pmatrix} p_z - \vartheta \boldsymbol{p}^2 \\ p_x + i p_y \end{pmatrix}. \tag{6.23}$$

Thereby, the general solution has the form

$$u(p,+s) = N_+ \begin{pmatrix} 1 \\ 0 \\ \dfrac{p_z - \vartheta \boldsymbol{p}^2}{E_\pm + m} \\ \dfrac{p_x + i p_y}{E_\pm + m} \end{pmatrix}, \tag{6.24}$$

where N_+ is a normalization constant. Using the normalization condition $\bar{u}(p,+s)\,u(p,+s) = 2m$, the N_+-constant is

$$N_+ = \sqrt{\frac{2m(E_\pm + m)^2}{2m(E_\pm + m) + \vartheta(2p_z \pm |\boldsymbol{p}|)\boldsymbol{p}^2}}\,. \tag{6.25}$$

The solution describing spin up is

$$\psi(x,+s) = \sqrt{\frac{2m(E_\pm + m)^2}{2m(E_\pm + m) + \vartheta(2p_z \pm |\boldsymbol{p}|)\boldsymbol{p}^2}} \begin{pmatrix} 1 \\ 0 \\ \dfrac{p_z - \vartheta \boldsymbol{p}^2}{E_\pm + m} \\ \dfrac{p_x + i p_y}{E_\pm + m} \end{pmatrix} e^{-ip\cdot x}\,. \tag{6.26}$$

For the case of the spin-down solution, the u_a-amplitude becomes

$$u_a(p,-s) = N_- \begin{pmatrix} 0 \\ 1 \end{pmatrix}, \tag{6.27}$$

and thus, we obtain

$$u_b(p,-s) = \frac{N_-}{E_\pm + m} \begin{pmatrix} p_x - i p_y \\ -p_z - \vartheta \boldsymbol{p}^2 \end{pmatrix}. \tag{6.28}$$

The general solution for $(-s)$ has the form

$$u(p,-s) = N_- \begin{pmatrix} 0 \\ 1 \\ \dfrac{p_x - i p_y}{E_\pm + m} \\ \dfrac{-p_z - \vartheta \boldsymbol{p}^2}{E_\pm + m} \end{pmatrix}, \tag{6.29}$$

where N_- is the correspondent normalization constant determined by the condition $\bar{u}(p,-s)$ $u(p,-s) = 2m$. Thereby, we obtain

$$N_- = \sqrt{\frac{2m(E_\pm + m)^2}{2m(E_\pm + m) - \vartheta(2p_z \mp |\boldsymbol{p}|)\boldsymbol{p}^2}}, \tag{6.30}$$

and the correspondent solution is given by

$$\psi(x,-s) = \sqrt{\frac{2m(E_\pm + m)^2}{2m(E_\pm + m) - \vartheta(2p_z \mp |\boldsymbol{p}|)\boldsymbol{p}^2}} \begin{pmatrix} 0 \\ 1 \\ \dfrac{p_x - i p_y}{E_\pm + m} \\ \dfrac{-p_z - \vartheta \boldsymbol{p}^2}{E_\pm + m} \end{pmatrix} e^{-ip\cdot x}. \tag{6.31}$$

The limit $\vartheta \to 0$ recovers all known results of the usual Dirac equation. Notice that, the normalization constants are not equal by the introduction of ϑ-scale, *i.e.*, $N_+ \neq N_-$. Consequently, the introduction of the LQG-scale breaks the symmetry in the Dirac equation solutions, and still includes degenerate solutions $(\pm)$ in Eqs. (6.26) and (6.31), respectively.

We can better understand this difference in the normalization constants by considering the role played by helicity in this modified Dirac equation scenario. In this sense, it is important to note that it is possible to construct polarized states along an arbitrary direction $\boldsymbol{r}$, as discussed in Section C.4 of Appendix C. In general, the defining relation for such states is $\boldsymbol{\sigma}\cdot\hat{\boldsymbol{r}}\, w = \pm w$, where the spinor w corresponds to a particle polarized along the $+1$ or -1 direction of the unit vector $\hat{\boldsymbol{r}}$. From this point of view, we can rewrite the general solution

given in Eq. (6.16) in terms of a Pauli spinor ξ that is an eigenstate of $\boldsymbol{\sigma}\cdot\boldsymbol{p} = \pm|\boldsymbol{p}|\,\boldsymbol{\sigma}\cdot\hat{\boldsymbol{p}}$, with eigenvalue $\pm|\boldsymbol{p}|$. In this convenient form, the general solution can be written as

$$u_{\pm}(\boldsymbol{p}) = N\begin{pmatrix} \xi_{\pm}(\boldsymbol{p}) \\ \dfrac{\boldsymbol{\sigma}\cdot\boldsymbol{p} - \vartheta\boldsymbol{p}^2}{E_{\pm}+m}\xi_{\pm}(\boldsymbol{p}) \end{pmatrix}, \tag{6.32}$$

or,

$$u_{\pm}(\boldsymbol{p}) = N\begin{pmatrix} \xi_{\pm}(\boldsymbol{p}) \\ \dfrac{\pm|\boldsymbol{p}| - \vartheta\boldsymbol{p}^2}{E_{\pm}+m}\xi_{\pm}(\boldsymbol{p}) \end{pmatrix}. \tag{6.33}$$

To be more explicit, in spherical coordinates where $\boldsymbol{p} = |\boldsymbol{p}|(\sin\theta\cos\varphi, \sin\theta\sin\varphi, \cos\theta)$, comes

$$\boldsymbol{\sigma}\cdot\hat{\boldsymbol{p}} = \begin{pmatrix} \cos\theta & e^{-i\varphi}\sin\theta \\ e^{-i\varphi}\sin\theta & -\cos\theta \end{pmatrix}, \tag{6.34}$$

and this matrix has two eigenvectors

$$\xi_{+}(\boldsymbol{p}) = \begin{pmatrix} \cos\frac{\theta}{2} \\ e^{i\varphi}\sin\frac{\theta}{2} \end{pmatrix}, \quad \xi_{-}(\boldsymbol{p})\begin{pmatrix} \sin\frac{\theta}{2} \\ -e^{i\varphi}\cos\frac{\theta}{2} \end{pmatrix} \tag{6.35}$$

with eigenvalues $s = +1$ and $s = -1$, respectively. With this, the normalization constant is given by

$$N \to N_{\pm} = \sqrt{\frac{2m(E_{\pm}+m)^2}{2m(E_{\pm}+m) \mp 3\vartheta|\boldsymbol{p}|^3}}, \tag{6.36}$$

showing that the $(\pm)$ signs in the normalization constants indicate an explicit dependence on helicity.

6.3 The $U(1)$ conserved current

Consider $\hat{O}$ an operator that acts of generic mathematical objects A and B, such as scalars, vectors and spinors. Throughout the text, we assume the definitions $A\overleftarrow{\hat{O}}B = (\hat{O}A)B$ and $A\overleftrightarrow{\hat{O}}B \equiv (\hat{O}A)B - A(\hat{O}B)$. Then, assuming that the transform under global $U(1)$ for the matter field (ψ)

$$\psi \to \psi' = e^{-i\alpha}\psi, \tag{6.37}$$

the fermion action in Eq. (6.3) is invariant. On the other hand, if we introduce a local $U(1)$ transformation for an infinitesimal α-parameter, the fermion action in Eq. (6.3) at first order in α is

$$S \to S' = S - \int d^4x(\partial_\mu\alpha)\bar{\psi}\gamma^\mu\psi + i\vartheta\int d^4x(\boldsymbol{\nabla}\alpha)\cdot\bar{\psi}\gamma^0\gamma_5\overleftrightarrow{\boldsymbol{\nabla}}\psi. \tag{6.38}$$

The variation of Eq. (6.38) with respect to α-parameter yields the 4-current

$$J^{\mu} = (J^0, J^i) = \left(\bar{\psi}\gamma^0\psi, \bar{\psi}\gamma^i\psi - i\vartheta\bar{\psi}\gamma^0\gamma_5\overleftrightarrow{\partial}^i\psi\right), \tag{6.39}$$

that satisfies the continuity equation $\partial_\mu J^\mu = 0$. The minimal coupling with the electromagnetic field is introduced substituting the derivative operator by the covariant derivative operator $\partial_\mu \longmapsto D_\mu = \partial_\mu + ie\,A_\mu$. The new action for the QED is

$$\begin{aligned} S = \int d^4x \Big[&-\frac{1}{4}F_{\mu\nu}F^{\mu\nu} + \bar{\psi}\left(i\gamma^\mu\partial_\mu - \vartheta\gamma^0\gamma_5\,\boldsymbol{\nabla}^2 - m\right)\psi \\ &- eA_\mu\bar{\psi}\gamma^\mu\psi - i\vartheta e\boldsymbol{A}\cdot\bar{\psi}\gamma^0\gamma_5\overleftrightarrow{\boldsymbol{\nabla}}\psi + \vartheta e^2\boldsymbol{A}^2\,\bar{\psi}\gamma^0\gamma_5\psi\Big], \end{aligned} \tag{6.40}$$

which includes a new quartic coupling involving the quadratic vector potential with the fermions fields. Since the Bianchi identity is the usual expression, one can verify that magnetic Gauss and Faraday-Lenz laws are unchanged. Also the electric Gauss law is protected, once the new current does not affect the electrical charge density

$$\boldsymbol{\nabla}\cdot\boldsymbol{E} = -e\,\psi^\dagger\,\psi\,. \tag{6.41}$$

Just the Ampère-Maxwell law is modified by the spatial current density

$$\boldsymbol{\nabla}\times\boldsymbol{B} = \partial_t\boldsymbol{E} + e\bar{\psi}\boldsymbol{\gamma}\psi - 2\vartheta e^2\boldsymbol{A}\bar{\psi}\gamma^0\gamma_5\psi + ie\vartheta\bar{\psi}\gamma^0\gamma_5\overleftrightarrow{\boldsymbol{\nabla}}\psi\,. \tag{6.42}$$

The displacement current on the right-hand side of Eq. (6.42) coincides with the spatial part of $U(1)$ current in Eq. (6.39). Thereby, we can conclude that the conserved $U(1)$ and the electromagnetic current is the same in this approach.

Substituting the solutions given by Eq. (6.21) in the spatial current density of Eq. (6.39), we obtain the result in the momentum space

$$\boldsymbol{J} = \frac{1}{E_\pm + m}\,u_a^\dagger(p')\left\{\left[1 - \frac{\vartheta^2}{2}\left(\boldsymbol{q}^2 + \boldsymbol{\ell}^2\right)\right]\boldsymbol{\ell} - (\boldsymbol{q}\times\boldsymbol{\sigma}) - \frac{\vartheta}{2}\boldsymbol{q}^2\boldsymbol{\sigma} - \vartheta\left(\frac{\boldsymbol{\ell}^2}{2}\delta_{ij} - \boldsymbol{\ell}_i\boldsymbol{\ell}_j\right)\boldsymbol{\sigma}_j\right\}u_a(p)\,, \tag{6.43}$$

where we have omitted the spins projections $(\pm s)$, and also have defined the photon's transfer 3-momentum $\boldsymbol{q} = \boldsymbol{p}' - \boldsymbol{p}$, and the total 3-momentum $\boldsymbol{\ell} = \boldsymbol{p} + \boldsymbol{p}'$. Since the term proportional to ϑ^2 is too small, the only contribution of a granular space-time in the current comes from a helicity-type interaction with respect to the transfer momentum $\boldsymbol{q}$, and a projection of the spin on $\boldsymbol{\ell}$-direction.

6.4 The Gordon decomposition

In this Section, we introduce the Gordon decomposition procedure for the modified Dirac equation, in which the interpretation of the current coupled to the electromagnetic field is an important key to understand the form factors, as well as the electron's magnetic and electric dipole momentum. In order, we must emphasize that the conserved current of

the model given by Eq. (6.39) has the interesting aspect of temporal and spatial sectors have different interpretations. This fact suggests that the usual procedure for deducing Gordon's identity can no longer be applied at least to the spatial part of Eq. (6.39), which differs form the usual case by the LSV terms. Thereby, we have two Gordon identities, the first for the time component of Eq. (6.39), and the second one for the spatial part. For the current's time-component, we go back to the Eq. (6.1), whose Dirac conjugate equation for $\bar{\psi}(x)$ is given by Eq. (6.5), and combining Eq. (6.1) with Eq. (6.5), we multiply by $\gamma^0\psi(x)$ at the right-hand side of Eq. (6.5), and also multiply by $\bar{\psi}(x)\gamma^0$ at the left-hand side. By subtracting these equations, we get

$$J^0 = \frac{i}{2m}\bar{\psi}\overleftrightarrow{\partial}_t\psi - \frac{1}{m}\partial_\mu(\bar{\psi}\Sigma^{\mu 0}\psi) - \frac{\vartheta}{2m}\bar{\psi}\gamma_5\overleftrightarrow{\nabla}^2\psi\,, \tag{6.44}$$

which is the Gordon identity for J^0-component of the conserved current.

For the spatial part of the conserved current, we repeat the procedure above by multiplying by $\gamma\psi + i\vartheta(\overleftarrow{\nabla})\gamma^0\gamma_5\psi - i\vartheta\gamma^0\gamma_5(\nabla\psi)$ on the right-hand side of Eq. (6.5), and also multiplying by $\bar{\psi}\gamma + i\vartheta(\nabla\bar{\psi})\gamma^0\gamma_5 - i\vartheta\bar{\psi}\gamma^0\gamma_5\nabla$ the left-hand side, with the LSV terms being necessary due to the new structure of the current. Therefore, the Gordon identity for J^i becomes as given below:

$$J^i = \frac{i}{2m}\bar{\psi}\partial^i\psi - \frac{1}{m}\partial_\mu(\bar{\psi}\Sigma^{\mu i}\psi) + \frac{\vartheta}{2m}(\partial_t\bar{\psi})\gamma_5\partial^i\psi - \frac{2i\vartheta}{m}(\nabla\bar{\psi})\Sigma^{0i}\gamma_5\cdot(\nabla\psi) + \frac{i\vartheta^2}{2m}\partial^i(\bar{\psi}\overleftrightarrow{\nabla}^2\psi). \tag{6.45}$$

The structure of both the components of the current as given in Eqs. (6.44) and (6.45) shall be applied in the next Section, where we shall be calculating the interparticle electron-electron (e^-e^-) non-relativistic potential mediated by a photon exchange by means of an elastic scattering. The role of the components of the currents will become clear after the expression for the e^-e^- potential will be written down with the spin and velocity corrections on the Coulombian term.

From the action in Eq. (6.40), the three-vertex coupling of the leptons current with the EM field is described by

$$S^{(3)}_{\rm int} = -e\int d^4x\Big[\,\bar{\psi}\gamma^\mu\psi A_\mu + i\vartheta\boldsymbol{A}\cdot\bar{\psi}\gamma^0\gamma_5\overleftrightarrow{\nabla}\psi\,\Big]\,, \tag{6.46}$$

which, in the momentum space, reads as

$$S^{(3)}_{\rm int} = -e\int\frac{d^4p'}{(2\pi)^4}\frac{d^4p}{(2\pi)^4}\Big[\,\bar{u}(p')\gamma^\mu u(p)A_\mu(q) - \vartheta\,\bar{u}(p')\gamma^0\gamma_5 u(p)(\boldsymbol{p}'+\boldsymbol{p})\cdot\boldsymbol{A}(q)\,\Big]. \tag{6.47}$$

Using the Gordon identities, the time-component for the coupling is

$$\bar{u}(p')\gamma^0 u(p)A_0(q) = \bar{u}(p')\left[\,\frac{\ell^0}{2m} - \frac{iq_\mu}{m}\Sigma^{\mu 0} - \vartheta\frac{\boldsymbol{\ell}\cdot\boldsymbol{q}}{2m}\gamma_5\,\right]u(p)A_0(q)\,, \tag{6.48}$$

where $q^\mu = p'^\mu - p^\mu$ and $\ell = p'^\mu + p^\mu$ are the photon's transfer and total 4-momentums, respectively. This coupling is interpreted as the interaction energy between the charge density and

the scalar potential $A^0 \equiv V$. In configuration space, the ϑ-term in Eq. (6.48) for the electrostatic case becomes

$$-\vartheta \frac{\boldsymbol{\ell}\cdot\boldsymbol{q}}{2m} V \gamma_5 = -\frac{i\vartheta}{2m}(\boldsymbol{\ell}\cdot\boldsymbol{E})\gamma_5 , \tag{6.49}$$

where $\boldsymbol{q} \to -i\boldsymbol{\nabla}$, and $\boldsymbol{E} = -\boldsymbol{\nabla} V$. Thus, the electric dipole momentum emerges with $\boldsymbol{\ell}\cdot\boldsymbol{E}$, and the ratio $(\vartheta/2m)$ modulates the LQG contribution to the electron's electric dipole momentum.

From the spatial part, the current density is

$$\begin{aligned}\bar{u}(p')\left[\gamma - \vartheta\ell\gamma^0\gamma_5\right]u(p)\cdot\boldsymbol{A}(q) = \bar{u}(p')\Bigg[&\frac{\boldsymbol{\ell}}{2m} - \frac{iq_\mu}{m}\Sigma^{\mu i} + \frac{\vartheta q^0 \boldsymbol{\ell}}{2m}\gamma_5 \\ &- \frac{i\vartheta(\boldsymbol{\ell}^2 - \boldsymbol{q}^2)}{2m}\Sigma^{0i}\gamma_5 - \frac{\vartheta^2(\boldsymbol{q}\cdot\boldsymbol{\ell})\boldsymbol{q}}{2m}\Bigg]u(p)\cdot\boldsymbol{A}(q).\end{aligned} \tag{6.50}$$

In coordinate space, the last term can be eliminated by the Coulomb gauge, $\boldsymbol{\nabla}\cdot\boldsymbol{A} = 0$.

An important aspect arising from the Gordon decomposition in Eq. (6.50) is the contribution to the electron's electric dipole moment (EDM). Specifically, it is associated with the term proportional to $\Sigma^{0i}\gamma_5$. This term defines an interaction action for the EDM in momentum space such that

$$S_{\text{EDM}} = \int \frac{d^4p'}{(2\pi)^4}\frac{d^4p}{(2\pi)^4}\bar{u}(p')d_e\boldsymbol{\Sigma}\cdot\boldsymbol{E}(q)u(p), \tag{6.51}$$

where $\boldsymbol{E}(q)$ is the momentum space version of the electric field,

$$\boldsymbol{\Sigma} = \begin{pmatrix}\boldsymbol{\sigma} & 0\\ 0 & \boldsymbol{\sigma}\end{pmatrix}, \tag{6.52}$$

and the EDM is

$$d_e = \frac{\vartheta e}{8m}\left(\frac{\boldsymbol{\ell}^2 - \boldsymbol{q}^2}{q_0}\right) = \frac{\vartheta e}{2m}\left(\frac{\boldsymbol{p}'\cdot\boldsymbol{p}}{q_0}\right). \tag{6.53}$$

The corresponding Lagrangian density is

$$\mathscr{L}_{\text{EDM}} = \bar{u}(p')\, d_e\, \boldsymbol{\Sigma}\cdot\boldsymbol{E}(q)\, u(p)\,. \tag{6.54}$$

The most recent experimental results for the EDM, obtained by using electrons confined inside molecular ions subjected to a huge intramolecular electric field, provide an upper bound of $d_e < 4.1\times10^{-30}\ e\cdot$ cm [28]. We can use this result to estimate a bound on the ϑ-parameter. In order, the Eq. (6.53) can be written as

$$d_e = \frac{\vartheta\, e}{2m}\left(\frac{|\boldsymbol{p}||\boldsymbol{p}'|\cos\alpha}{q_0}\right) \leq 4.1\times10^{-30}\,\text{e}\cdot\text{cm}\,, \tag{6.55}$$

where α is the angle between $\boldsymbol{p}$ and $\boldsymbol{p}'$. From the Eqs. (6.1) and (6.2), the ϑ-parameter is defined by

$$\vartheta = \frac{\kappa_7}{4\mathscr{L}}\left(\frac{\ell_P}{\mathscr{L}}\right)^{\Upsilon_f}\ell_P^2. \tag{6.56}$$

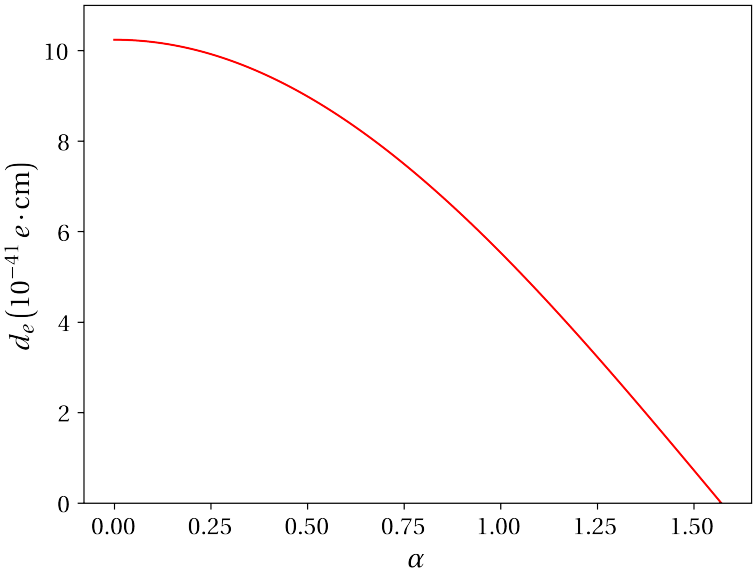

Figure 5 – Upper bounds on the d_e as function of the α-angle. In this plot, we fix the momenta and the energy at the MeV QED scale : $|\boldsymbol{p}| = |\boldsymbol{p}'| = q_0 = 1$ MeV.

In Ref. [256], it is argued that $\Upsilon_f = -1$ and $\kappa_7 = 37.5$ for neutrinos. Here, it is necessary to carry on a similar analysis to determine the values of these parameters, when dealing with electrons. To follow this path, we base our analysis on the data from Ref. [**?**], which studies the LSV effects in the propagation velocity of a charged lepton, not just in neutrinos and photons, as it is the case in Ref. [256]. Following the steps described in Ref. [**?**], we can express the modulus of our group velocity, Eq. (6.15), in the form

$$|\boldsymbol{v}_\pm| = 1 - \frac{m^2}{2\boldsymbol{p}^2} \pm \frac{|\boldsymbol{p}|}{E_{\mathrm{LSV}}}, \tag{6.57}$$

which, to match the general results presented in Ref. [**?**], requires that $\Upsilon_f = -1$ and, consequently,

$$\frac{\kappa_7 \ell_P}{2} = \frac{1}{E_{\mathrm{LSV}}}, \tag{6.58}$$

with $E_{\mathrm{LSV}} \gtrsim 9.4 \times 10^{25}$ GeV for the highest-energy event from the Crab Nebula [259]. All of this implies that $\kappa_7 \approx 2.6 \times 10^{-7}$. Then, considering a energy scale at $|\boldsymbol{p}| = |\boldsymbol{p}'| = q_0 = 1$ MeV, and the electron mass of $m = 0.5$ MeV, we can illustrate our d_e values as a function of the α-angle in the plot of the FIG. 5. Since all d_e values in FIG. 5 are on the order of 10^{-40} to 10^{-41} e·cm, the EDM predicted by this LQG model falls within the current experimental limit of $d_e < 4.1 \times 10^{-30}$ e·cm [28].

It is also important to emphasize that this result is consistent with the Standard-Model prediction for the EDM of charged leptons using hadron effective models as given by [29]: $d_e = 5.8 \times 10^{-40}$ e·cm, with an error bar of 70%, exceeding the conventionally known four-loop level elementary contribution by several orders of magnitude.

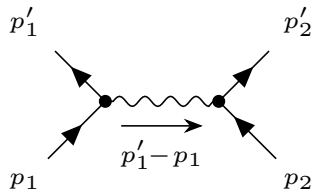

Figure 6 – An $e^- e^-$ tree-level elastic scattering involves incoming 4-momenta p_1 and p_2, and outgoing 4-momenta p_1' and p_2', mediated by a photon that transfers 4-momentum $p_1' - p_1 = -(p_2' - p_2)$ during the process.

6.5 Electromagnetic Interaction Between Fermions

In this section, we aim to elucidate the implications of the preceding electromagnetic current Gordon decomposition structure by examining its influence on the Coulomb potential. To achieve this, we analyze the interaction between two fermions, as described by the solutions in Eqs. (6.24) and (6.29), in a tree-level elastic scattering considering the possibility of spin-flip. The amplitude of this process can be characterized by the Feynman diagram depicted in Figure 6. This interparticle potential procedure will also play an important role in Chapter 7, in the context of particle physics beyond the SM. This would justify the inclusion of an Appendix with all the technical details of its derivation. However, we have recently published a pedagogical article in which we show, in detail, how to apply this procedure starting from the action and ending with the final expression for the potential; see Ref. [260].

In this tree-level elastic scattering, the two fermions, each with charges e_1 and e_2, possess incoming 4-momenta denoted as ${p_1}^\mu = (E_1, \boldsymbol{p}_1)$ and ${p_2}^\mu = (E_1, \boldsymbol{p}_1)$, and outgoing 4-momenta denoted as ${p_1'}^\mu = (E_1', \boldsymbol{p}_1')$ and ${p_2'}^\mu = (E_2', \boldsymbol{p}_2')$, respectively. Furthermore, it is convenient for us to work in the center of mass reference frame, with the parameterization in terms of the following independent momenta: the transferred momentum, $q = p_1' - p_1 = -(p_2' - p_2)$, and the average momentum, $\frac{\ell}{2} = \frac{(p_1' + p_1)}{2} = \frac{(p_2' + p_2)}{2}$. Through the conservation of energy and momentum, we have that $q^0 = 0$ and $\boldsymbol{q} \cdot \boldsymbol{\ell} = 0$ to simplify the amplitude of Figure 6.

In order to include spin and velocity corrections to the potential, we shall employ the method described in [261, 262]. The prescription is that the potential, V, can be obtained from the first Born approximation, i.e., by performing the Fourier integral of the non-relativistic (NR) amplitude, $\mathscr{M}_{\rm NR}$, with respect to the transferred momentum $\boldsymbol{q}$,

$$V(\boldsymbol{x}) = -\int \frac{d^3\boldsymbol{q}}{(2\pi)^3} \mathscr{M}_{\rm NR} e^{i\boldsymbol{q}\cdot\boldsymbol{x}}, \tag{6.59}$$

where $\mathscr{M}_{\rm NR}$ is related to the relativistic Feynman amplitude, $\mathscr{M}$, according to the conventions of [263], through

$$\mathscr{M}_{\rm NR} = \frac{1}{\sqrt{2E_1}} \frac{1}{\sqrt{2E_1'}} \frac{1}{\sqrt{2E_2}} \frac{1}{\sqrt{2E_2'}} \mathscr{M}. \tag{6.60}$$

The amplitude $\mathscr{M}$ is obtained by applying Feynman rules, incorporating the fields, interaction vertices, and propagators. In the case to be considered here, it can be rewritten as

$\mathscr{M} \sim J_{(1)}\langle \text{prop}\rangle J_{(2)}$, where $J_{(1)}$ and $J_{(2)}$ represent the sources/currents, and $\langle \text{prop}\rangle$ denotes the propagator, with the possible Lorentz indices of the representations being omitted. Therefore, taking the photon propagator in the Feynman gauge,

$$\langle A_\mu A_\nu\rangle = i\frac{\eta_{\mu\nu}}{q^2}, \tag{6.61}$$

for the process in Figure 6 we have the amplitude

$$i\mathscr{M} = -e_1 e_2 J^\mu_{(1)}\langle A_\mu A_\nu\rangle J^\mu_{(2)} = -e_1 e_2\,\bar{u}(p_1')\gamma^\mu u(p_1)\langle A_\mu A_\nu\rangle \bar{u}(p_2')\gamma^\nu u(p_2), \tag{6.62}$$

with J^μ here denoting the vector current of the model given by Eq. (6.39) in the momentum space. Then, utilizing the continuity equation $q_\mu J^\mu = 0$ and $q^0 = 0$, in the NR limit yields

$$\mathscr{M}_{\text{NR}} = -\frac{e_1 e_2}{\boldsymbol{q}^2}\frac{J^\mu_{(1)}J_{(2)\mu}}{4E_1E_2} - \frac{e_1 e_2}{\boldsymbol{q}^2}\frac{J^0_{(1)}J^0_{(2)} - \boldsymbol{J}_{(1)}\cdot\boldsymbol{J}_{(2)}}{4E_1E_2}. \tag{6.63}$$

Expressing both $J^0_{(1)}$ and $\boldsymbol{J}_{(1)}$ in terms of their respective Gordon decompositions and positive energy solutions, Eqs. (6.24) and (6.29), in the NR limit,

$$u_{\text{NR}}(p_1) \approx \sqrt{2m}\begin{pmatrix}\chi_1\\ \dfrac{\boldsymbol{\sigma}\cdot\boldsymbol{p}_1 - \vartheta\boldsymbol{p}_1^2}{2m}\chi_1\end{pmatrix} \tag{6.64}$$

and

$$\bar{u}_{\text{NR}}(p_1') \approx \sqrt{2m}\left(\chi_1'^{\,\dagger}, \chi_1'^{\,\dagger}\frac{\boldsymbol{\sigma}\cdot\boldsymbol{p}_1' - \vartheta\boldsymbol{p}_1'^{\,2}}{2m}\right), \tag{6.65}$$

with spin up and down respectively given by

$$\chi_1 = \begin{pmatrix}1\\0\end{pmatrix} \text{ and } \chi_1 = \begin{pmatrix}0\\1\end{pmatrix} \tag{6.66}$$

and the same for Dirac's conjugate solution with

$$\chi_1'^{\,\dagger} = (1,0) \text{ and } \chi_1'^{\,\dagger} = (0,1), \tag{6.67}$$

together the conditions of elastic scattering, we obtain

$$J^0_{(1)} = \left[2m_1 + \frac{1}{8m_1}(\boldsymbol{\ell}^2 + 7\boldsymbol{q}^2)\right]\delta_1 + \frac{3}{4m_1}i(\boldsymbol{q}\times\boldsymbol{\ell})\cdot\langle\boldsymbol{S}_1\rangle \tag{6.68}$$

and

$$\boldsymbol{J}_{(1)} = \left[1 + \frac{(\boldsymbol{q}^2 - \boldsymbol{\ell}^2)}{16m_1^2}\right]\boldsymbol{\ell}\delta_1 - 2i\varepsilon_{ijk}\boldsymbol{q}_j\langle\boldsymbol{S}_{1k}\rangle + \vartheta(\boldsymbol{\ell}^2 - \boldsymbol{q}^2)\langle\boldsymbol{S}_1\rangle, \tag{6.69}$$

where we defined the quantities

$$\chi_1'^{\,\dagger}\chi_1 = \delta_1, \tag{6.70}$$

$$\chi_1'^{\,\dagger}\frac{\boldsymbol{\sigma}}{2}\chi_1 = \langle\boldsymbol{S}_1\rangle. \tag{6.71}$$

To express $J^0_{(2)}$ and $\boldsymbol{J}_{(2)}$, one simply needs to replace the index 1 with 2 in Eqs. (6.68) and (6.69), as well as replace the momenta $\boldsymbol{q}$ and $\boldsymbol{\ell}$ with $-\boldsymbol{q}$ and $-\boldsymbol{\ell}$, respectively. With these result and still in the NR limit, one can write the expression for the interparticle potential in the form

$$V(\boldsymbol{x}) = V_{\text{QED}}(x) + V_{\text{LQG}}(x), \tag{6.72}$$

with

$$\begin{aligned} V_{\text{QED}} = &-e_1e_2\left[\frac{\delta_1\delta_2}{8}\left(\frac{1}{m_1^2}+\frac{1}{m_2^2}\right)+\frac{2}{3}\frac{\langle \boldsymbol{S}_1\rangle\cdot\langle \boldsymbol{S}_2\rangle}{m_1m_2}\right]\delta^{(3)}(\boldsymbol{x}) + \frac{e_1e_2}{4\pi|\boldsymbol{x}|}\delta_1\delta_2\left(1+4\frac{\boldsymbol{\ell}^2}{m_1m_2}\right) \\ &+\frac{e_1e_2}{4\pi|\boldsymbol{x}|^3}\left\{\boldsymbol{Q}_{ij}\frac{\langle \boldsymbol{S}_1\rangle_i\langle \boldsymbol{S}_2\rangle_j}{m_1m_2} - \boldsymbol{L}\cdot\left[\langle \boldsymbol{S}_1\rangle\delta_2\left(\frac{1}{2m_1^2}+\frac{1}{m_1m_2}\right)+(1)\leftrightarrow(2)\right]\right\} \end{aligned} \tag{6.73}$$

and

$$\begin{aligned} V_{\text{LQG}}(x) = &\, e_1e_2\vartheta\left\{2\boldsymbol{P}\cdot\left[\langle \boldsymbol{S}_1\rangle\delta_b\left(\frac{1}{4m_1^2}+\frac{1}{m_1m_2}\right)-(1)\leftrightarrow(2)\right]-2\left(\frac{\langle \boldsymbol{S}_1\rangle\times\langle \boldsymbol{S}_2\rangle}{m_1m_2}\right)\cdot\boldsymbol{\nabla}\right]\right\}\delta^{(3)}(\boldsymbol{x}) \\ &+\frac{e_1e_2}{4\pi|\boldsymbol{x}|}\vartheta\left\{32\boldsymbol{\ell}^2\boldsymbol{\ell}\cdot\left[\langle \boldsymbol{S}_1\rangle\delta_2\left(\frac{1}{4m_1^2}-\frac{1}{m_1m_2}\right)-(1)\leftrightarrow(2)\right]\right\} \\ &-\frac{e_1e_2}{4\pi|\boldsymbol{x}|^3}\vartheta\left[\frac{32\boldsymbol{\ell}^2}{m_1m_2}\boldsymbol{x}\cdot\left(\langle \boldsymbol{S}_1\rangle\times\langle \boldsymbol{S}_2\rangle\right)\right], \end{aligned} \tag{6.74}$$

where $\boldsymbol{L} = \boldsymbol{x}\times\dfrac{\boldsymbol{\ell}}{2}$ is the angular momentum and $\boldsymbol{Q}_{ij} = \delta_{ij} - 3\frac{\boldsymbol{x}_i\boldsymbol{x}_j}{|\boldsymbol{x}|^2}$. As anticipated in Section 6.4, the linear contributions in the ϑ parameter are explicitly calculated and we pay attention to the Coulomb-like term in ϑ with dependence on the spin. Also, it is worth to highlight the spin correction coming from the ϑ-contribution to the contact term.

In the case of the e^-e^- scattering, $m_1 = m_2 = m_e$ and $e_1 = e_2 = e$, with m_e and e being the electron mass and charge, respectively. Then, in the situation of an e^-e^- scattering with spin-flip, both δ_1 and δ_2 are zero. In this sense, the potential given by Eq. (6.72) assumes the form

$$V_1(\boldsymbol{x}) = \frac{e^2}{4\pi|\boldsymbol{x}|^2}\left[\frac{\boldsymbol{Q}_{ij}\langle \boldsymbol{S}_{1,i}\rangle\langle \boldsymbol{S}_{2,j}\rangle - 32\vartheta\boldsymbol{\ell}^2\hat{\boldsymbol{x}}\cdot\left(\langle \boldsymbol{S}_2\rangle\times\langle \boldsymbol{S}_1\rangle\right)}{m_e^2}\right] - 2\frac{\vartheta e^2}{m_e^2}\left(\langle \boldsymbol{S}_1\rangle\times\langle \boldsymbol{S}_2\rangle\right)\cdot\boldsymbol{\nabla}\delta^{(3)}(\boldsymbol{x}). \tag{6.75}$$

In the case where the e^-e^- scattering does not have the spin-flip, $\delta_1 = \delta_2 v \equiv \delta$ and $\langle \boldsymbol{S}_1\rangle = \langle \boldsymbol{S}_2\rangle \equiv \langle \boldsymbol{S}\rangle$, and the Eq. (6.72) reduces to

$$V_2(\boldsymbol{x}) = \frac{e^2}{4\pi|\boldsymbol{x}|}\left(1+4\frac{\boldsymbol{\ell}^2}{4m_e^2}\right)\delta^2 + \frac{e^2}{m_e^2}\left[\left(\frac{\delta^2}{4}-\frac{2\langle \boldsymbol{S}\rangle\cdot\langle \boldsymbol{S}\rangle}{3}\right)\delta^{(3)}(\boldsymbol{x}) + \frac{\boldsymbol{Q}_{ij}\langle \boldsymbol{S}_i\rangle\langle \boldsymbol{S}_j\rangle}{4\pi|\boldsymbol{x}|^2} + \frac{3\delta}{2|\boldsymbol{x}|^3}\boldsymbol{L}\cdot\langle \boldsymbol{S}\rangle\right]. \tag{6.76}$$

The contribution from LQG arises specifically in scenarios involving scattering without spin-flip, as outlined in Eq. (6.75). Notably, this contribution does not take into account the typical Coulomb-like term. The Coulombian interaction, being a gauge interaction, preserves the chirality of the particles. Hence, it follows that, in the absence of spin-flip, as Eq. (6.76) shows, Coulomb potential comes out.

6.6 The coupling with the EM field and the non-relativistic Hamiltonian

The gauge principle applied to the Eq. (6.3) means to introduce the minimal coupling with the EM field via the usual redefinition of the 4-momentum $p_\mu \longmapsto p_\mu - e\,A_\mu$ in which the modified Dirac Eq. (6.1) is given by

$$\left[\gamma^\mu\left(p_\mu - eA_\mu\right) + \vartheta\left(\boldsymbol{p} - e\boldsymbol{A}\right)^2\gamma^0\gamma_5 - m\right]u(p) = 0\,. \tag{6.77}$$

Using the previous notation for the u-amplitude in the momentum space, *i.e.*, $u = (u_a \;\; u_b)^t$, the system of Eqs. in (6.77) is read as

$$\left(E - e\phi - m\right)u_a - \left[\boldsymbol{\sigma}\cdot\left(\boldsymbol{p} - e\boldsymbol{A}\right) - \vartheta\left(\boldsymbol{p} - e\boldsymbol{A}\right)^2\right]u_b = 0, \tag{6.78}$$

$$\left(E - e\phi + m\right)u_b - \left[\boldsymbol{\sigma}\cdot\left(\boldsymbol{p} - e\boldsymbol{A}\right) - \vartheta\left(\boldsymbol{p} - e\boldsymbol{A}\right)^2\right]u_a = 0. \tag{6.79}$$

From (6.79), we have the relation

$$u_b = \frac{\boldsymbol{\sigma}\cdot\left(\boldsymbol{p} - e\boldsymbol{A}\right) - \vartheta\left(\boldsymbol{p} - e\boldsymbol{A}\right)^2}{E - e\phi + m}\,u_a\,, \tag{6.80}$$

that allows us to write the spinor $u(p)$ in the form

$$u(p) = \begin{pmatrix} 1 \\ \dfrac{\boldsymbol{\sigma}\cdot\left(\boldsymbol{p} - e\boldsymbol{A}\right) - \vartheta\left(\boldsymbol{p} - e\boldsymbol{A}\right)^2}{E - e\phi + m} \end{pmatrix} u_a\,. \tag{6.81}$$

In the non-relativistic regime, the linear momentum is $\boldsymbol{p} \ll m$, and the dominant energy term is of the order of the rest energy of the particle, that is, $E \approx m$. The kinetic and potential energy are much smaller than the rest energy, that is, the approximation $e\phi \ll m$ is valid in the previous relations. Therefore, the relations between the Eqs. (6.80) and (6.81) are simplified as

$$u_b \approx \frac{\boldsymbol{\sigma}\cdot\boldsymbol{\pi} - \vartheta\boldsymbol{\pi}^2}{2m}\,u_a, \tag{6.82}$$

$$u_{\mathrm{NR}}(p) \approx \begin{pmatrix} 1 \\ \dfrac{\boldsymbol{\sigma}\cdot\boldsymbol{\pi} - \vartheta\boldsymbol{\pi}^2}{2m} \end{pmatrix} u_a, \tag{6.83}$$

where $\boldsymbol{\pi} \equiv \boldsymbol{p} - e\boldsymbol{A}$. Substituting Eq. (6.82) in Eq. (6.78), the Eq. (6.78) is so written in the form $E_{\mathrm{NR}}\,u = (E - m)\,u = Hu$, in which E_{NR} is the energy of a particle, and H is the Hamiltonian operator in the NR limit:

$$H = e\phi + \frac{\left(\boldsymbol{\sigma}\cdot\boldsymbol{\pi} - \vartheta\boldsymbol{\pi}^2\right)^2}{2m}\,. \tag{6.84}$$

The kinetic term yields the operator

$$\left(\boldsymbol{\sigma}\cdot\boldsymbol{\pi} - \vartheta\boldsymbol{\pi}^2\right)^2 = (\boldsymbol{\sigma}\cdot\boldsymbol{\pi})^2 + \vartheta^2\boldsymbol{\pi}^4 - \vartheta\boldsymbol{\pi}^2\,(\boldsymbol{\sigma}\cdot\boldsymbol{\pi}) - \vartheta\,(\boldsymbol{\sigma}\cdot\boldsymbol{\pi})\,\boldsymbol{\pi}^2, \tag{6.85}$$

in which new terms as $\boldsymbol{\pi}^4$ and $\boldsymbol{\pi}^2(\boldsymbol{\sigma}\cdot\boldsymbol{\pi})$ emerge with the ϑ-parameter. We use the following relations

$$(\boldsymbol{\pi}\cdot\boldsymbol{\sigma})^2 = \big(\boldsymbol{p}-e\boldsymbol{A}\big)^2 - e\boldsymbol{\sigma}\cdot\boldsymbol{B}, \tag{6.86}$$

$$\boldsymbol{\pi}^2(\boldsymbol{\sigma}\cdot\boldsymbol{\pi}) = (\boldsymbol{\sigma}\cdot\boldsymbol{\pi})\boldsymbol{\pi}^2 + e\boldsymbol{\sigma}\cdot\partial_t\boldsymbol{E} + 2e^2\boldsymbol{\sigma}\cdot\big[\boldsymbol{A}\times\big(\boldsymbol{p}\times\boldsymbol{A}\big)\big], \tag{6.87}$$

for a magnetic field ($\boldsymbol{B}$), in which $\boldsymbol{B} = \boldsymbol{\nabla}\times\boldsymbol{A}$. Therefore, the Hamiltonian operator is

$$\begin{aligned} H = e\phi + \frac{\big(\boldsymbol{p}-e\boldsymbol{A}\big)^2}{2m} - \frac{e}{2m}\boldsymbol{\sigma}\cdot\boldsymbol{B} - \frac{\vartheta}{m}(\boldsymbol{\sigma}\cdot\boldsymbol{\pi})\big(\boldsymbol{p}-e\boldsymbol{A}\big)^2 \\ - \frac{\vartheta e}{2m}\boldsymbol{\sigma}\cdot\partial_t\boldsymbol{E} - \frac{\vartheta e^2}{m}\boldsymbol{\sigma}\cdot\big[\boldsymbol{A}\times\big(\boldsymbol{p}\times\boldsymbol{A}\big)\big] + \frac{\vartheta^2}{2m}\boldsymbol{\pi}^4. \end{aligned} \tag{6.88}$$

In the particular case of a weak and homogeneous magnetic field, the vector potential is $\boldsymbol{A} = (\boldsymbol{B}\times\boldsymbol{x})/2$, and we can neglect quadratic terms in $\boldsymbol{A}$. Thereby, we can approximate the terms

$$\boldsymbol{\pi}^2 \approx \boldsymbol{p}^2 - e(\boldsymbol{B}\cdot\boldsymbol{L}), \tag{6.89}$$

$$\boldsymbol{\pi}^4 \approx \boldsymbol{p}^4 - 2e\boldsymbol{p}^2(\boldsymbol{B}\cdot\boldsymbol{L}), \tag{6.90}$$

also

$$\boldsymbol{\sigma}\cdot\big[\boldsymbol{A}\times\big(\boldsymbol{p}\times\boldsymbol{A}\big)\big] \approx 0 \tag{6.91}$$

and

$$\boldsymbol{\sigma}\cdot(\boldsymbol{p}-e\boldsymbol{A})(\boldsymbol{p}-e\boldsymbol{A})^2 \approx -e\boldsymbol{p}^2\boldsymbol{B}\cdot(\boldsymbol{r}\times\boldsymbol{S}) + \frac{1}{2}(\boldsymbol{S}\cdot\boldsymbol{p})\big(\boldsymbol{p}^2 - e\boldsymbol{B}\cdot\boldsymbol{L}\big), \tag{6.92}$$

where we have used that $\boldsymbol{S} = \boldsymbol{\sigma}/2$. Under these conditions, the Hamiltonian operator is

$$\begin{aligned} H = e\phi + \frac{\boldsymbol{p}^2}{2m}\Big[1 + 2\vartheta\big(e\boldsymbol{B}\cdot(\boldsymbol{x}\times\boldsymbol{S}) - 2\boldsymbol{S}\cdot\boldsymbol{p}\big) + \vartheta^2\big(\boldsymbol{p}^2 - 2\boldsymbol{B}\cdot\boldsymbol{L}\big)\Big] \\ - \frac{e}{2m}(\boldsymbol{L}+2\boldsymbol{S})\cdot\boldsymbol{B} - \frac{\vartheta e}{m}\boldsymbol{S}\cdot\partial_t\boldsymbol{E} + \frac{2\vartheta e}{m}(\boldsymbol{B}\cdot\boldsymbol{L})\big(\boldsymbol{S}\cdot\boldsymbol{p}\big). \end{aligned} \tag{6.93}$$

The term $\boldsymbol{S}\cdot\partial_t\boldsymbol{E}$ is projection of the electric field on the spin direction. It emerges from the Faraday law, and expresses the electric dipole momentum variable with the time. In the case of a electrostatic field, as the Coulomb electric field, this term is null. The other terms have contribution of the uniform magnetic field, of the linear momentum, and also of angular momentum ($\boldsymbol{L}$) for the NR particle.

6.7 Renormalizability

The presence of a $\boldsymbol{\nabla}^2$ in the modified Dirac action introduces a higher-order space derivative. Besides gauge symmetry, causality, and renormalizability, that are fundamental ingredients of a consistent quantum field theory can be checked in this model. From the

discussions in Section 6.1 and 6.3, respectively, we see that there are configurations in which tachyon modes are avoided, and that $U(1)$ gauge symmetry is ensured if minimal coupling with the EM field is introduced . The missing point, regarding renormalizability, is a relevant discussion and let us take into consideration the fact that the modified fermion propagator given by Eq. (6.7) becomes more convergent with respect to the usual case of QED. Thus, we conclude that the model is super-renormalizable. This is the matter discussed in the present Section.

The ultraviolet behavior of the modified fermion propagator in the Eq. (6.7) goes with $\sim 1/p^2$. Thereby, we obtain that the superficial degree of divergence of the primitively divergent diagrams is given by

$$\delta_{\text{graph}} = 4 - E_\gamma - E_\psi - V_{\text{QED}}\,, \tag{6.94}$$

where E_γ and E_ψ are the number of external photonic and the fermionic lines, respectively, and V_{QED} is the usual QED vertex with two fermionic lines, one photonic line, and without momentum. Since that V_{QED} appears with a negative coefficient, the conclusion is in favor to a super-renormalizability model from the point of view of a quantum field theory. This unexpected result is consequence of the behavior of the modified fermion propagator given by Eq. (6.7) in the ultraviolet regime.

6.8 Concluding remarks

In this paper, we study the solutions of a modified Dirac equation by the effects of the LQG, and it coupling with the EM field through the $U(1)$ gauge symmetry. The modification of the Dirac action is due to presence of a length scale (ϑ) introduced by the LQG, where the Dirac kinetic term contains the higher order derivative term $\vartheta\,\bar{\psi}\gamma^0\gamma_5\,\boldsymbol{\nabla}^2\psi$. We obtain the plane solutions in the momentum space associated with the positive and negative energies for the modified Dirac operator. These solutions express an asymmetry in these solutions due to Lorentz symmetry breaking induced by the ϑ-length scale. This is the consequence of the asymmetry for the frequencies associated with the fermion dispersion relations. The group velocity for fermions is showed for the positive energy solution. The fermion propagator in this LSV scenario is obtained in the momentum space. In the ultraviolet regime, the propagator has an improved behavior in which it goes to zero with the squared inverse of the momentum ($\sim 1/k^2$).

The $U(1)$ global symmetry in the LQG Dirac action motivates us to calculate the correspondent conserved current through the Noether theorem. The term $\vartheta\,\bar{\psi}\gamma^0\gamma_5\,\boldsymbol{\nabla}^2\psi$ with the Laplacian operator implies that the spatial-component for the conserved current is altered with new terms that depend on the ϑ-parameter, whereas that time-component is unaltered. The next step is so to investigate the $U(1)$ local symmetry of this theory. The minimal coupling with the electromagnetic (EM) field preserves the $U(1)$ local transformation, that leads us to a QED emerged from the LQG. Thereby, we study the coupling of the conserved current

with the EM field through the Gordon identity. New terms emerge in the current that can be interpreted as contributions to the lepton's electric dipole momentum due exclusively to the ϑ-length scale. Afterwards, we obtain the non-relativistic limit in the Dirac equation, where the Hamiltonian for the NR particle acquires terms that depend on the spin and orbital angular momentum projected on the uniform magnetic field, and also the projection on the particle linear momentum. A new term that depends on the interaction of the electric dipole momentum emerges in the NR limit. All these new effects are removed whenever $\vartheta \to 0$.

Also, to render clearer the terms that appear after carrying out the Gordon decomposition of the electric magnetic current, we have devoted special attention to the calculation of the e^-e^- interparticle potential and the linear corrections in the ϑ parameter shows us how LQG effects correct the usual spin- and velocity-dependent contributions present in the potential.

To end up, we briefly investigate the power-counting renormalizability of the model. Since the fermion propagator exhibits a more convergent ultraviolet behavior, $D^{-1} \sim 1/k^2$, the model becomes super-renormalizable. Thus, this conclusion motivates us to investigate new effects of this modified QED, such as the corrections to the $g-2$ factor for the electron and muon, which are decisive precision measurements in QED. Furthermore, the study of the scalar sector and of the EM modified by the LQG, as described in the Ref. [256], are interesting challenges for a forthcoming project. As a perspective, it is worth noting that one can explore the effects of the Hamiltonian in Eq. (6.93) on spectral lines, e.g., of the Hydrogen atom.

Here ends our Lorentz-symmetry violation endeavor in this Part I of the thesis. In Part II, what follows is a new perspective in the search for physics beyond the Standard Model, based on particle physics. We leave the general conclusions of Part I, as well as perspectives for future works, to Chapter 8 in Part III.

Part II

Pathways to particle physics beyond the Standard Model

Chapter

7

Experimental signatures of Kalb-Ramond like particles

In this Chapter, we slightly change the direction of our search for physics beyond the SM. We explore how particle physics can contribute in this context by studying the rank-2 antisymmetric field, commonly known in the literature as the Kalb–Ramond (KR) field, which, as we emphasize, has many applications in a wide variety of low- and high-energy physics scenarios. The results of our efforts in this chapter were published in Ref. [264].

Antisymmetric fields of rank-2 were introduced in 1966 in the context of quantum field theory [265] (for a review, see Ref.[266]) and eight years later in the dawn of string theory when Kalb and Ramond showed that such fields naturally couple to strings as gauge mediators [267]. It was later demonstrated that KR fields are necessary to ensure some gauge-invariance properties of a string model describing strong interactions [268]. More recently, other aspects of KR fields in string theory, such as in string dualities, have been thoroughly discussed [269]. Stringy KR fields, particularly from low-scale models [270], are interesting due to their phenomenological impact. One such case is that of massless KR fields behaving as singlets under the gauge group of the SM and interacting with fermions via tensor and pseudo-tensor couplings [271]. Tensor currents interacting directly with KR fields appear in the context of dark matter to generate dipole couplings that strongly suppress the interaction with the visible sector of the SM [272–274]. Incidentally, KR fields – connected to string theories or not – are used in investigations of confinement [275–279], condensed matter [280], holography [281], the Casimir effect [282, 283], quantum electrodynamics (QED) [284], the coupling of KR fields to branes [285], Lorentz-symmetry violation [286–288], gravitation [289–291] and cosmology [292–294].

Interestingly enough, antisymmetric rank-2 fields are a possible representation of the Lorentz group in four dimensions, $(1,0)\oplus(0,1)$. This allows a paradigm change to treat the field excitations as particles in their own right: KR-like particles (KRLPs) [295], which may be investigated as new degrees of freedom beyond the SM with phenomenological consequences. Massive KRLPs describe spin-1 particles, analogous – but not equivalent – to the de Broglie-Proca field. This suggests a duality [296] between the two descriptions: in the massive case, the noninteracting KR field is dual to a pseudovector [297]. In the massless and noninteracting limit, the KR field is dual to a pseudoscalar field, prompting the connection to

axion-like particles (ALPs) [298–302]. Similarly, string theory gives rise the so-called hidden photons (HPs), spin-1 particles kinetically mixed with the photon [303–307]. Just like in the case of de Broglie-Proca, HPs are parity-odd vectors, whereas the KR field is parity-even. For more details on the KR dualities, see Ref. [308]. Both ALPs and HPs are well-motivated dark-matter candidates [309–313].

As mentioned above, the dualities of the massless and massive KRL theories suggest a comparison with pseudoscalars and pseudovectors. The most prominent example of pseudoscalars are ALPs, which can have a variety of couplings [314–316]. For example, ALPs may couple to photons via $\mathscr{L}_{\text{int}} \supset aF_{\mu\nu}\tilde{F}^{\mu\nu}$, where $\tilde{F}^{\mu\nu}$ is the dual of the electromagnetic field-strength tensor and a is the ALP field. This coupling leads to ALP-photon oscillations, a feature not shared with KRLPs. Electrons and nucleons can also interact with ALPs via $\mathscr{L}_{\text{int}} \supset a\bar{\psi}\gamma^5\psi$ or $\mathscr{L}_{\text{int}} \supset (\partial_\mu a)\,\bar{\psi}\gamma^\mu\gamma^5\psi$, the latter being analogous to our pseudovector (PV) coupling, see Eq. (7.3).

Also relevant are HPs, light spin-1 particles kinetically mixed to photons with a parameter $\chi \ll 1$. Upon diagonalization, the kinetic terms of the HP and the usual photon decouple, but now the electric current couples to the HP with an effective charge $e\chi$, implying that the fermions acquire a "millicharge" under the new $U_\chi(1)$ [317]. Moreover, the mass terms are not diagonal and we have HP-photon oscillations, which is absent from the dynamics of KRLPs, further differentiating the two in their phenomenology. Finally, HPs are true vectors, whereas KRLPs are parity-even tensors, thus causing the respective couplings to matter to differ. There are two natural couplings possible: $\mathscr{L}_{\text{int}} \supset e\chi X_\mu\bar{\psi}\gamma^\mu\psi$ and $\mathscr{L}_{\text{int}} \supset X_{\mu\nu}\bar{\psi}\sigma^{\mu\nu}\psi$, where X_μ and $X_{\mu\nu}$ are the HP 4-vector and its field-strength tensor, respectively. The first has no parallel in the case of KRLPs because of the parity properties of the fields involved. The second is similar to the tensor (T) interaction, which will be investigated in this work, see Eq. (7.3). Note that for HPs, this coupling is actually derivative because of the presence of the HP field-strength tensor, but in the case of KRLPs it is the field itself that couples to the T current.

Here we confine ourselves to massive interacting KRLPs, not distinguishing among the possible underlying ultraviolet theories. Similarly to HPs, KRLPs may be broadly described as generic Z' bosons feebly interacting with SM particles [318,319]. However, contrary to HPs – or even axions or ALPs – we do not consider a direct coupling of the KRLPs to photons, only to spin-1/2 matter. The aforementioned PV and T couplings to fermions would give rise to modifications of well-measured quantities, such as spectral lines and differential cross sections. Here we compare the predictions including KRLP-mediated interactions with experimental data to set exclusion limits on the PV and T couplings, as well as on the KRLP mass.

This Chapter is organized as follows: in Section 7.1 we set up the basics of the theory of KRLPs and introduce the interaction to matter. Next, in Section 7.2 we investigate possible phenomenological signatures of KRLPs. In Section 7.2.1 we obtain limits from the hyperfine

structure of hydrogen, whereas in Section 7.2.2 we study the tree-level unitarity bounds for $e^- + e^+ \to \ell^- + \ell^+$ ($\ell \neq e$) and in Section 7.2.3 we analyse Bhabha scattering in lepton colliders. Finally, in Section 7.3 we present our conclusions. The flat metric is $\eta_{\mu\nu} = \text{diag}(+,-,-,-)$ and the totally antisymmetric Levi-Civita symbol $\epsilon^{\mu\nu\lambda\kappa}$ is defined such that $\epsilon^{0123} = +1$ with $\epsilon^{0ijk} = -\epsilon_{0ijk} = \epsilon^{ijk} = \epsilon_{ijk}$ (Greek indices run from 0 to 3; Latin indices run from 1 to 3). We use natural units ($\hbar = c = 1$) throughout. The calculations of Section 7.2.3 were cross checked with the FeynCalc Mathematica Package [320–323].

7.1 Kalb-Ramond-like particles and their interactions

In order to determine what kind of experimental signatures a KRLP could produce as a kind of Z′, it is important to discuss its properties, as well as those from the fermion currents with which it could couple.

The dynamics of the real antisymmetric rank-2 KR field $B_{\mu\nu}$ is described by the Lorentz-invariant action

$$S = \int d^4x \left[\frac{1}{6} H_{\mu\nu\lambda} H^{\mu\nu\lambda} - \frac{1}{2} m^2 B_{\mu\nu} B^{\mu\nu} + \mathscr{L}_{\text{int}} \right], \tag{7.1}$$

where the rank-3 field-strength tensor is $H_{\mu\nu\lambda} = \partial_\mu B_{\nu\lambda} + \partial_\nu B_{\lambda\mu} + \partial_\lambda B_{\mu\nu}$ and $m > 0$ is the mass of the KRLP. The KR field has canonical mass dimension one, whereas its field-strength tensor has dimension two. Here $\mathscr{L}_{\text{int}}$ describes the interaction with matter, to be discussed below. In the massless theory, the field-strength tensor allows for a gauge symmetry, namely, $B_{\mu\nu} \to B_{\mu\nu} + \partial_\mu \Omega_\nu - \partial_\nu \Omega_\mu$, with the 4-vector $\Omega_\mu(x)$ being an arbitrary function. Note that, besides the aforementioned gauge transformation, $B_{\mu\nu}$ is itself left unchanged under $\Omega_\mu \to \Omega_\mu + \partial_\mu \lambda$ for a generic $\lambda(x)$. For $m \neq 0$ the model is not gauge invariant – this is the paradigm assumed from here on.

Let us first focus on the case without interactions with equations of motion

$$\partial_\mu H^{\mu\nu\lambda} - m^2 B^{\nu\lambda} = 0. \tag{7.2}$$

Due to its antisymmetry, $B_{\mu\nu}$ has six independent components. However, the subsidiary condition $\partial_\mu B^{\mu\nu} = 0$ contributes with three linearly independent equations, reducing the number of degrees of freedom to three: KRLPs are neutral, parity-even, massive spin-1 particles.

The fundamental field is the parity-even $B_{\mu\nu}$, to which a parity-odd field-strength tensor $H^{\mu\nu\lambda}$ is associated. We can also define its dual, $\tilde{H}_\mu = \frac{1}{6} \epsilon_{\mu\nu\rho\sigma} H^{\nu\rho\sigma}$, which is a pseudovector. The fermionic currents coupling to either $B_{\mu\nu}$ or $\tilde{H}_\mu$ are of two distinct types: pseudovector (PV) and tensor (T), given by $j^\mu_{\text{PV}} = \bar{\psi}\gamma^\mu\gamma^5\psi$ and $j^{\mu\nu}_{\text{T}} = \bar{\psi}\sigma^{\mu\nu}\psi$, respectively, with $\sigma^{\mu\nu} = \frac{i}{2}[\gamma^\mu, \gamma^\nu]$. Here ψ denotes a massive spin-1/2 fermion f. The PV current couples to $\tilde{H}_\mu$, whereas the T current couples directly to the KRL field, $B_{\mu\nu}$, so the natural choices for $\mathscr{L}_{\text{int}}$ are

$$\mathscr{L}_{\text{PV}} = \frac{g^f_{\text{PV}}}{\Lambda} \tilde{H}_\mu \bar{\psi}\gamma^\mu\gamma^5\psi \quad \text{or} \quad \mathscr{L}_{\text{T}} = g^f_{\text{T}} B_{\mu\nu} \bar{\psi}\sigma^{\mu\nu}\psi. \tag{7.3}$$

The real and dimensionless coupling constants $g^f_{\mathrm{PV},T}$ may depend on the fermion species f; we only consider vertices connecting fermions of the same family. The real parameter Λ has dimension of mass and is related to the energy scale of the underlying physics. These are free parameters that, together with m, form the parameter space of the theory.

In QED the vector current $j^\mu_{\mathrm{V}} = \bar{\psi}\gamma^\mu\psi$ is conserved due the local $U(1)_{\mathrm{em}}$ symmetry, a remanent of the $SU(2)_{\mathrm{L}} \otimes U(1)_{\mathrm{Y}}$ electroweak symmetry. Other, less trivial, current structures $j = \bar{\psi}\Gamma\psi$ with $\Gamma = \{\gamma_\mu\gamma_5, \sigma_{\mu\nu}, ...\}$ are nonetheless possible. Pseudovector currents naturally arise in weak interactions due to the embedded V-A structure [325], but also in axion-nucleon effective interactions [326]. Tensor currents, for example, are necessary to describe mesons in the Nambu–Jona-Lasinio model [327], also if one includes dark vector bosons [328]. Similarly, tensor currents have been proposed to explain the discrepancies between theory and experiment concerning the anomalous magnetic moment of the muon with massive dark bosons [329], as fundamental ingredients of dimension-six operators involving a novel massless spin-1 boson [330].

Current conservation translates to $\partial \cdot j = 0$, where the current is either the vector current $j^\mu_{\mathrm{V}} = \bar{\psi}\gamma^\mu\psi$ of electrodynamics, the PV current $j^\mu_{\mathrm{PV}} = \bar{\psi}\gamma^\mu\gamma^5\psi$ or the T current $j^{\mu\nu}_{\mathrm{T}} = \bar{\psi}\sigma^{\mu\nu}\psi$. The vector current is conserved, since the Lagrangian is invariant under $U(1)_{\mathrm{em}}$. In fact, by using the Dirac equation we can show that

$$\partial_\mu j^\mu_{\mathrm{PV}} = 2im_f\bar{\psi}\gamma^5\psi\,, \tag{7.4}$$

$$\partial_\mu j^{\mu\nu}_{\mathrm{T}} = -2m_f j^\nu_{\mathrm{V}} + i\left[\bar{\psi}\left(\partial^\nu\psi\right) - \left(\partial^\nu\bar{\psi}\right)\psi\right]. \tag{7.5}$$

The PV current is only conserved in the case of massless fermions; the T current, on the other hand, is not. For $m = 0$, the KRLP Lagrangian exhibits gauge symmetry (see comment below Eq. (7.1)) and a tensor current would be conserved [331]. In the massive case, however, these currents are not conserved, meaning that the momentum-dependent contributions from the longitudinal parts of the propagator will not automatically vanish.

From Eq. (7.3) we read off the Feynman rule for the T vertex:

$$V^{\mu\nu}_{\mathrm{T}} = ig^f_{\mathrm{T}}\sigma^{\mu\nu}. \tag{7.6}$$

The PV vertex is more involved. Since $B_{\mu\nu}$ is the fundamental field, this interaction is derivative, thus introducing factors of the 4-momentum carried by the KRLP. Using $\partial_\mu \to -ik_\mu$ with the 4-momenta flowing into the vertex defined as positive, the PV interaction vertex is

$$V^{\alpha\beta}_{\mathrm{PV}} = \frac{g^f_{\mathrm{PV}}}{4\Lambda}\epsilon^{\mu\nu\alpha\beta}\left(k_\nu\gamma_\mu - k_\mu\gamma_\nu\right)\gamma^5. \tag{7.7}$$

The propagator may be obtained by writing the free KRLP action in bilinear form as $S = \frac{1}{2}\int d^4x B^{\nu\lambda}\mathcal{O}_{\nu\lambda,\alpha\beta}(x)B^{\alpha\beta}$. In momentum space we have

$$\begin{aligned}\mathcal{O}^{\nu\lambda,\alpha\beta}(k) = \frac{1}{2}\Big[&\left(\eta^{\nu\alpha}\eta^{\lambda\beta} - \eta^{\lambda\alpha}\eta^{\nu\beta}\right)(k^2 - m^2)\\ &+\left(\eta^{\nu\beta}k^\lambda - \eta^{\lambda\beta}k^\nu\right)k^\alpha + \left(\eta^{\lambda\alpha}k^\nu - \eta^{\nu\alpha}k^\lambda\right)k^\beta\Big],\end{aligned} \tag{7.8}$$

which is antisymmetric in $(\nu\lambda)$ and $(\alpha\beta)$. Note the symmetry in the exchange $(\nu\lambda) \leftrightarrow (\alpha\beta)$. The propagator is defined as the inverse of this operator, $\Delta(k) = i\mathcal{O}^{-1}(k)$, and is calculated in App. C.1; here we quote the result with adequate indices for convenience

$$\Delta_{\nu\lambda,\alpha\beta}(k) = \frac{i}{k^2 - m^2}\left[\left(1^{a.s.}\right)_{\nu\lambda,\alpha\beta} - \frac{k^2}{m^2}\left(P_e^1\right)_{\nu\lambda,\alpha\beta}\right], \tag{7.9}$$

where $\left(1^{a.s.}\right)_{\nu\lambda,\alpha\beta}$ is the antisymmetric identity and P_e^1 is one of the projection operators for rank-2 tensors, both defined in App. C.1. The presence of the pole at $k^2 = m^2$ confirms that the KRLP is indeed massive.

7.2 Phenomenology

Having developed the basics of KRLPs as an alternative description of massive spin-1 particles, now we analyse their phenomenology. To this end we use experimental data from different sources, in particular, spectroscopy and scattering at high energies. These are chosen, respectively, due to their high precision and high energies attained. We also study perturbative unitarity to establish a consistent scale for the KRLP couplings to fermions and its mass.

7.2.1 Atomic physics

In order to calculate the shift in the spectral lines caused by the exchange of a KRLP, we must first determine the interaction potential between spin-1/2 point sources. The positive-energy solution of the Dirac equation for a fermion f with mass m_f, spin s and 4-momentum $p^\mu = (E, \boldsymbol{p})$ satisfying $E^2 - \boldsymbol{p}^2 = m_f^2$ is

$$u_s(p) = N_{\mathrm{R}}\begin{pmatrix} \xi_s \\ \dfrac{\boldsymbol{\sigma}\cdot\boldsymbol{p}}{E + m_f}\xi_s \end{pmatrix} \tag{7.10}$$

with $\boldsymbol{\sigma}$ the Pauli spin-matrix vector and $N_{\mathrm{R}} = \sqrt{E + m_f}$ being the relativistic normalization; in a non-relativistic (NR) treatment we change it to $N_{\mathrm{R}} \to N_{\mathrm{NR}} = N_{\mathrm{R}}/\sqrt{2E}$ [332]. The spinor normalization is $u_s^\dagger(p)u_{s'}(p) = 2E\delta_{ss'}$ and here we will ignore spin flip, so $s = s'$.

We are interested in the tree-level interaction of fermion a with initial and final 4-momenta p_1 and p_3, respectively, with fermion b, whose initial and final 4-momenta are p_2 and p_4, respectively. In this case only one Feynman diagram – the t-channel diagram, analogous to those in Figure 8 – contributes and the amplitude reads (suppressing spin indices for clarity)

$$i\mathcal{M} = \bar{u}(p_3)V_v^{\mu\nu}u(p_1)\Delta_{\mu\nu,\alpha\beta}(q)\bar{u}(p_4)V_v^{\alpha\beta}u(p_2), \tag{7.11}$$

where the propagator of the KRLP is given by Eq. (7.9) with $q = p_3 - p_1 = p_2 - p_4$. Here $v = \{\mathrm{PV}, T\}$ indicates the specific interaction being considered; we only consider the potentials

generated by vertices of the same type, that is, the vertices are either both PV or T, but not a mixture (see Refs. [333, 334] for a discussion). More explicitly, the relativistic PV and T amplitudes are

$$\begin{aligned}\mathscr{M}_{\rm PV} = &-\frac{g^a_{\rm PV} g^b_{\rm PV}}{2\Lambda^2(q^2-m^2)}\Big\{q^2\Big[\bar{u}^{(s_3)}(p_3)\gamma_\mu\gamma_5 u^{(s_1)}(p_1)\Big]\Big[\bar{v}^{(s_2)}(p_2)\gamma^\mu\gamma_5 v^{(s_4)}(p_4)\Big]\\ &-q_\mu q_\nu\Big[\bar{u}^{(s_3)}(p_3)\gamma^\mu\gamma_5 u^{(s_1)}(p_1)\Big]\Big[\bar{v}^{(s_2)}(p_2)\gamma^\nu\gamma_5 v^{(s_4)}(p_4)\Big]\Big\}\end{aligned} \tag{7.12}$$

and

$$\begin{aligned}\mathscr{M}_{\rm T} = &-\frac{g^a_{\rm T} g^b_{\rm T}}{(q^2-m^2)}\Big\{\Big[\bar{u}^{(s_3)}(p_3)\sigma_{\mu\nu} u^{(s_1)}(p_1)\Big]\Big[\bar{v}^{(s_2)}(p_2)\sigma^{\mu\nu} v^{(s_4)}(p_4)\Big]\\ &+\frac{2q^\nu q_\alpha}{m^2}\Big[\bar{u}^{(s_3)}(p_3)\sigma_{\mu\nu} u^{(s_1)}(p_1)\Big]\Big[\bar{v}^{(s_2)}(p_2)\sigma^{\mu\alpha} v^{(s_4)}(p_4)\Big]\Big\}.\end{aligned} \tag{7.13}$$

From scattering theory, the interaction potential is related to the amplitude (at leading order) by the first Born approximation [332]

$$V(r) = -\int \frac{d^3\boldsymbol{q}}{(2\pi)^3}\mathscr{M}_{\rm NR}(\boldsymbol{q})\, e^{i\boldsymbol{q}\cdot\boldsymbol{r}}, \tag{7.14}$$

where $\boldsymbol{q}$ is the 3-momentum carried by the mediator and $r = |\boldsymbol{r}|$ is the distance between the sources. We must now consider the NR limit of the amplitudes (7.12) and (7.13). For this we use the spinor (7.10) with $N_{\rm R} \to N_{\rm NR} = N_{\rm R}/\sqrt{2E}$, as well as the approximation of an elastic scattering, to evaluate the bilinears. For further details, please refer to App. C.2. The results are the NR amplitudes for PV and T sources, see Eqs. (C.21) and (C.23), which can be used to compute the respective potentials with the help of the Fourier integrals listed in App. C.2.3. The ensuing parity-even potentials due to the exchange of a KRLP between fermions a and b in the NR limit are (see Ref. [260] for a pedagogical approach to this type of calculation)

$$\begin{aligned}V_{\rm PV}(r) = &\left(\frac{g^a_{\rm PV} g^b_{\rm PV}}{2\Lambda^2}\right)\Big\{\left[\frac{2}{3}\delta^3(\boldsymbol{r}) - \left(1+mr+m^2r^2\right)\frac{e^{-mr}}{4\pi r^3}\right]\boldsymbol{\sigma}_a\cdot\boldsymbol{\sigma}_b\\ &+\left(3+3mr+m^2r^2\right)\frac{e^{-mr}}{4\pi r^3}\left(\hat{\boldsymbol{r}}\cdot\boldsymbol{\sigma}_a\right)\left(\hat{\boldsymbol{r}}\cdot\boldsymbol{\sigma}_b\right)\Big\},\end{aligned} \tag{7.15}$$

$$\begin{aligned}V_{\rm T}(r) = &-\left(\frac{2g^a_{\rm T} g^b_{\rm T}}{m^2}\right)\Big\{\left[\frac{2}{3}\delta^3(\boldsymbol{r}) - (1+mr)\frac{e^{-mr}}{4\pi r^3}\right]\boldsymbol{\sigma}_a\cdot\boldsymbol{\sigma}_b\\ &+\left(3+3mr+m^2r^2\right)\frac{e^{-mr}}{4\pi r^3}\left(\hat{\boldsymbol{r}}\cdot\boldsymbol{\sigma}_a\right)\left(\hat{\boldsymbol{r}}\cdot\boldsymbol{\sigma}_b\right)\Big\}.\end{aligned} \tag{7.16}$$

A few comments are in order. The heaviest fermion in our analysis is the proton, the electron is the lightest. Even though we make no assumption regarding the scale of m, it is possible that the KRLP is lighter than either of the fermions (but not strictly massless). We may thus generally neglect terms $O\left(|\boldsymbol{P}|^2/m_a m_b\right)$ in the amplitudes. From the decomposition of the fermionic bilinears, see App. C.2.2, and the structure of the propagator (7.9) we see that

the $0i$ and ij components do not mix in the NR amplitudes, causing the only momentum contributions to be automatically of second order. The typical velocity of the electron in the hydrogen atom is $\approx \alpha \approx 1/137$, so all things being equal, the velocity-dependent terms are suppressed by a factor $\approx 5 \times 10^{-5}$. We therefore work in the static limit.

The presence of the spins of both fermions is also relevant, though this is not new in the literature of exotic potentials [333–341]. It shows that the energy shifts resulting from using the PV and T potentials as perturbations will have a structure similar to that of the hyperfine interaction [342]. Moreover, both potentials have contact terms $\sim \delta^3(\boldsymbol{r})$, also featured in other potentials involving the exchange of spin-1 mediators [333–339]. These terms are not important in interactions at macroscopic distances, but they do play a role in atomic phenomena, specially when one considers wave functions that are finite at the origin [337, 342].

The limit of a light KRLP is noteworthy. The PV potential is unproblematic, but the T potential is enhanced due to the pre-factor $1/m^2$. A similar feature appears in the context of the Proca-mediated interaction between spin-1/2 fermions with PV couplings $\sim V_\mu \bar{\psi}\gamma^\mu\gamma^5\psi$, where V_μ is the massive mediator [334]. This kind of PV coupling is also considered in Refs. [336, 337], with similar conclusions. Note that this PV interaction differs from the one we consider, see Eq. (7.3), where the dual field-strength tensor $\tilde{H}_\mu$ couples to the PV current, not to $B_{\mu\nu}$ itself, thus bringing extra factors of the momentum transfer, $\boldsymbol{q}$, which eventually lead to the cancelling of the overall $1/m^2$ factor present in the NR amplitude. Interestingly, the vertex for T couplings does not carry momentum factors [295]; here the coupling of the T current is directly to $B_{\mu\nu}$ and the $1/m^2$ factor survives. For a truly massless mediator, the divergence caused by $\sim q_\mu q_\nu/m^2$ does not occur, since the mediator has no longitudinal degree of freedom [337].

7.2.1.1 Limits from the hyperfine structure of hydrogen atom

The potentials calculated above may be understood as quantum-mechanical operators acting as small corrections to the unperturbed Hamiltonian of hydrogen (we make $a, b \to p, e$). The potentials (7.15) and (7.16) will then cause certain energy levels to slightly shift and split, thereby inducing the transition frequency between said levels to deviate from those experimentally observed and theoretically calculated using QED. Here we obtain these energy differences between the split levels – the so-called hyperfine splitting intervals – of the $n = 1$ and $n = 2$ states of hydrogen with $\ell = 0$, that is, the $1s_{1/2}$ and $2s_{1/2}$ states.

In the standard treatment of the hydrogen atom the spin of the electron first appears in the context of the spin-orbit interaction caused by the coupling of the electron's magnetic moment to its orbital motion – these corrections are of order $\approx 10^{-4}$ eV, marking the energy scale of the fine structure. The spin of the proton enters the picture when we consider the direct coupling of its magnetic moment to that of the electron [342, 343]: this hyperfine interaction breaks the degeneracy of the $\ell = 0$, spherically symmetric $1s_{1/2}$ and $2s_{1/2}$ states. The associated hyperfine energy splitting is of order $\approx 10^{-6}$ eV for the $1s_{1/2}$ level, which is

broken in (three-fold degenerate) triplet and singlet energy states [342–346].

The calculation of the splitting caused by the PV and T potentials closely resembles that of the standard hyperfine structure [342]. To start with, we must calculate the matrix elements of the potentials between the states $|\psi_n\rangle = |\psi_{n00}\rangle \otimes |m_{z,e} m_{z,p}\rangle$ with $n = 1, 2$; here $m_{z,(e,p)} = \pm 1/2$ are the projections of the respective spins, $\boldsymbol{S}_{e,p} = \boldsymbol{\sigma}_{e,p}/2$, along the quantization axis. The normalized unperturbed wave functions for the $1s_{1/2}$ and $2s_{1/2}$ states of hydrogen are

$$\langle \mathrm{R}|\psi_{100}\rangle = \psi_{100}(r) = \sqrt{\frac{k^3}{\pi}} e^{-kr}\,, \tag{7.17}$$

$$\langle \mathrm{R}|\psi_{200}\rangle = \psi_{200}(r) = \frac{1}{2}\sqrt{\frac{k^3}{2\pi}} \left(1 - \frac{kr}{2}\right) e^{-kr/2}\,, \tag{7.18}$$

with $k = 1/a_0$, where $a_0 = 2.68 \times 10^{-4}\,\mathrm{eV}^{-1}$ is the Bohr radius ($k = 3.73 \times 10^3$ eV).

Let us work out the case of the PV potential. Setting $\boldsymbol{\sigma} = 2\boldsymbol{S}$, the matrix elements are

$$\langle \psi_n | V_{\mathrm{PV}} | \psi_n \rangle = C_{\mathrm{PV}} \langle \psi_n | \left\{ \left[\frac{8\pi}{3} \delta^3(\boldsymbol{r}) - F_1(r) \right] \boldsymbol{S}_e \cdot \boldsymbol{S}_p + F_2(r) \left(\hat{\boldsymbol{r}} \cdot \boldsymbol{S}_e\right) \left(\hat{\boldsymbol{r}} \cdot \boldsymbol{S}_p\right) \right\} | \psi_n \rangle\,, \tag{7.19}$$

where $C_{\mathrm{PV}} = g_{\mathrm{PV}}^e g_{\mathrm{PV}}^p / 2\pi\Lambda^2$ and we defined the functions $F_1(r) = \left(1 + mr + m^2 r^2\right) e^{-mr}/r^3$ and $F_2(r) = \left(3 + 3mr + m^2 r^2\right) e^{-mr}/r^3$. Writing $\langle \psi_n | V_{\mathrm{PV}} | \psi_n \rangle = C_{\mathrm{PV}} \left(A_c - A_1 + A_2\right)$, we find

$$A_c = \frac{8\pi}{3} \langle \boldsymbol{S}_e \cdot \boldsymbol{S}_p \rangle |\psi_{n00}(0)|^2\,, \tag{7.20}$$

$$A_1 = 4\pi \langle \boldsymbol{S}_e \cdot \boldsymbol{S}_p \rangle \int dr\, r^2\, F_1(r) |\psi_{n00}(r)|^2\,, \tag{7.21}$$

$$\begin{aligned} A_2 &= \langle (\boldsymbol{S}_e)_i \cdot \left(\boldsymbol{S}_p\right)_j \rangle \int d\Omega \left(\hat{\boldsymbol{r}}_i \hat{\boldsymbol{r}}_j\right) \int dr\, r^2\, F_2(r) |\psi_{n00}(r)|^2\,, \\ &= \frac{4\pi}{3} \langle \boldsymbol{S}_e \cdot \boldsymbol{S}_p \rangle \int dr\, r^2\, F_2(r) |\psi_{n00}(r)|^2 \end{aligned} \tag{7.22}$$

where, in the last line, we used $\int d\Omega \left(\hat{\boldsymbol{r}}_i \hat{\boldsymbol{r}}_j\right) = 4\pi\delta_{ij}/3$ due to spherical symmetry. Putting it all together we get

$$\begin{aligned} \langle \psi_n | V_{\mathrm{PV}} | \psi_n \rangle &= \frac{8\pi}{3} C_{\mathrm{PV}} \langle \boldsymbol{S}_e \cdot \boldsymbol{S}_p \rangle \left\{ |\psi_{n00}(0)|^2 + \frac{1}{2} \int_0^\infty dr\, r^2 \left[F_2(r) - 3F_1(r)\right] |\psi_{n00}(r)|^2 \right\}, \\ &= \frac{8\pi}{3} C_{\mathrm{PV}} \langle \boldsymbol{S}_e \cdot \boldsymbol{S}_p \rangle \left\{ |\psi_{n00}(0)|^2 - m^2 \int_0^\infty dr\, r\, e^{-mr} |\psi_{n00}(r)|^2 \right\}. \end{aligned} \tag{7.23}$$

Let us now address the factor $\langle \boldsymbol{S}_e \cdot \boldsymbol{S}_p \rangle = \langle m_{z,e} m_{z,p} | \boldsymbol{S}_e \cdot \boldsymbol{S}_p | m_{z,e} m_{z,p} \rangle$. The total angular momentum of the system is $\boldsymbol{F} = \boldsymbol{S}_e + \boldsymbol{S}_p$, since we are dealing with zero orbital angular momentum. Both the electron and the proton have spin $1/2$, whose addition can only generate $\boldsymbol{F}$ with eigenvalues $F = 0, 1$: the four eigenstates of the perturbation will have only two distinct energy levels. Noting that $\boldsymbol{S}_e \cdot \boldsymbol{S}_p = \left(\boldsymbol{F}^2 - \boldsymbol{S}_e^2 - \boldsymbol{S}_p^2\right)/2 = \left(\boldsymbol{F}^2 - 3/2\right)/2$ we may diagonalize this operator to find that its eigenvalues are $\lambda_F = \left[F(F+1) - 3/2\right]/2$, so that $\lambda_F = -3/4, +1/4$ for $F = 0, 1$, respectively. We are interested in corrections to $\Delta E_{\mathrm{hfs}}(ns)$, which is the energy difference between the triplet ($F = 1$) and singlet ($F = 0$) states for the $n = 1, 2$

levels. Since $\lambda_{F=1} - \lambda_{F=0} = 1/4 - (-3/4) = 1$, the PV splitting interval is

$$\Delta E^{(\mathrm{PV})}_{\mathrm{hfs}}(ns) = \frac{8\pi}{3} C_{\mathrm{PV}} \left\{ |\psi_{n00}(0)|^2 - m^2 \int_0^\infty dr\, r\, e^{-mr} |\psi_{n00}(r)|^2 \right\}. \tag{7.24}$$

Using the normalized wave functions (7.17) and (7.18) we obtain

$$\Delta E^{(\mathrm{PV})}_{\mathrm{hfs}}(1s) = \frac{4 g^e_{\mathrm{PV}} g^p_{\mathrm{PV}}}{3\pi\Lambda^2} k^3 \left[1 - \frac{m^2}{(m+2k)^2} \right], \tag{7.25}$$

$$\Delta E^{(\mathrm{PV})}_{\mathrm{hfs}}(2s) = \frac{g^e_{\mathrm{PV}} g^p_{\mathrm{PV}}}{6\pi\Lambda^2} k^3 \left[1 - \frac{m^2 \left(k^2 + 2m^2\right)}{2\,(m+k)^4} \right]. \tag{7.26}$$

Note that in the massless limit we have $\Delta E^{(\mathrm{PV})}_{\mathrm{hfs}}(1s)/\Delta E^{(\mathrm{PV})}_{\mathrm{hfs}}(2s) = 8$.

The steps above may be repeated for the T potential, see Eq. (7.16), but here we must make the substitution $F_1(r) \to F_3(r) = (1+mr)\, e^{-mr}/r^3$. This leads to

$$\begin{aligned} \langle \psi_n | V_{\mathrm{T}} | \psi_n \rangle &= -\frac{8\pi}{3} C_{\mathrm{T}} \langle \boldsymbol{S}_e \cdot \boldsymbol{S}_p \rangle \left\{ |\psi_{n00}(0)|^2 + \frac{1}{2} \int_0^\infty dr\, r^2 \left[F_2(r) - 3F_3(r) \right] |\psi_{n00}(r)|^2 \right\} \\ &= -\frac{8\pi}{3} C_{\mathrm{T}} \langle \boldsymbol{S}_e \cdot \boldsymbol{S}_p \rangle \left\{ |\psi_{n00}(0)|^2 + \frac{m^2}{2} \int_0^\infty dr\, r\, e^{-mr} |\psi_{n00}(r)|^2 \right\}, \end{aligned} \tag{7.27}$$

with $C_{\mathrm{T}} = 2 g^{e^-}_{\mathrm{T}}\, g^{p^+}_{\mathrm{T}} / \pi m^2$. The hyperfine splitting interval due to the T potential is then

$$\Delta E^{(\mathrm{T})}_{\mathrm{hfs}}(ns) = -\frac{8\pi}{3} C_{\mathrm{T}} \left\{ |\psi_{n00}(0)|^2 + \frac{m^2}{2} \int_0^\infty dr\, r\, e^{-mr} |\psi_{n00}(r)|^2 \right\}, \tag{7.28}$$

which for $n = 1, 2$ is explicitly given by

$$\Delta E^{(\mathrm{T})}_{\mathrm{hfs}}(1s) = -\frac{16 g^e_{\mathrm{T}} g^p_{\mathrm{T}}}{3\pi m^2} k^3 \left[1 + \frac{m^2}{2\,(m+2k)^2} \right], \tag{7.29}$$

$$\Delta E^{(\mathrm{T})}_{\mathrm{hfs}}(2s) = -\frac{2 g^e_{\mathrm{T}} g^p_{\mathrm{T}}}{3\pi m^2} k^3 \left[1 + \frac{m^2 \left(k^2 + 2m^2\right)}{4\,(m+k)^4} \right]. \tag{7.30}$$

The hyperfine structure is caused by finite wave functions at $r = 0$ and is sensitive to the finite size of the proton. The precision of theoretical calculations is dominated by uncertainties in the modelling of the proton's internal structure. It is thus convenient to consider Sternheim's splitting interval $D_{21} = 8\Delta E_{\mathrm{hfs}}(2s) - \Delta E_{\mathrm{hfs}}(1s)$ [347], which reduces the uncertainty from nuclear-structure effects since $|\psi_{100}(0)|^2 = 8|\psi_{200}(0)|^2$, see Eqs. (7.17) and (7.18). The results above give

$$D^{(\mathrm{PV})}_{21} = \frac{4 g^e_{\mathrm{PV}} g^p_{\mathrm{PV}}}{3\pi\Lambda^2} m^2 k^3 \left[\frac{1}{(m+2k)^2} - \frac{\left(k^2 + 2m^2\right)}{2\,(m+k)^4} \right], \tag{7.31}$$

$$D^{(\mathrm{T})}_{21} = \frac{4 g^e_{\mathrm{T}} g^p_{\mathrm{T}}}{3\pi} k^3 \left[\frac{2}{(m+2k)^2} - \frac{\left(k^2 + 2m^2\right)}{(m+k)^4} \right]. \tag{7.32}$$

In order to constrain the unknown KRLP parameters we must compare our predictions for D_{21} to a reference value ΔD. Following Refs. [336–338, 348] we obtain ΔD by evaluating

$$\int_{-\Delta D}^{\Delta D} \frac{1}{\sqrt{2\pi}\sigma} e^{-(x-\mu)^2/(2\sigma^2)} dx = f(\Delta D). \tag{7.33}$$

Here $\sigma = \sqrt{\sigma_{\rm Th}^2 + \sigma_{\rm exp}^2}$ is the combined error from theory and experiment and μ is the (mean) deviation of experiment from the theoretical prediction. Choosing $f(\Delta D) = 0.95$ gives a 95% confidence-level (CL) limit. The meaning of Eq. (7.33) is simple: the best theoretical calculations are statistically compatible with the best measurements of D_{21}. Therefore, our contributions to D_{21}, see Eqs. (7.31) and (7.32), cannot be arbitrarily large and ΔD is the largest deviation from the mean μ which still preserves the agreement between experiment and standard theory.

The most recent measurement of the hyperfine splitting of the $2s_{1/2}$ level in hydrogen gives $D_{21}^{\rm exp} = 48.9592(68)$ kHz [346], whereas the theoretical prediction is $D_{21}^{\rm Th} = 48.9541(23)$ kHz [349]. Here we merely quote the transition frequencies without explicitly converting them to energies. We have $\mu = D_{21}^{\rm Th} - D_{21}^{\rm exp} = -0.0051$ kHz with $\sigma = 0.0072$ kHz [338]; plugging these values in Eq. (7.33) yields $\Delta D = 0.0170\,\text{kHz} = 7.04 \times 10^{-14}$ eV at 95% CL. Setting $|D_{21}^{(\rm PV,\,T)}| \leq \Delta D$, we obtain the exclusion plots in Figure 7. The central upward peaks are due to the structure of Sternheim's splitting, which introduces the difference of the hyperfine splittings of the $1s$ and $2s$ states. From Eqs. (7.31) and (7.32) we see that both peaks occur at $m^\star = (\sqrt{10} - 2)k/3 \approx 1.45$ keV. For the PV coupling the limit behaves as $1/m^2$ for $m \ll m^\star$ and as m^2 for $m \gg m^\star$, whereas for the T coupling the limit is constant for $m \ll m^\star$ and goes as m^4 for $m \gg m^\star$.

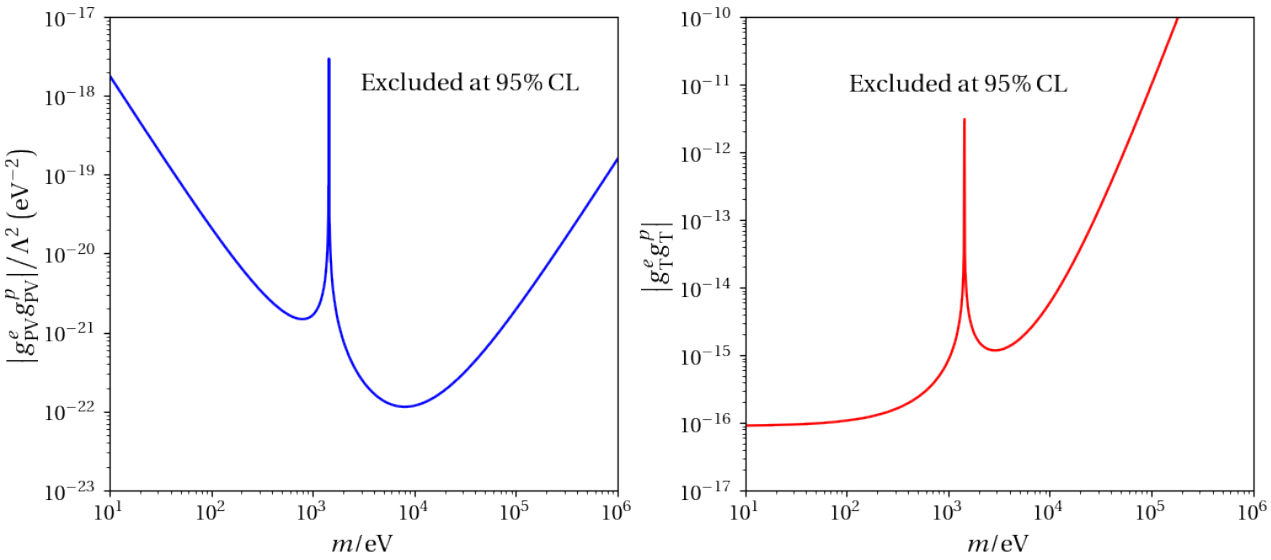

Figure 7 – Constraints on the parameter space of KRLPs coupled to electrons and protons at 95% CL extracted by comparing experimental and theoretical values for Steinheim's splitting interval $D_{21} = 8\Delta E_{\rm hfs}(2s) - \Delta E_{\rm hfs}(1s)$ in hydrogen.

The worsening of the bounds for large masses is expected, since a heavy mediator can be hardly excited at low energies and the photon-mediated interaction dominates, thus causing the bound to weaken. The case of small masses is more involved. A truly massless theory is fundamentally different than a massive one, even if the mediator is light relative to the pertinent energy scales: the former is gauge invariant and the latter is not. Let us then focus on the case of a light, but massive, mediator. In this regime the PV potential (7.15) reduces to the standard Maxwellian dipole-dipole interaction [343], apart from an overall constant.

This means that, for small KRLP masses, the strength of the dipole-dipole interaction in pure QED is simply re-scaled by $\sim (1 + g_{\rm PV}^2)$. The consequence is that KRLP exchange becomes unobservable and the PV bound worsens; a similar situation occurs for hidden photons [350, 351].

For the bound on T interactions the argument is different. The saturation for small masses can be explained as in Ref. [337] using the toy-model example of the Z boson from the SM with only axial-vector couplings to fermions. In this case the potential also displays a (longitudinal) contribution with a pre-factor g^2/m_Z^2, where g is the universal electroweak coupling constant and m_Z is the Z-boson mass. The mass-generation mechanism involves a Higgs boson with g and m_Z related to its vacuum expectation value v by $g^2/m_Z^2 = 4/v^2$. This shows that g^2/m^2 is actually constant for the energy shifts (7.29) and (7.30) to leading order. However, in Figure 7 we use Sternheim's splitting interval $D_{21} = 8\Delta E_{\rm hfs}(2s) - \Delta E_{\rm hfs}(1s)$, which kills this leading-order behavior of the energy shifts – the remaining expression is constant for small m, as visible in the plot.

Finally, it is worth noting the similarity of the shape of our bounds to those obtained in Ref. [337], specially their Figs. 5 and 10 for Sternheim's interval D_{21} in hydrogen, where the authors study generic spin-dependent potentials between spin-1/2 sources with couplings to pseudoscalar and pseudovector mediators. The reason for this resemblance is the fact that the potentials considered, their $V_{\rm pp}$ and $V_{\rm AA}$ – or rather $\mathcal{V}_3$ – are functionally similar to our $V_{\rm PV}$ and $V_{\rm T}$, respectively.

7.2.2 Tree-level unitarity in $e^- + e^+ \to \ell^- + \ell^+$ ($\ell \neq e$) scattering

In this and the next section we focus on the scatterings $e^- + e^+ \to \ell^- + \ell^+$ for $\ell = \{e, \mu, \tau\}$, which are well described by pure QED at energies up to the vicinity of the Z-pole, where electroweak (EW) effects become relevant. Particularly important is Bhabha scattering, $e^- + e^+ \to e^- + e^+$, which is frequently used as a luminosity monitor to calibrate cross-section measurements at lepton colliders [352–356]. Corrections from diagrams with Z-boson exchange alter the QED differential cross section at the level of $1 - 2\%$ [357] and generally improve the fit of the theory to the data – these processes were crucial in the early studies of the properties of the Z boson [358–360]. The EW corrections are of the same order of magnitude as the experimental errors, so we shall include $\ell\ell Z$ vertices along those of QED in our analysis, where the KRLP-mediated diagrams with either PV or T vertices will enter as small perturbations.

The processes $e^- + e^+ \to \ell^- + \ell^+$ with $\ell = e$ or $\ell \neq e$ are physically distinct, but have some common aspects. Here we study tree-level unitarity applied to the case $\ell \neq e$ and in Sec. 7.2.3 we analyse Bhabha scattering ($\ell = e$). Below we state the necessary kinematics and the amplitudes for the t- and s-channels; only the latter is relevant for the discussion of tree-level unitarity in Sec. 7.2.2.2, whereas both are needed to describe Bhabha scattering in Sec. 7.2.3.

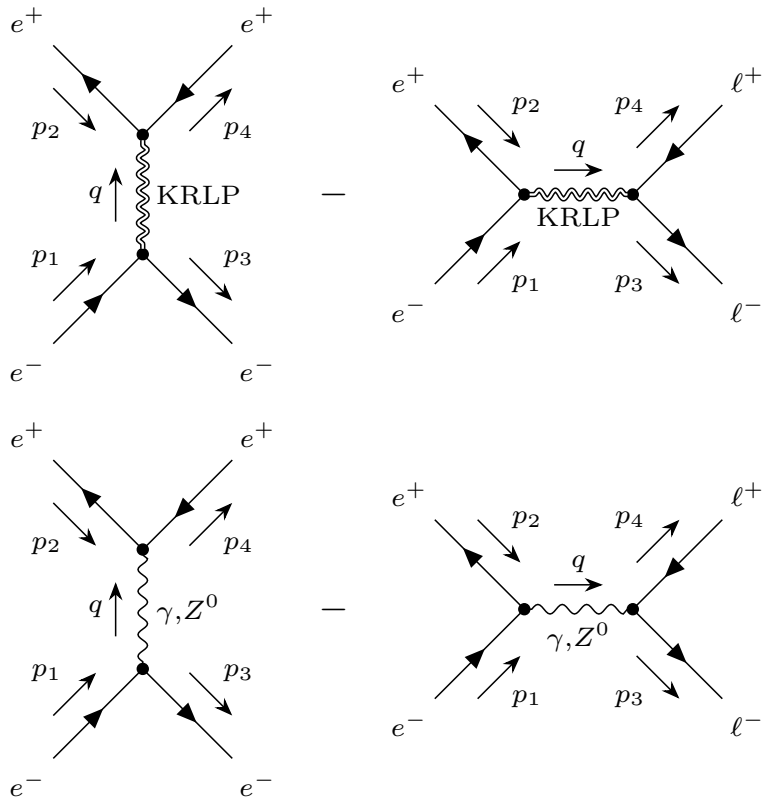

Figure 8 – Tree-level Feynman diagrams contributing to the scattering $e^- + e^+ \to \ell^- + \ell^+$ for $\ell = \{e, \mu, \tau\}$. If $\ell = e$ we have Bhabha scattering with both s- and t-diagrams, whereas for $\ell = \{\mu, \tau\}$ only the s-channel contributes at tree level. The minus signs indicate that the corresponding amplitudes must be subtracted.

7.2.2.1 Kinematic definitions and amplitudes

We work in the center-of-mass (CM) frame, where the particles have the same energy $E \gg m_\ell$ and opposite 3-momenta. The 4-momenta of the leptons are the following: the in-coming electron has $p_1 = (E, \boldsymbol{p})$ and the in-coming positron has $p_2 = (E, -\boldsymbol{p})$, whereas the out-going lepton has $p_3 = (E, \boldsymbol{p}')$ and the out-going anti-lepton has $p_4 = (E, -\boldsymbol{p}')$. The CM energy is $\sqrt{s} = 2E$ and $|\boldsymbol{p}| = |\boldsymbol{p}'|$. The initial 3-momenta are taken to be on the z-axis, $\boldsymbol{p} = \left(\sqrt{s}/2\right)\hat{\boldsymbol{z}}$, with the final momentum $\boldsymbol{p}' = \left(\sqrt{s}/2\right)(\sin\theta\cos\phi, \sin\theta\sin\phi, \cos\theta)$.

The relevant Feynman diagrams are illustrated in Figure 8. The total tree-level amplitudes are the combination of the SM contribution and that of new physics containing KRLP-mediated PV or T interactions: $\mathscr{M}_{\text{tot}} = \mathscr{M}_{\text{SM}} + \mathscr{M}_{\text{PV},T}$. The amplitude from the SM is itself the sum of the photon-mediated amplitudes

$$\mathscr{M}^{(t)}_{\text{QED}} = -\frac{e^2}{t}\left[\bar{u}^{(s_3)}(p_3)\gamma^\mu u^{(s_1)}(p_1)\right]\left[\bar{v}^{(s_2)}(p_2)\gamma_\mu v^{(s_4)}(p_4)\right], \tag{7.34}$$

$$\mathscr{M}^{(s)}_{\text{QED}} = \frac{e^2}{s}\left[\bar{v}^{(s_2)}(p_2)\gamma^\mu u^{(s_1)}(p_1)\right]\left[\bar{u}^{(s_3)}(p_3)\gamma_\mu v^{(s_4)}(p_4)\right] \tag{7.35}$$

with $t = -s(1-\cos\theta)/2$ and of the Z-mediated amplitudes

$$\mathscr{M}_{\rm EW}^{(t)} = -\frac{g_Z^2}{4(t-m_Z^2+im_Z\Gamma_Z)}\left[\eta_{\mu\nu}-\frac{(p_1-p_3)_\mu(p_1-p_3)_\nu}{m_Z^2}\right] \times\left[\bar{u}^{(s_3)}(p_3)(g_V-g_A\gamma_5)\gamma^\mu u^{(s_1)}(p_1)\right]\left[\bar{v}^{(s_2)}(p_2)(g_V-g_A\gamma_5)\gamma^\nu v^{(s_4)}(p_4)\right], \tag{7.36}$$

$$\mathscr{M}_{\rm EW}^{(s)} = \frac{g_Z^2}{4(s-m_Z^2+im_Z\Gamma_Z)}\left[\eta_{\mu\nu}-\frac{(p_1+p_2)_\mu(p_1+p_2)_\nu}{m_Z^2}\right] \times\left[\bar{v}^{(s_2)}(p_2)(g_V-g_A\gamma_5)\gamma^\mu u^{(s_1)}(p_1)\right]\left[\bar{u}^{(s_3)}(p_3)(g_V-g_A\gamma_5)\gamma^\nu v^{(s_4)}(p_4)\right]. \tag{7.37}$$

The $\ell\ell Z$ coupling is $g_Z = e/(\sin\theta_W\cos\theta_W)$, where $\sin^2\theta_W = 0.23$ is the Weinberg angle, $\Gamma_Z = 2.5$ GeV is the Z-boson width and $G_F = 1.17\times10^{-5}\,\text{GeV}^{-2}$ is the Fermi constant [39]. Furthermore, $g_V = -1/2+2\sin^2\theta_W$ and $g_A = +1/2$ are the vector and axial couplings. The longitudinal pieces of the Z-boson propagator are negligible by virtue of the Dirac equation: for the incoming electron we have $p_1^\mu\gamma_\mu u^{(s_1)}(p_1) = m_e u^{(s_1)}(p_1)$. Similar results hold for the other leptons and the longitudinal term contributes with $\sim m_\ell^2/m_Z^2 \lesssim 10^{-4}$, being henceforth ignored; see Refs. [361,362] for a complementary discussion of ultra-heavy fermions.

The KRLP-mediated t- and s-channel diagrams with PV vertices are

$$\mathscr{M}_{\rm PV}^{(t)} = -\frac{g_{\rm PV}^e g_{\rm PV}^e}{2\Lambda^2(t-m^2)}\Big\{t\left[\bar{u}^{(s_3)}(p_3)\gamma_5\gamma_\mu u^{(s_1)}(p_1)\right]\left[\bar{v}^{(s_2)}(p_2)\gamma_5\gamma^\mu v^{(s_4)}(p_4)\right] - q_\mu q_\nu\left[\bar{u}^{(s_3)}(p_3)\gamma_5\gamma^\mu u^{(s_1)}(p_1)\right]\left[\bar{v}^{(s_2)}(p_2)\gamma_5\gamma^\nu v^{(s_4)}(p_4)\right]\Big\}, \tag{7.38}$$

$$\mathscr{M}_{\rm PV}^{(s)} = \frac{g_{\rm PV}^e g_{\rm PV}^\ell}{2\Lambda^2(s-m^2)}\Big\{s\left[\bar{v}^{(s_2)}(p_2)\gamma_5\gamma_\mu u^{(s_1)}(p_1)\right]\left[\bar{u}^{(s_3)}(p_3)\gamma_5\gamma^\mu v^{(s_4)}(p_4)\right] - q_\mu q_\nu\left[\bar{v}^{(s_2)}(p_2)\gamma_5\gamma^\mu u^{(s_1)}(p_1)\right]\left[\bar{u}^{(s_3)}(p_3)\gamma_5\gamma^\nu v^{(s_4)}(p_4)\right]\Big\} \tag{7.39}$$

and the KRLP-mediated amplitudes with T vertices are

$$\mathscr{M}_{\rm T}^{(t)} = -\frac{g_{\rm T}^e g_{\rm T}^e}{(t-m^2)}\Big\{\left[\bar{u}^{(s_3)}(p_3)\sigma_{\mu\nu}u^{(s_1)}(p_1)\right]\left[\bar{v}^{(s_2)}(p_2)\sigma^{\mu\nu}v^{(s_4)}(p_4)\right] + \frac{2q^\nu q_\alpha}{m^2}\left[\bar{u}^{(s_3)}(p_3)\sigma_{\mu\nu}u^{(s_1)}(p_1)\right]\left[\bar{v}^{(s_2)}(p_2)\sigma^{\mu\alpha}v^{(s_4)}(p_4)\right]\Big\}, \tag{7.40}$$

$$\mathscr{M}_{\rm T}^{(s)} = \frac{g_{\rm T}^e g_{\rm T}^\ell}{(s-m^2)}\Big\{\left[\bar{v}^{(s_2)}(p_2)\sigma_{\mu\nu}u^{(s_1)}(p_1)\right]\left[\bar{u}^{(s_3)}(p_3)\sigma^{\mu\nu}v^{(s_4)}(p_4)\right] + \frac{2q^\nu q_\alpha}{m^2}\left[\bar{v}^{(s_2)}(p_2)\sigma_{\mu\nu}u^{(s_1)}(p_1)\right]\left[\bar{u}^{(s_3)}(p_3)\sigma^{\mu\alpha}v^{(s_4)}(p_4)\right]\Big\}. \tag{7.41}$$

If $\ell \neq e$ only the s-channel diagrams are allowed and if $\ell = e$ we have Bhabha scattering with the two channels. Here q is the 4-momentum carried by the KRLP: for the s-channel $q = p_1+p_2 = p_3+p_4$ and $q^2 = s$, while for the t-channel $q = p_1-p_3 = -(p_2-p_4)$ and $q^2 = t$.

7.2.2.2 Perturbative unitarity for $\ell \neq e$

The scattering matrix $S = 1 + iT$ describes the interaction of particles. Non-trivial interactions are encoded in the transition matrix T, which takes the system from the initial state $|i\rangle$ to the final state $|f\rangle$. Its matrix elements, $T_{if} = \langle i|T|f\rangle$, are expressed in terms of the Lorentz-invariant amplitude $\mathscr{M}_{i\to f}$ as $T_{if} = (2\pi)^4 \delta^4\left(P_i - P_f\right)\mathscr{M}_{i\to f}$, where $P_{i,f}$ are the sum of 4-momenta of the $|i\rangle, |f\rangle$ states, respectively.

The amplitude for $e^-(h) + e^+(\bar{h}) \to \ell^-(h') + \ell^+(\bar{h}')$ may be labeled by the helicities of the particles as $\mathscr{M}_{h\bar{h}\to h'\bar{h}'}$ with $\{h, \bar{h}, h', \bar{h}'\} = \pm 1$ (or $\pm$ for short); these indicate the eigenvalues of the helicity operator, see App. C.4. For a given helicity configuration, the amplitude depends on the CM energy and on the scattering angle. It is convenient to decompose it in terms of partial waves of total angular momentum J in the limit of high energies via [363, 364]

$$\mathscr{M}_{h\bar{h}\to h'\bar{h}'}(\sqrt{s}, \cos\theta) = 16\pi \sum_{J=0}^{\infty} (2J+1)\, d^J_{\mu_i,\mu_f}(\theta)\, a^J_{h\bar{h}\to h'\bar{h}'}(\sqrt{s})\,. \tag{7.42}$$

Here $d^J_{\mu_i,\mu_f}(\theta)$ are the Wigner small-d functions with $\mu_i = \frac{1}{2}(h - \bar{h})$, $\mu_f = \frac{1}{2}(h' - \bar{h}')$ and $\mu_{i,f} = -J, -J+1, \cdots, J-1, J$ [365].

The generally complex coefficients $a^J_{h\bar{h}\to h'\bar{h}'}(\sqrt{s})$, the partial waves, may be expressed in terms of the amplitude as [363, 366]

$$a^J_{h\bar{h}\to h'\bar{h}'}(\sqrt{s}) = \frac{1}{32\pi}\int_{-1}^{1} d(\cos\theta)\, d^J_{\mu_i,\mu_f}(\theta)\, \mathscr{M}_{h\bar{h}\to h'\bar{h}'}(\sqrt{s}, \cos\theta)\,. \tag{7.43}$$

Limiting the number of particles in the intermediate states to two, the same as in $|i\rangle$ and $|f\rangle$, the real and imaginary parts of the partial wave (7.43) are bounded from above by [363, 364]

$$\mathrm{Re}\left(a^J_{h\bar{h}\to h'\bar{h}'}\right) \leq \frac{1}{2} \quad \text{and} \quad \mathrm{Im}\left(a^J_{h\bar{h}\to h'\bar{h}'}\right) \leq 1\,. \tag{7.44}$$

These are the unitarity bounds, from which the first inequality is the most useful, since tree-level amplitudes are real. If more than one amplitude contributes to a certain partial wave, the bounds above are applied to the (absolute value of the) largest eigenvalue.

These bounds are satisfied by the complete, renormalizable theory from which the non-perturbative amplitude is calculated. We are, however, pursuing a perturbative treatment, but we may still apply the bounds (7.44) to each term in the series expansion of the amplitude. If the tree-level amplitude violates unitarity and we know that a complete theory should respect it, we have an indication that higher-order terms must restore unitarity: the perturbative expansion in the coupling parameter is not reliable, since the lower-order terms are not a good approximation of the full amplitude. Thus, the bounds (7.44) represent limits on the perturbative unitarity and may be used to fix the range of validity of the parameters of an effective theory.

A classical example is the "Higgsless" EW theory. The scattering of longitudinal W bosons would violate unitarity at tree level – the four-point interaction amplitudes and s- and t-channel photon and Z-boson exchange grow as $\sim s/v_F^2$, where $v_F \approx 246$ GeV. Therefore,

in a "Higgsless" SM, perturbative unitarity would be violated in high energies [364,367]. If, however, a scalar Higgs boson with mass m_H is included, the added amplitudes with Higgs exchange exactly cancel and the aforementioned problem is avoided.

Moreover, taking other channels which proceed via Higgs exchange into account, the final amplitude turns out to be $\sim m_H^2/v_F^2$. Once again, applying Eq. (7.44) one finds that $m_H \lesssim 710$ GeV [368,369], thus providing an upper limit on the Higgs mass based on perturbative unitarity. Naturally, corrections at higher orders may also break the perturbative expansion [370]. A similar argument (at tree level) was responsible for the introduction of intermediate vector bosons in the context of the old Fermi theory of weak interactions [371]: above the Fermi scale new degrees of freedom – the massive W and Z bosons – were expected to emerge if (perturbative) unitarity was to be respected.

Let us move on to the case of interest, $e^- + e^+ \to \ell^- + \ell^+$ with $\ell \neq e$. Working in the ultra-relativistic regime, where $\sqrt{s} \gg m_\ell$, the leptons are essentially massless and in App. C.4 we construct the corresponding spinors, see Eq. (C.41), which are eigenvectors of the helicity operator with eigenvalues h. The leptons are propagating with the following angular parameters $\{\theta,\phi\}$: incoming $e^-(p_1,h)$ with $\{0,0\}$, incoming $e^+(p_2,\bar{h})$ with $\{\pi,\pi\}$, outgoing $\ell^-(p_3,h')$ with $\{\theta,0\}$ and outgoing $\ell^+(p_4,\bar{h}')$ with $\{\pi-\theta,\pi\}$. The amplitudes may thus be naturally labelled $\mathscr{M}_{h\bar{h}\to h'\bar{h}'}$. For $\ell \neq e$ only the s-channel diagrams contribute, see Figure 8, and the non-zero helicity amplitudes for pure QED, see Eq. (7.35), are

$$\mathscr{M}^{\text{QED}}_{+-\to+-} = \mathscr{M}^{\text{QED}}_{-+\to-+} = e^2(1+\cos\theta)\,, \tag{7.45}$$

$$\mathscr{M}^{\text{QED}}_{+-\to-+} = \mathscr{M}^{\text{QED}}_{-+\to+-} = e^2(1-\cos\theta)\,. \tag{7.46}$$

For the Z-mediated amplitude, see Eq. (7.37), neglecting the width of the Z boson and setting $z = \sqrt{s}/m_Z$, we have

$$\mathscr{M}^{\text{EW}}_{+-\to+-} = \frac{g_Z^2\left(g_V+g_A\right)^2 z^2(1+\cos\theta)}{4(1-z^2)} \xrightarrow[z\gg1]{} -\frac{g_Z^2\left(g_V+g_A\right)^2(1+\cos\theta)}{4}\,, \tag{7.47}$$

$$\mathscr{M}^{\text{EW}}_{-+\to-+} = \frac{g_Z^2\left(g_V-g_A\right)^2 z^2(1+\cos\theta)}{4(1-z^2)} \xrightarrow[z\gg1]{} -\frac{g_Z^2\left(g_V-g_A\right)^2(1+\cos\theta)}{4}\,, \tag{7.48}$$

$$\mathscr{M}^{\text{EW}}_{+-\to-+} = \mathscr{M}^{\text{EW}}_{-+\to+-} = \frac{g_Z^2(g_V^2-g_A^2)z^2\,(1-\cos\theta)}{4\left(1-z^2\right)} \xrightarrow[z\gg1]{} -\frac{g_Z^2(g_V^2-g_A^2)\,(1-\cos\theta)}{4}\,. \tag{7.49}$$

The KRLP-mediated amplitudes, Eqs. (7.39) and (7.41), have a more complex momentum structure involving $q_\mu = (p_1+p_2)_\mu = \sqrt{s}(1,0,0,0)$. With this, the longitudinal term becomes $(p_1+p_2)_\mu(p_1+p_2)_\nu = \text{diag}(s,0,0,0)$ and the PV helicity amplitudes read ($y = \sqrt{s}/m$)

$$\mathscr{M}^{\text{PV}}_{+-\to+-} = \mathscr{M}^{\text{PV}}_{-+\to-+} = \left(\frac{g^e_{\text{PV}}g^\ell_{\text{PV}}}{\Lambda^2}\right)\frac{m^2y^4(1+\cos\theta)}{2(1-y^2)} \xrightarrow[y\gg1]{} -\left(\frac{g^e_{\text{PV}}g^\ell_{\text{PV}}}{\Lambda^2}\right)\frac{s(1+\cos\theta)}{2}\,, \tag{7.50}$$

$$\mathscr{M}^{\text{PV}}_{+-\to-+} = \mathscr{M}^{\text{PV}}_{-+\to+-} = -\left(\frac{g^e_{\text{PV}}g^\ell_{\text{PV}}}{\Lambda^2}\right)\frac{m^2y^4(1-\cos\theta)}{2(1-y^2)} \xrightarrow[y\gg1]{} \left(\frac{g^e_{\text{PV}}g^\ell_{\text{PV}}}{\Lambda^2}\right)\frac{s(1-\cos\theta)}{2}\,, \tag{7.51}$$

and

$$\mathcal{M}^{\mathrm{T}}_{++\to++} = \mathcal{M}^{\mathrm{T}}_{--\to--} = \left(g^e_{\mathrm{T}} g^\ell_{\mathrm{T}}\right) \frac{2y^2(2+y^2)\cos\theta}{(1-y^2)} \underset{y\gg1}{\longrightarrow} -\left(g^e_{\mathrm{T}} g^\ell_{\mathrm{T}}\right) \frac{2s\cos\theta}{m^2}, \tag{7.52}$$

$$\mathcal{M}^{\mathrm{T}}_{++\to--} = \mathcal{M}^{\mathrm{T}}_{--\to++} = \left(g^e_{\mathrm{T}} g^\ell_{\mathrm{T}}\right) \frac{2y^4\cos\theta}{(1-y^2)} \underset{y\gg1}{\longrightarrow} -\left(g^e_{\mathrm{T}} g^\ell_{\mathrm{T}}\right) \frac{2s\cos\theta}{m^2}. \tag{7.53}$$

All other amplitudes are either identically zero in the s-channel or vanish in the ultra-relativistic limit. The QED and EW amplitudes are independent of the CM energy, whereas the KRLP-mediated amplitudes grow with $\sim s$. The physical reason behind this is two-fold. First we have that the fermion currents in QED and EW are conserved; for the PV and T currents this is not so, see Eqs. (7.4) and (7.5). The second is the much richer momentum structure of the KRLP propagator in comparison with its QED and EW counterparts. These two factors connected give rise to extra 4-momentum contributions in the amplitudes. Furthermore, in the high-energy limit, the KRLP mass is absent from the amplitudes involving PV vertices, but not from those with T vertices.

In the CM frame, the initial and final $\ell\bar{\ell}$ pairs have the same energies, moving with equal and opposite 3-momenta; the system has zero orbital angular momentum. Also, in the ultra-relativistic regime the spins are aligned parallel or anti-parallel to the particle's 3-momentum. Since the external states are composed of pairs of spin-1/2 fermions, we have total angular momentum (projection) $J = 0, 1$. For $J = 0$ we have $\mu_{i,f} = 0$ and only the helicities $\{h\bar{h}\} = \{++, --\}$ are compatible – the relevant amplitudes are $\mathcal{M}_{++\to++}$, $\mathcal{M}_{--\to--}$ and $\mathcal{M}_{++\leftrightarrow--}$. The allowed helicity combinations can be found only in the KRLP-mediated T amplitudes, see Eqs. (7.52) and (7.53), since the corresponding QED, EW and PV amplitudes are zero. However, using Eq. (7.43) with $J = 0$, for which $d^0_{0,0}(\theta) = 1$, we find that $a^{J=0}_{\mathrm{T}} = 0$. Therefore, no useful bounds on the PV and T couplings can be derived from perturbative unitarity in the sector $J = 0$.

The sector $J = 1$ is much richer, because now $\mu_{i,f} = 0, \pm1$. Let us start by the KRLP-mediated PV interaction. We already know that the sub-sector $\mu_{i,f} = 0$ does not contribute to the partial wave, but the sub-sectors $\mu_{i,f} = \pm1$ do – only amplitudes with initial and final states with helicities $\{h\bar{h}\} = \{+-, -+\}$ are relevant in this case. From Eq. (7.43) with $J = 1$ and using that $d^1_{1,1}(\theta) = d^1_{-1,-1}(\theta) = (1+\cos\theta)/2$ and $d^1_{1,-1}(\theta) = d^1_{-1,1}(-\theta) = (1-\cos\theta)/2$ the partial-wave matrix for the PV coupling, in the basis $\{+-, -+\}$, becomes

$$a^{J=1}_{\mathrm{PV}} \approx \frac{s}{48\pi}\left(\frac{g^e_{\mathrm{PV}} g^\ell_{\mathrm{PV}}}{\Lambda^2}\right)\begin{pmatrix} -1 & 1 \\ 1 & -1 \end{pmatrix}. \tag{7.54}$$

Applying Eq. (7.44) to the absolute value of the largest eigenvalue of $a^{J=1}_{\mathrm{PV}}$, we get

$$\left|\frac{g^e_{\mathrm{PV}} g^\ell_{\mathrm{PV}}}{\Lambda^2}\right| \leq \frac{12\pi}{s} = 3.8\times10^{-17}\,\mathrm{eV}^{-2}\left(\frac{\mathrm{GeV}}{\sqrt{s}}\right)^2. \tag{7.55}$$

Since we assumed very high energies, in particular $\sqrt{s} \gg m_Z$, the result above can be more simply stated as $|g^e_{\mathrm{PV}} g^\ell_{\mathrm{PV}}/\Lambda^2| \ll 4.6\times10^{-21}\,\mathrm{eV}^{-2}$. The PV coupling constant g^f_{PV} is dimensionless and we may as well assume it to be $\sim O(1)$, that is, we allow Λ to determine the

overall magnitude (and canonical dimension) of the PV coupling $g^f_{\rm PV}/\Lambda$. In this context the bound (7.55) may be converted into $\Lambda \geq 1.6\times 10^8\,\text{eV}\left(\frac{\sqrt{s}}{\text{GeV}}\right)$.

Finally, let us analyse the KRLP-mediated interactions involving T couplings that contribute to the sector $J=1$. As already mentioned, only the sub-sector $\mu_{i,f}=0$ with helicities $\{h\bar{h}\}=\{++,--\}$ is relevant and the QED and EW amplitudes are zero. Using Eqs. (7.52) and (7.53) together with $d^1_{0,0}(\theta)=\cos\theta$, we find that the partial-wave matrix in the basis $\{++,--\}$ is

$$a_{\rm T}^{J=1}\approx -\frac{s}{24\pi}\left(\frac{g^e_{\rm T}g^\ell_{\rm T}}{m^2}\right)\begin{pmatrix}1 & 1\\ 1 & 1\end{pmatrix}, \tag{7.56}$$

so that, taking the absolute value of the largest eigenvalue and imposing (7.44), we get

$$|g^e_{\rm T}g^\ell_{\rm T}|\leq 6\pi\left(\frac{m}{\sqrt{s}}\right)^2 = 1.9\times 10^{-17}\left(\frac{m}{\text{eV}}\right)^2\left(\frac{\text{GeV}}{\sqrt{s}}\right)^2. \tag{7.57}$$

Once more, the result above was obtained under the condition that $\sqrt{s}\gg m_Z$, and it can thus be translated into $|g^e_{\rm T}g^\ell_{\rm T}|\ll 2.3\times 10^{-21}\,(m/\text{eV})^2$.

Contrary to the PV case, here we are not allowed to assume $g^f_{\rm T}\sim O(1)$ in order to convert the limit above into a more direct limit on m. The reason is that $g^f_{\rm T}$ is the actual (dimensionless) coupling of the T interaction, see Eq. (7.3), that is used to establish the perturbative expansion that is ultimately constrained by unitarity. The PV interaction is parametrized not only by $g^f_{\rm PV}$, but by the (energy) parameter Λ in the combination $g^f_{\rm PV}/\Lambda$, and in this case we may assume that $g^f_{\rm PV}\sim O(1)$ and transfer the size of the PV interaction to Λ. This is not so for $g^f_{\rm T}$ and the KRLP mass m cannot be bounded independently.

7.2.3 Bhabha scattering

In Sec. 7.2.2.1 we stated the amplitudes and obtained limits on the PV and T couplings from perturbative unitarity. Now we move on to study the unpolarized differential cross section of Bhabha scattering mediated by KRLPs. Before stating the final result including the new interactions, let us first quote the expected background result from the SM, which includes photon- and Z-mediated tree-level diagrams as shown in Figure 8.

Working in the ultra-relativistic limit ($\sqrt{s}\gg m_e$), the unpolarized differential cross section from EW theory is [357]

$$\frac{d\sigma_{\rm SM}}{d(\cos\theta)}=\frac{\pi\alpha^2}{s}\left[|A(t)|^2\left(\frac{s}{t}\right)^2+|A(s)|^2\left(\frac{t}{s}\right)^2+\frac{1}{2}\left(|A_+|^2+|A_-|^2\right)\left(1+\frac{t}{s}\right)^2\right], \tag{7.58}$$

where $\alpha=e^2/4\pi\approx 1/137$ is the fine structure constant and

$$A(a)=1+\left(g_V^2-g_A^2\right)\xi(a)\quad\text{and}\quad A_\pm=1+\frac{s}{t}+\left(g_V\pm g_A\right)^2\left[\xi(s)+\frac{s}{t}\xi(t)\right] \tag{7.59}$$

with $\xi(a)=\frac{G_F}{\pi\alpha\sqrt{8}}\frac{am_Z^2}{(a-m_Z^2+im_Z\Gamma_Z)}$. Here $g_V=-1/2+2\sin^2\theta_W$ and $g_A=+1/2$ are the vector and axial couplings of the Z boson to fermions. The QED contribution is obtained from Eq. (7.58)

turning off purely EW effects, that is, by setting $g_V = g_A = 0$:

$$\frac{d\sigma_{\rm QED}}{d(\cos\theta)} = \frac{\pi\alpha^2(3+\cos^2\theta)^2}{2s(1-\cos\theta)^2}\,. \tag{7.60}$$

The total differential cross section is

$$\frac{d\sigma}{d(\cos\theta)} = \frac{d\sigma_{\rm SM}}{d(\cos\theta)} + \frac{d\sigma_\gamma^{{\rm PV},T}}{d(\cos\theta)} + \frac{d\sigma_{\rm Z}^{{\rm PV},T}}{d(\cos\theta)} + \frac{d\sigma^{{\rm PV},T}}{d(\cos\theta)}\,. \tag{7.61}$$

The first term is the SM result, Eq. (7.58). The second and third terms represent contributions from the interference of diagrams with KRLP exchange and diagrams with photon and Z-boson exchange, respectively. The fourth term is purely due to KRLP-mediated diagrams. The aforementioned unpolarized differential cross sections are given in App. C.3 and their general behaviors are summarized in Table 3.

Due to the non-conservation of the PV and T currents the longitudinal part of the KRLP propagator does not cancel, leading to extra energy factors in the amplitudes causing the (differential) cross sections to generally grow with the CM energy, see Table 3. This is in stark contrast with QED, where $d\sigma/d(\cos\theta) \sim 1/s$, see Eq. (7.60), thus creating an unexpected – and unobserved – excess in the number of events at higher energies. This would, in turn, convert into potentially strong bounds on the couplings of KRLPs to electrons and positrons.

	QED interf. PV	pure PV	QED interf. T	pure T
$m \ll \sqrt{s}$	$\sim (g^2/\Lambda^2)\alpha$	$\sim (g^4/\Lambda^4)s$	$\sim g^2\alpha/m^2$	$\sim g^4 s/m^4$
$m \gg \sqrt{s}$	$\sim (g^2/\Lambda^2)\alpha s/m^2$	$\sim (g^4/\Lambda^4)s^3/m^4$	$\sim g^2\alpha s/m^4$	$\sim g^4 s/m^4$

Table 3 – Behavior of the differential cross sections for PV and T couplings as a function of m and $\sqrt{s}$ for the limiting cases of $m \ll \sqrt{s}$ and $m \gg \sqrt{s}$. Angular factors are omitted and the couplings are stripped of super- and subscripts for notational clarity, being denoted simply by g. The interference terms with the Z-mediated diagrams follow the same patterns as the interference with QED for both PV and T couplings.

7.2.3.1 Limits from deviations from pure QED

Particularly interesting for our purposes is the analysis from Ref. [357] reporting on dedicated Bhabha measurements at $\sqrt{s} = 29$ GeV in the angular range $|\cos\theta| < 0.55$ performed with the high resolution spectrometer at the PEP e^+e^- storage ring facility at SLAC. One of their main results is the determination of upper bounds on deviations of the data from the predictions of QED (at 95% CL):

$$\left|\frac{d\sigma/d(\cos\theta)}{d\sigma_{\rm QED}/d(\cos\theta)} - 1\right| \lesssim \frac{3s}{E^2_{\text{cut-off}}} \tag{7.62}$$

with $E_{\text{cut-off}} \approx 200$ GeV. This relation may be used to constrain new physics (see e.g. Refs. [372–375]), since the left-hand side is the ratio of the differential cross sections due to new physics

relative to that of QED, see Eq. (7.60). We thus have

$$\left| \frac{d\sigma_\gamma^{\mathrm{PV},T}/d(\cos\theta) + d\sigma^{\mathrm{PV},T}/d(\cos\theta)}{d\sigma_{\mathrm{QED}}/d(\cos\theta)} \right| \lesssim 0.063\,. \tag{7.63}$$

Typically, one would neglect the pure PV or T contribution in comparison with the respective interference term with photon-mediated diagrams based on the powers of the coupling constant. However, the differential cross sections are relatively complex functions of the KRLP mass and there may be values of the KRLP couplings and mass for a given energy that violate our intuition. We thus choose to keep the pure PV or T contributions and numerically evaluate the constraint (7.63). The 95%-CL upper bounds on the parameters of the KRLP-mediated interactions are shown in Figure 9, labelled "pure QED". For the bounds we use $\cos\theta = -0.3$, maximizing the bound for PV couplings; the results for T couplings are rather insensitive to the angle chosen.

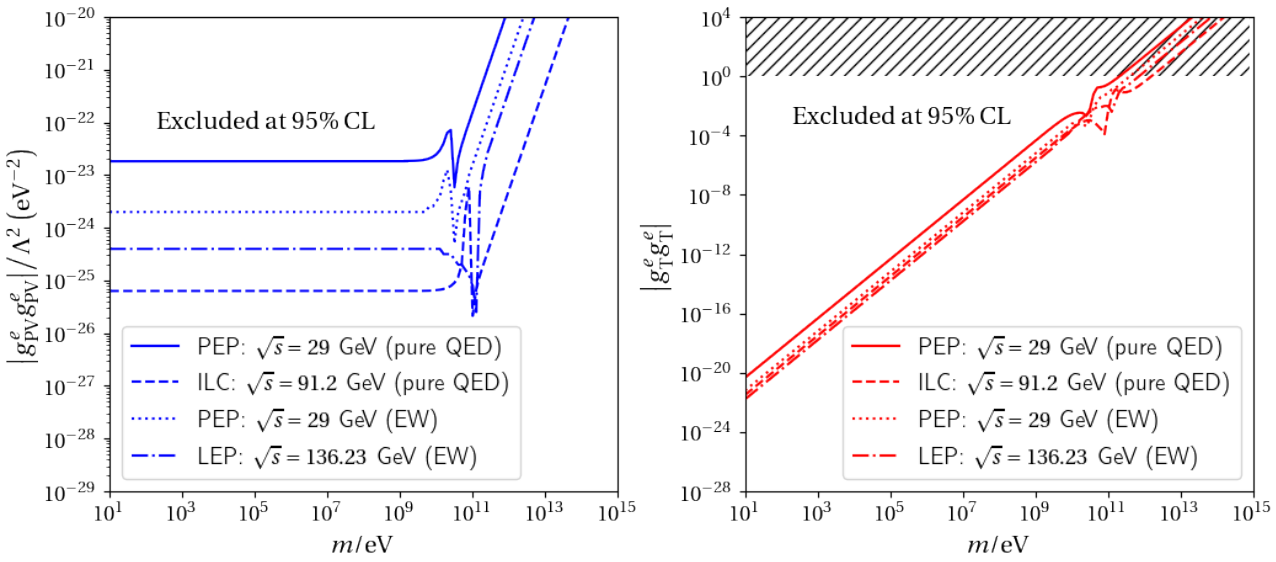

Figure 9 – Constraints on PV and T couplings of KRLPs from Bhabha scattering. The bounds obtained by using upper limits for deviations from pure QED are from PEP and the ILC (projected), both labelled "pure QED", see Sec. 7.2.3.1. For the data from PEP we used $\sqrt{s} = 29$ GeV [357], whereas for the projected sensitivities for the ILC we used $\sqrt{s} = m_Z$ [377]. For both we set $\cos\theta = -0.3$. The remaining bounds were extracted using experimental data at various angles from PEP and LEP, see Sec. 7.2.3.2, at $\sqrt{s} = 29$ GeV [357] and $\sqrt{s} = 136.23$ GeV [376], respectively. All bounds are at 95% CL. The hatched region in the right panel is excluded since there $|g^e_{\mathrm{T}} g^e_{\mathrm{T}}| \gtrsim O(1)$ and the perturbative treatment becomes meaningless.

A few features displayed by the bounds in Figure 9 are noteworthy. First is the change in slope of the bound for the PV couplings, as could be anticipated from Table 3. In the region $m \lesssim \sqrt{s}$ the PV differential cross sections are independent of m, leading to the plateau dominated by the QED interference. Moving towards larger masses, the pure PV term is suppressed and the bound relaxes after passing by $m = \sqrt{s}$, since now Eq. (C.30) behaves as $\sim y^2 = s/m^2$; the bound becomes $|g^e_{\mathrm{PV}} g^e_{\mathrm{PV}}/\Lambda^2| \sim m^2$.

For the T couplings the situation is different. For $m \lesssim \sqrt{s}$ the pure-T differential cross section is enhanced by s/m^4, thus compensating the higher order in the coupling constants relative to the QED interference term – the bound then goes as $|g_{\rm T}^e g_{\rm T}^e| \sim m^2$. Around $m \approx \sqrt{s}$ the bound reaches $|g_{\rm T}^e g_{\rm T}^e| \sim O(1)$ and, going further, the high-mass region lies in the range $|g_{\rm T}^e g_{\rm T}^e| \gtrsim O(1)$. This is problematic: the theory becomes strongly coupled and a perturbative treatment as the one undertaken here is no longer justified. Therefore, the bounds above are not reliable for $|g_{\rm T}^e g_{\rm T}^e| \gtrsim O(1)$ – this is indicated in Figure 9 by the hatched region.

Future lepton colliders, such as the International Linear Collider (ILC) [377] and other "Higgs factories" [378], will operate at much higher energies with improved precision. Also at the ILC Bhabha scattering at small angles – as low as $|\cos\theta| = 0.996$ – will play a central role in the calibration of cross-section measurements. The ILC is planned to reach $\sqrt{s} = 500$ GeV, but luminosity measurements will be particularly critical during its Giga-Z phase at $\sqrt{s} = m_Z$, where an enhancement in the number of Bhabha events is expected. The target precision in the determination of the number of such events, and consequently also of the (differential) cross section, is 0.1%. Setting twice this value as the upper bound on deviations from pure QED to reach 95% CL we obtain the projected bounds shown in Figure 9.

7.2.3.2 Limits from electroweak data at $\sqrt{s} = 29$ GeV and 136.23 GeV

A complementary possibility to constrain KRLP-mediated interactions with Bhabha scattering at the GeV scale is to go beyond QED and analyse the full tree-level EW contributions. The SM result (7.58) fits well all data so far and deviations caused by the KRLP-mediated interactions will appear as small corrections that must generally fit within experimental error.

In order to extract bounds on the PV and T couplings and the KRLP mass we will perform simple chi-squared analyses of differential cross section data available from lepton colliders. We scan the parameter space and search for the minimum of

$$\chi^2 = \sum_{i=1}^{N} \frac{\left[y^i_{\rm obs} - y^i_{\rm Th}\right]^2}{\delta y^2}, \tag{7.64}$$

where y stands for $d\sigma/d\cos\theta$, "obs" and "th" label the observed quantities and the theoretical values obtained using Eq. (7.61), respectively, N is the number of data points and δy_i are the associated experimental errors. We use the data sets available in Table XII of Ref. [357] at $\sqrt{s} = 29$ GeV for $|\cos\theta| \leq 0.525$ with $N = 22$ and Table 2 of Ref. [376] at $\sqrt{s} = 136.23$ GeV for $|\cos\theta| \leq 0.9$ with $N = 9$. In Ref. [357] the polar angles are quoted as the central value of the respective bins; in contrast, in Ref. [376] the bins are given and we have used the respective central values. In evaluating Eq. (7.64) we assume the SM parameters $\{\alpha, m_Z, \Gamma_Z, \sin^2\theta_W\}$ to be fixed and given by their latest accepted values [39].

Following Table 40.2 of Ref. [39], we set 95%-CL limits on $\{g_{\rm PV}^e g_{\rm PV}^e/\Lambda^2; m\}$ and $\{g_{\rm T}^e g_{\rm T}^e; m\}$ by identifying the parameters that satisfy $\chi^2 - \chi^2_{\rm min} = 5.99$. We find: $\chi^2_{\rm min}/N_{\rm dof} = 1.12$ for PV and $\chi^2_{\rm min}/N_{\rm dof} = 1.14$ for T at $\sqrt{s} = 29$ GeV [357], and $\chi^2_{\rm min}/N_{\rm dof} = 3.74$ for PV and $\chi^2_{\rm min}/N_{\rm dof} = 4.13$ fot T at $\sqrt{s} = 136.23$ GeV [376], where $N_{\rm dof} = N - 2$. The ensuing 95%-CL bounds are shown in

Figure 9, labeled "EW", together with those from deviations of pure QED, see Sec. 7.2.3.1, where visible improvements over the latter are achieved.

7.3 Final considerations

In this work we analysed the phenomenological impact of a neutral and massive spin-1 boson expressed as an antisymmetric rank-2 tensor coupled to pseudovector and tensor fermionic currents. Since these fundamentally differ from the usual vector current from electromagnetism or the V-A current from the electroweak interactions, we can expect that KRLPs would induce distictive signals that could be experimentally probed. Furthermore, despite the dualities relating it to ALPs and HPs, particular in the massless case, a massive and interacting KRLP is physically distinct due to its parity-transformation properties, as well as the fact that the couplings of the fundamental field and its field-strength tensor to fermions is different than those of ALPs or HPs. These features plainly justify the investigation of KRLPs and their phenomenology.

We studied a variety of systems and processes including KRLPs as small perturbations and analysed how well–measured observables would be affected. In Figure 10 we display the bounds – all at 95% CL, except those from unitarity – in case the couplings of the KRLPs to fermions are universal, that is, they are independent of the fermion species: $g^f_{\mathrm{PV},T} = g_{\mathrm{PV},T}$. In general, we found that the scattering amplitudes including KRLPs contain extra factors of the 4-momenta, implying that these amplitudes will be enhanced at high energies. This is visible in Figure 10, where the bounds from spectroscopy at energy scales $\sim 1/a_0 \sim O(\mathrm{KeV})$ are, despite the outstanding precision in the associated measurements, weaker than those from collider experiments at $\sqrt{s} \sim O(\mathrm{GeV})$. In fact, the strongest bounds are obtained from LEP data at $\sqrt{s} = 136.23$ GeV [376], displayed as solid blue (PV) and red (T) lines.

The next generation of lepton colliders may further improve our bounds, since we observed that the differential cross sections generally increase with the CM energy. Incidentally, this feature is already manifest in the bounds from perturbative unitarity, Eqs. (7.55) and (7.57), showing how the allowed range for the couplings must decrease with s to safeguard unitarity. In Sec. 7.2.3 we also obtained the projected bounds from the ILC at $\sqrt{s} = m_Z$, shown in dashed lines in Figs. 9 and 10. These are stronger than those from LEP due to the improved detection precision of Bhabha events.

There are several proposals for e^-e^+ colliders besides the ILC: FCC-ee [379], CEPC [380], CCC [381] and CLIC [382]; also for $\mu^-\mu^+$ colliders [383]. These are primarily designed as Z-boson and Higgs factories for precision tests of EW physics. Making the simplifying assumption of coupling universality and $m \ll \sqrt{s}$, from Eqs. (7.60) and (7.62) and using Eqs. (C.30) and (C.35), we see that

$$\frac{g_{\mathrm{PV}}}{\Lambda} \lesssim 4 \times 10^{-11}\,\mathrm{eV}^{-1} \left(\frac{\delta}{0.1\%}\right)^{1/2} \left(\frac{\mathrm{GeV}}{\sqrt{s}}\right), \tag{7.65}$$

$$g_{\rm T} \lesssim 9 \times 10^{-11} \left(\frac{m}{\rm eV}\right) \left(\frac{\delta}{0.1\%}\right)^{1/4} \left(\frac{\rm GeV}{\sqrt{s}}\right), \tag{7.66}$$

where δ is the expected precision in the determination of Bhabha events – these are rough numerical values not taking into account angular factors and EW corrections. Clearly, smaller δ only mildly improves the bounds and higher energies offer optimal leverage and we expect that, if these proposals come to fruition, stronger limits will be derived.

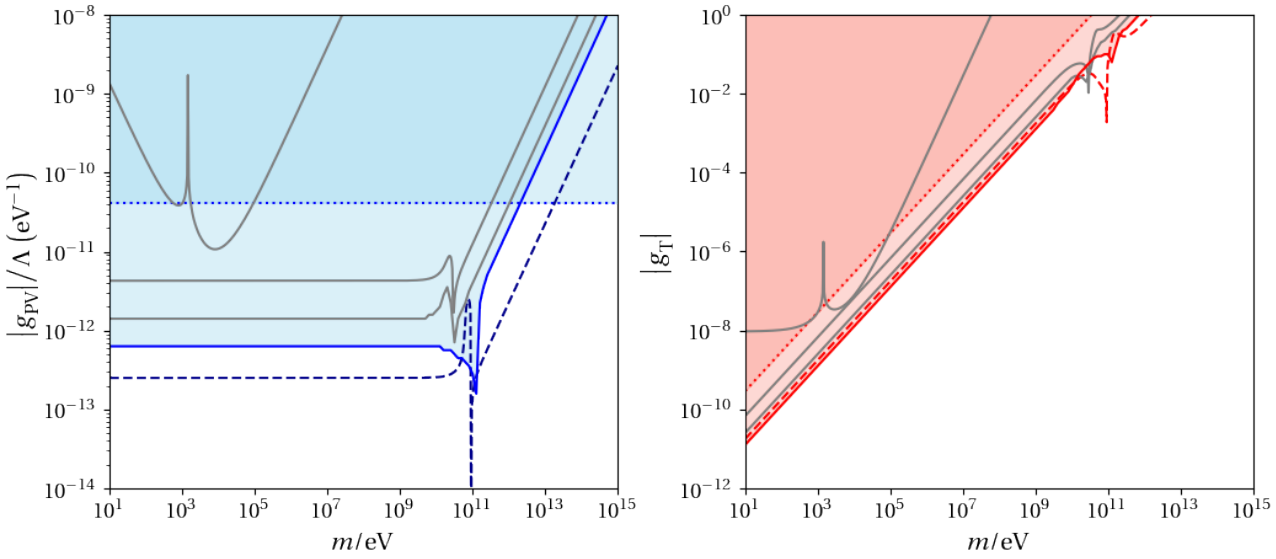

Figure 10 – Excluded regions in parameter space for KRLP-mediated interactions assuming that the couplings are independent of the fermion species. The solid lines and the colored regions correspond to the strongest bounds (at 95% CL) coming from Bhabha scattering at $\sqrt{s} = 136.23$ GeV, see Sec. 7.2.3.2. The projections for Bhabha scattering at the ILC are shown as the dashed lines, see Sec. 7.2.3.1. The bounds from perturbative unitarity, see Sec. 7.2.2.2, are shown as dotted lines; the limit from spectroscopy is also shown in grey for completeness. Above $|g_{\rm T}| \sim O(1)$ the bounds on the right panel are unreliable.

As a closing remark, let us briefly discuss other portals of KRLPs to SM degrees of freedom. Here we assigned a Proca-like mass to the KRLP, see Eq. (7.1), but this is not the only option. Another possibility is a massless KRLP: in this case the solution to the equations of motion $\partial_\mu H^{\mu\nu\lambda} = 0$ is $H^{\mu\nu\lambda} = \epsilon^{\mu\nu\lambda\kappa}\partial_\kappa a$, where a is a pseudoscalar field, akin to the string-motivated axion [298]. The fundamental field of the theory is now a, not $B_{\mu\nu}$ and the kinetic term in the action (7.1) turns into the usual one for a spin-0 field and the interactions with fermions, for example through the PV current, see Eq. (7.3), involve the dual field-strength tensor $\tilde{H}_\mu \sim \partial_\mu a$, similar to the case of massless axions coupled to electrons [324]. The associated phenomenology will therefore differ from the one analysed here.

Alternatively, we may keep a massive KRLP, but model the mass term differently: instead of the Proca term that does not allow for gauge invariance, we introduce a Chern-Simons-like term [**?**] $\sim m\epsilon^{\mu\nu\alpha\beta} A_\mu \partial_\nu B_{\alpha\beta}$, where $B_{\alpha\beta}$ is the KR field and A_μ is an Abelian field. This topological term is gauge invariant and the pair $\{A_\mu, B_{\alpha\beta}\}$ carries three degrees of freedom, describing a massive spin-1 field. This scenario has been studied in different contexts: spin-dependent

interactions [333], cosmic strings [384], dark electrodynamics [385], dualities between Stueckelberg and BF gauge theories [308, 386] and scenarios with Lorentz-symmetry violation [387]. In this topological formulation the KR field is coupled to a 4-potential, usually associated with the photon, but this is not an absolute requirement: for example, in Ref. [272] the authors study dark fermions with a portal to the $U_Y(1)$ sector of the SM via dipole couplings (see also Ref. [273]). If we use the weak hypercharge field Y_μ instead of the electromagnetic 4-potential A_μ, the topological term becomes $m\epsilon^{\mu\nu\alpha\beta}\, Y_\mu \partial_\nu B_{\alpha\beta}$ retaining the EW gauge invariance and, through the mixing of mass eigenstates, resulting in $m\epsilon^{\mu\nu\alpha\beta}\left(\cos\theta_W A_\mu - \sin\theta_W Z_\mu\right)\partial_\nu B_{\alpha\beta}$. We thus generate a direct coupling not only to the photon, but also to the Z boson. The theoretical and phenomenological aspects of this topic will be addressed elsewhere.

Part III

What comes next?

Chapter

8

Conclusive considerations and perspectives

We conclude this thesis with some general remarks and criticisms about the works developed, and we outline a few perspectives for future research. We emphasize that the conclusions and possible continuations of each study carried out throughout the thesis were already properly presented in the corresponding Chapters. This final part is divided into two sections. In the first one, we discuss perspectives related to LSV, while in the second we present ideas concerning particle physics beyond the SM.

8.1 On Lorentz-symmetry Violation

First of all, it is important to emphasize that no unambiguous or decisive experimental evidence for LSV has been found so far. Perhaps the most promising signals in this direction are possible deviations in the propagation speeds of light and neutrinos in vacuum due to modified dispersion relations, as discussed and referenced in Chapter 6. Such effects could be related to gravitational phenomena and also to LSV.

However, all these possibilities must be treated with great caution. The Data Tables reporting limits on several Lorentz-violating parameters within the SME framework show extremely small bounds, with some coefficients appearing to be consistent with zero [76]. Even so, many efforts based on high-precision experiments and sophisticated astrophysical observations have been devoted to testing these ideas, as discussed throughout Chapter 2. Therefore, LSV cannot yet be ruled out as a possible route to physics beyond the Standard Model and as a potential path toward quantum gravity.

From an aesthetic point of view, giving up relativistic invariance, even only in an active sense, may seem unnatural or unattractive. However, the idea of exact symmetries in nature appears to work mainly as a human abstraction. Symmetries serve as a starting point to organize, parametrize, and give structure to the fundamental building blocks of a theoretical description of a given sector of nature, as is the case for internal gauge symmetries for example. The real world, however, seems to be less ordered and may be described only by approximate symmetries. The history of physics strongly supports this view. Therefore, there is no clear reason to believe that spacetime symmetries should be immune to such

imperfections of nature when we look at smaller and smaller scales. For this reason, there is no fundamental argument to rule out LSV from the outset, and the search for LSV should continue until clear experimental or theoretical evidence completely excludes this possibility. In the author's view, such a complete exclusion seems unlikely. In the early Universe, when space and time themselves were being formed, the absence of exact invariance appears to be natural. It is therefore reasonable to ask whether some effects from that era could have survived until the present day. In this sense, the search for LSV remains well motivated and should be pursued.

In an attempt to continue contributing to this search, some additional works that were not included in this thesis are currently under development. For example, we have investigated how the inclusion of the CFJ term in the Maxwell electromagnetic action affects the magnetostatics of the magnetic field produced by a solenoid. In this context, we have analyzed the consequences of the Lorentz-violating parameter k_{AF} on the magnetic flux and its implications for the Aharonov–Bohm effect. We have also studied interparticle potentials in scenarios where the fermion sector is affected by a Lorentz-violating term of the form $b_\mu \gamma^\mu \gamma_5$. This modification changes the role of the electromagnetic current in scattering processes and leads to distinct and interesting effects depending on whether the background vector b_μ is timelike, spacelike, or lightlike.

As future work, we plan to explore the fact that Lorentz symmetry and its violation are well-established experimental features in condensed matter systems. Recently, excitations corresponding to a spin-3/2 mode have been reported in Rarita–Schwinger–Weyl $(2+1)$D semimetals [391, 392]. Following an approach similar to that of Ref. [393], where $(2+1)$D Weyl semimetals were described using $(3+1)$D fermions in the presence of a privileged direction—allowing for a better description of the tilt of the Dirac cone and of chiral symmetry breaking—we intend to develop a closely related formulation. In our case, we aim to describe Rarita–Schwinger–Weyl semimetals in $(2+1)$D using Rarita–Schwinger fermions in $(3+1)$D and to investigate the resulting effects on the Dirac cone, which determines the band structure of these materials.

Since the Rarita–Schwinger field has been mentioned, one may also consider a formulation of supergravity in which a gauge theory for spin-3/2 fields is realized through the introduction of supersymmetry and their interaction with the gravitational field [394, 395]. In this framework, it would be possible to integrate out the Rarita–Schwinger fermions, in a way similar to what was done in Chapter 4, in order to obtain a purely gravitational effective theory. Such a theory would contain contributions to graviton–graviton scattering, playing the role of a gravitational analogue of the Euler–Heisenberg effective action. Within this perspective, one could also consider the inclusion of Lorentz-symmetry-violating terms in the Rarita–Schwinger fermion sector and study how this symmetry breaking manifests itself in the resulting effective description of gravity.

8.2 On particle physics beyond the Standard Model

Many proposals involving new particle spectra and anomalies beyond the SM have been presented in recent years [40]. These ideas aim to address some of the main problems of the Standard Model discussed in Chapter 1, as well as to explain the dark matter content of the Universe. However, experimental results and observational data have so far shown a strong consistency with the Standard Model [40]. As a consequence, the international physics community has mainly been able to place exclusion limits on the parameter spaces of these new fields, rather than obtain direct evidence for new physics [40]. This is the case in our work [] related to Chapter 7.

One of the great successes of the SM, besides placing our understanding of the fundamental interactions on solid ground, was its ability to predict new particles and later confirm them with high precision. This experience gives us confidence that particle physics is a valid and serious path to search for new physics, even though there have been many negative results along the way, such as in the case of supersymmetric particles. However, there are still very promising candidates. This is the case for particles generically called axions. These can be classified as QCD axions (see Chapter 1) or as axion-like particles (ALPs), which naturally appear in many effective field theory scenarios [396–402]. Another important candidate is the so-called dark photon. This particle is a vector boson that acts as a mediator of a new symmetry group, $U(1)_{\text{Dark}}$, with no direct relation to the interactions of the SM. The idea is that this new gauge boson, similar to the photon, can interact with SM particles through kinetic mixing in the action. This mechanism was first introduced in the context of supersymmetry [403, 404] and was later generalized. A clear introduction to dark photon physics can be found in the book [405], and several excellent reviews are available in Refs. [406, 407]. Axion-like particles and dark photons currently play a central role in the search for new particles beyond the SM.

In this direction, we are currently developing works involving axions with kinetic mixing with the ordinary photon, and also a scenario in which an axion mediates kinetic mixing between dark photons and ordinary photons. We study the mixing matrices of both models after linearization in the presence of a strong external magnetic background. Within this framework, we derive the modified propagators of the theory, as well as the mixed propagators. Using these results, we discuss the possibility of particle transitions such as photon–axion, axion–dark photon, and photon–dark photon transitions mediated by the axion, which acts as a portal between the ordinary sector and the dark sector. This type of particle conversion is known as the Primakoff effect. We also investigate how this linearized scenario in a strong magnetic background leads to optical effects in vacuum, which can be compared with recent experimental results.

For the future, we intend to revisit the Maxwell electrodynamics in the presence of axions, incorporating higher-order derivative effects in two distinct scenarios: modifications in the photon kinetic sector and radiative corrections to the Axion-Photon coupling. We can also

propose to jointly investigate the effects of LSV and axion physics in three frameworks: through the k_F term in the CPT-even sector of the Standard-Model Extension; by modifying the axion kinetic term via $(\eta_{\mu\nu} + c_{\mu\nu})(\partial^\mu a)(\partial^\nu a)$; and by including LSV directly in the Axion-Photon-Photon interaction vertex. Our models can be applied to a range of phenomenological scenarios: studies of modified dispersion relations, associated optical properties, vacuum birefringence effects under background magnetic fields, stability and unitarity analyses, and the Axion-Photon transition. Unifying axions and LSV in a single action may, at first glance, seem like an arbitrary combination of effects. However, this approach seeks to understand how the parameters associated with these sectors mutually influence each other in the presence of external electric and magnetic fields. This entire effort will be contextualized in light of current experiments such as ALPS I and II, ATLAS, CMS, PVLAS, among others, allowing for the imposition of relevant phenomenological constraints. Furthermore, both axion-like excitations and LSV effects are present in condensed matter systems, strengthening the experimental relevance of this study. Additionally, both topics have deep implications in Cosmology and Astrophysics.

Appendix

A

Auxiliary results for the derivation of effective actions

A.1 Conventions for the Wick rotation

The calculation of the effective action performed in Chapter 4 is well defined in Euclidean space, $\mathbb{E}^4$. In this Appendix, we summarize the conventions adopted and the corresponding relations used to implement the Wick rotation from Minkowski spacetime, $\mathbb{M}^{1,3}$, with metric tensor $\eta_{\mu\nu} = \text{diag}(1,-1,-1,-1)$, to Euclidean space $\mathbb{E}^4$, endowed with the metric $\hat{g}_{\mu\nu} = -\delta_{\mu\nu}$. In $\mathbb{M}^{1,3}$, Greek indices run over $\mu,\nu = (0,1,2,3)$, whereas in $\mathbb{E}^4$ they run over $\mu,\nu = (1,2,3,4)$.

At the outset, the conventions adopted for the Wick rotation affect the coordinates x^μ, the partial derivatives ∂_μ, and the four-vectors v^μ defined in $\mathbb{M}^{1,3}$. The correspondence between these quantities in $\mathbb{M}^{1,3}$ and their counterparts in $\mathbb{E}^4$ is given, respectively, by

$$\{x^0 \to -i\hat{x}_4, \quad x^i \to \hat{x}_i\}, \tag{A.1}$$

$$\{\partial_0 \to i\hat{\partial}_4, \quad \nabla_i \to \hat{\nabla}_i\}, \tag{A.2}$$

$$\{v^0 \to -i\hat{v}_4, \quad v^i \to \hat{v}_i\}, \tag{A.3}$$

where the bar denotes quantities defined in Euclidean space. These definitions imply that the scalar product of four-vectors is transformed in the following manner

$$u_\mu v^\mu \to -\hat{u}_\mu \hat{v}^\mu, \tag{A.4}$$

$$\partial_\mu v^\mu \to \hat{\partial}_\mu \hat{v}^\mu. \tag{A.5}$$

For the Dirac gamma matrices, we adopt the following conventions:

$$\{\gamma^i \to i\hat{\gamma}^i; \quad \gamma^0 \to \hat{\gamma}^4\}, \tag{A.6}$$

with the Euclidean gamma matrices taken to be Hermitian, i.e., $\hat{\gamma}^{i\dagger} = \hat{\gamma}^i$ and $\hat{\gamma}^{4\dagger} = \hat{\gamma}^4$. The consequences of these conventions for the Clifford algebra are

$$\{\gamma^\mu,\gamma^\nu\} = 2\eta^{\mu\nu} \to \{\hat{\gamma}^\mu,\hat{\gamma}^\nu\} = 2\hat{g}^{\mu\nu} = -2\delta^{\mu\nu}. \tag{A.7}$$

In this case, the matrix γ_5 transforms accordingly as

$$\gamma_5 = -i\gamma^0\gamma^1\gamma^2\gamma^3 \to \hat{\gamma}^1\hat{\gamma}^2\hat{\gamma}^3\hat{\gamma}^4 = \hat{\gamma}_5. \tag{A.8}$$

It is straightforward to verify that $\hat{\gamma}_5$ is Hermitian, $\hat{\gamma}_5^\dagger = \gamma_5$. The contraction of gamma matrices with the derivative operator and an arbitrary four-vector follows the rules

$$\gamma^\mu \partial_\mu \to i\hat{\gamma}^\mu \hat{\partial}_\mu, \tag{A.9}$$

$$v_\mu \gamma^\mu \to -i\hat{v}_\mu \hat{\gamma}^\mu. \tag{A.10}$$

Finally, we show how the components of the Lorentz group generator $\Sigma^{\mu\nu} = \frac{i}{4}[\gamma^\mu, \gamma^\nu]$ transform according to the prescriptions above. This yields

$$\Sigma^{0i} \to i\hat{\Sigma}^{4i}, \quad \Sigma^{ij} \to -\hat{\Sigma}^{ij}. \tag{A.11}$$

Thus, the contraction of two arbitrary four-vectors u_μ and v_ν with $\Sigma^{\mu\nu}$ transforms as

$$u_\mu v_\nu \Sigma^{\mu\nu} \to -\hat{u}_\mu \hat{v}_\nu \hat{\Sigma}^{\mu\nu}. \tag{A.12}$$

For the electromagnetic field-strength tensor, we have

$$F_{0i} \to -i\hat{F}_{4i}, \quad F^{ij} \to -\hat{F}^{ij}, \tag{A.13}$$

which implies that $F_{\mu\nu}^2 = \hat{F}_{\mu\nu}^2$.

To determine the correspondence for terms involving the dual electromagnetic field-strength tensor, it is necessary to examine how the four-dimensional Levi-Civita symbol transforms. We adopt the conventions $\varepsilon^{0123} = +1$ and $\varepsilon_{0123} = -1$ for the Levi-Civita symbol in Minkowski spacetime. Under the Wick rotation, the corresponding relations in Euclidean space are

$$\varepsilon^{0123} = +1 \to i\hat{\varepsilon}^{1234} = +i, \tag{A.14}$$

$$\varepsilon_{0123} = -1 \to -i\hat{\varepsilon}_{1234} = -i. \tag{A.15}$$

With these definitions of the Levi-Civita symbol, we can establish the mapping of the dual field-strength tensor, $\tilde{F}^{\mu\nu} = \frac{1}{2}\varepsilon^{\mu\nu\kappa\lambda}F_{\kappa\lambda}$, from Minkowski spacetime $\mathbb{M}^{1,3}$ to Euclidean space $\mathbb{E}^4$. In particular, the components transform as

$$\tilde{F}_{0i} \to -\hat{\tilde{F}}_{4i}, \quad \tilde{F}_{ij} \to -i\hat{\tilde{F}}_{ji}. \tag{A.16}$$

From these relations, it follows that $\tilde{F}_{\mu\nu}F^{\mu\nu} \to i\hat{\tilde{F}}_{\mu\nu}\hat{F}^{\mu\nu}$. We can also determine the correspondence of contractions involving the Lorentz generators $\Sigma^{\mu\nu}$ and the tensors $F_{\mu\nu}$ and $\tilde{F}_{\mu\nu}$:

$$\Sigma^{\mu\nu}F_{\mu\nu} \to \hat{\Sigma}^{\mu\nu}\hat{F}_{\mu\nu}, \tag{A.17}$$

$$\Sigma^{\mu\nu}\tilde{F}_{\mu\nu} \to -i\hat{\Sigma}^{\mu\nu}\hat{\tilde{F}}_{\mu\nu}. \tag{A.18}$$

Finally, according to these conventions, the components of the covariant derivative $D_\mu = \partial_\mu + ieA_\mu$ transforms as

$$\{D_0 \to i\hat{D}_4, \quad D_i \to \hat{D}_i\}. \tag{A.19}$$

Thus, contractions involving covariant derivatives take the form

$$\gamma^\mu D_\mu \to i\hat{\gamma}^\mu \hat{D}_\mu, \tag{A.20}$$

$$D_\mu v^\mu \to \hat{D}_\mu \hat{v}^\mu. \tag{A.21}$$

These are the main conversions from Minkowski spacetime to Euclidean space adopted in this work. The same relations can be applied in reverse to rewrite the effective actions in Sections 6.2 and in Minkowski spacetime. These conventions were also used to express the quadratic photon-field action in Sections and 6.3 in Minkowski spacetime.

A.2 Proper-time integrals

In the calculations of the effective actions presented in Chapter 4, we implement the following proper-time integrals:

$$I_1 = \int ds\, e^{-sm^2/\mu^2} = \frac{\mu^2}{m^2}; \tag{A.22}$$

$$I_2 = \int ds\, e^{-sm^2/\mu^2} s = \frac{\mu^4}{m^2}; \tag{A.23}$$

$$I_3 = \int ds\, e^{-sm^2/\mu^2} s^2 = \frac{2\mu^6}{m^6}; \tag{A.24}$$

$$I_4 = \int ds\, e^{-sm^2/\mu^2} \frac{1}{s} = -\frac{1}{\epsilon_{\text{div}}} - \ln\left(\frac{m^2}{\mu^2}\right) + \gamma_E; \tag{A.25}$$

$$I_5 = \int ds\, e^{-sm^2/\mu^2} \frac{1}{s^2} = -\frac{m^2}{\mu^2}\left[\frac{1}{\epsilon_{\text{div}}} + \ln\left(\frac{m^2}{\mu^2}\right) + 1 - \gamma_E\right]. \tag{A.26}$$

The proper-time integrals over s are performed in the interval $(-\infty, +\infty)$, γ_E denotes the Euler–Mascheroni constant, and ϵ_{div} is the divergence regulator introduced in dimensional regularization, which is ultimately taken to zero. We also encountered terms containing integrations over two proper-time variables:

$$I_6 = \int d\tau \int ds\, e^{-(\tau+s)m^2/\mu^2} \frac{s}{(s+\tau)^2} = \frac{\mu^2}{2m^2}; \tag{A.27}$$

$$I_7 = \int d\tau \int ds\, e^{-(\tau+s)m^2/\mu^2} \frac{\tau}{(s+\tau)^2} = I_6; \tag{A.28}$$

$$I_8 = \int d\tau \int ds\, e^{-(\tau+s)m^2/\mu^2} \frac{s^2}{(s+\tau)^2} = \frac{\mu^2}{3m^2}; \tag{A.29}$$

$$I_9 = \int d\tau \int ds\, e^{-(\tau+s)m^2/\mu^2} \frac{\tau^2}{(s+\tau)^2} = I_8; \tag{A.30}$$

$$I_9 = \int d\tau \int ds\, e^{-(\tau+s)m^2/\mu^2} \frac{s\tau}{(s+\tau)^2} = \frac{I_8}{2}; \tag{A.31}$$

$$I_{10} = \int d\tau \int ds\, e^{-(\tau+s)m^2/\mu^2} \frac{1}{(s+\tau)^2} = -\frac{m^2}{\mu^2}\left[\frac{1}{\epsilon_{\text{div}}} + \ln\left(\frac{m^2}{\mu^2}\right) + 1 - \gamma_E\right]. \tag{A.32}$$

Appendix

B

Results on SUSY with LSV

B.1 The alternative case of a vector superfield

In this Appendix, we show the result of supersymmetrization following the second approach cited in the Section 5.2.3, in which we define a vector superfield in the form

$$V = C + \theta\zeta + \bar{\theta}\bar{\zeta} + (\theta\sigma^{\mu}\bar{\theta})\,v_{\mu} + \theta^2 M + \bar{\theta}^2 M^* + \theta^2\bar{\theta}\bar{\rho} + \bar{\theta}^2\theta\rho + \theta^2\bar{\theta}^2 D. \tag{B.1}$$

Here, the terms in (5.30) comes out from the combination $V\left(\Phi_{\mathrm{L}} e^{eA_{\mathrm{WZ}}}\bar{\Phi}_{\mathrm{L}} - \Phi_{\mathrm{R}} e^{-eA_{\mathrm{WZ}}}\bar{\Phi}_{\mathrm{R}}\right)\big|_{\sim\theta^2\bar{\theta}^2}$. Then, after some algebra, one can verify that

$$\begin{aligned} S = -\int d^4x \Bigg\{ & \int d^2\theta d^2\bar{\theta} \left[\bar{\Phi}_{\mathrm{L}} e^{eA_{\mathrm{WZ}}}\Phi_{\mathrm{L}} + \bar{\Phi}_{\mathrm{R}} e^{-eA_{\mathrm{WZ}}}\Phi_{\mathrm{R}} + V\left(\bar{\Phi}_{\mathrm{L}} e^{eA_{\mathrm{WZ}}}\Phi_{\mathrm{L}} - \bar{\Phi}_{\mathrm{R}} e^{-eA_{\mathrm{WZ}}}\Phi_{\mathrm{R}}\right)\right] \\ & - \frac{1}{4}\left(\int d^2\theta\, W^2 + c.c.\right) - m\left(\int d^2\theta\, \Phi_{\mathrm{R}}\Phi_{\mathrm{L}} + c.c.\right)\Bigg\}. \end{aligned} \tag{B.2}$$

where

$$\begin{aligned} V\Phi_{\mathrm{L}} e^{eA_{\mathrm{WZ}}}\bar{\Phi}_{\mathrm{L}}\Big|_{\sim\theta^2\bar{\theta}^2} = & -\frac{1}{2}v_{\mu}(\bar{\psi}\bar{\sigma}^{\mu}\psi) - \frac{i}{2}v_{\mu}\left[\left(\tilde{\partial}^{\mu}\varphi^*\right)\varphi - \varphi^*\tilde{\partial}^{\mu}\varphi\right] + \varphi^*\varphi D + f^*\varphi M + f\varphi^* M^* \\ & - \frac{1}{\sqrt{2}}\left[\varphi\bar{\psi}\bar{\rho} + \varphi^*\psi\rho + f^*\psi\zeta + f\bar{\psi}\bar{\zeta}\right] + \frac{i}{2\sqrt{2}}\left[\varphi\left(\tilde{\partial}_{\mu}\bar{\psi}\right)\bar{\sigma}^{\mu}\zeta + (\bar{\zeta}\bar{\sigma}^{\mu}\psi)\tilde{\partial}_{\mu}\varphi^*\right. \\ & \left. - (\bar{\psi}\bar{\sigma}^{\mu}\zeta)\tilde{\partial}_{\mu}\varphi - \varphi^*\bar{\zeta}\bar{\sigma}^{\mu}\tilde{\partial}_{\mu}\psi\right] + C\left[f^* f + \left(\tilde{\partial}^{\mu}\varphi^*\right)\tilde{\partial}_{\mu}\varphi\right] - \frac{i}{2}C\left[\bar{\psi}\bar{\sigma}^{\mu}\tilde{\partial}_{\mu}\psi\right. \\ & \left. - \left(\tilde{\partial}_{\mu}\bar{\psi}\right)\bar{\sigma}^{\mu}\psi\right] + e\left\{\frac{iC}{\sqrt{2}}\left[\varphi^*(\lambda\psi) - \varphi(\bar{\lambda}\bar{\psi})\right] - \frac{1}{2}C\left[i(\varphi\tilde{\partial}^{\mu}\varphi^* - \varphi^*\tilde{\partial}^{\mu}\varphi)\right.\right. \\ & \left. + \bar{\psi}\bar{\sigma}^{\mu}\psi\right]\tilde{a}_{\mu} - \frac{1}{2\sqrt{2}}\left[\varphi(\bar{\psi}\bar{\sigma}^{\mu}\zeta) + \varphi^*(\bar{\zeta}\bar{\sigma}^{\mu}\psi)\right]\tilde{a}_{\mu} + \frac{1}{2}\varphi^*\varphi\left[i(\lambda\zeta - \bar{\lambda}\bar{\zeta})\right. \\ & \left.\left. + v^{\mu}\tilde{a}_{\mu} + C\left(K + \frac{e}{2}\tilde{a}^2\right)\right]\right\}, \end{aligned} \tag{B.3}$$

and right sector contribution is

$$
\begin{aligned}
V\Phi_{\mathrm{R}}e^{-eA_{\mathrm{WZ}}}\bar{\Phi}_{\mathrm{R}}\Big|_{\sim\theta^2\bar{\theta}^2} = &-\frac{1}{2}v_\mu(\bar{\chi}\bar{\sigma}^\mu\chi)+\frac{i}{2}v_\mu\Big[(\tilde{\partial}^\mu s^*)s-s^*\tilde{\partial}^\mu s\Big]+s^*sD+gs^*M+g^*sM^*\\
&-\frac{1}{\sqrt{2}}\Big[s^*\bar{\chi}\bar{\rho}+s\chi\rho+g\chi\zeta+g^*\bar{\chi}\bar{\zeta}\Big]+\frac{i}{2\sqrt{2}}\Big[s^*(\tilde{\partial}_\mu\bar{\chi})\bar{\sigma}^\mu\zeta+(\bar{\zeta}\bar{\sigma}^\mu\chi)\tilde{\partial}_\mu s\\
&-(\bar{\chi}\bar{\sigma}^\mu\zeta)\tilde{\partial}_\mu s^*-s\bar{\zeta}\bar{\sigma}^\mu\tilde{\partial}_\mu\chi\Big]+C\Big[g^*g+(\tilde{\partial}^\mu s^*)\tilde{\partial}_\mu s\Big]-\frac{i}{2}C\Big[\bar{\chi}\bar{\sigma}^\mu\tilde{\partial}_\mu\chi\\
&-(\tilde{\partial}_\mu\bar{\chi})\bar{\sigma}^\mu\chi\Big]-e\Big\{\frac{iC}{\sqrt{2}}\Big[s(\lambda\chi)-s^*(\bar{\lambda}\bar{\chi})\Big]-\frac{1}{2}C\Big[i(s^*\tilde{\partial}^\mu s-s\tilde{\partial}^\mu s^*)\\
&+\bar{\chi}\bar{\sigma}^\mu\chi\Big]\tilde{a}_\mu-\frac{1}{2\sqrt{2}}\Big[s^*(\bar{\chi}\bar{\sigma}^\mu\zeta)+s(\bar{\zeta}\bar{\sigma}^\mu\chi)\Big]\tilde{a}_\mu+\frac{1}{2}s^*s\Big[i(\lambda\zeta-\bar{\lambda}\bar{\zeta})\\
&+v^\mu\tilde{a}_\mu+C\Big(K-\frac{e}{2}\tilde{a}^2\Big)\Big]\Big\}. \qquad \text{(B.4)}
\end{aligned}
$$

In this case, using the constraints obtained from the field equations for the auxiliary fields, namely, f, g, and D, we get

$$
\begin{aligned}
S_2 = &\int d^4x\Big\{-\frac{1}{4}\mathscr{F}_{\mu\nu}^2+\frac{i}{2}\Big[(\tilde{\partial}_\mu\bar{\lambda})\bar{\sigma}^\mu\lambda-\bar{\lambda}\bar{\sigma}^\mu\tilde{\partial}_\mu\lambda\Big]+\frac{i}{2}(1+C)\Big[\bar{\psi}\bar{\sigma}^\mu(\tilde{\partial}_\mu\psi)-(\tilde{\partial}_\mu\bar{\psi})\bar{\sigma}^\mu\psi\Big]\\
&+\frac{i}{2}(1-C)\Big[\bar{\chi}\bar{\sigma}^\mu(\tilde{\partial}_\mu\chi)-(\tilde{\partial}_\mu\bar{\chi})\bar{\sigma}^\mu\chi\Big]+\frac{1}{2}v_\mu(\bar{\psi}\bar{\sigma}^\mu\psi-\bar{\chi}\bar{\sigma}^\mu\chi)-m(\bar{\psi}\bar{\chi}+\chi\psi)-(1+C)\\
&\times(\tilde{\partial}^\mu\varphi^*)\tilde{\partial}_\mu\varphi-(1-C)(\tilde{\partial}^\mu s^*)\tilde{\partial}_\mu s+\frac{i}{2}v_\mu\Big[(\tilde{\partial}^\mu\varphi^*)\varphi-\varphi^*\tilde{\partial}^\mu\varphi+(\tilde{\partial}^\mu s^*)s-s^*\tilde{\partial}^\mu s\Big]\\
&+\left[\frac{m^2}{(1-C)}+\frac{M^*M}{(1+C)}\right]\varphi^*\varphi+\left[\frac{m^2}{(1+C)}+\frac{M^*M}{(1-C)}\right]s^*s-\frac{m}{\sqrt{2}}\left[\frac{1}{(1-C)}(\varphi\chi\zeta+\varphi^*\bar{\chi}\bar{\zeta})\right.\\
&\left.-\frac{1}{(1+C)}(s\bar{\psi}\bar{\zeta}+s^*\psi\zeta)\right]-\frac{i}{2\sqrt{2}}\Big[\varphi(\tilde{\partial}_\mu\bar{\psi})\bar{\sigma}^\mu\zeta-(\bar{\psi}\bar{\sigma}^\mu\zeta)\tilde{\partial}_\mu\varphi-\varphi^*\bar{\zeta}\bar{\sigma}^\mu\tilde{\partial}_\mu\psi+(\bar{\zeta}\bar{\sigma}^\mu\psi)\tilde{\partial}_\mu\varphi^*\\
&+s\bar{\zeta}\bar{\sigma}^\mu\tilde{\partial}_\mu\chi-(\bar{\zeta}\bar{\sigma}^\mu\chi)\tilde{\partial}_\mu s-s^*(\tilde{\partial}_\mu\bar{\chi})\bar{\sigma}^\mu\zeta+(\bar{\chi}\bar{\sigma}^\mu\zeta)\tilde{\partial}_\mu s^*\Big]+\frac{1}{\sqrt{2}}\Big[(\varphi\bar{\psi}-s^*\bar{\chi})\bar{\rho}\\
&+(\varphi^*\psi-s\chi)\rho\Big]+\frac{1}{2(1+C)}\Big[\bar{\zeta}\bar{\psi}\zeta\psi-\sqrt{2}(M\varphi\bar{\zeta}\bar{\psi}+M^*\varphi^*\zeta\psi)\Big]+\frac{1}{2(1-C)}\Big[\bar{\zeta}\bar{\chi}\zeta\chi\\
&-\sqrt{2}(Ms^*\bar{\zeta}\bar{\chi}+M^*s\zeta\chi)\Big]-(\varphi^*\varphi-s^*s)D-\frac{e}{2}(\varphi^*\varphi+s^*s)\Big[i(\lambda\zeta-\bar{\lambda}\bar{\zeta})+v^\mu\tilde{a}_\mu\Big]\\
&+\frac{e}{2\sqrt{2}}(\varphi\bar{\psi}\bar{\sigma}^\mu\zeta+\varphi^*\bar{\zeta}\bar{\sigma}^\mu\psi+s^*\bar{\chi}\bar{\sigma}^\mu\zeta+s\bar{\zeta}\bar{\sigma}^\mu\chi)\tilde{a}_\mu-\frac{e}{2}(1+C)\Big[i\sqrt{2}(\varphi^*\lambda\psi-\varphi\bar{\lambda}\bar{\psi})\\
&+(\bar{\psi}\bar{\sigma}^\mu\psi)\tilde{a}_\mu-i(\varphi\tilde{\partial}^\mu\varphi^*-\varphi^*\tilde{\partial}^\mu\varphi)\tilde{a}_\mu\Big]+\frac{e}{2}(1-C)\Big[i\sqrt{2}(s\lambda\chi-s^*\bar{\lambda}\bar{\chi})\\
&+i(s\tilde{\partial}^\mu s^*-s^*\tilde{\partial}^\mu s)\tilde{a}_\mu-(\bar{\chi}\bar{\sigma}^\mu\chi)\tilde{a}_\mu\Big]-\frac{e^2}{4}\Big[(1+C)\varphi^*\varphi+(1-C)s^*s\Big]\tilde{a}^2\\
&-\frac{e^2}{8}\Big[(1+C)\varphi^*\varphi-(1-C)s^*s\Big]^2\Big\}. \qquad \text{(B.5)}
\end{aligned}
$$

As in the first approach, the gauge sector is given by (5.36). For the other sectors, we have

- fermionic sector

$$
\begin{aligned}
S_{\text{fermion}} = &\int d^4x\Big\{\frac{i}{2}\Big[\bar{\Psi}\gamma^\mu\tilde{\partial}_\mu\Psi-(\tilde{\partial}_\mu\bar{\Psi})\gamma^\mu\Psi\Big]+\frac{1}{2}v_\mu(\bar{\Psi}\gamma^\mu\Psi)-m\bar{\Psi}\Psi\\
&+\frac{e}{2}(\bar{\Psi}\gamma^\mu\gamma_5\Psi-C\bar{\Psi}\gamma^\mu\Psi)\tilde{a}_\mu-\frac{i}{2}C\Big[\bar{\Psi}\gamma^\mu\gamma_5\tilde{\partial}_\mu\Psi-(\tilde{\partial}_\mu\bar{\Psi})\gamma^\mu\gamma_5\Psi\Big]\Big\}. \qquad \text{(B.6)}
\end{aligned}
$$

- scalar sector

$$\begin{aligned} S_{\text{scalar}} = -\int d^4x \Big\{ & (1+C)(\tilde{D}^\mu\varphi^*)\tilde{D}_\mu\varphi + (1-C)(\tilde{D}^\mu s^*)\tilde{D}_\mu s + (\varphi^*\varphi - s^* s)D \\ & + i v_\mu\big(\varphi^*\tilde{D}^\mu\varphi + s^*\tilde{D}^\mu s\big) - \left[\frac{m^2}{(1-C)} + \frac{M^* M}{(1+C)}\right]\varphi^*\varphi \\ & - \left[\frac{m^2}{(1+C)} + \frac{M^* M}{(1-C)}\right] s^* s \Big\}. \end{aligned} \tag{B.7}$$

- gaugino and matter self-interaction sector

$$\begin{aligned} S_{\text{int}} = \int d^4x \Big\{ & \frac{ie}{\sqrt{2}}\Big[(1+C)(\varphi\bar{\Psi}\mathscr{P}_{\text{R}}\Lambda - \varphi^*\bar{\Lambda}\mathscr{P}_{\text{L}}\Psi) + (1-C)(s\bar{\Psi}\mathscr{P}_{\text{L}}\Lambda - s^*\bar{\Lambda}\mathscr{P}_{\text{R}}\Psi)\Big] \\ & + \frac{1}{\sqrt{2}}\Big[\bar{\Psi}(\varphi\mathscr{P}_{\text{R}} - s\mathscr{P}_{\text{L}})R + \bar{R}(\varphi^*\mathscr{P}_{\text{L}} - s^*\mathscr{P}_{\text{R}})\Psi\Big] - \frac{i}{2\sqrt{2}}\Big[(\tilde{D}^*_\mu\bar{\Psi})\gamma^\mu(\varphi\mathscr{P}_{\text{L}} - s\mathscr{P}_{\text{R}})Z \\ & - \bar{Z}\gamma^\mu(\varphi^*\mathscr{P}_{\text{L}} - s^*\mathscr{P}_{\text{R}})\tilde{D}_\mu\Psi - \bar{\Psi}\gamma^\mu\big(\tilde{\partial}_\mu\varphi\mathscr{P}_{\text{L}} - \tilde{\partial}_\mu s\mathscr{P}_{\text{R}}\big)Z \\ & + \bar{Z}\gamma^\mu\big(\tilde{\partial}_\mu\varphi^*\mathscr{P}_{\text{L}} - \tilde{\partial}_\mu s^*\mathscr{P}_{\text{R}}\big)\Psi\Big] - \frac{m}{\sqrt{2}}\Big[\frac{1}{(1-C)}(\varphi\bar{\Psi}\mathscr{P}_{\text{L}}Z + \varphi^*\bar{Z}\mathscr{P}_{\text{R}}\Psi) \\ & - \frac{1}{(1+C)}(s\bar{\Psi}\mathscr{P}_{\text{R}}Z + s^*\bar{Z}\mathscr{P}_{\text{L}}\Psi)\Big] + \frac{1}{2(1+C)}\Big[(\bar{\Psi}\mathscr{P}_{\text{R}}Z)(\bar{Z}\mathscr{P}_{\text{L}}\Psi) \\ & - \sqrt{2}(M\varphi\bar{\Psi}\mathscr{P}_{\text{R}}Z + M^*\varphi^*\bar{Z}\mathscr{P}_{\text{L}}\Psi)\Big] + \frac{1}{2(1-C)}\Big[(\bar{Z}\mathscr{P}_{\text{R}}\Psi)(\bar{\Psi}\mathscr{P}_{\text{L}}Z) \\ & - \sqrt{2}(Ms^*\bar{Z}\mathscr{P}_{\text{R}}\Psi + M^* s\bar{\Psi}\mathscr{P}_{\text{L}}Z)\Big] - \frac{ie}{4}(\varphi^*\varphi + s^* s)\big[\bar{\Lambda}\gamma_5 Z + \bar{Z}\gamma_5\Lambda\big] \\ & - \frac{e^2}{8}\Big[(1+C)\varphi^*\varphi - (1-C)s^* s\Big]^2\Big\}, \end{aligned} \tag{B.8}$$

where

$$R = \begin{pmatrix} \rho_\alpha \\ \bar{\rho}^{\dot{\alpha}} \end{pmatrix}. \tag{B.9}$$

B.2 Useful results

We collect here some useful results related to the calculation of dispersion relations in Sect. 5.3.3.

$$\begin{aligned} X^{(1)}(\varphi_0, s_0) = \frac{1}{16}\Big\{ & \Big[2m^2(\tilde{p}\cdot\zeta) - 2(\tilde{p}^2 - \tilde{p}\cdot\mathscr{R} - \tilde{p}\cdot\zeta)(\tilde{p}^2 + 2\tilde{p}\cdot\mathscr{R} - 2\tilde{p}\cdot\zeta \\ & + \mathscr{R}^2 - 2\zeta\cdot\mathscr{R} + \zeta^2)\Big]h - 2\Big[2m^2\tilde{p}^2 - 3m^2\tilde{p}\cdot\zeta - \tilde{p}^4 - 2(\tilde{p}\cdot\mathscr{R})^2 \\ & - (\tilde{p}\cdot\zeta)(2\tilde{p}\cdot\zeta + 3\mathscr{R}^2 - 2\zeta\cdot\mathscr{R} - \zeta^2) - (\tilde{p}\cdot\mathscr{R})(\mathscr{R}^2 - 2\zeta\cdot\mathscr{R} + \zeta^2) \\ & + \tilde{p}^2(\tilde{p}\cdot\mathscr{R} + 3\tilde{p}\cdot\zeta + 3\mathscr{R}^2 - 2\zeta\cdot\mathscr{R} - \zeta^2)\Big]h^* + 2m^2\big(m^2 + \tilde{p}\cdot\mathscr{R} \\ & + \mathscr{R}^2 - \tilde{\zeta}^2\big)(h + h^*)\Big\}\varphi_0 + \frac{1}{16}\Big\{4m^5 + 4m^3\big(2\tilde{p}\cdot\tilde{\zeta} + \mathscr{R}^2 - \tilde{\zeta}^2\big) \\ & - 4m\Big[\tilde{p}^2\big(\tilde{p}^2 - 2\tilde{p}\cdot\tilde{\zeta} + 3\mathscr{R}^2 + \tilde{\zeta}^2\big) - 4(\tilde{p}\cdot\mathscr{R})\big(\tilde{p}\cdot\mathscr{R} - \zeta\cdot\mathscr{R}\big) \\ & - 4\tilde{p}\cdot\zeta\mathscr{R}^2\Big] - m\big(m^2 - \tilde{p}^2 + 2\tilde{p}\cdot\tilde{\zeta} + \mathscr{R}^2 - \tilde{\zeta}^2\big)h^{*2}\Big\}s_0, \end{aligned} \tag{B.10}$$

$$
\begin{aligned}
X^{(2)}(\varphi_0, s_0) = &-\frac{1}{16}\Big\{4m^3(m^2-2\tilde{p}^2+2\tilde{p}\cdot\mathscr{R}+4\tilde{p}\cdot\zeta+\mathscr{R}^2-\zeta^2)+4m\Big[\tilde{p}^2(\tilde{p}^2-2\tilde{p}\cdot\mathscr{R}\\
&-4\tilde{p}\cdot\zeta-5\mathscr{R}^2+\zeta^2)+2(\tilde{p}\cdot\mathscr{R})(2\tilde{p}\cdot\mathscr{R}+2\tilde{p}\cdot\zeta+\mathscr{R}^2-2\zeta\cdot\mathscr{R}-\zeta^2)\\
&+2(\tilde{p}\cdot\zeta)(2\tilde{p}\cdot\zeta+3\mathscr{R}^2-\zeta^2)+m(m^2-\tilde{p}^2+2\tilde{p}\cdot\zeta+\mathscr{R}^2-\zeta^2)h^*h\Big]\Big\}\varphi_0\\
&+\frac{1}{16}\Big\{4m^2(m^2-2\tilde{p}^2+3\tilde{p}\cdot\zeta+\mathscr{R}^2-\zeta^2)+4\Big[\tilde{p}^2(\tilde{p}^2-3\tilde{p}\cdot\zeta-3\mathscr{R}^2\\
&-2\zeta\cdot\mathscr{R}+\zeta^2)+2(\tilde{p}\cdot\mathscr{R})(\tilde{p}\cdot\mathscr{R}+\tilde{p}\cdot\zeta-\zeta\cdot\mathscr{R}-\zeta^2)\\
&+(\tilde{p}\cdot\zeta)(2\tilde{p}\cdot\zeta+3\mathscr{R}^2+2\zeta\cdot\mathscr{R}-\zeta^2)\Big]\Big\}h^*s_0,
\end{aligned}
\tag{B.11}
$$

$$
\begin{aligned}
\mathscr{M}^{(1)}(\varphi_0, s_0) = &\frac{1}{16}\Big\{\Big[2m^2(\tilde{p}\cdot\zeta)-2(\tilde{p}^2-\tilde{p}\cdot\mathscr{R}-\tilde{p}\cdot\zeta)(\tilde{p}^2+2\tilde{p}\cdot\mathscr{R}-2\tilde{p}\cdot\zeta+\mathscr{R}^2\\
&-2\zeta\cdot\mathscr{R}+\zeta^2)\Big]h+\Big[4m^2\tilde{p}^2-6m^2\tilde{p}\cdot\zeta-2\big[\tilde{p}^4+2(\tilde{p}\cdot\mathscr{R})^2\\
&+(\tilde{p}\cdot\zeta)(2\tilde{p}\cdot\zeta+3\mathscr{R}^2-2\zeta\cdot\mathscr{R}-\zeta^2)\big]+(\tilde{p}\cdot\mathscr{R})(\mathscr{R}^2-2\zeta\cdot\mathscr{R}+\zeta^2)\\
&+\tilde{p}^2(-\tilde{p}\cdot\mathscr{R}-3\tilde{p}\cdot\zeta-3\mathscr{R}^2+2\zeta\cdot\mathscr{R}+\zeta^2)\Big]h^*+2m^2\big(m^2+\tilde{p}\cdot\mathscr{R}\\
&+\mathscr{R}^2-\tilde{\zeta}^2\big)(h-h^*)\Big\}\varphi_0+\frac{1}{16}\Big\{4m^5+4m^3\big(2\tilde{p}\cdot\tilde{\zeta}+\mathscr{R}^2-\tilde{\zeta}^2\big)\\
&-4m\Big[\tilde{p}^2\big(\tilde{p}^2-2\tilde{p}\cdot\tilde{\zeta}+3\mathscr{R}^2+\tilde{\zeta}^2\big)-4(\tilde{p}\cdot\mathscr{R})\big(\tilde{p}\cdot\mathscr{R}-\zeta\cdot\mathscr{R}\big)\\
&-4(\tilde{p}\cdot\zeta)\mathscr{R}^2\Big]+m\big(m^2-\tilde{p}^2+2\tilde{p}\cdot\tilde{\zeta}+\mathscr{R}^2-\tilde{\zeta}^2\big)h^{*2}\Big\}s_0,
\end{aligned}
\tag{B.12}
$$

$$
\begin{aligned}
\mathscr{M}^{(2)}(\varphi_0, s_0) = &\frac{1}{16}\Big\{4m^3(m^2-2\tilde{p}^2+2\tilde{p}\cdot\mathscr{R}+4\tilde{p}\cdot\zeta+\mathscr{R}^2-\zeta^2)+4m\Big[\tilde{p}^2(\tilde{p}^2-2\tilde{p}\cdot\mathscr{R}\\
&-4\tilde{p}\cdot\zeta-5\mathscr{R}^2+\zeta^2)+2(\tilde{p}\cdot\mathscr{R})(2\tilde{p}\cdot\mathscr{R}+2\tilde{p}\cdot\zeta+\mathscr{R}-2\zeta\cdot\mathscr{R}-\zeta^2)\\
&+2(\tilde{p}\cdot\zeta)(2\tilde{p}\cdot\zeta+3\mathscr{R}^2-\zeta^2)\Big]+m(m^2-\tilde{p}^2+2\tilde{p}\cdot\zeta+\mathscr{R}^2-\zeta^2)h^*h\Big\}\varphi_0\\
&-\frac{1}{16}\Big[4m^2(\tilde{p}\cdot\mathscr{R})-4(\tilde{p}\cdot\mathscr{R})(\tilde{p}^2-2\tilde{p}\cdot\zeta)+\mathscr{R}^2-\zeta^2)\Big]h^*s_0,
\end{aligned}
\tag{B.13}
$$

$$
\begin{aligned}
Y_\alpha^{(1)}(\varphi_0, s_0) = &-\frac{1}{16}\Big[4m\big(m^2-\tilde{p}^2+2\tilde{p}\cdot\zeta-\mathscr{R}^2-\zeta^2\big)\tilde{p}_\alpha+8m\mathscr{R}^2\zeta_\alpha-4m\big(m^2-\tilde{p}^2\\
&+2\tilde{p}\cdot\mathscr{R}+2\tilde{p}\cdot\zeta-\mathscr{R}^2-\zeta^2\big)\mathscr{R}_\alpha\Big]h^* s_0+\frac{1}{16}\Big\{\Big[4m^2\big(m^2-2\tilde{p}^2+4\tilde{p}\cdot\zeta\\
&-\mathscr{R}^2-2\zeta\cdot\mathscr{R}-\zeta^2\big)+4\tilde{p}^2\big(\tilde{p}^2-4\tilde{p}\cdot\mathscr{R}-4\tilde{p}\cdot\zeta+\mathscr{R}^2-2\zeta\cdot\mathscr{R}+\zeta^2\big)\\
&+8(\tilde{p}\cdot\mathscr{R})\big(-2\tilde{p}\cdot\mathscr{R}+4\tilde{p}\cdot\zeta+\mathscr{R}^2-\zeta^2\big)+8(\tilde{p}\cdot\zeta)\big(2\tilde{p}\cdot\zeta+\mathscr{R}^2-\zeta^2\big)\Big]\tilde{p}_\alpha\\
&+\Big[4m^2\big(m^2-2\tilde{p}^2+4\tilde{p}\cdot\zeta+3\mathscr{R}^2+2\zeta\cdot\mathscr{R}-\zeta^2\big)+4\tilde{p}^2\big(\tilde{p}^2+2\tilde{p}\cdot\mathscr{R}\\
&-2\tilde{p}\cdot\zeta-3\mathscr{R}^2+2\zeta\cdot\mathscr{R}+\zeta^2\big)+8(\tilde{p}\cdot\mathscr{R})\big(2\tilde{p}\cdot\mathscr{R}-2\tilde{p}\cdot\zeta\big)\Big]\zeta_\alpha\\
&+4\Big[m^2\big(m^2+2\tilde{p}\cdot\mathscr{R}+2\tilde{p}\cdot\zeta+\mathscr{R}^2-2\zeta\cdot\mathscr{R}-3\zeta^2\big)+\tilde{p}^2\big(3\tilde{p}^2-2\tilde{p}\cdot\mathscr{R}\\
&+6\tilde{p}\cdot\zeta+\mathscr{R}^2-\zeta\cdot\mathscr{R}-\zeta^2\big)+4(\tilde{p}\cdot\zeta)\big(\tilde{p}\cdot\zeta-\tilde{p}\cdot\mathscr{R}\big)\Big]\mathscr{R}_\alpha\\
&-16i\big(\tilde{p}^2-\tilde{p}\cdot\mathscr{R}-\tilde{p}\cdot\zeta\big)\varepsilon_\alpha{}^{\mu\nu\kappa}\tilde{p}_\mu\mathscr{R}_\nu\zeta_\kappa\Big\}\varphi_0,
\end{aligned}
\tag{B.14}
$$

$$
\begin{aligned}
Y_\alpha^{(2)}(\varphi_0, s_0) = &\frac{1}{16}\Big\{m\Big[4\big(m^2-\tilde{p}^2+2\tilde{p}\cdot\mathscr{R}+2\tilde{p}\cdot\zeta+2\mathscr{R}^2-\zeta\cdot\mathscr{R}-\zeta^2\big)\tilde{p}_\alpha-2\big(m^2-\tilde{p}^2\\
&+4\tilde{p}\cdot\mathscr{R}+2\tilde{p}\cdot\zeta+3\mathscr{R}^2-2\zeta\cdot\mathscr{R}-\zeta^2\big)\zeta_\alpha+2\big(m^2-5\tilde{p}^2-2\tilde{p}\cdot\mathscr{R}\\
&+8\tilde{p}\cdot\zeta+\mathscr{R}^2+\zeta\cdot\mathscr{R}-3\zeta^2\big)\mathscr{R}_\alpha-4i\varepsilon_\alpha{}^{\mu\nu\kappa}\tilde{p}_\mu\mathscr{R}_\nu\zeta_\kappa\Big]h-\Big[4\big(\mathscr{R}^2+\zeta\cdot\mathscr{R}\big)\tilde{p}_\alpha\\
&-2\big(m^2-\tilde{p}^2+2\tilde{p}\cdot\zeta+3\mathscr{R}^2+2\zeta\cdot\mathscr{R}-\zeta^2\big)\zeta_\alpha-2\big(m^2-\tilde{p}^2+2\tilde{p}\cdot\mathscr{R}\\
&+4\tilde{p}\cdot\zeta+\mathscr{R}^2-2\zeta\cdot\mathscr{R}-3\zeta^2\big)\mathscr{R}_\alpha-4i\varepsilon_\alpha{}^{\mu\nu\kappa}\tilde{p}_\mu\mathscr{R}_\nu\zeta_\kappa\Big]h^*\Big\}\varphi_0\\
&+\frac{1}{16}\Big\{\Big[\big(m^2-\tilde{p}^2-2\tilde{p}\cdot\mathscr{R}+2\tilde{p}\cdot\zeta+3\mathscr{R}^2+2\zeta\cdot\mathscr{R}-\zeta^2\big)\tilde{p}_\alpha-\big(m^2-\tilde{p}^2\\
&-2\tilde{p}\cdot\mathscr{R}+2\tilde{p}\cdot\zeta-3\mathscr{R}^2+2\zeta\cdot\mathscr{R}-\zeta^2\big)\zeta_\alpha-\big(m^2-3\tilde{p}^2+2\tilde{p}\cdot\mathscr{R}\\
&+6\tilde{p}\cdot\zeta+\mathscr{R}^2-2\zeta\cdot\mathscr{R}-3\zeta^2\big)\mathscr{R}_\alpha\Big]h^{*2}+4\Big[3m^4+\tilde{p}^4+4(\tilde{p}\cdot\mathscr{R})^2\\
&+4(\tilde{p}\cdot\zeta)^2-2(\tilde{p}\cdot\mathscr{R}-\tilde{p}\cdot\zeta)\mathscr{R}^2+2(\tilde{p}\cdot\mathscr{R}-\tilde{p}\cdot\zeta)\zeta^2-m^2(\tilde{p}^2-8\tilde{p}\cdot\zeta\\
&-5\mathscr{R}^2+2\zeta\cdot\mathscr{R}+3\zeta^2)-\tilde{p}^2(4\tilde{p}\cdot\zeta+\mathscr{R}^2+2\zeta\cdot\mathscr{R}-\zeta^2)\Big]\tilde{p}_\alpha\\
&-4\Big[m^4-\tilde{p}^4+4(\tilde{p}\cdot\mathscr{R})^2+4(\tilde{p}\cdot\mathscr{R})(\tilde{p}\cdot\zeta)+m^2(2\tilde{p}\cdot\mathscr{R}+2\tilde{p}\cdot\zeta+3\mathscr{R}^2\\
&-2\zeta\cdot\mathscr{R}-\zeta^2)-\tilde{p}^2(2\tilde{p}\cdot\mathscr{R}-2\tilde{p}\cdot\zeta+\mathscr{R}^2+2\zeta\cdot\mathscr{R}+\zeta^2)\Big]\zeta_\alpha\\
&+4\Big[m^4+\tilde{p}^4+4(\tilde{p}\cdot\zeta)(\tilde{p}\cdot\mathscr{R}+\tilde{p}\cdot\zeta)-m^2(2\tilde{p}^2+2\tilde{p}\cdot\mathscr{R}-6\tilde{p}\cdot\zeta-\mathscr{R}^2\\
&-2\zeta\cdot\mathscr{R}+3\zeta^2)-\tilde{p}^2(2\tilde{p}\cdot\mathscr{R}+2\tilde{p}\cdot\zeta-\mathscr{R}^2+2\zeta\cdot\mathscr{R}-\zeta^2)\Big]\mathscr{R}_\alpha\\
&-16i(\tilde{p}^2-\tilde{p}\cdot\mathscr{R}-\tilde{p}\cdot\zeta)\varepsilon_\alpha{}^{\mu\nu\kappa}\tilde{p}_\mu\mathscr{R}_\nu\zeta_\kappa\Big\}s_0.
\end{aligned}
\tag{B.15}
$$

Appendix

C

Results on Kalb-Ramond like particle

C.1 Spin projectors and the KRLP propagator

In Sec. 7.1 we obtained the wave operator $\mathcal{O}^{\nu\lambda,\alpha\beta}(k)$, see Eq. (7.8), and mentioned that its inverse is the propagator. The inversion of the operator is best performed by using the spin projectors acting on antisymmetric 2-forms [384, 388, 389]

$$\left(P_b^1\right)_{\mu\nu,\rho\sigma} \equiv \frac{1}{2}\left(\theta_{\mu\rho}\theta_{\nu\sigma} - \theta_{\mu\sigma}\theta_{\nu\rho}\right), \tag{C.1}$$

$$\left(P_e^1\right)_{\mu\nu,\rho\sigma} \equiv \frac{1}{2}\left(\theta_{\mu\rho}\omega_{\nu\sigma} + \theta_{\nu\sigma}\omega_{\mu\rho} - \theta_{\mu\sigma}\omega_{\nu\rho} - \theta_{\nu\rho}\omega_{\mu\sigma}\right), \tag{C.2}$$

with $\theta_{\mu\nu} = \eta_{\mu\nu} - \dfrac{k_\mu k_\nu}{k^2}$ and $\omega_{\mu\nu} = \dfrac{k_\mu k_\nu}{k^2}$. The antisymmetric identity is defined as

$$\left(P_b^1 + P_e^1\right)_{\mu\nu,\rho\sigma} = \frac{1}{2}\left(\eta_{\mu\rho}\eta_{\nu\sigma} - \eta_{\mu\sigma}\eta_{\nu\rho}\right) \equiv \left(1^{a.s.}\right)_{\mu\nu,\rho\sigma} \tag{C.3}$$

and the algebra fulfilled by these operators is:

$$\left(P_b^1\right)_{\mu\nu,\alpha\beta}\left(P_b^1\right)^{\alpha\beta}{}_{,\rho\sigma} = \left(P_b^1\right)_{\mu\nu,\rho\sigma}, \tag{C.4}$$

$$\left(P_e^1\right)_{\mu\nu,\alpha\beta}\left(P_e^1\right)^{\alpha\beta}{}_{,\rho\sigma} = \left(P_e^1\right)_{\mu\nu,\rho\sigma}, \tag{C.5}$$

$$\left(P_b^1\right)_{\mu\nu,\alpha\beta}\left(P_e^1\right)^{\alpha\beta}{}_{,\rho\sigma} = 0, \tag{C.6}$$

$$\left(P_e^1\right)_{\mu\nu,\alpha\beta}\left(P_b^1\right)^{\alpha\beta}{}_{,\rho\sigma} = 0. \tag{C.7}$$

The operator $\mathcal{O}$ may be written in terms of the projectors as (omitting tensor indices for clarity)

$$\mathcal{O} = \left(k^2 - m^2\right)P_b^1 - m^2 P_e^1. \tag{C.8}$$

The propagator is such that $-i\Delta = \mathcal{O}^{-1} = aP_e^1 + bP_b^1$ with a, b free coefficients to be determined. Imposing that $\Delta\mathcal{O} = 1^{a.s.}$ we obtain $a = -1/m^2$ and $b = 1/(k^2 - m^2)$, so that

$$\Delta = \frac{i}{k^2 - m^2}\left(P_b^1\right) - \frac{i}{m^2}\left(P_e^1\right). \tag{C.9}$$

C.2 Calculation of the non-relativistic amplitudes

In this appendix we detail the calculation of the NR amplitudes for the KRLP-mediated PV and T interactions. For the sake of generality, we make no prior assumption about the hierarchy of the fermion masses; adequate approximations may be made in a case-by-case basis. The two fermions are labelled $f = a, b$ with initial and final 4-momenta p_1 and p_3, and p_2 and p_4, respectively. As stated in the main text, we will express our results as expansions in $|\boldsymbol{p}_n|/m_f$ ($n = 1,2,3,4$) and we will keep terms only up to and including second order.

It is convenient to consider the problem in the CM frame, where the total initial and final 3-momenta are zero: $\boldsymbol{p}_1 + \boldsymbol{p}_2 = \boldsymbol{0} = \boldsymbol{p}_3 + \boldsymbol{p}_4$. Here we use the average 4-momentum of fermion a, $P = (p_1 + p_3)/2$, and the momentum transfer, $q = p_3 - p_1$, as main variables. In the CM frame, the 3-momenta of the fermion a and b translate to $\boldsymbol{p}_1 = \boldsymbol{P} - \boldsymbol{q}/2$ and $\boldsymbol{p}_3 = \boldsymbol{P} + \boldsymbol{q}/2$, and $\boldsymbol{p}_2 = -\boldsymbol{P} + \boldsymbol{q}/2$ and $\boldsymbol{p}_4 = -\boldsymbol{P} - \boldsymbol{q}/2$, respectively. Noting that $\boldsymbol{p}_n^2 = \boldsymbol{P}^2 + \boldsymbol{q}^2/4$, one sees that the initial and final energies of the fermions are roughly the same, that is, $q^0 \approx 0$ and $q^2 \approx -\boldsymbol{q}^2$, thus characterizing an elastic interaction. In the $\{\boldsymbol{P}, \boldsymbol{q}\}$ basis, our approximations imply that terms of order higher than $O(|\boldsymbol{P}|^2/m_f^2)$ and $O(|\boldsymbol{q}|^2/m_f^2)$ will be neglected.

A direct consequence of our approximation scheme is that the NR normalization factors for the spinors, see Eq. (7.10), are now mass and momentum dependent. The NR normalization is given by $N_{\rm NR} = \sqrt{(m_f + E)/2E}$, but up to second order we have $E \approx m_f\left(1 + \boldsymbol{p}_n^2/2m_f^2\right)$, therefore $N_{\rm NR} \to N_{{\rm NR},f}$. For a given bilinear we always have the normalization factor squared, $N_{{\rm NR},f}^2$, which may be expanded as (using $\boldsymbol{P}\cdot\boldsymbol{q} = 0$)

$$N_{{\rm NR},f}^2 \approx 1 - \frac{1}{4m_f^2}\left(\boldsymbol{P}^2 + \frac{\boldsymbol{q}^2}{4}\right) \to N_{{\rm NR},a}^2 N_{{\rm NR},b}^2 \approx 1 - \frac{1}{4}\left(\frac{1}{m_a^2} + \frac{1}{m_b^2}\right)\left(\boldsymbol{P}^2 + \frac{\boldsymbol{q}^2}{4}\right). \tag{C.10}$$

This momentum-dependent pre-factor must be consistently accounted for in the calculation of the fermionic bilinears up to second order [334].

C.2.1 Fermionic bilinears

Here we explicitly calculate the fermionic bilinears that appear in the PV and T currents in the NR approximation. We use the standard Dirac representation of the gamma matrices

$$\gamma^0 = \begin{pmatrix} \boldsymbol{1} & \boldsymbol{0} \\ \boldsymbol{0} & \boldsymbol{-1} \end{pmatrix}, \quad \gamma^k = \begin{pmatrix} \boldsymbol{0} & \sigma^k \\ -\sigma^k & \boldsymbol{0} \end{pmatrix} \quad \text{and} \quad \gamma^5 = \begin{pmatrix} \boldsymbol{0} & \boldsymbol{1} \\ \boldsymbol{1} & \boldsymbol{0} \end{pmatrix}. \tag{C.11}$$

The PV fermionic bilinear is $O_{\rm PV}^{\mu\nu} = \epsilon^{\mu\nu}{}_{\beta\alpha}\bar{u}(p_f)\left(q^\alpha\gamma^\beta - q^\beta\gamma^\alpha\right)\gamma^5 u(p_i)$. In order to evaluate its components, it is worth quoting the identity

$$\bar{u}(p_f)\gamma^\mu\gamma^5 u(p_i) = \frac{1}{2m_f}\bar{u}(p_f)\left(q^\mu + 2iP_\nu\sigma^{\mu\nu}\right)\gamma^5 u(p_i), \tag{C.12}$$

which can be obtained by using the Dirac equation and the fact that $\gamma^\mu\gamma^\nu = \eta^{\mu\nu} - i\sigma^{\mu\nu}$. Using these results we find that

$$O^{0k}_{\rm PV} = -4\epsilon_{klm}\left(\boldsymbol{p}_f - \boldsymbol{p}_i\right)_l \langle\boldsymbol{\sigma}_m\rangle \quad \text{and} \quad O^{kl}_{\rm PV} = -\frac{2}{m_f}\epsilon_{klm}\left(\boldsymbol{p}_f - \boldsymbol{p}_i\right)_m \left[\left(\boldsymbol{p}_i + \boldsymbol{p}_f\right)\cdot\langle\boldsymbol{\sigma}\rangle\right], \tag{C.13}$$

where we retained only terms of up to second order. In obtaining the results above we used $\sigma_i\sigma_j = \delta_{ij} + i\epsilon_{ijk}\sigma_k$ and $\sigma_i\sigma_j\sigma_l = \delta_{ij}\sigma_l - \delta_{il}\sigma_j + \delta_{jl}\sigma_i + i\epsilon_{ijl}$. For the T interaction the fermionic bilinear is $O^{\mu\nu}_{\rm T} = \bar{u}(p_f)\dfrac{i}{2}\left(\gamma^\mu\gamma^\nu - \gamma^\nu\gamma^\mu\right)u(p_i)$. Its components are given by

$$O^{0k}_{\rm T} = -\frac{1}{2m_f}\epsilon_{klm}\left(\boldsymbol{p}_i + \boldsymbol{p}_f\right)_l\langle\boldsymbol{\sigma}_m\rangle - \frac{i}{2m_f}\left(\boldsymbol{p}_f - \boldsymbol{p}_i\right)_k \tag{C.14}$$

$$O^{kl}_{\rm T} = \epsilon_{klm}\left\{\langle\boldsymbol{\sigma}_m\rangle - \frac{1}{4m_f^2}\left[\left(\boldsymbol{p}_i\right)_m\left(\boldsymbol{\sigma}\cdot\boldsymbol{p}_f\right) + \left(\boldsymbol{p}_f\right)_m\left(\boldsymbol{\sigma}\cdot\boldsymbol{p}_i\right) - \left(\boldsymbol{p}_i\cdot\boldsymbol{p}_f\right)\boldsymbol{\sigma}_m\right]\right.$$
$$\left. - \frac{i}{4m_f^2}\left[\left(\boldsymbol{p}_i\right)_k\left(\boldsymbol{p}_f\right)_l - \left(\boldsymbol{p}_i\right)_l\left(\boldsymbol{p}_f\right)_k\right]\right\}. \tag{C.15}$$

All fermionic bilinears, momentarily omitting the NR normalization, Eq. (C.10), satisfy our limitation of keeping terms up to at most $O(|\boldsymbol{P}|^2/m_f^2)$ and $O(|\boldsymbol{q}|^2/m_f^2)$.

Note that the bilinears are antisymmetric, as expected, and we have omitted the factor $\xi^\dagger_a\xi_b = \delta_{ab}$ from the spinor normalization; this accounts for the impossibility of a spin flip. Moreover, the results above are 2-rank tensors, so that $O^{0k} = -O_{0k}$ and $O^{kl} = O_{kl}$.

C.2.2 Non-relativistic amplitudes

The NR PV amplitude for the KRLP-mediated interaction between two fermions labelled a and b is given by (see Eqs. (7.7) and (7.11))

$$i\mathscr{M}^{\rm PV}_{\rm NR} = \left(\frac{g^a_{\rm PV}g^b_{\rm PV}}{16\Lambda^2}\right)O^{\mu\nu}_a\Delta_{\mu\nu,\alpha\beta}O^{\alpha\beta}_b\,. \tag{C.16}$$

The operators $O^{\mu\nu}_{a,b}$ are understood to represent the PV bilinears. Due to the antisymmetry of the vertices, the terms in the propagator with four factors of the 4-momentum transfer automatically vanish and, after long, but straightforward manipulations, we are left with

$$\mathscr{M}^{\rm PV}_{\rm NR} = -\left(\frac{g^a_{\rm PV}g^b_{\rm PV}}{16\Lambda^2}\right)\frac{1}{\boldsymbol{q}^2 + m^2}\left[O_{a,\mu\nu}O^{\mu\nu}_b - \frac{2}{m^2}O_{a,\alpha\nu}O^{\alpha\beta}_b q^\nu q_\beta\right], \tag{C.17}$$

which may be further expanded using

$$O_{a,\mu\nu}O^{\mu\nu}_b = -2O^{0i}_aO^{0i}_b + O^{ij}_aO^{ij}_b\,, \tag{C.18}$$

$$O_{a,\alpha\nu}O^{\alpha\beta}_b q^\nu q_\beta = -\boldsymbol{q}_i\boldsymbol{q}_j\left(O^{ki}_aO^{kj}_b - O^{0i}_aO^{0j}_b\right). \tag{C.19}$$

We evaluate the expressions above using Eq. (C.13). Keeping in mind that $\boldsymbol{q}\to-\boldsymbol{q}$ and $\boldsymbol{P}\to-\boldsymbol{P}$ in passing from the vertex for fermion a to fermion b, we obtain

$$\frac{1}{8}O_{a,\mu\nu}O^{\mu\nu}_b = \boldsymbol{q}^2\left[\langle\boldsymbol{\sigma}\rangle_a\cdot\langle\boldsymbol{\sigma}\rangle_b + \frac{1}{m_am_b}\left(\boldsymbol{P}\cdot\langle\boldsymbol{\sigma}\rangle_a\right)\left(\boldsymbol{P}\cdot\langle\boldsymbol{\sigma}\rangle_b\right)\right] - \left(\boldsymbol{q}\cdot\langle\boldsymbol{\sigma}\rangle_a\right)\left(\boldsymbol{q}\cdot\langle\boldsymbol{\sigma}\rangle_b\right), \tag{C.20}$$

whereas $O_{a,\alpha\nu}O_b^{\alpha\beta}q^\nu q_\beta = 0$ due to symmetry. The NR PV amplitude at tree level is then

$$\begin{aligned}\mathscr{M}_{\rm NR}^{\rm PV} &= \left(\frac{g^a_{\rm PV}g^b_{\rm PV}}{2\Lambda^2}\right)\frac{1}{\boldsymbol{q}^2+m^2}\Big\{(\boldsymbol{q}\cdot\langle\boldsymbol{\sigma}\rangle_a)(\boldsymbol{q}\cdot\langle\boldsymbol{\sigma}\rangle_b)\\ &- \boldsymbol{q}^2\left[\langle\boldsymbol{\sigma}\rangle_a\cdot\langle\boldsymbol{\sigma}\rangle_b+\frac{1}{m_am_b}(\boldsymbol{P}\cdot\langle\boldsymbol{\sigma}\rangle_a)(\boldsymbol{P}\cdot\langle\boldsymbol{\sigma}\rangle_b)\right]\Big\}. \end{aligned} \tag{C.21}$$

The NR T amplitude follows a similar structure as for the PV case, see Eq. (C.16), namely

$$\mathscr{M}_{\rm NR}^{\rm T} = -\frac{g^a_{\rm T}g^b_{\rm T}}{\boldsymbol{q}^2+m^2}\left[O_{a,\mu\nu}O_b^{\mu\nu}-\frac{2}{m^2}O_{a,\alpha\nu}O_b^{\alpha\beta}q^\nu q_\beta\right] \tag{C.22}$$

with the operators now referring to the T bilinears. Considering Eqs. (C.14) and (C.15) and keeping contributions only up to and including $O(|\boldsymbol{P}|^2/m_f^2)$ and $O(|\boldsymbol{q}|^2/m_f^2)$, we find

$$\begin{aligned}\mathscr{M}_{\rm NR}^{\rm T} &= \left(\frac{2g^a_{\rm T}g^b_{\rm T}}{m^2}\right)\left[\langle\boldsymbol{\sigma}\rangle_a\cdot\langle\boldsymbol{\sigma}\rangle_b-\frac{1}{\boldsymbol{q}^2+m^2}(\boldsymbol{q}\cdot\langle\boldsymbol{\sigma}\rangle_a)(\boldsymbol{q}\cdot\langle\boldsymbol{\sigma}\rangle_b)\right]\\ &- \left(\frac{2g^a_{\rm T}g^b_{\rm T}}{m_am_b}\right)\frac{1}{\boldsymbol{q}^2+m^2}\Big\{\langle\boldsymbol{\sigma}\rangle_a\cdot\langle\boldsymbol{\sigma}\rangle_b\left(C_P\boldsymbol{P}^2+C_q\boldsymbol{q}^2\right)+\frac{1}{4}\boldsymbol{q}^2\\ &+ (\boldsymbol{P}\cdot\langle\boldsymbol{\sigma}\rangle_a)(\boldsymbol{P}\cdot\langle\boldsymbol{\sigma}\rangle_b)-\frac{i}{2}\boldsymbol{q}\cdot[\boldsymbol{P}\times(\langle\boldsymbol{\sigma}\rangle_a+\langle\boldsymbol{\sigma}\rangle_b)]\Big\}, \end{aligned} \tag{C.23}$$

where we defined the coefficients

$$C_P = \frac{1}{4}\left(\frac{m_a}{m_b}+\frac{m_b}{m_a}-4\right) \quad \text{and} \quad C_q = \frac{1}{16}\left(\frac{m_a}{m_b}+\frac{m_b}{m_a}\right). \tag{C.24}$$

Similar to the PV amplitude, Eq. (C.21), we have essentially a spin-spin interaction with small second-order corrections due to the velocity of the fermions. It is worth noting that Eq. (C.23) presents an apparent divergence in the limit of a massless mediator, indicating that the interparticle potentials, as well as other quantities derived from this amplitude, will have an enhancement for light KRLPs. The velocity-dependent part of the NR T amplitude remains finite independently of m, but it is generally suppressed in a NR context.

C.2.3 Relevant integrals

Following Ref. [332], the potential may be obtained by taking the Fourier transform of the NR amplitudes, as defined in Eq. (7.14). To do that the necessary integrals are

$$\int\frac{d^3\mathbf{q}}{(2\pi)^3}\frac{1}{\boldsymbol{q}^2+m^2}e^{i\mathbf{q}\cdot\mathbf{r}} = \frac{1}{r}y(r), \tag{C.25}$$

$$\int\frac{d^3\mathbf{q}}{(2\pi)^3}\frac{\boldsymbol{q}^2}{\boldsymbol{q}^2+m^2}e^{i\mathbf{q}\cdot\mathbf{r}} = \delta^3(\boldsymbol{r})-\frac{m^2}{r}y(r), \tag{C.26}$$

$$\int\frac{d^3\mathbf{q}}{(2\pi)^3}\frac{\boldsymbol{q}_j}{\boldsymbol{q}^2+m^2}e^{i\mathbf{q}\cdot\mathbf{r}} = \frac{i(1+mr)}{r^2}\frac{r_j}{r}y(r), \tag{C.27}$$

$$\int\frac{d^3\mathbf{q}}{(2\pi)^3}\frac{\boldsymbol{q}_i\boldsymbol{q}_j}{\boldsymbol{q}^2+m^2}e^{i\mathbf{q}\cdot\mathbf{r}} = \frac{\delta_{ij}}{3}\delta^3(\mathbf{r})+\frac{1}{r^3}\left[(1+mr)\delta_{ij}-(3+3mr+m^2r^2)\frac{r_ir_j}{r^2}\right]y(r) \tag{C.28}$$

with $i,j=1,2,3$ and $y(r)=e^{-mr}/4\pi$. The Dirac delta in Eq. (C.28) stems from the fact that Eq. (C.26) = Tr {Eq. (C.28)} [340, 390].

C.3 The KRLP-mediated differential cross sections

In Sec. (7.2.2.1) we stated the s- and t-channel amplitudes for $2 \to 2$ lepton scattering in the CM frame. Assuming $s = E_{\rm CM}^2 \gg m_f^2$, the unpolarized differential cross section is [332]

$$\frac{d\sigma}{d\Omega} = \frac{1}{64\pi^2 s}\langle|\mathscr{M}|^2\rangle\,, \tag{C.29}$$

where $d\Omega = d\cos\theta d\phi$ and $\phi = [0, 2\pi]$. Here $\langle|\mathscr{M}|^2\rangle$ indicates averaging the amplitude squared over initial spins and summing over final spins; typically the result is independent of the azimuthal angle ϕ. If the amplitude is $\mathscr{M} = \mathscr{M}_1 + \mathscr{M}_2$ we will have "pure" contributions $\sim |\mathscr{M}_{1,2}|^2$, but also so-called interference terms $\sim |\mathscr{M}_1^\star \mathscr{M}_2|^2$.

For the KRLP scenario with PV vertices we find the following interference contributions with photon-mediated diagrams

$$\frac{d\sigma_\gamma^{\rm PV}}{d(\cos\theta)} = \frac{\alpha g_{\rm PV}^e g_{\rm PV}^e}{16\Lambda^2}\frac{y^2\left[\left(11-10x+12x^2+2x^3+x^4\right)-y^2\left(5-8x-6x^2+8x^3+x^4\right)\right]}{(1-x)\left(1-y^2\right)\left[2+(1-x)y^2\right]} \tag{C.30}$$

and with Z-mediated diagrams

$$\begin{aligned}
\frac{d\sigma_{\rm Z}^{\rm PV}}{d(\cos\theta)} = {}& \frac{g_{\rm PV}^e g_{\rm PV}^e}{32\pi\Lambda^2}\frac{g_Z^2 y^2 z^2}{\left(1-y^2\right)\left[2+(1-x)y^2\right]}\,\frac{1}{\left[\left(1-z^2\right)^2+w^2\right]\left[\left(z^2(1-x)+2\right)^2+4w^2\right]} \\
&\times\Bigg\{\left(g_V^2-g_A^2\right)\Bigg[(1+w^2)(1-x^2)-z^2\Big(\left(3-3x+x^2-x^3\right)-2w^2\left(1-2x+x^2\right)\Big) \\
&+\frac{1}{4}z^4\left(3-2x^2-x^4\right)+\frac{1}{4}z^6\left(5-12x+10x^2-4x^3+x^4\right)-\frac{1}{2}y^2\Big(\left(1+w^2\right)\left(5-7x+3x^2-x^3\right) \\
&-z^2\Big(\left(6-3x-5x^2+3x^3-x^4\right)-w^2\left(1-x-x^2+x^3\right)\Big)-\frac{1}{4}z^4\left(3-27x+30x^2-6x^3-x^4+x^5\right) \\
&+\frac{1}{4}z^6\left(7-11x-2x^2+10x^3-5x^4+x^5\right)\Big)\Bigg]+\left(g_V^2+g_A^2\right)\Bigg[\left(1+w^2\right)\left(x^3+3x^2+3x+1\right) \\
&-\frac{1}{4}z^2\Big(3\left(1+4x+6x^2+4x^3+x^4\right)+w^2\left(1+4x+6x^2+4x^3+x^4\right)\Big) \\
&-\frac{1}{8}z^4\left(3+3x-10x^2-18x^3-9x^4-x^5\right)+\frac{1}{8}z^6\left(1+3x+2x^2-2x^3-3x^4-x^5\right) \\
&+2y^2\Big(\left(1+w^2\right)\left(1+x-x^2-x^3\right)-\frac{1}{4}z^2\Big(3(1+2x-2x^3-x^4)+w^2\left(1+2x-2x^3-x^4\right)\Big)\Big) \\
&-\frac{1}{8}z^4\left(3-3x-10x^2+2x^3+7x^4+x^5\right)+\frac{1}{8}z^6\left(1+x-2x^2-2x^3+x^4+x^5\right)\Bigg]\Bigg\}\,,
\end{aligned} \tag{C.31}$$

where $x = \cos\theta$, $y = \sqrt{s}/m$, $z = \sqrt{s}/m_Z$ and $w = \Gamma_Z/m_Z$. Note the resonance at $y = 1$ ($\sqrt{s} = m$), as well as the forward divergence as $x \to 1$ inherited from QED. The pure PV diffferential cross section is

$$\begin{aligned}
\frac{d\sigma^{\rm PV}}{d(\cos\theta)} = {}& \left(\frac{g_{\rm PV}^e g_{\rm PV}^e}{\Lambda^2}\right)^2\frac{m^2}{256\pi}\frac{y^6}{\left(1-y^2\right)^2\left[2+(1-x)\,y^2\right]^2} \\
&\times\Big[\left(9-12x+14x^2+4x^3+x^4\right)+4y^2\left(3x+x^2-3x^3-x^4\right) \\
&+y^4(1-x)^2\left(9+6x+5x^2\right)\Big]\,.
\end{aligned} \tag{C.32}$$

The leading-order contribution from KRLPs with T vertices stems from interference with pure QED:

$$\frac{d\sigma_\gamma^{\mathrm{T}}}{d(\cos\theta)} = -\frac{\alpha g_{\mathrm{T}}^e g_{\mathrm{T}}^e}{8m^2}\frac{y^2\left[\left(3-24x+6x^2-x^4\right)-y^2\left(3-2x^2-x^4\right)\right]}{(1-x)\left(1-y^2\right)\left[2+(1-x)\,y^2\right]}, \tag{C.33}$$

where again the resonance at $y=1$ ($\sqrt{s}=m$) and the forward divergence at $x\to 1$ are present. The interference with Z-mediated diagrams is

$$\begin{aligned}\frac{d\sigma_{\mathrm{Z}}^{\mathrm{T}}}{d(\cos\theta)} = {}& \frac{g_{\mathrm{T}}^e g_{\mathrm{T}}^e}{32\pi m^2}\frac{g_Z^2(g_V^2-g_A^2)y^2z^2}{\left(1-y^2\right)\left[2+\left(1-x\right)y^2\right]}\frac{1}{\left[\left(1-z^2\right)^2+w^2\right]\left[\left(z^2\left(1-x\right)+2\right)^2+4w^2\right]}\\
&\times\left\{\left(1+w^2\right)\left(3+3x+x^2+x^3\right)-z^2\left[x\left(15-x+x^2+x^3\right)+w^2\left(3-9x+5x^2+x^3\right)\right.\right.\\
&-\frac{1}{4}z^4\left(9-21x-22x^2+6x^3-3x^4-x^5\right)-\frac{1}{4}z^6\left(3-27x+30x^2-6x^3-x^4+x^5\right)\Big]\\
&-y^2\left[\left(1+w^2\right)\left(3-9x+5x^2+x^3\right)+z^2\left(x\left(3+x-3x^2-x^3\right)-3w^2\left(1-x-x^2+x^3\right)\right)\right.\\
&\left.\left.-\frac{1}{4}z^4\left(9-21x+26x^2-10x^3-3x^4-x^5\right)-\frac{1}{4}z^6\left(3-3x-2x^2+2x^3-x^4+x^5\right)\right]\right\}.\end{aligned} \tag{C.34}$$

Finally, we also have the pure T contribution:

$$\begin{aligned}\frac{d\sigma^{\mathrm{T}}}{d(\cos\theta)} = {}& \frac{\left(g_{\mathrm{T}}^e g_{\mathrm{T}}^e\right)^2}{4\pi m^2}\frac{y^2}{\left(1-y^2\right)^2\left[2+(1-x)\,y^2\right]^2}\\
&\times\left[9\,(1+x)^2-\frac{9}{2}y^2\left(5+3x-x^2+x^3\right)+\frac{1}{8}y^4\left(153-60x+34x^2-52x^3+5x^4\right)\right.\\
&\left.+\frac{1}{4}y^6\left(27+15x+23x^2-15x^3+4x^4\right)+\frac{1}{8}y^8(1-x)^2\left(9+12x+7x^2\right)\right].\end{aligned} \tag{C.35}$$

C.4 Helicity eigenspinors: a brief overview

The evaluation of the unitarity bounds (7.44) depends on the calculation of the amplitudes with all possible helicity states consistent with the total angular momentum J of the partial wave under consideration. For this we must first find the basic spinors pointing at a generic direction $\hat{\boldsymbol{n}}=(\sin\theta\cos\phi,\sin\theta\sin\phi,\cos\theta)$, where θ is the polar angle relative to the (positive) z-axis and ϕ is the azimuthal angle for a counter-clockwise rotation on the $x-y$ plane. We choose the coordinate system so that the initial electron-positron beam runs on the z-axis. It is therefore convenient to quantize the spin on the z-axis and take the eigenvectors of σ_z as the basic spinors

$$\xi_+=\begin{pmatrix}1\\0\end{pmatrix}\quad\text{and}\quad\xi_-=\begin{pmatrix}0\\1\end{pmatrix}. \tag{C.36}$$

We must now rotate $\xi_\pm$ toward $\hat{\boldsymbol{n}}$ by means of the matrix $U(\omega)=\exp\left(-i\omega_{\mu\nu}S^{\mu\nu}/2\right)$, where $S^{\mu\nu}=(i/4)\left[\gamma^\mu,\gamma^\nu\right]$ are the generators of Lorentz boosts and spatial rotations. Starting at

$\theta = \phi = 0$ we first rotate around the y-axis by an angle $\omega_{31} = -\omega_{13} = \theta$ and then around the z-axis by an angle $\omega_{12} = -\omega_{21} = \phi$. The unitary operator that accomplishes this is $U(\theta,\phi) = e^{-i(\phi/2)\sigma_z} e^{-i(\theta/2)\sigma_y}$, which can be explicitly written as

$$U(\theta,\phi) = e^{-i\phi/2} \begin{pmatrix} \cos\frac{\theta}{2} & -\sin\frac{\theta}{2} \\ e^{i\phi}\sin\frac{\theta}{2} & e^{i\phi}\cos\frac{\theta}{2} \end{pmatrix}. \tag{C.37}$$

The overall phase factor is inconsequential and will be henceforth omitted. The basic spinors along $\hat{\boldsymbol{n}}$ are then $U(\theta,\phi)\xi_\pm = \xi'_\pm$, namely

$$\xi'_+ = \begin{pmatrix} \cos\frac{\theta}{2} \\ e^{i\phi}\sin\frac{\theta}{2} \end{pmatrix} \quad \text{and} \quad \xi'_- = \begin{pmatrix} -\sin\frac{\theta}{2} \\ e^{i\phi}\cos\frac{\theta}{2} \end{pmatrix}. \tag{C.38}$$

As expected, these basic spinors also form an orthonormal basis.

Again starting from a particle moving in the positive z-direction described by the spinor (7.10) with $\boldsymbol{p} = (0,0,|\boldsymbol{p}|)$ we find the associated rotated spinor by applying $U(\theta,\phi)$ to the upper and lower components. For the upper component we get simply $\xi'_\pm$, whereas the lower component is proportional to $U(\theta,\phi)\sigma_z\xi_\pm$. However, we know that the basic spinors $\xi_\pm$ are eigenvectors of σ_z with $\sigma_z\xi_\pm = \pm\xi_\pm$, so that the lower component turns out to be $\dfrac{\pm|\boldsymbol{p}|}{E+m_f}\xi'_\pm$. This makes sense, since the rotated spinors are eigenvectors of $\boldsymbol{\sigma}\cdot(|\boldsymbol{p}|\hat{\boldsymbol{n}})$. A similar procedure must be applied to the spinor for anti-particles. Therefore, the spinors for particles and anti-particles moving with 3-momentum of magnitude $|\boldsymbol{p}|$ in a generic direction $\hat{\boldsymbol{n}}$ are

$$u^\pm(p) = N_{\mathrm{R}} \begin{pmatrix} \xi'_\pm \\ \dfrac{\pm|\boldsymbol{p}|}{E+m_f}\xi'_\pm \end{pmatrix} \quad \text{and} \quad v^\pm(p) = \pm N_{\mathrm{R}} \begin{pmatrix} \dfrac{\mp|\boldsymbol{p}|}{E+m_f}\xi'_\mp \\ \xi'_\mp \end{pmatrix} \tag{C.39}$$

with $N_{\mathrm{R}} = \sqrt{E+m_f}$. These spiunors satisfy $u^\dagger_\pm u_\pm = v^\dagger_\pm v_\pm = 2E$ and $\bar{u}_\pm u_\pm = -\bar{v}_\pm v_\pm = 2m$; all other combinations are zero.

The helicity operator, given by $\hat{h} = \boldsymbol{\Sigma}\cdot\hat{\boldsymbol{p}}$ with $\boldsymbol{\Sigma} = \mathrm{diag}(\boldsymbol{\sigma},\boldsymbol{\sigma})$ and $\hat{\boldsymbol{p}} = \boldsymbol{p}/|\boldsymbol{p}| = \hat{\boldsymbol{n}}$, projects the spin along the direction of motion. Noting that $(\boldsymbol{\sigma}\cdot\hat{\boldsymbol{n}})\xi'_\pm = \pm\xi'_\pm$ and keeping in mind that the helicity operator applied to anti-particles is defined as $\hat{h}_v \equiv -\hat{h}$, we find

$$\hat{h}u^\pm(p) = \pm u^\pm(p) \quad \text{and} \quad \hat{h}_v v^\pm(p) = \pm v^\pm(p). \tag{C.40}$$

The subscripts $\pm$ label the helicity eigenvalues of the spinors, ±1. Finally, in the ultra-relativist regime, where $E = \sqrt{s}/2 \gg m_f$, the spinors (C.39) simplify to

$$u^\pm(p) = \sqrt{E}\begin{pmatrix} \xi'_\pm \\ \pm\xi'_\pm \end{pmatrix} \quad \text{and} \quad v^\pm(p) = \pm\sqrt{E}\begin{pmatrix} \mp\xi'_\mp \\ \xi'_\mp \end{pmatrix}. \tag{C.41}$$

References

[1] J. Bernstein, *Spontaneous symmetry breaking, gauge theories, Higgs mechanism an all that*, Rev. Mod. Phys. **46**, 7 (1974).

[2] M.E. Peskin, *Lectures on the theory of the weak interaction*, arXiv:1708.09043.

[3] F.J. Gilman, K. Kleinknecht , and B Renk, *The Cabibbo-Kobayashi-Maskawa quark mixing matrix: in Review of Particle Physics (RPP 2000)*, Eur. Phys. J. C **15**, 110 (2000).

[4] A. Hook, *TASI Lectures on the Strong CP Problem and Axions*, arXiv:1812.02669v3.

[5] Super-Kamiokande Collaboration, *Evidence for Oscillation of Atmospheric Neutrinos*, Phys. Rev. Lett. **81**, 1562 (1998).

[6] C. Giganti, S. Lavignac, and M. Zito, *Neutrino oscillations: The rise of the PMNS paradigm*, Prog. Part. Nucl. Phys. **98**, 1 (2018).

[7] C. Giganti, S. Lavignac, M. Zito, *Neutrino oscillations: The rise of the PMNS paradigm*, Prog. Part. Nucl. Phys. **98**, 1 (2018).

[8] A. Gouvêa, *Neutrino mass models*, Annu. Rev. Nucl. Part. Sci. **66**, 197 (2016).

[9] N. Craig, *Naturalness: past, present, and future*, Eur. Phys.J. C **83**, 825 (2023).

[10] M.E. Peskin, *What is the Hierarchy Problem?*, Nucl. Phys. B **1018**, 116971 (2025).

[11] G.G. Ross, *SUSY: Quo Vadis?*, Eur. Phys. J. C **74**, 2699 (2014).

[12] N. Arkani-Hamed, L. Hall, D. Smith, and N. Weiner, *Solving the hierarchy problem with exponentially large dimensions*, Phys. Rev. D **62**, 105002 (2000).

[13] V. Baluni, *CP-nonconserving effects in quantum chromodynamics*, Phys. Rev. D **19**, 2227 (1979).

[14] R. J. Crewther, P. Di Vecchia, G. Veneziano e E. Witten, *Chiral estimate of the electric dipole moment of the neutron in quantum chromodynamics*, Phys. Lett. B **88**, 123 (1979); *Erratum* Phys. Lett. B **91**, 487(E) (1980).

[15] C. Abel *et al.*, *Measurement of the permanent electric dipole moment of the neutron*, Phys. Rev. Lett. **124**, 081803 (2020).

[16] R. D. Peccei e H. R. Quinn, *CP Conservation in the Presence of Pseudoparticles*, Phys. Rev. Lett. **38**, 1440 (1977).

[17] R. D. Peccei e H. R. Quinn, *Constraints imposed by CP conservation in the presence of pseudoparticles*, Phys. Rev. D. **16**, 1791 (1977).

[18] G. von Gersdorff and L. Modesto, *Inequalities for Standard Model Yukawa couplings*, JHEP **09**, 140 (2025).

[19] J.L. Feng, *Naturalness and the Status of Supersymmetry*, Annu. Rev. Nucl. Part. Sci. **63**, 351 (2013).

[20] B. Bellazzini, C. Csáki, and J. Serra, *Composite Higgses*, Eur. Phys. J. C **74**, 2766 (2014).

[21] P. Draper and H. Rzehak, *A review of Higgs mass calculations in supersymmetric models*, Phys. Rep. **619**, 1 (2016).

[22] D.J.E. Callaway, *Triviality pursuit: Can elementary scalar particles exist?*, Phys. Rep. **167**, 241 (1988).

[23] M.S. Chanowitz, *New physics and the Landau pole*, Phys. Rev. D **63**, 076002 (2001).

[24] K. Lane, *An introduction to technicolor*, arXiv:hep-ph/9401324.

[25] BABAR Collaboration, *Evidence for an excess of* $\bar{B} \to D^{(*)}\tau^-\bar{\nu}_\tau$ *decays*, Phys. re. Lett. **109**, 101802 (2012).

[26] HFLAV Collaboration, *Averages of b-hadron, c-hadron, and* τ^- *lepton properties as of summer 2016*, Eur. Phys. J. C **75**, 895 (2016).

[27] ACME Collaboration, *Improved limit on the electric dipole moment of the electron*, Nature **562**, 355 (2018).

[28] S. Roussy *et al.*, *An improved bound on the electron's electric dipole moment*, Science **381**, 46 (2023).

[29] Y. Yamaguchi and N. Yamanaka, *Large long-distance contributions to the electric dipole moments of charged leptons in the standard model*. Phys. Rev. Lett. **125**, 241802 (2020).

[30] Muon $g-2$ Collaboration, *Measurement of the Positive Muon Anomalous Magnetic Moment to* 0.46 *ppm*, Phys. Rev. Lett. **126**, 141801 (2021).

[31] Muon $g-2$ Collaboration, *Measurement of the Positive Muon Anomalous Magnetic Moment to* 0.20 *ppm*, Phys. Rev. Lett. **131**, 161802 (2023).

[32] T. Aoyama *et al.*, *The anomalous magnetic moment of the muon in the Standard Model*, Phys. Rep. **887**, 1 (2020).

[33] Muon $g-2$ Collaboration, *Measurement of the Positive Muon Anomalous Magnetic Moment to* 127 *ppb*, Phys. Rev. Lett. **131**, 101802 (2025).

[34] R. Aliberti *et al.*, *The anomalous magnetic moment of the muon in the standard model: An update*, Phys. Rept. **1143**, 1 (2025).

[35] J-PARC muon g-2/EDM experiment (E34), https://inspirehep.net/experiments/1394980?ui-citation-summary=true.

[36] D.S. Pereira, J. Ferraz, F.S.N. Lobo, and J.P. Mimoso, *Baryogenesis: A Symmetry Breaking in the Primordial Universe Revisited*, Symmetry **16**, 13 (2024).

[37] W. Buchmüller, R.D. Peccei, and T. Yanagida, *Leptogenesis as the Origin of Matter*, Annu. Rev. Nucl. Part. Sci. **55**, 311 (2005).

[38] K. Arun, S.B. Gudennavar, and C Sivaram, *Dark matter, dark energy, and alternate models: A review*, Adv. Space Res. **60**, 166 (2017).

[39] S. Navas *et al.*, *Particle Data Group*, Phys. Rev. D **110**, 030001 (2024) and 2025 update.

[40] A. Crivellin and B. Mellado, *Anomalies in particle physics and their implications for physics beyond the standard model*, Nat. Rev. Phys. **6**, 294 (2024).

[41] V.A. Kostelecký and M. Mewes, *Signals for Lorentz Violation in Electrodynamics*, Phys. Rev. D **66**, 056005 (2002).

[42] J.P.S. Melo and J.A. Helayël-Neto, *From the Aether questioned by Dirac to the Standard Model: the diachrony of Lorentz-symmetry violation*, Rev. Bras. Ens. Fis. **45**, e20220211 (2023).

[43] P.A.M. Dirac, *Is there an aether?*, Nature **168**, 906 (1951).

[44] H. Bondi and T. Gold, *Is there an aether?*, Nature **169**, 146 (1952).

[45] J.D. Bjorken, *A dynamical origin for the electromagnetic field*, Ann. Phys. **24**, 174 (1963).

[46] T.G. Pavlopoulos, *Breakdown of Lorentz invariance*, Phys. Rev. **159**, 1106 (1967).

[47] P.R. Phillips, *Is the graviton a goldstone boson?*, Phys. Rev. **146**, 966 (1966).

[48] L.B. Rédei, *Validity of special relativity at small distances and the velocity dependence of the muon lifetime*, Phys. Rev. **162**, 1299 (1967).

[49] H.B. Nielsen and M. Ninomiya, *Lorentz invariance as a low energy phenomenon*, Nucl. Phys. B **141**, 153 (1978).

[50] J. Ellis, M.K. Gaillard, D.V. Nanopoulos, and S. Rudaz, *Uncertainties in the proton lifetime*, Nucl. Phys. B **176**, 61 (1980).

[51] A. Zee, *Perhaps proton decay violates Lorentz invariance*, Phys. Rev. D **25**, 1864 (1982).

[52] H.B. Nielsen and I. Picek, *The Rédei-like model and testing Lorentz invariance*, Phys. Lett. B **114**, 141 (1982).

[53] H.B. Nielsen and S. Chadha, *Lorentz invariance as a low energy phenomenon*, Nucl. Phys. B **217**, 125 (1983).

[54] H.B. Nielsen and I. Picek, *Lorentz non-invariance*, Nucl. Phys. B **211**, 269 (1983).

[55] V.A. Kostelecký and S. Samuel, *Spontaneous breaking of Lorentz symmetry in string theory*, Phys. Rev. D **39**, 683 (1989).

[56] V.A. Kostelecký and S. Samuel, *Phenomenological gravitational constraints on strings and higher-dimensional theories*, Phys. Rev. Lett. **63**, 224 (1989).

[57] S.M. Carroll, G.B. Field and R. Jackiw, *Limits on a Lorentz- and parity-violating modification of electrodynamics*, Phys. Rev. D **41**, 1231 (1990).

[58] C. Adam and F.R. Klinkhamer, *Causality and CPT violation from an Abelian Chern–Simons-like term*, Nucl. Phys. B **607**, 247 (2001).

[59] A.P. Baêta Scarpelli, H. Belich, J.L. Boldo, and J.A. Helayël-Neto, *Aspects of causality and unitarity and comments on vortexlike configurations in an Abelian model with a Lorentz-breaking term*, Phys. Rev. D **67**, 085021 (2003).

[60] D. Colladay and V.A. Kostelecký, *CPT violation and the standard model*, Phys. Rev. D **55**, 6760 (1997).

[61] D. Colladay and V.A. Kostelecký, *Lorentz-violating extension of the standard model,* Phys. Rev. D **58**, 116002 (1998).

[62] V.A. Kostelecký, *Gravity, Lorentz violation, and the standard model*, Phys. Rev. D **69**, 105009 (2004).

[63] G. Amelino-Camelia, J. Ellis, N. Mavromatos, and D.V. Nanopoulos, *Distance measurement and wave dispersion in a Liouville-string approach to quantum gravity*, Int. J. Mod. Phys. A **12**, 607 (1997).

[64] G. Amelino-Camelia, J.R. Ellis, N.E. Mavromatos, D.V. Nanopoulos, and S. Sarkar, *Tests of quantum gravity from observations of gamma-ray bursts*, Nature **393**, 763 (1998).

[65] J. Ellis, N. Mavromatos, and D.V. Nanopoulos, *Probing models of quantum space–time foam*, arXiv:gr-qc/9909085.

[66] R. Aloisio, P. Blasi, P.L. Ghia, and A.F. Grillo, *Probing the structure of space-time with cosmic rays*, Phys. Rev. D **62**, 053010 (2000).

[67] R. Gambini and J. Pullin, *Nonstandard optics from quantum space-time*, Phys. Rev. D **59**, 124021 (1999).

[68] G. Amelino-Camelia and S. Majid, *Waves on noncommutative spacetime and gamma-ray bursts*, Int. J. Mod. Phys. A **15**, 4301 (2000).

[69] J. Alfaro, H.A. Morales-Tecotl, and L.F. Urrutia, *Loop quantum gravity and light propagation*, Phys. Rev. D **65**, 103509 (2002).

[70] N. Seiberg and E. Witten, *String theory and noncommutative geometry*, JHEP **09**, 032 (1999).

[71] S.M. Carroll, J.A. Harvey, V.A. Kostelecký, C.D. Lane, and T. Okamoto, *Noncommutative field theory and Lorentz violation*, Phys. Rev. Lett. **87**, 141601 (2001).

[72] S. Coleman and S.L. Glashow, *High-energy tests of Lorentz invariance*, Phys. Rev. D **59**, 116008 (1999).

[73] G. Amelino-Camelia, *Doubly-special relativity: first results and key open problems*, Int. J. Mod. Phys. D, **11**, 1643 (2002).

[74] J. Magueijo, *New varying speed of light theories*, Rept. Prog. Phys. **66**, 2025 (2003).

[75] J. Kowalski-Glikman, *Introduction to doubly special relativity*, Lect. Notes Phys. **669**, 131 (2005).

[76] V.A. Kostelecký and N. Russel, *Data tables for Lorentz and CPT violation*, arXiv:0801.0287v18.

[77] J. Bolmont and C. Perennes, *Probing modified dispersion relations in vacuum with high-energy γ-ray sources: review and prospects*, J. Phys.: Conf. Ser. **1586**, 012033 (2020).

[78] R. Bluhm, V.A. Kostelecký, C. Lane, and N. Russell, *Clock-Comparison Tests of Lorentz and CPT Symmetry in Space*, Phys. Rev. Lett. **88**, 090801 (2002).

[79] R. Bluhm, V.A. Kostelecký, C. Lane, and N. Russell, *Probing Lorentz and CPT Violation with Space-Based Experiments*, Phys. Rev. D **68**, 125008 (2003).

[80] P. Delva, *et al.*, *Test of special relativity using a fiber network of optical clocks*, Phys. Rev. Lett. **118**, 221102 (2017).

[81] V.A. Kostelecký and A.J. Vargas, *Lorentz and CPT Tests with Clock-Comparison Experiments*, Phys. Rev. D **98**, 036003 (2018).

[82] C. Sanner, N. Huntemann, R. Lange, C. Tamm, E. Peik, M.S. Safronova, and S.G. Porsev, *Optical clock comparison for Lorentz symmetry testing*, Nature **567**, 204 (2019).

[83] V.A. Kostelecký and M. Mewes, *Cosmological constraints on Lorentz violation in electrodynamics*, Phys. Rev. Lett. **87**, 251304 (2001).

[84] V.A. Kostelecký and M. Mewes, *Astrophysical Tests of Lorentz and CPT violation with photons*, Astrophys. J. Lett. **689**, L1 (2008).

[85] V.A. Kostelecký and M. Mewes, *Constraints on relativity violations from gamma-ray bursts*, Phys. Rev. Lett. **110**, 201601 (2013).

[86] S. Meuren, C.H. Keitel, and A. Di Piazza, *High-energy vacuum birefringence and dichroism in an ultrastrong laser field sergey bragin*, Phys. Rev. Lett. **119**, 250403 (2017).

[87] G.W. Bennett, *et al.*, *Search for Lorentz and CPT violation effects in muon spin precession*, Rev. Lett. **100**, 091602 (2008).

[88] F. Allmendinger, W. Heil, S. Karpuk, W. Kilian, A. Scharth, U. Schmidt, A. Schnabel, Y. Sobolev, and K. Tullney, *New limit on Lorentz-invariance- and CPT-violating neutron spin interactions using a free-spin-precession ^{3}He-^{129}Xe comagnetometer*, Phys. Rev. Lett. **112**, 110801 (2014).

[89] A. Gomes, V.A. Kostelecký, and A.J. Vargas, *Laboratory tests of Lorentz and CPT symmetry with muons*, Phys. Rev. D **90**, 076009 (2014).

[90] Y. Ding and V.A. Kostelecký, *Lorentz-Violating Spinor Electrodynamics and Penning Traps*, Phys. Rev. D **94**, 065008 (2016).

[91] L.S. Dreissen, C.-H. Yeh, H.A. Fürst, K.C. Grensemann, and T.E. Mehlstäubler, *Improved bounds on Lorentz violation from composite pulse Ramsey spectroscopy in a trapped ion*, Nature Commun. **13**, 7314 (2022).

[92] G. Amelino-Camelia, D. Guetta, and T. Piran, *IceCube neutrinos and Lorentz invariance violation*, ApJ **806**, 269 (2015).

[93] G. Amelino-Camelia, L. Barcaroli, G. D'Amico, N. Loret, and G. Rosati, *IceCube and GRB neutrinos propagating in quantum spacetime*, Phys. Lett. B **761**, 318 (2016).

[94] J.S. Diaz, *Testing Lorentz and CPT invariance with neutrinos*, Symmetry **8**, 105 (2016).

[95] J.S. Diaz and T. Schwetz, *Limits on CPT violation from solar neutrinos*, Phys. Rev. D **93**, 093004 (2016).

[96] G. Amelino-Camelia, G. D'Amico, G. Rosati, and N. Loret, *In-vacuo-dispersion features for GRB neutrinos and photons*, Nature Astron. **1**, 0139 (2017).

[97] Y. Huang and B.-Q. Ma, *Lorentz violation from gamma-ray burst neutrinos*, Commun. Phys. **1**, 62 (2018).

[98] Y. Huang, H. Li and B.-Q. Ma, *Consistent Lorentz violation features from near-TeV IceCube neutrinos*, Phys. Rev. D **99**, 123018 (2019).

[99] Y. Huang and B.-Q. Ma, *Ultra-high energy cosmic neutrinos from gamma-ray bursts*, Fundam. Res. (2022).

[100] L. Shao, Z. Xiao and B.-Q. Ma, *Lorentz violation from cosmological ob jects with very high energy photon emissions*, Astropart. Phys. **33**, 312 (2010).

[101] S. Zhang and B.-Q. Ma, *Lorentz violation from gamma-ray bursts*, Astropart. Phys. **61**, 108 (2015).

[102] H. Xu and B.-Q. Ma, *Light speed variation from gamma-ray bursts*, Astropart. Phys. **82**, 72 (2016).

[103] H. Xu and B.-Q. Ma, *Light speed variation from gamma-ray burst GRB 160509A*, Phys. Lett. B **760**, 602 (2016).

[104] Y. Liu and B.-Q. Ma, *Light speed variation from gamma ray bursts: criteria for low energy photons*, EPJ C **78**, 825 (2018).

[105] H. Li and B.-Q. Ma, *Light speed variation from active galactic nuclei*, Sci. Bull. **65**, 262 (2020).

[106] J. Zhu and B.-Q. Ma, *Pre-burst events of gamma-ray bursts with light speed variation*, Phys. Lett. B **820**, 136518 (2021).

[107] G. Amelino-Camelia, G. D'Amico, F. Fiore, S. Puccetti, and M. Ronco, *In vacuo dispersion-Like spectral lags in gamma-ray bursts*, Symmetry **13**, 541 (2021).

[108] Y.M.P. Gomes and P.C. Malta, *Laboratory-based limits on the Carroll-Field-Jackiw Lorentz-violating electrodynamics*, Phys. Rev. D **94**, 025031 (2016).

[109] M. Schreck, *Fermionic Lorentz violation and its implications for interferometric gravitational-wave detection*, Class. Quant. Grav. **34**, 135009 (2017).

[110] J.B. Araujo, B. Hiller, I.G. da Paz, M.M. Ferreira Jr., and Marcos Sampaio, *Measuring QED cross sections via entanglement*, Phys. Rev. D **100**, 105018 (2019).

[111] Y.M.P. Gomes, P.C. Malta, and M.J. Neves, *Testing Lorentz-symmetry violation via electroweak decays*, Phys. Rev. D **101**, 075001 (2022).

[112] A. Crivellin, F. Kirk, and M. Schreck, *Impact of Lorentz violation on anomalous magnetic moments of charged leptons*, JHEP **11**, 109 (2022).

[113] C.-G. Qin, T. Liu, J.-Z. Dong, X.-Y. Dai, Yu-Jie Tan, and C.-G. Shao, *Tidal Effects and Clock Comparison Experiments*, Universe **9**, 133 (2023).

[114] V.A. Kostelecký, R. Lehnert, N. McGinnis, M. Schrecke, and B. Seradjeh, *Lorentz violation in Dirac and Weyl semimetals*, Phys. Rev. Res. **4**, 023106 (2022).

[115] V.A. Kostelecký, R. Lehnert, M. Schreck, B. Seradjeh, *Physical interpretation of large Lorentz violation via Weyl semimetals*, New Journal Physics **27**, 073901 (2025).

[116] V.A. Kostelecký, R. Lehnert, M. Schreck, B. Seradjeh, *Nonperturbative Lorentz Violation and Field Quantization*, Phys. Lett. B **865**, 139414 (2025)

[117] O.W. Greenberg, *CPT violation implies violation of Lorentz invariance*, Phys. Rev. Lett. **89**, 231602 (2002).

[118] O.W. Greenberg, *Why is CPT fundamental?*, Found. Phys. **36**, 1535 (2006).

[119] R. Lehnert, *CPT symmetry and its violation*, Simmetry **11**, 114 (2016).

[120] V.A. Kostelecký and M. Mewes, *Lorentz and CPT violation in neutrinos*, Phys. Rev. D **69**, 016005 (2004).

[121] R. Bluhm and Y. Zhi, *Spontaneous and Explicit Spacetime Symmetry Breaking in Einstein–Cartan Theory with Background Fields*, Symmetry **16**, 25 (2024).

[122] J.P.S. Melo and J.A. Helayël-Neto, *Re-assessing special aspects of Dirac fermions in presence of Lorentz-symmetry violation*, Annals Phys. **470**, 169790 (2024).

[123] R. Lehnert, *Beta-decay spectrum and Lorentz violation*, Phys. Lett. B **828**, 137017 (2022).

[124] V.A. Kostelecký and J. Tasson, *Matter-gravity couplings and Lorentz violation* Phys. Rev. D **83**, 016013 (2011).

[125] V.A. Kostelecký, *Riemann-Finsler geometry and Lorentz-violating kinematics*, Phys. Lett. B **701**, 137 (2011).

[126] V.A. Kostelecký and M. Mewes, *Testing local Lorentz invariance with gravitational waves*, Phys. Lett. B **757**, 510 (2016).

[127] B. Altschul, *Eliminating the CPT-odd f coefficient from the Lorentz-violating standard model extension*, J. Phys. A: Math. Gen. **39**, 13757 (2006).

[128] D. Colladay and P. McDonald, *Redefining spinors in Lorentz-violating quantum electrodynamics*, J. Math. Phys. **43**, 3554 (2002).

[129] V.A. Kostelecký and R. Lehnert, *Stability, causality, and Lorentz and CPT violation*, Phys. Rev. D **63**, 065008 (2001).

[130] R. Jackiw and V. Alan Kostelecký, *Radiatively Induced Lorentz and CPT Violation in Electrodynamics*, Phys. Rev. Lett. **82**, 3572 (1999).

[131] V.A. Kostelecký and M. Mewes, *Electrodynamics with Lorentz-violating operators of arbitrary dimension*, Phys. Rev. D **80**, 015020 (2009).

[132] V.A. Kostelecký and M. Mewes, *Fermions with Lorentz-violating operators of arbitrary dimension*, Phys. Rev. D **88**, 096006 (2013).

[133] P.D.S. Silva, L. Lisboa-Santos, M.M. Ferreira Jr., and M. Schreck, *Effects of CPT-odd terms of dimensions three and five on electromagnetic propagation in continuous matter*, Phys. Rev. D **104**, 116023 (2021).

[134] V. A Kostelecký, *Progress in Lorentz and CPT Violation*, arXiv:2512.23873.

[135] V.A. Kostelecký, R. Lehnert, M. Schreck, B. Seradjeh, *Lorentz violation and momentum-space geometric phases*, arXiv:2512.01156.

[136] V.A. Kostelecký and Z. Li, *Searches for beyond-Riemann gravity*, Phys. Rev. D **104**, 044054 (2021).

[137] C. Pfeifer, *Finsler spacetime geometry in physics*, Int. J. Geom. Methods Mod. Phys. **16**, 941004 (2019).

[138] J. Zhu, B.-Q. Ma, *Lorentz Violation in Finsler Geometry*, Symmetry **15**, 978 (2023).

[139] V.A. Kostelecký *Riemann-Finsler geometry and Lorentz-violating kinematics*, Phys. Lett. B **701**, 137 (2011).

[140] J. Alfaro and L.F. Urrutia, *Gauge invariant nonlinear electrodynamics motivated by a spontaneous breaking of the Lorentz symmetry*, Phys. Rev. D **81**, 025007 (2010).

[141] F. Gliozzi, *Dirac-Born-Infeld action from spontaneous breakdown of Lorentz symmetry in brane-world scenarios*, Phys. Rev. D **84**, 027702 (2011).

[142] R. Bufalo, *Born-Infeld electrodynamics in very special relativity* , Phys. Lett. B **746**, 251 (2015).

[143] J.M.A. Paixão, L.P.R. Ospedal, M.J. Neves, and J.A. Helayël-Neto, *Probing the interference between non-linear, axionic and space-time-anisotropy effects in the QED vacuum*, JHEP **05**, 029 (2024).

[144] W. Heisenberg and H. Euler, Z. Physik, *Consequences of Dirac Theory of the Positron*, *98*, 714 (1936), arXiv:physics/0605038.

[145] J.S. Shwinger, *On Gauge Invariance and Vacuum Polarization*, Phys. Rev. **82**, 664 (1951).

[146] I.N. McArthur and T.D. Gargett, *A "Gaussian" approach to computing supersymmetric effective actions*, Nucl. Phys. B **497**, 525 (1997).

[147] ATLAS Collaboration, *Evidence for light-by-light scattering in heavy-ion collisions with the ATLAS detector at the LHC*, Nat. Phys. **13**, 852 (2017).

[148] ATLAS Collaboration, *Observation of Light-by-Light Scattering in Ultraperipheral Pb + Pb Collisions with the ATLAS Detector*, Phys. Rev. Lett. **123**, 052001 (2019).

[149] CMS Collaboration, *Evidence for light-by-light scattering and searches for axion-like particles in ultraperipheral PbPb collisions at* $\sqrt{s_{NN}} = 5.02$ *TeV*, Phys. Lett. B **797**, 134826 (2019).

[150] C.-L. Zhang, C. M. Wang, Z. Yuan, X. Xu, G. Wang, C.-C. Lee, L. Pi, C. Xi, H. Lin, N. Harrison, H.-Z. Lu, J. Zhang, and S. Jia, *Non-saturating quantum magnetization in Weyl semimetal TaAs*, Nat. Commun. **10**, 1028 (2019).

[151] A. Iwasa, A. Kondo, S. Kawachi, K. Akiba, Y. Nakanishi, M. Yoshizawa, M. Tokunaga, and K. Kindo, *Thermodynamic evidence of magnetic-field-induced complete valley polarization in bismuth*, Sci. Rep. **9**, 1672 (2019).

[152] A.C. Keser, Y. Lyanda-Geller, and O.P. Sushkov, *Nonlinear Quantum Electrodynamics in Dirac Materials*, Phys. Rev. Lett. **128**, 066402 (2022).

[153] J. Furtado and T. Mariz, *Lorentz-violating Euler-Heisenberg effective action*, Phys. Rev. D **89**, 025021 (2014).

[154] L.H.C. Borges, A.G. Dias, A.F. Ferraria, J.R. Nascimento, and A.Yu. Petrov, *Generation of higher derivatives operators and electromagnetic wave propagation in a Lorentz-violation scenario*, Phys. Lett. B **756**, 332 (2016).

[155] A.F. Ferrari, J. Furtado, J.F. Assunção, T. Mariz, and A.Yu. Petrov, *One-loop calculations in Lorentz-breaking theories and proper-time method*, EPL **136**, 21002 (2021).

[156] L.C.T. Brito, J.C.C. Felipe, A.C. Lehum, J.R. Nascimento, and A.Yu. Petrov *Modified Euler-Heisenberg effective action and Proper-Time Method in Lorentz-Violating Scalar QED*, Int. J. Mod. Phys. A **40**, 255067 (2025).

[157] R. Araújo, T. Mariz, J.R. Nascimento, and A.Yu. Petrov, *One-loop Euler-Heisenberg action in Lorentz-violating QED revisited*, Phys. Lett. B **873**, 140213 (2026).

[158] Filip Přeučil and Jiří Hořejší, *Effective Euler–Heisenberg Lagrangians in models of QED*, J. Phys. G: Nucl. Part. Phys. **45**, 085005 (2018).

[159] M. Marklund and P.K. Shukla, *Nonlinear collective effects in photon-photon and photon-plasma interactions*, Rev. Mod. Phys. **78**, 591 (2006).

[160] B. Altschul, *Improved Bounds on Lorentz Symmetry Violation from High-Energy Astrophysical Sources*, Symmetry **13**, 688 (2021).

[161] A.V. Ivanov and N.V. Kharuk, *Heat kernel: proper time method, Fock-Schwinger gauge, path integral representation, and Wilson line*, Theor. Math. Phys. **205**, 1456 (2020).

[162] D.M. Nenno, C.A.C. Garcia, J. Gooth, C. Felser, and P. Narang, *Axion physics in condensed-matter systems*, Nat. Rev. Phys. **2**, 682 (2020).

[163] J. Gooth *et. al.*, *Axionic charge-density wave in the Weyl semimetal* $(TaSe_4)_2I$, Nature **575**, 315 (2019).

[164] A. Sekine and K. Nomura, *Axion electrodynamics in topological materials*, J. Appl. Phys. **129**, 141101 (2021).

[165] A.A. Grigoreva, A.V. Andreev, and L.I. Glazman, *Axion Electrodynamics and Giant Magnetic Birefringence in Weyl Excitonic Insulators* Phys. Rev. Lett. **135**, 21660 (2025).

[166] P. Sikivie, *Invisible Axion Search Methods*, Rev. Mod. Phys. **93**, 15004 (2021).

[167] Wolfram Research, Inc., *Mathematica,* (Version 14.0, Champaign, IL, 2025); and for details related to the xAct package see https://www.xact.es/index.html.

[168] W.H. Furry, *On Bound States and Scattering in Positron Theory*, Phys, Rev. **81**, 115 (1951).

[169] V.A. Kostelecký, C.D. Lane, and A.G.M. Pickering, *One-loop renormalization of Lorentz-violating electrodynamics*, Phys. Rev. D **65**, 056006 (2002).

[170] T. Kubota, *Overview of Triple and Quartic Gauge Coupling Measurements at the LHC*, arXiv:1408.6604v1.

[171] A. Kupco, *Triple and quartic gauge boson couplings at the LHC*, Nuovo Cim. C **40**, 202 (2018).

[172] J.S. Dowker, *On the relevance of the multiplicative anomaly,* arXiv:hep-th/9803200.

[173] T.S. Evans, *Regularization schemes and the multiplicative anomaly,* Phys. Lett. B **457**, 127 (1999).

[174] B. Gonçalves, G. de Berredo-Peixoto and I.L. Shapiro, *One-loop corrections to the photon propagator in curved-space QED,* Phys. Rev. D **80**, 104013 (2009).

[175] R. Bluhm, V.A. Kostelecký, *Spontaneous Lorentz Violation, Nambu-Goldstone Modes, and Gravity*, Phys. Rev. D **71**, 065008 (2005).

[176] L. Bonetti, L.R. dos Santos Filho, J.A. Helayël-Neto, and A.D.A.M. Spallicci, *Photon sector analysis of Super and Lorentz symmetry breaking: effective photon mass, bi-refringence and dissipation*, Eur. Phys. J. C, **78** 811 (2018).

[177] E.R. Tracy, A.J. Brizard, A.S. Richardson, and A.N. Kaufman, *Ray Tracing and Beyond: Phase Space Methods in Plasma Wave Theory*, (Cambridge University Press, New York, 2014).

[178] B. Goncalves, G. Berredo-Peixoto, and I.L. Shapiro, *Exact formfactors in the one-loop curved-space QED and the nonlocal multiplicative anomaly*, Int. J. Mod. Phys. A **25**, 2382 (2010).

[179] M. Gomes, J.R. Nascimento, A.Yu. Petrov, and A.J. da Silva, *Aetherlike Lorentz-breaking actions*, Phys. Rev. D **81**, 045018 (2010).

[180] T. Higaki and R. Kitano, *Supersymmetric effective theories of axions*, Phys. Rev. D **86**, 075027 (2012).

[181] C. Roldán-Domínguez, H. Belich, W. Spalenza, A.L.M.A. Nogueira, M. Reetz, and J.A. Helayël-Neto, *A Supersymmetric Extension of Axionic Electrodynamics: From Axions and Photons to Axinos and Photinos*, arXiv:2509.26089v4.

[182] M.S. Berger and V.A. Kostelecký, *Supersymmetry and Lorentz violation,* Phys. Rev. D **65**, 091701(R) (2002).

[183] M.S. Berger, *Superfield realizations of Lorentz and CPT violation,* Phys. Rev. D **68**, 115005 (2003).

[184] P.A. Bolokhov, S.G. Nibbelink, and M. Pospelov, *Lorentz violating supersymmetric quantum electrodynamics,* Phys. Rev. D **72**, 015013 (2005).

[185] A. Katz and Y. Shadmi, *Lorentz violation and superpartner masses,* Phys. Rev. D **74**, 115021 (2006).

[186] D. Friedan, Z. Qiu, and S. Shenker, *Conformal Invariance, Unitarity, and Critical Exponents in Two Dimensions,* Phys. Rev. Lett. **52**, 1575 (1984).

[187] M. Ezawa, *Supersymmetric structure of quantum Hall effects in graphene,* Phys. Lett. **A372**, 924 (2008).

[188] E.M.C. Abreu, M.A. De Andrade, L.P.G. De Assis, J.A. Helayël-Neto, Á.L.M.A. Nogueira, and R.C. Paschoal, *A supersymmetric model for graphene,* J. High Energ. Phys. **2011**, 1 (2011).

[189] C.A. Dartora and G.G. Cabrera, *Wess–Zumino supersymmetric phase and superconductivity in graphene,* Phys. Lett. A **377**, 907 (2013).

[190] S.-S. Lee, *Emergence of supersymmetry at a critical point of a lattice model,* Phys. Rev. B **76**, 075103 (2007).

[191] T. Grover, D.N. Sheng, and A. Vishwanath, *Emergent space-time supersymmetry at the boundary of a topological phase,* Science **344**, 280 (2014).

[192] P. Ponte and S.-S. Lee, *Emergence of supersymmetry on the surface of three-dimensional topological insulators,* New J. Phys. **16**, 013044 (2014).

[193] S.-K. Jian, Y.-F. Jiang, and H. Yao, *Emergent Spacetime Supersymmetry in* $3D$ *Weyl Semimetals and* $2D$ *Dirac Semimetals,* Phys. Rev. Lett. **114**, 237001 (2015).

[194] T. Wehling, A. Black-Schaffer, and A. Balatsky, *Dirac materials,* Advances in Physics **63**, 1 (2014).

[195] B.Q. Lv, *et al.*, *Experimental discovery of Weyl semimetal TaAs,* Phys. Rev. **X5**, 031013 (2015).

[196] A. Tamai, *et al.*, *Fermi arcs and their topological character in the candidate type-II Weyl semimetal* $MoTe_2$, Phys. Rev. **X6**, 031021 (2016).

[197] B. Yan and C. Felser, *Topological Materials: Weyl Semimetals,* Annu. Rev. Condens. Matter Phys. **8**, 337 (2017).

[198] N.P. Armitage, E.J. Mele, and A. Vishwanath, *Weyl and Dirac Semimetals in Three Dimensional Solids,* Rev. Mod. Phys. **90**, 015001 (2018).

[199] H. Gao, J.W.F. Venderbos, Y. Kim, and A.M. Rappe, *Topological Semimetals from First Principles,* Annu. Rev. Mater. Res. **49**, 153 (2019).

[200] S.H. Lee, *et al.*, *Evidence for a Magnetic-Field-Induced Ideal Type-II Weyl State in Antiferromagnetic Topological Insulator* $Mn(Bi_{1-x}Sb_x)_2$, Phys. Rev. **X11**, 031032 (2021).

[201] X.-L. Qi, T. L. Hughes, and S.-C. Zhang, *Topological field theory of time-reversal invariant insulators,* Phys. Rev. B **78**, 195424 (2008).

[202] H. Zhang, C.-X. Liu, X.-L. Qi, X. Dai, Z. Fang, and S.-C. Zhang, *Topological insulators in* Bi_2Se_3, Bi_2Te_3 *and* Sb_2Te_3 *with a single Dirac cone on the surface,* Nature Physics **5**, 438 (2009).

[203] M.Z. Hasan and C.L. Kane, *Topological Insulators,* Rev. Mod. Phys. **82**, 3045 (2010).

[204] S. Ryu, A.P. Schnyder, A. Furusaki, and A.W.W. Ludwig, *Topological insulators and superconductors: tenfold way and dimensional hierarchy,* New J. Phys. **12**, 065010 (2010).

[205] Y. Ando and L. Fu, *Topological Crystalline Insulators and Topological Superconductors: From Concepts to Materials,* Annu. Rev. Condens. Matter Phys. **6**, 361 (2015).

[206] E. Xu, *et al.*, *Enhanced thermoelectric properties of topological crystalline insulator PbSnTe nanowires grown by vapor transport,* Nano Res. **9**, 820 (2016).

[207] S. Reja, H.A. Fertig, L. Brey, and S. Zhang, *Surface magnetism in topological crystalline insulators,* Phys. Rev. B **96**, 201111(R) (2017).

[208] K.S. Novoselov *et al.*, *Electric field effect in atomically thin carbon films,* Science **306**, 666 (2004).

[209] A.H. Castro Neto, F. Guinea, N.M.R. Peres, K.S. Novoselov, and A.K. Geim, *The electronic properties of graphene,* Rev. Mod. Phys. **81**, 109 (2009).

[210] X. Wan, A.M. Turner, A. Vishwanath, and S. Y. Savrasov, *Topological semimetal and Fermi-arc surface states in the electronic structure of pyrochlore iridates,* Phys. Rev. B **83**, 205101 (2011).

[211] A.G. Grushin, *Consequences of a condensed matter realization of Lorentz violating QED in Weyl semi-metals,* Phys. Rev. D **86**, 045001 (2012).

[212] A.A. Soluyanov, D. Gresch, Z. Wang, Q. Wu, M. Troyer, X. Dai, and B. Andrei Bernevig, *Type-II Weyl semimetals,* Nature **527**, 495 (2015).

[213] S. Tchoumakov, M. Civelli, and M.O. Goerbig, *Magnetic-field-induced relativistic properties in type-I and type-II Weyl semimetals,* Phys. Rev. Lett. **117**, 086402 (2016).

[214] Y.M.P. Gomes and M.J. Neves, *A Lorentz-violating low-energy model for the bilayer graphene,* EPJ Plus **138**, 543 (2023).

[215] H. Isobe and N. Nagaosa, *Theory of a quantum critical phenomenon in a topological insulator: (3+1)-dimensional quantum electrodynamics in solids,* Phys. Rev. B **86**, 165127 (2012).

[216] H. Belich, J.L. Boldo, L.P. Colatto, J.A. Helayël-Neto, and Á.L.M.A. Nogueira, *Supersymmetric extension of the Lorentz- and CPT-violating Maxwell-Chern-Simons model,* Phys. Rev. D **68**, 065030 (2003).

[217] A.P. Baêta Scarpelli, H. Belich, J.L. Boldo, L.P. Colatto, J.A. Helayël-Neto, and Á.L.M.A. Nogueira, *Remarks on the causality, unitarity and supersymmetric extension of the Lorentz and CPT-violating Maxwell-Chern-Simons model,* Nucl. Phys. B **127**, 105 (2004).

[218] A. Katz and Y. Shadmi, *Lorentz Violation and Superpartner Masses,* Phys. Rev. D **74**, 115021 (2006).

[219] J.P.S. Melo, W.C. e Silva, and J.A. Helayël-Neto, *SUSY QED with Lorentz-Asymmetric Fermionic Matter and a Glance at the Electron's EDM*, Fortsch. Phys. **73**, 2400203 (2025).

[220] A. Salam and J. Strathdee, *Super-gauge transformations,* Nucl. Phys. B **76**, 477 (1974).

[221] S.J. Gates, M.T. Grisaru, M. Rocek, and W. Siegel, *Superspace, or One thousand and one lessons in supersymmetry,* Front. Phys. **58**, 1 (1983).

[222] A. Bilal, *Introduction to Supersymmetry*, arXiv:hep-th/0101055.

[223] H. Belich, L.D. Bernald, P. Gaete, and J.A. Helayël-Neto, *The photino sector and a confining potential in a supersymmetric Lorentz-symmetry-violating model,* Eur. Phys. J. C **73**, 2632 (2013).

[224] L. Bonetti, L.R. dos Santos Filho, J.A. Helayël-Neto, and A.D.A.M. Spallicci, *Photon sector analysis of Super and Lorentz symmetry breaking: effective photon mass, birefringence and dissipation,* Eur. Phys. J. C **78**, 811 (2018).

[225] R.C. Terin, W. Spalenza, H. Belich, and J.A. Helayël-Neto, *Aspects of the gauge boson-gaugino mixing in a supersymmetric scenario with Lorentz-symmetry violation,* Phys. Rev. D **105**, 115006 (2022).

[226] S.G. Nibbelink and M. Pospelov, *Lorentz Violation in Supersymmetric Field Theories,* Phys. Rev. Lett. **94**, 081601 (2005).

[227] H. Belich, L.D. Bernald, P. Gaete, J.A. Helayël-Neto, and F.J.L. Leal, *Aspects of CPT-even Lorentz-symmetry violating physics in a supersymmetric scenario,* Eur. Phys. J. C **75**, 291 (2015).

[228] V.A. Kostelecký and R. Potting, *CPT, strings, and meson factories,* Phys. Rev. D **51**, 13923 (1995).

[229] B.L. Roberts and W.J. Marciano, *Lepton dipole moments*, (World Scientific, Singapore, 2010).

[230] N. Yamanaka, *Analysis of the electric dipole moment in the R-parity violating supersymmetric standard model*, (Springer, Berlin, 2014).

[231] W. Bernreuther and M. Suzuki, *The electric dipole moment of the electron,* Rev. Mod. Phys. **63**, 313 (1991).

[232] C. Rovelli, *Loop quantum gravity*, Living Rev. Rel. **1**, 1 (1998).

[233] A. Ashtekar and J. Lewandowski, *Background independent quantum gravity: A status report*, Class. Quant. Grav. **21**, 15R53 (2004).

[234] A. Ashtekar, *New variables for classical and quantum gravity*, Phys. Rev. Lett. **57**, 2244 (1986).

[235] T. Jacobson and L. Smolin, *The left-handed spin connection as a variable for canonical gravity*, Phys. Lett. B **196**, 39 (1987).

[236] C. Rovelli and L. Smolin, *Knot theory and quantum gravity*, Phys. Rev. Lett. **61**, 1155 (1988).

[237] A. Ashtekar and C. Rovelli, *A loop representation for the quantum Maxwell field*, Class. Quant. Grav. **9**, 1121 (1992).

[238] H.A. Morales-Técotl and C. Rovelli, *Fermions in quantum gravity*, Phys. Rev. Lett. **72**, 3642 (1994).

[239] C. Rovelli and L. Smolin, *The physical Hamiltonian in nonperturbative quantum gravity*, Phys. Rev. Lett. **72**, 446 (1994).

[240] C. Rovelli and L. Smolin, *Discreteness of area and volume in quantum gravity*, Nucl. Phys. B. **442**, 593 (1995).

[241] C. Rovelli, *Black hole entropy from loop quantum gravity*, Phys. Rev. Lett. **77**, 3288 (1996).

[242] T. Thiemann, *Anomaly-free formulation of nonperturbative four-dimensional Lorentzian quantum gravity*, Phys. Lett. **380**, 257 (1996).

[243] J.C. Baez, *Spin networks in gauge theory*, Adv. Math. **117**, 253 (1996).

[244] H. Fort, R. Gambini, and Jorge Pullin, *Lattice knot theory and quantum gravity in the loop representation*, Phys. Rev. D **56**, 2127 (1997).

[245] A. Perez, *The spin-foam approach to quantum gravity*, Living Rev. Rel. **16**, 3 (2013).

[246] M. Han, Z. Huang, and A. Zipfel, *Emergent four-dimensional linearized gravity from a spin foam model*, Phys. Rev. D **100**, 024060 (2019).

[247] J. Alfaro, H.A. Morales-Tecotl, and L.F. Urrutia, *Quantum gravity and spin 1/2 particles effective dynamics*, Phys. Rev. D **66**, 124006 (2002).

[248] L. L. Graef, R.O. Ramos, and G.S. Vicente, *Gravitational particle production in loop quantum cosmology*, Phys. Rev. D **102**, 043518 (2020).

[249] L.N. Barboza, G.L.L.W. Levy, L.L. Graef, and R.O. Ramos, *Constraining the Barbero-Immirzi parameter from the duration of inflation in loop quantum cosmology*, Phys. Rev. D **106**, 103535 (2022).

[250] S. Vagnozzi, et al., *Horizon-scale tests of gravity theories and fundamental physics from the Event Horizon Telescope image of Sagittarius A^**, Class. Quant. Grav. **40**, 165007 (2023).

[251] M. Afrin, S. Vagnozzi, and S.G. Ghosh, *Tests of loop quantum gravity from the Event Horizon Telescope results of Sgr A**, Astrophys. J. **944**, 149 (2023).

[252] J.-M. Yan, C. Liu, T. Zhu, Q. Wu, and A. Wang, *Observational tests of a quantum extension of Schwarzschild spacetime in loop quantum gravity with stars in the Galactic Center*, Phys. Rev. D **107**, 084043 (2023).

[253] R.-T. Chen, S. Li, L.-G. Zhu, and J.-P. Wu, *Constraints from Solar System tests on a covariant loop quantum black hole*, Phys. Rev. D **109**, (2024) 024010.

[254] T. Zhu and A. Wang, *Observational tests of the self-dual spacetime in loop quantum gravity*, Phys. Rev. D **102**, 124042 (2020).

[255] E. K. Anderson, *et al.*, *Observation of the effect of gravity on the motion of antimatter*, Nature **621**, 716 (2023).

[256] H. Li and B.-Q. Ma, *Speed variations of cosmic photons and neutrinos from loop quantum gravity*, Phys. Lett. B **836**, 137613 (2023).

[257] Y. Chen and B.-Q. Ma, *Novel pre-burst stage of gamma-ray bursts from machine learning*, JHEAp **32**, 78 (2021).

[258] H. Xu and B.-Q. Ma, *Regularity of high energy photon events from gamma ray bursts*, JCAP **1801**, 050 (2018).

[259] Z. Cao, *et al.*, *Peta–electron volt gamma-ray emission from the Crab Nebula*, Science **73**, 6553 (2021).

[260] J.P.S. Melo, M. Reetz, L.P.R. Ospedal, and J.A. Helayël-Neto, *From interacting fields to interparticle potentials: a pedagogical approach*, Rev. Bras. Ens. Fís. **48**, e20250466 (2026).

[261] J.E. Moody and F. Wilczek, *New macroscopic forces?*, Phys. Rev. D **30**, 130 (1984).

[262] B.A. Dobrescu and I. Mocioiu, *Spin-dependent macroscopic forces from new particle exchange*, JHEP **11**, 005 (2006).

[263] M. Maggiore, *A modern introduction to quantum field theory*, (Oxford University Press, New York, 2005).

[264] P.C. Malta, J.P.S. Melo, and C.A.D. Zarro, *Experimental signatures of Kalb-Ramond-like particles*, JHEP **05**, 093 (2025).

[265] V. I. Ogievetsky and I. V. Polubarinov, *The notoph and its possible interactions*, Yad. Fiz. **4**, 216 (1966) [Sov. J. Nucl. Phys. **4**, 156 (1967)].

[266] E. A. Ivanov, *Gauge Fields, Nonlinear Realizations, Supersymmetry*, Phys. Part. Nucl. **47**, 508 (2016).

[267] M. Kalb and P. Ramond, *Classical Direct Interstring Action*, Phys. Rev. D **9**, 2273 (1974).

[268] E. Cremmer and J. Scherk, *Spontaneous dynamical breaking of gauge symmetry in dual models*, Nuclear Physics **72**, 117 (1974).

[269] K. Becker, M. Becker, and J. H. Schwarz, *String theory and M-theory: A modern introduction*, (Cambridge University Press, Cambridge, 2006).

[270] I. Antoniadis, N. Arkani-Hamed, S. Dimopoulos, and G.R. Dvali, *New dimensions at a millimeter to a fermi and superstrings at a TeV*, Phys. Lett. B **436**, 257 (1998).

[271] S. Tiwary and R. Dick, *Constraints on antisymmetric tensor fields from Bhabha scattering*, Eur. Phys. J. C **81**, 1115 (2021).

[272] A. Dashko and R. Dick, *The shadow of dark matter as a shadow of string theory*, Eur. Phys. J. C **79**, 312 (2019).

[273] J.M. Cline, G.D. Moore, and A.R. Frey, *Composite magnetic dark matter and the 130 GeV line*, Phys. Rev. D **86**, 115013 (2012).

[274] A. J. Magnus, J. G. Fenwick, and R. Dick, *Antisymmetric tensor portals to dark matter*, arXiv:2409.05915.

[275] Y. Nambu, *III. Magnetic and electric confinement of quarks* Phys. Rep. **23**, 250 (1976).

[276] J. Greensite, *An Introduction to Confinement Problem*, second edition (Springer, Berlin, 2020).

[277] L. S. Grigorio, M. S. Guimaraes, R. Rougemont, and C. Wotzasek, *Confinement, brane symmetry and the Julia-Toulouse approach for condensation of defects*, JHEP **08**, 118 (2011).

[278] M. S. Guimaraes, R. Rougemont, C. Wotzasek, and C. A. D. Zarro, *Massive photons and Dirac monopoles: electric condensate and magnetic confinement*, Phys. Lett. B **723**, 422-426 (2013).

[279] A. Smailagic and E. Spallucci, *Cornell potential in Kalb-Ramond scalar QED via Higgs mechanism*, Phys. Lett. B **803**, 135304 (2020).

[280] M. Franz, *Vortex-boson duality in four space-time dimensions*, EPL, **77**, 47005 (2007).

[281] R. Rougemont, J. Noronha, C. A. D. Zarro, C. Wotzasek, M. S. Guimaraes, and D. R. Granado, *Vanishing DC holographic conductivity from a magnetic monopole condensate*, JHEP **07**, 070 (2015).

[282] F. A. Barone, L. M. De Moraes, and J. A. Helayel-Neto, *Casimir effect for gauge scalars: The Kalb-Ramond case*, Phys. Rev. D **72**, 105012 (2005) [erratum: Phys. Rev. D **73**, 089901 (2006)].

[283] H. Belich, L. M. Silva, J. A. Helayel-Neto, and A. E. Santana, *Casimir Effect at finite temperature for the Kalb-Ramond field*, Phys. Rev. D **84**, 045007 (2011).

[284] A. Smailagic and E. Spallucci, *Kalb–Ramond scalar QED multiple vacua*, J. Phys. G **48**, 125002 (2021).

[285] F. A. Barone, F. E. Barone, and J. A. Helayel-Neto, *Charged branes interactions via Kalb-Ramond field*, Phys. Rev. D **84**, 065026 (2011).

[286] J. F. Assunção, T. Mariz, J. R. Nascimento, and A. Yu. Petrov, *Dynamical Lorentz symmetry breaking in a tensor bumblebee model*, Phys. Rev. D **100**, 085009 (2019).

[287] L. H. C. Borges, A. G. Dias, A. F. Ferrari, J. R. Nascimento, and A. Yu. Petrov, *Generation of Axion-Like Couplings via Quantum Corrections in a Lorentz Violating Background*, Phys. Rev. D **89**, 045005 (2014).

[288] A. J. G. Carvalho, A. G. Dias, A. F. Ferrari, T. Mariz, J. R. Nascimento, and A. Yu. Petrov, *Axion-Photon Interaction from Nonminimal Dimension-5 Lorentz-Violating Operators*, Phys. Rev. D **107**, 085021 (2023).

[289] C. N. Ferreira, J. A. Helayel-Neto, and N. A. Tomimura, *Plane Gravitational Radiation from Neutrinos Source with Kalb-Ramond Coupling*, Int. J. Mod. Phys. A **24**, 1537 (2009).

[290] S. Chakraborty and S. Sengupta, *Packing extra mass in compact stellar structures: An interplay between Kalb-Ramond field and extra dimensions*, JCAP **05**, 032 (2018).

[291] E.L.B. Junior, J.T.S.S. Junior, F.S.N.Lobo, M.E.Rodrigues, D. Rubiera-Garcia, L.F.D. da Silva, and H.A. Vieira, *Spontaneous Lorentz symmetry-breaking constraints in Kalb-Ramond gravity*, Eur. Phys. J. C **84**, 1257 (2024).

[292] D. Maity, P. Majumdar, and S. SenGupta, *Parity violating Kalb-Ramond-Maxwell interactions and CMB anisotropy in a brane world*, JCAP **06**, 005 (2004).

[293] J. P. Beltrán Almeida, A. Guarnizo, and C. A. Valenzuela-Toledo, *Arbitrarily coupled p-forms in cosmological backgrounds*, Class. Quant. Grav. **37**, 035001 (2020).

[294] J. P. B. Almeida, A. Guarnizo, R. Kase, S. Tsujikawa, and C. A. Valenzuela-Toledo, *Arbitrarily coupled p-forms in cosmological backgrounds*, JCAP **03**, 025 (2019).

[295] C. Capanelli, L. Jenks, E. W. Kolb, and E. McDonough, *Cosmological implications of Kalb-Ramond-like particles*, JHEP **06**, 075 (2024).

[296] S. E. Hjelmeland and U. Lindstrom, *Duality for the nonspecialist*, arXiv:hep-th/9705122.

[297] A. Hell, *On the duality of massive Kalb-Ramond and Proca fields*, JCAP **01**, 056 (2022).

[298] P. Svrcek and E. Witten, *Axions In String Theory*, JHEP **06**, 051 (2006).

[299] A. Arvanitaki, S. Dimopoulos, S. Dubovsky, N. Kaloper, and J. March-Russell, *String Axiverse*, Phys. Rev. D **81**, 123530 (2010).

[300] R.D. Peccei and H.R. Quinn, *CP Conservation in the Presence of Instantons*, Phys. Rev. Lett. **38**, 1440 (1977).

[301] S. Weinberg, *A New Light Boson?*, Phys. Rev. Lett. **40**, 223 (1978).

[302] F. Wilczek, *Problem of Strong P and T Invariance in the Presence of Instantons*, Phys. Rev. Lett. **40**, 279 (1978).

[303] L.B. Okun, *Limits of electrodynamics: paraphotons?*, Sov. Phys. JETP **56**, 502 (1982).

[304] B. Holdom, *Two U(1)'s and epsilon charge shifts*, Phys. Lett. B **166**, 196 (1986).

[305] S.A. Abel, M.D. Goodsell, J. Jaeckel, V.V. Khoze, and A. Ringwald, *Kinetic mixing of the photon with hidden $U(1)$'s in string phenomenology*, JHEP **807**, 124 (2008).

[306] S. Abel and J. Santiago, *Constraining the string scale: from Planck to Weak and back again*, J. Phys. G **30**, (2004).

[307] P. Fayet, *Extra $U(1)$'s and new forces*, Nucl. Phys. B **347**, 743 (1990).

[308] A. Smailagic and E. Spallucci, *The dual phases of massless/massive Kalb-Ramond fields*, J. Phys. A: Math. Gen. **34** L435 (2001).

[309] K.M. Zurek, *Dark Matter Candidates of a Very Low Mass*, arXiv:2401.03025.

[310] J.L. Feng *Dark Matter Candidates from Particle Physics and Methods of Detection*, Ann. Rev. Astron. Astrophys. **48**, 495 (2010).

[311] F. Chadha-Day, J. Ellis, and D.J.E. Marsh, *Axion Dark Matter: What is it and Why Now?*, arXiv:2105.01406.

[312] A.E. Nelson and J. Scholtz, *Dark Light, Dark Matter and the Misalignment Mechanism*, Phys. Rev. D **84**, 103501 (2011).

[313] E. Massó, F. Rota, and G. Zsembinszki, *Planck-Scale Effects on Global Symmetries: Cosmology of Pseudo-Goldstone Bosons*, Phys. Rev. D **70**, 115009 (2004).

[314] P.W. Graham *et al.*, *Experimental Searches for the Axion and Axion-Like Particles*, Ann. Rev. Nucl. Part. Sci. **65**, 485 (2015).

[315] F. Capozzi *et al.*, *New Constraints on ALP Electron and Photon Couplings from ArgoNeuT and the MiniBooNE Beam Dump*, arXiv:2307.03878.

[316] P. Agrawal *et al.*, *Feebly-interacting particles: FIPs 2020 Workshop Report (2021)*, arXiv:2102.12143.

[317] J. Jaeckel, *A force beyond the Standard Model - Status of the quest for hidden photons*, arXiv:1303.1821.

[318] A. Leike, *The phenomenology of extra neutral gauge bosons*, Phys. Rept. **317**, 143 (1999).

[319] P. Langacker, *The physics of heavy Z' gauge bosons*, Rev. Mod. Phys. **81**, 1199 (2009).

[320] V. Shtabovenko, R. Mertig, and F. Orellana, *FeynCalc 10: Do multiloop integrals dream of computer codes?*, arXiv:2312.14089.

[321] V. Shtabovenko, R. Mertig, and F. Orellana, *FeynCalc 9.3: New features and improvements*, arXiv:2001.04407.

[322] V. Shtabovenko, R. Mertig, and F. Orellana, *New Developments in FeynCalc 9.0*, Comput. Phys. Commun. **207**, 432, (2016).

[323] R. Mertig, M. Böhm, and A. Denner, *Feyn Calc - Computer-algebraic calculation of Feynman amplitudes*, Comput. Phys. Commun. **64**, 345 (1991).

[324] J. Liu, Y. Luo, and M. Song, *Investigation of the concurrent effects of ALP-photon and ALP-electron couplings in Collider and Beam Dump Searches*, JHEP **09**, 104 (2023).

[325] Y. Nambu, *Axial vector current conservation in weak interactions*, Phys. Rev. Lett. **4**, 380 (1960).

[326] X.-H. Cao and Z.-H. Guo, *Comprehensive study of axion photoproduction off the nucleon in chiral effective field theory*, Phys. Rev. D **110**, 095025 (2024).

[327] M. Chizhov and M. Naydenov, *Isospin-invariant Nambu–Jona-Lasinio model with complete set of spin-1 excitations*, AIP Conf. Proc. **2075**, 090025 (2019).

[328] M. Naydenov and V. Kozhuharov, *Dark boson mediation of the $\pi^0 \to \gamma e^+ e^-$ decay*, Nucl. Phys. B **978**, 115723 (2022).

[329] M. Naydenov and V. Kozhuharov, *Dark sector tensor currents contribution to lepton's anomalous magnetic moment*, arXiv:hep-ph/2212.02242.

[330] B.A. Dobrescu, *Massless Gauge Bosons other than the Photon*, Phys. Rev. Lett. **94**, 151802 (2005).

[331] B. Altschul, Q.G. Bailey, and V.A. Kostelecký, *Lorentz violation with an antisymmetric tensor*, Phys. Rev. D **81**, 065028 (2010).

[332] M. Maggiore, *A modern introduction to quantum field theory*, (Oxford University Press, New York, 2005).

[333] F.A. Gomes Ferreira, P.C. Malta, L.P.R. Ospedal, and J.A. Helayël-Neto, *Topologically massive spin-1 particles and spin-dependent potentials*, Eur. Phys. J. C **75**, 238 (2015).

[334] P.C. Malta, L.P.R. Ospedal, K. Veiga, and J.A. Helayël-Neto, *Comparative aspects of spin-dependent interaction potentials for spin-1/2 and spin-1 matter fields*, Adv. High Energy Phys. **2016** (2016) 2531436, [erratum Adv. High Energy Phys. **2017** (2017) 9152437].

[335] G.P. de Brito, P.C. Malta, and L.P.R. Ospedal, *Spin- and velocity-dependent nonrelativistic potentials in modified electrodynamics*, Phys. Rev. D **95**, 016006 (2017).

[336] P. Fadeev, Y.V. Stadnik, F. Ficek, M.G. Kozlov, V.V. Flambaum, and D. Budker, *Revisiting spin-dependent forces mediated by new bosons: Potentials in the coordinate-space representation for macroscopic- and atomic-scale experiments*, Phys. Rev. A **99**, 022113 (2019).

[337] P. Fadeev, F. Ficek, M.G. Kozlov, D. Budker, and V.V. Flambaum, *Pseudovector and pseudoscalar spin-dependent interactions in atoms*, Phys. Rev. A **105**, 022812 (2022).

[338] L. Cong, F. Ficek, P. Fadeev, and D. Budker, *Improved constraints on exotic interactions between electron and proton in hydrogen*, arXiv:2408.11009.

[339] L. Cong *et al.*, *Spin-dependent exotic interactions*, arXiv:2408.15691.

[340] B.A. Dobrescu and I. Mocioiu, *Spin-Dependent Macroscopic Forces from New Particle Exchange*, JHEP **0611**, 005 (2006).

[341] J. P. S. Melo, M. J. Neves, J. M. A. Paixão, and J. A. Helayël-Neto. *Loop quantum gravity effects on electromagnetic properties of charged leptons*, Eur. Phys. J. C **84**, 938 (2024).

[342] Claude Cohen-Tannoudji, Bernard Diu, and Franck Laloë, *Quantum Mechanics (vol. I, II)*, 2nd edition, (Wiley, New York, 1977).

[343] D. Griffiths, *Hyperfine Splitting in the ground state of Hydrogen*, Am. J. Phys. **50**, 698 (1982).

[344] N. Kolachevsky, A. Matveev, J. Alnis, C.G. Parthey, S.G. Karshenboim, and T.W. Haensch, *New Measurement of the 2S Hyperfine Interval in Atomic Hydrogen*, Phys. Rev. Lett. **102**, 213002 (2009).

[345] C.G. Parthey *et al.*, *Improved Measurement of the Hydrogen 1S - 2S Transition Frequency*, Phys. Rev. Lett. **107**, 203001 (2011).

[346] R. G. Bullis, C. Rasor, W. L. Tavis, S. A. Johnson, M. R. Weiss, and D. C. Yost, *Ramsey Spectroscopy of the $2S_{1/2}$ Hyperfine Interval in Atomic Hydrogen*, Phys. Rev. Lett. **130**, 203001 (2023).

[347] M.M. Sternheim, *State-Dependent Mass Corrections to Hyperfine Structure in Hydrogenic Atoms*, Phys. Rev. **130**, 211 (1963).

[348] F. Ficek and D. Budker, *Constraining Exotic Interactions*, Annalen der Physik **531**, 1800273 (2019).

[349] V.A. Yerokhin and U.D. Jentschura, *Electron Self-Energy in the Presence of a Magnetic Field: Hyperfine Splitting and g Factor*, Phys. Rev. Lett. **100**, 163001 (2008).

[350] J. Jaeckel and S. Roy, *Spectroscopy as a test of Coulomb's law - A probe of the hidden sector*, Phys. Rev. D **82**, 125020 (2010).

[351] D. Kroff and P.C. Malta, *Constraining hidden photons via atomic force microscope measurements and the Plimpton-Lawton experiment*, Phys. Rev. D **102**, 095015 (2020).

[352] G. Montagna, O. Nicrosini, and F. Piccinini, *Precision physics at LEP*, Riv. Nuovo Cim. 21N9, 1-162 (1998).

[353] SLD collaboration, *Polarized Bhabha scattering and a precision measurement of the electron neutral current couplings*, Phys. Rev. Lett. **74**, 2880 (1995).

[354] I. Bozovic-Jelisavcic, S. Lukic, M. Pandurovic, and I. Smiljanic, *Precision luminosity measurement at ILC*; arXiv:1403.7348.

[355] M. Bicer *et al.*, TLEP Design Study Working Group, JHEP **01**, 164 (2014).

[356] H. Baer *et al.*, *The International Linear Collider Technical Design Report – Volume 2: Physics*, arXiv:1306.6352.

[357] M. Derrick *et al.*, *Experimental study of the reactions $e^- e^+ \to e^- e^+$ and $e^- e^+ \to \gamma\gamma$ at 29 GeV*, Phys. Rev. D **34**, 3286 (1986).

[358] M.E. Levi *et al.*, *Weak Neutral Currents in e^+e^- Collisions at $\sqrt{s} = 29$ GeV*, Phys. Rev. Lett. **51**, 1941 (1983).

[359] G. S. Abrams *et al.*, *Measurement of Z decays into lepton pairs*, Phys. Rev. Lett. **63**, 2780 (1989).

[360] G. S. Abrams *et al.*, *Measurements of Z-boson resonance parameters in e^+e^- annihilation*, Phys. Rev. Lett. **63**, 2173 (1989).

[361] M.S. Chanowitz, M.A. Furman, and I. Hinchliffe, *Weak Interactions of Ultraheavy Fermions*, Phys. Lett. B **78**, 285 (1978).

[362] M.S. Chanowitz, M.A. Furman, and I. Hinchliffe, *Weak Interactions of Ultraheavy Fermions (II)*, Nucl. Phys. B **153**, 402 (1979).

[363] M. Jacob and G. C. Wick, *On the general theory of collisions for particles with spin*, Annals Phys. **7**, 404 (1959).

[364] H. E. Logan, *Lectures on perturbative unitarity and decoupling in Higgs physics*, arXiv:2207.01064.

[365] D.A. Varshalovich, A.N. Moskalev, and V.K. Khersonskii, *Quantum Theory of Angular Momentum: Irreducible Tensors, Spherical Harmonics, Vector Coupling Coefficients, 3nj Symbols*, (World Scientific Publishing Company, Singapura, 1988).

[366] L. Di Luzio, J. F. Kamenik, and M. Nardecchia, *Implications of perturbative unitarity for scalar di-boson resonance searches at LHC*, Eur. Phys. J. C **77**, 30 (2017).

[367] M. S. Chanowitz, *Strong WW scattering at the end of the 90's: Theory and experimental prospects*, arXiv:hep-ph/9812215.

[368] B. W. Lee, C. Quigg, and H. B. Thacker, *Weak Interactions at Very High-Energies: The Role of the Higgs Boson Mass*, Phys. Rev. D **16**, 1519 (1977).

[369] B. W. Lee, C. Quigg, and H. B. Thacker, *Strength of Weak Interactions at Very High Energies and the Higgs Boson Mass*, Phys. Rev. Lett. **38**, 883 (1977).

[370] J.J. Van Der Bij, *Two-loop large higgs mass correction to vector boson masses*, Nucl. Phys. B **248**, 141 (1984).

[371] A. Djouadi, *The Anatomy of electro-weak symmetry breaking. I: The Higgs boson in the standard model*, Phys. Rept. **457**, 1 (2008).

[372] G. P. de Brito, J. T. Guaitolini Junior, D. Kroff, P. C. Malta, and C. Marques, *Lorentz violation in simple QED processes*, Phys. Rev. D **94**, 056005 (2016).

[373] S. Dutta, P. Konar, B. Mukhopadhyaya, and S. Raychaudhuri, *Bhabha scattering with radiated gravitons at linear colliders*, Phys. Rev. D **68**, 095005 (2003).

[374] R. Bufalo, *On the Bhabha scattering for $z = 2$ Lifshitz QED*, Int. J. Mod. Phys. A **30**, 1550086 (2015).

[375] R. Bufalo, B.M. Pimentel, and D.E. Soto, *Causal approach for the electron-positron scattering in Generalized Quantum Electrodynamics*, Phys. Rev. D **90**, 085012 (2014).

[376] OPAL Collaboration, *Test of the four-fermion contact interaction in $e + e^-$ collisions at 130-40 GeV*, Phys. Lett. B **387**, 432 (1996).

[377] The International Linear Collider. URL: http://www.linearcollider.org/cms/.

[378] P. Bechtle, S. Heinemeyer, J. List, G. Moortgat-Pick, and G. Weiglein, *Physics case for an e^+e^- collider at 500 GeV and above*, arXiv:2410.16191.

[379] FCC collaboration, *FCC-ee: The Lepton Collider: Future Circular Collider Conceptual Design Report Volume 2*, Eur. Phys. J. ST **228**, 261 (2019).

[380] CEPC Study Group collaboration, *CEPC Conceptual Design Report: Volume 2 - Physics & Detector*, arXiv:1811.10545.

[381] C. Vernieri *et al.*, *Strategy for Understanding the Higgs Physics: The Cool Copper Collider*, JINST **18**, P07053 (2023).

[382] CLIC collaboration, *The Compact Linear e^+e^- Collider (CLIC): Physics Potential*, arXiv:1812.07986.

[383] C. Accettura *et al.*, *Towards a muon collider*, Eur. Phys. J. C **83**, 864 (2023).

[384] C.N. Ferreira, J.A. Helayël-Neto, and M.B.D.S.M. Porto, *Cosmic string configuration in the supersymmetric CSKR theory*, Nucl. Phys. B **620** (2002) 181.

[385] D. Cocuroci, M.J. Neves, L.P.R. Ospedal, and J.A. Helayël-Neto, *A 3-form Gauge Potential in 5D in connection with a Possible Dark Sector of 4D-Electrodynamics*, Eur. Phys. J. C **75**, 322 (2015).

[386] E.Harikumar and M. Sivakumar, *Duality and Massive Gauge Invariant Theories*, Phys. Rev. D **57**, 3794 (1998).

[387] J. R. Nascimento, A. Y. Petrov, C. Wotzasek, and C. A. D. Zarro, *"Three-dimensional Lorentz-violating action"*, Phys. Rev. D **89**, 065030 (2014).

[388] R.J. Rivers, *Lagrangian theory for neutral massive spin-2 fields*, Nuovo Cimento **34**, 387 (1964).

[389] R. Kuhfuss and J. Nitsch, *Propagating modes in gauge field theories of gravity*, Gen. Rel. Grav. **18**, 1207 (1986).

[390] G.S. Adkins, *Three-dimensional Fourier transforms, integrals of spherical Bessel functions, and novel delta function identities*, arXiv:1302.1830.

[391] I. Boettcher, *Interplay of Topology and Electron-Electron Interactions in Rarita-Schwinger-Weyl semimetals*, Phys. Rev. Lett. **124**, 127602 (2020).

[392] J.M. Link, I. Boettcher, I.F. Herbut, *d-wave superconductivity and Bogoliubov-Fermi surfaces in Rarita-Schwinger-Weyl semimetals*, Phys. Rev. B **101**, 184503 (2020).

[393] Y.M.P. Gomes and R.O. Ramos, *Tilted Dirac cone effects and chiral symmetry breaking in a planar four-fermion model*, Phys. Rev. B **104**, 245111 (2021).

[394] P. van Nieuwenhuizen, *Supergravity*, Phys. Rep. **68**, 189 (1981).

[395] D.Z. Freedman and A.V. Proeyen, *Supergravity*, (Cambridge Univ. Press, Cambridge, UK, 2012).

[396] P. Svrček e E. Witten, *Axions In String Theory*, JHEP **06**, 051 (2006).

[397] K.-S. Choi, H.P. Nilles, S. Ramos-Sanchez e P.K.S. Vaudrevange, *Accions*, Phys. Lett. B **675**, 381 (2009).

[398] J. Halverson, C. Long e P. Nath, *An Ultralight Axion in Supersymmetry and Strings and Cosmology at Small Scales*, Phys. Rev. D **96**, 056025 (2017).

[399] M. Demirtas, C. Long, L. McAllister e M. Stillman, *The Kreuzer-Skarke Axiverse*, arXiv:1808.01282 **[hep-th]**.

[400] A. Dashko e R. Dick, *The shadow of dark matter as a shadow of string theory*, Eur. Phys. J. C **79**, 312 (2019).

[401] A. Hell, *On the duality of massive Kalb-Ramond and Proca fields*, JCAP **01**, 056 (2022).

[402] A.J. Magnus, J.G. Fenwick e R. Dick, *Antisymmetric tensor portals to dark matter*, J. Subatomic Part. Cosmol. **3**, 100022 (2025).

[403] P. Fayet, *Effects of the Spin 1 partner of the Goldstino (Gravitino) on neutral current phe-nomenology*, Phys. Lett. B **95**, 285–289 (1980).

[404] P. Fayet, *On the search for a new Spin 1 Boson*, Nucl. Phys. B **187**, 184–204 (1981).

[405] M. Fabbrichesi, E. Gabrielli, G. Lanfranchi *The Physics of the Dark Photon: A Primer*, (SpringerBriefs in Physics, 2021).

[406] Y. Hochberg, Y.F. Kahn, R.K. Leane, S. Rajendran, K.V. Tilburg, T.-T. Yu e K.M. Zurek, *New approaches to dark matter detection*, Nature Rev. Phys. **4**, 637 (2022).

[407] J.M. Cline, *Status of Dark Photons*, arXiv:2405.08534.